CARBON DIOXIDE AS SOLVENT AND C1 BUILDING BLOCK IN CATALYSIS
Ariadna Campos Carrasco

UNIVERSITAT ROVIRA I VIRGILI

Carbon Dioxide as Solvent and C1 Building Block in Catalysis

Ariadna Campos Carrasco

TESIS DOCTORAL

Dirigida per la Dra. Anna Maria Masdeu i Bultó

Departament de Química Física i Inorgànica

TARRAGONA, April 2011

UNIVERSITAT ROVIRA I VIRGILI

Departament de Química Física i Inorgànica

La Dra. ANNA MARIA MASDEU I BULTÓ, Professora Titular del Departament de Química Física i Inorgànica de la Facultat de Química de la Universitat Rovira i Virgili

CERTIFICA:

Que la present memòria que porta per títol "**CARBON DIOXIDE AS SOLVENT AND C1 BUILDING BLOCK IN CATALYSIS**", que presenta Ariadna Campos Carrasco per a obtenir el grau de Doctor en Química, ha estat realitzada sota la meva direcció al Departament de Química Física i Inorgànica de la Universitat Rovira i Virgili i compleix amb els requeriments per a poder optar a Menció Europea.

Tarragona, Abril de 2011

Dra. Anna Maria Masdeu i Bultó

Agraïments

Això gairebé ja està... ara toca fer memòria dels moments bons i difícils que han passat durant aquests quatre anys i mig, en els quals tots vosaltres heu participat i heu fet possible que aquesta tesis es portés a terme i finalitzes amb èxit. Per això vull agrair-vos a tots el suport i els moments passats, ja que LA TESIS NO ÉS COSA D'UN SOL.

En primer lloc voldria agrair a la meva directora de Tesis, la Dra. Anna Mª Masdeu i Bultó, sense la qual aquesta tesis no hauria estat possible. Gràcies Anna per confiar en mi, donar-me l'oportunitat de formar part del grup de les "supercrítiques", ensenyar-me tot el que saps, tenir la paciència necessària per aguantar-me durant aquest quatre anys i donar-me l'oportunitat de conèixer món i a persones tan diferents que han aportat tant en la meva Tesis i al meu creixement personal.

A tota la resta de professores del departament: a Carmen por todas sus cenas de navidad, de verano y multiculturales, así como los momentos pasados en las Tesis de Holanda; a la Mar per tota la paciència i ajuda amb els càlculs teòrics; a la Yolanda i la Pilar pels moments de pràctiques passats juntes; a la Núria, l'Aurora, la Montse, l'Oscar, l'Elena, el Francesc i la Magdalena. Ha estat un plaer compartir aquest temps amb vosaltres i haver-me animat en tot moment a seguir endavant.

A les que m'han ensenyat a treballar al laboratori: la Clara que va tenir la paciència necessària per ensenyar-me síntesis i caracterització amb tots els aparells possibles; i a l'Arantxa, que sempre estava allí quan la necessitaves, ajudant-te en tot el que fos possible i proposant-te solucions, sense la qual aquesta Tesis no hauria estat possible... Sempre estaràs en la nostra memòria.

A tots els que passen desapercebuts però que fan que el dia a dia de la recerca sigui més fàcil: a la María José, con la que he pasado muchos momentos en el laboratorio y algún que otro susto y me ha acompañado en tantos momentos que he estado sola en el labo…; al Jordi, tantes converses i compres que vam fer....; a les secretaries del departament, per l'ajuda amb tot el papeleo; a la gent de recursos científics: en especial al Ramón, el Miguel i la Rosa; el Ramón sempre disposat a ajudar en tot, químic i no químic, buscar solucions als problemes més insòlits i motivar-te en tot moment a tirar endavant sense perdre mai el bon humor i la paciència, al Miguel, per la seva perseverança i sense el qual el PGSE no hagués sortit endavant; i la Rosa, la qual m'ha ajudat molt amb el "MALDITOf".

Agraïments

Que dir dels amics i companys de laboratori... aquesta part tant important de la Tesis sense els quals no hagués estat possible superar molts moments difícils i recordar els bons moments, tot fent decantar la balança cap al costat positiu.

Agrair als doctors del grup que amb la seva experiència m'han fet veure els problemes una mica més senzill del que jo els plantejava: a l'Aitor i al Cyril per totes les discussions químiques i propostes per solucionar els problemes químics sorgits; a l'Ali per estar sempre disposat a ajudar i compartir amb mi els seus coneixements de química i en especial dels policarbonats; a l'Henrik, a l'Olivier, al Nicolas i al nouvingut Bernabé.

A tots els companys dels laboratoris 216 i 217: la Vero, l'Angèlica, l'Amadeu, el Javi, l'Oriol, la Carolina i el Manuel, per tots els bons moments passats en congressos, cursos, sopars i excursions durant aquest quatre anys i haver-me escoltat i aconsellat en algun que altre problema químic. Sense oblidar a les Heterogènies, bueno, les GreenCat, la Isa i la Tati, tot i que hem coincidit menys, també hem passat molt bons moments, ànims i molta sort que això ja està.

Que puc dir-vos a vosaltres que no us hagi dit ja... aix... tots els moments que hem passat... qui ho diria... A la més beterana, la Dra. Raluy ;) moltes gràcies Eva per tot, per haver-me ajudat en els moments més difícils, haver compartit riures i festes, i estar sempre present, dins i fora del labo i dins i fora del país. Sobretot, sobretot, per la teva amistat, que no té preu. La Mercè, que sempre se'n recorda de totes, moooltes gràcies per tots els moments passats juntes i per tot el suport que m'has donat sempre. La Sabi, quina mala sort que has tingut, espero que et recuperis aviat i tornis a estar al 100% pel labo ;) i puguem compartir molts moments dins i fora. La Cris Pubill, ets la pera, no canviïs mai. La Dolores, gracias por compartir tantos momentos en el seminario y darme siempre tu opinión. La Cris Solé, merci per ser com ets, sempre tan directa, clara i sincera, no perdis mai aquesta espontaneïtat i bon humor. La Raquel, tot i que ens hem conegut al final, ha estat intens. Sempre disposada a ajudar i aprendre, a estat un goig compartir amb tu el labo 218. Ja us queda poc per acabar... molta sort i merci a totes per tot, espero que l'amistat continuï.

Molts estudiants i doctorands han passat pels diferents grups durant aquests últims quatre anys; la Doris, la Lourdes, el Gwaine, la Kara, el Norbert, el Benjamin, la Tatiana, el Dagoberto, la Sarah, el Francesc i la Sheila, a tots molta sort en el vostre futur.

Desitjar-li a tots els que han començat fa poc; la Siham, l'Eli, la Jessica Cid, la Jessica Llop, al Marc i l'Helena; molta sort en la Tesis i no perdeu mai l'esperança, que sempre s'arriba al final.

I no m'oblido tampoc dels companys del departament d'orgànica; l'Isidre, el David Foix, la Irene i la Cristina, que sempre han estat presents i m'han donat un cop de mà sempre que ho he necessitat.

I would like to thank Prof. Dr. Dieter Vogt to accept me in his group and specially, I want to thank Dr. Christian Müller for introducing me to the phosphinines world, the excellent guidance during my project, all the help he provides me and also to pass onto me his enormous enthusiasm for chemistry and research, overall for crystal structure. As well as the beers, talks and laughs we had during the FORT, the Friday-borrels and the defence were very nice. I'm so sorry to not have you in the defence board, it would be a pleasure. Ton Staring to helping me with the GC and with the reactor, as well as for his inexhaustible patience.

My friend Katharina Kunna for the discussions, talks and many laughs we had, and to take care of me the first days and help me when I need it. Also for the weekends we expend together. Thanks to Daniel Totev to help me with all that was in his hands, as well as discussions and laughs we had together. Laura Bini, thank you very much to share with me your office, give me advice and also share funny moments in defence and Friday-borrels; enjoy your honey moon and good luck for the future. Dr. Jarl Ivar van der Vlugt for being so nice and friendly with me and all the discussions we had about my project, as well as your good ideas to try new things and solve my problems, and also to pass onto me your enormous motivation. Thanks as well for all the chats we had when I was in Trieste and to invite me for the nice dinner.

I would like to thank as well to all the other people of the whole SKA group for their help, our talks and drinks together; Marion, Jarno, Bart, Patrick, Mathijs, Leandra, Michéle, Andreas, Joost, Cristina and Evgeny.

Vorrei anche ringraziare la Dra. Barbara Milani per avermi accettato nel vostro gruppo e avermi insegnato molte cose, soprattutto a vedere la risonanza magnetica in modo diverso. Grazie anche per averte preoccupato per me sotto tutti gli aspetti, e discutere con me l'intera chimica e essere venuta anche Tarragona. E 'un peccato che

non può essere in tribunale nella mia tesi, sarei molto onorata. Vorrei inoltre ringraziare per tutto quello che Angela ha fatto per me mentre ero a Trieste, sia all'esterno che all'interno del laboratorio, senza il loro aiuto sarebbe molto dificil.

També m'agradaria agrair al Prof. Miquel A. Pericàs i a la Dra. Amaia Bastero per haver-me proporcionat els lligands aminoalcohols que m'han servit per poder estudiar la seva eficàcia com a catalitzadors de zinc en la copolimerització CO_2/CHO i per haver tingut sempre els braços oberts a discutir sobre els resultats obtinguts i proposar-nos nous sistemes catalítics.

També voldria agrair a la família Casasayas-Llurba pels anys compartits amb ells i el seu suport durant els primers anys de tesis així com les primeres estàncies.

I per últim agrair a les persones més importants; moltes gràcies Jordi per haver estat al meu costat en aquests moments tan difícils, sé que no ha estat fàcil per tu i que jo tampoc t'ho he posat fàcil... aquests nervis... merci per no haver desistit, per no haver perdut mai la paciència i el bon humor i compartir amb mi el teu amor; muchas gracias papas y Héctor, gracias por haberme animado a seguir adelante y apoyarme en todas las decisiones que he tomado; ayudarme a levantar, a superar los momentos difíciles y a continuar cuando me he equivocado; sin vosotros no habría llegado hasta aquí y no sería quién soy.

Moltes gràcies a tots. Muchas gracias a todos. Thank you very much everybody. Vielen Dank allen. Heel erg bedankt iedereen. Grazie a tutti.

Ariadna Campos Carrasco

El investigador sufre las decepciones, los largos meses pasados en una dirección equivocada, los fracasos. Pero los fracasos son también útiles, porque, bien analizados, pueden conducir al éxito.

Alexander Fleming

"Lo importante es no dejar de hacerse preguntas."

Albert Einstein

La duda no está por debajo del conocimiento, sino por encima de él.

Alain-Rene Lesage

Table of Contents

Table of Contents

Table of Contents

Chapter - 1

Carbon Dioxide as Solvent and C1 Building Block in Catalysis: General Introduction

In the last decades homogeneous catalysis has achieved an important role in chemical industries. An aspect that is receiving increasing attention is the use of less hazardous reagents or solvents for environmental friendly reactions. This also leads to explore the possibilities of reuse, recover and recycle the emissions (basically carbon dioxide) prior to their release into the environment. One possible application of carbon dioxide is as an environmental benign reaction medium in its compressed form (liquid or supercritical, $scCO_2$), also providing opportunities for facilitating the recovery and recycling of the catalyst. On the other hand, CO_2 could be reused as a remarkable C_1 feedstock because of its low cost, its natural abundance and relatively low toxicity.

The literature reveals that uses of CO_2 have great potential in the chemical industry and that careful application of CO_2 technology can result in products and processes that are cleaner, less expensive and of higher quality than with classical technologies.

This introductory chapter reviews the literature on the use of carbon dioxide as an alternative solvent to perform copolymerisation reactions of CO and vinyl arenes to obtain polyketones, and the use of carbon dioxide as C_1 building block in CO_2/epoxides copolymerisation reactions to produce polycarbonates.

General Introduction

1.1 Green Chemistry

Green chemistry appears during the second half of the 20th century as a new way to understand the chemistry. It is focused on minimizing the hazard and maximizing the efficiency of any chemical choice reducing waste, and reducing or eliminating pollution and environmental damage.[1]

Paul T. Anastas and John C. Warner developed the 12 principles of green chemistry.[1] These concepts help researchers to do greener chemistry in the way that when they design a new product they use renewable feedstocks, when possible, or at least less hazardous and toxic reagents. The synthetic route should prevent waste and minimize the derivatisation. The requirements of energy should be as low as possible, as well as the chemical risk. All these concepts are not always possible to incorporate in a new designed procedure, but as much as they are incorporated, greener chemistry will be done.

From the point of view of green chemistry, the organic synthesis has the problem of producing high amounts of waste in fine chemicals industry. Therefore, it could be advisable to replace classical stoichiometric reagents with cleaner and more selective catalytic alternatives.[2] On the other hand, one of the key transformations in organic synthesis is C-C bond formation. An important way to do it greener is using renewable feedstocks such as CO or CO_2, two gases widely use as C_1 building blocks in catalysis.

Another important issue in green chemistry is reducing the use of organic solvents. Since, so many of the solvents that are favoured by organic reactions have been blacklisted, researchers try to avoid them.[2] Indeed, the best solvent is no solvent and if a solvent is needed, then water or other non-classical reaction media (compressed carbon dioxide and/or ionic liquids) are preferred to avoid environmental problems and/or to facilitate catalyst recovery and recycling.

1.2 Homogeneous Catalysis

The main advantage of catalysis is that it can provide the desired product at lower temperature and pressure with higher selectivity and generating less waste than non-catalysed reactions. The responsible of these advantages is the catalyst, a substance that increases the rate of the reaction without being consumed or modified (Figure 1.1).

The catalyst combines with the reagents generating intermediate species, which are easily transformed into the desired products by the different steps of the catalytic cycle.
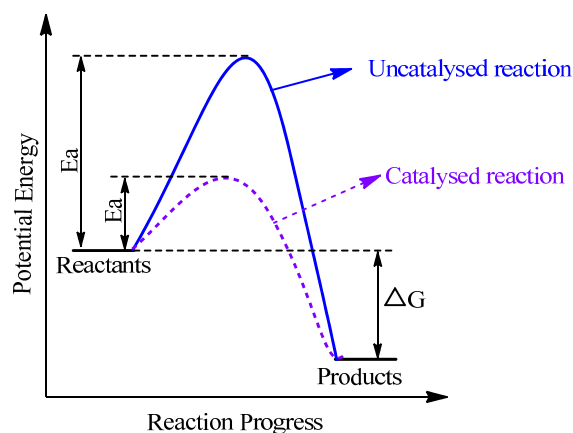
Figure 1.1. Catalyst's effect on the reaction.

Catalysis has been traditionally divided in two different kinds. One of those is homogeneous catalysis in which the catalyst, the reagents and products are in the same phase. The other is heterogeneous catalysis in which the catalysts are insoluble in the reaction medium, so the reaction occurs at the surface. Recently, other possibilities have been developed (biphasic catalysis, multiphasic, supported catalysis, etc.) making this classification between these two concepts less clear. Some homogeneous catalysts are based on coordination or organometallic complexes containing organic ligands, which can modulate the properties of the catalyst. In Table 1.1 different properties of both kinds of catalysis are compared. Despite the advantages presented by homogeneous in front of heterogeneous catalysis, homogeneous catalysis has the important drawback of catalyst separation, recovery and recycling.

Table 1.1. Comparison of homogeneous and heterogeneous catalysis.[3]

	Heterogeneous	**Homogeneous**
Catalyst form	Solid, often metal or metal oxide	Metal complex
Mode of use	Fixed bed or slurry	Dissolved in reaction medium
Solvent	Usually not required	Usually required – can be product or by-product
Selectivity	Usually poor	Can be tuned
Stability	Stable to high temperature	Often decompose ≥ 100ºC
Recyclability	Easy	Can be very difficult

General Introduction

Over the past few decades, methods and techniques in homogeneous catalysis achieved remarkable progress on catalyst separation, recovery and recycling. One of the first solutions studied was to heterogenise the homogeneous catalysts by attachment to organic or inorganic supports or by using semipermeable membranes.[4] However, this approach has some limitation such as poor catalytic activities, poor reproducibility, selectivity and leaching of the catalyst. Another solution was using liquid-liquid biphasic systems, where the catalyst was dissolved in one phase and the reactants and products in the second phase. The catalyst is easily recovered by phase separation. These systems can be formed by two immiscible organic solvents, water phase, fluorous solvents, ionic liquids or supercritical carbon dioxide.[5] Even more, recently it has been developed the concept of organic aqueous tuneable solvents (OATS),[6] which optimised the reactions and separations simultaneously. In these systems the reaction takes place in a miscible aqueous-organic solvent mixture, while the addition of modest pressure of CO_2 (50-60 bars) split the solvents into two immiscible phases, where the catalyst persists in the aqueous solution and the product in the organic one.

Especially carbon dioxide has been proposed as an environmental benign medium for catalytic reactions and extraction processes, since the catalyst can be easily separated from the products by releasing the pressure.

1.3 Supercritical fluids

A supercritical fluid (SCF) is any substance at pressure and temperature above the critical point. In this situation a new phase is formed with properties intermediate between gas and liquid.[7,8] The use of supercritical fluids is a green strategy to replace volatile organic compounds (VOCs) and to enable new and clean technologies, when non-toxic substances are used. One example, which has been practiced in industry for more than twenty years on various scales, is the extraction of natural products by supercritical carbon dioxide.[7]

The main advantage of supercritical fluids as reaction media is that some solvent properties can be modified from gas-like to liquid-like, changing pressure and temperature conditions. SCF can have liquid-like densities and solvent strength. Furthermore, the solvent strength of SCFs can be adjusted by modification of the medium density (and therefore the density-dependent solvent properties such as dielectric constant, viscosity, etc.) by pressure control giving more controllable and

4

selective reactions.[8,9] On the other hand, SCF also share many of the advantages of gases including low viscosities,[10] high gas miscibilities and high diffusivities,[11] providing faster reactions in case of diffusion-controlled processes involving gaseous reagents, for example hydrogen, oxygen or carbon monoxide.

Among supercritical fluids, carbon dioxide and water are the most commonly used. Particularly carbon dioxide is considered to be an alternative solvent for chemical synthesis[12] because of its practical physical and chemical properties. It has a readily accessible critical temperature and pressure (Figure 1.2, T_c = 31.1ºC, P_c = 73.8 bars, δ_c = 0.468 g/ml). Moreover, is non-toxic, non-flammable, inexpensive and abundant. [8,13]
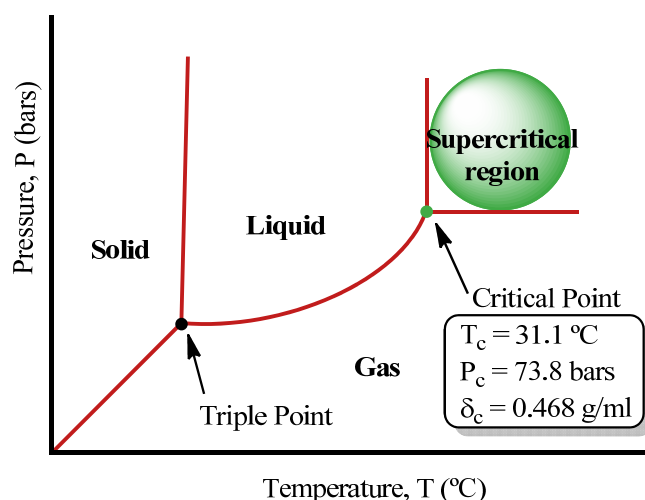
Figure 1.2. Qualitative representation of the CO_2 phase diagram.

Using a window adapted reactor the CO_2 phases can be easily observed. When the reactor is pressurized with the liquid at the vapour pressure, two separated phases can be observed, where the meniscus is clearly defined (Figure 1.3a). Once the temperature increases, the meniscus is less defined (Figure 1.3b and c), and finally at supercritical conditions only one phase is observed (Figure 1.3d).

(a)   *(b)*   *(c)*   *(d)*
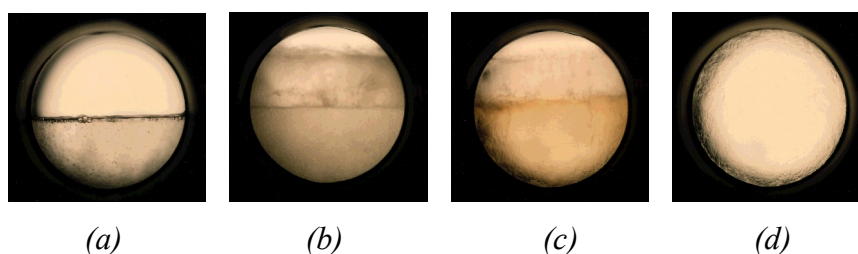
Figure 1.3. Phases adopted by carbon dioxide.

General Introduction

Although CO_2 is the most popular solvent, its low polarity causes problems of solubility, especially in homogeneous catalysis where the catalysts are often polar substances. It is known that most organic molecules of molecular weights below 1000 and with low to medium polarity are moderately soluble in $scCO_2$, and their solubility increases greatly with increasing volatility of the compound. The presence of highly polar functional groups like carboxylic acids, their salts or aromatic rings strongly reduces the solubility.[14] Solubility of the catalysts in $scCO_2$ can be adjusted by introducing CO_2-philic group in the ligands.[8] The type of ligands that are known to be sufficiently CO_2-philic or at least sufficiently non-polar to be soluble or usable in $scCO_2$ include highly fluorinated ligands (such as highly fluorinated phosphines),[15,16] carboxylates, diketonates,[17] trialkylphosphines,[15,18] carbonyl ligands[19] and ligands functionalized with trimethylsilyl or polysiloxane groups.[20] Moreover, the solubility of the complexes can be increased by the addition of co-solvents or surfactants.[21]

The introduction of the perfluorinated groups in *meta* or *para* position of the aromatic ring are normally done using $-(CH_2)_x-(CF_2)_y-CF_3$ "ponytails" where x ranges generally from 0 to 3 and y ranges from 0 to 8. Some examples of these ligands used in catalytic systems in compressed carbon dioxide are depicted in Figure 1.4.[8,15,22-26] The solubility of the catalyst is sensitive to the length and number of fluorinated ponytails, longer or more tails decreases the pressure required for solubility.[27] Besides, $-CF_2-$ groups have electron-withdrawing effect and the methylene spacers $-(CH_2)_x-$ between the aromatic ring and the perfluoroalkyl chain are inserted in order to minimize it. However, in some cases are avoided, due to beneficial effects in catalysis.

On contrast, it should be noted that even cationic catalyst precursors can be used in $scCO_2$ if the anion is carefully chosen so as to optimize the solubility. Anions that are preferred are those that are large and highly fluorinated such as $BArF^-$ (tetrakis(3,5-bis(trifluoromethyl)phenyl)borate). One example is found in the asymmetric hydrogenation of α-amidoacrylic acid reaction in supercritical carbon dioxide.[28] The catalyst involved is based on [Rh(cod)(Et-Duphos)][BArF] (cod = 1,5-cyclooctadiene, Et-Duphos = 1,2-bis[(*R,R*)-2,5-diethylphospholano]benzene) and the results are better than the ones obtained in conventional solvents.
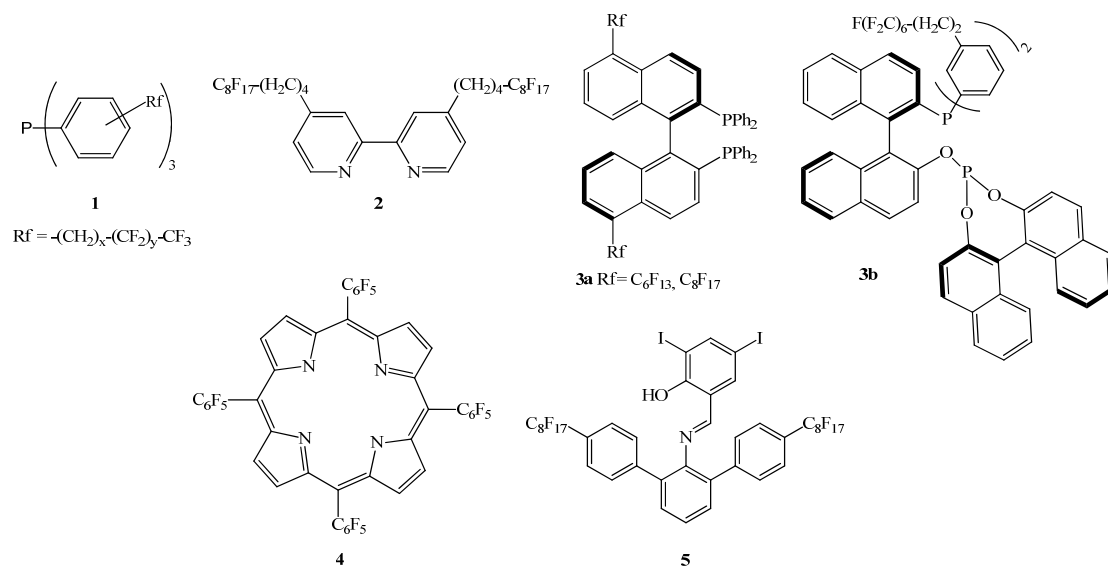
Figure 1.4. Some examples of perfluorinated ligands used in compressed carbon dioxide.

Furthermore, an advantage of supercritical fluids as reaction media is the recovery and reuse of the catalyst. There are a wide variety of ways in which homogeneous catalysis can be recovered. In some cases the catalyst precipitates by lowering the pressure[16a,29] or cooling the SCF.[16a,29,30] In other cases, is the product which precipitates from the reaction media.[31] Another type of separation processes are based on the use of a second solvent in which the catalyst or the products are soluble[21b,27b,32,33] on catalyst immobilization[34] and on a selective separation of the catalyst through membrane.[35]

Another possibility which has been taken into consideration is the use of other liquids together with compressed CO_2. In the mixture the liquid expands volumetrically forming a single phase gas-expanded liquid (GXL), above the bubble point curve but below the critical composition.[36] The properties of the resulting liquid phase are considerably different from those at atmospheric pressure. This phenomenon may have a positive effect in catalysis and it should be taken into consideration when the liquid and/or reactants occupy more than 5% of the reactor volume. Expanded liquids combine the beneficial properties of compressed gases (CO_2) and the solvent (or substrate), leading to a new class of tuneable solvents. Some of these advantages are raised solubility of gases and catalysts (solvent power), the possibility to work under milder pressures (tens of bars) compared to $scCO_2$ (hundreds of bars) and enhanced transport

General Introduction

rate. One example is found in oxidation reactions of substituted phenols and cyclohexene.[37]

Not all liquids expand equally in the presence of CO_2 pressure, as they have different ability to dissolve in CO_2. So, we can found liquids divided in three different classes depending on their ability to dissolve in CO_2. The first (class I) contains liquids which are not sufficiently soluble in CO_2 and therefore do not expand significantly and only change the acidity. One example of class I is water. The second (class II) includes liquids which dissolve in large amount in CO_2 and consequently expand greatly. Their expansion only depends on the mole fraction of CO_2 in the liquid phase. Examples of class II are common organic solvents such as hexane, methanol, etc. Finally, the class III are liquids which dissolve in moderate quantities, and then expand only moderately. Examples of class III are ionic liquids, liquid polymers and crude oils.[36]

1.4   C-C bond reactions using CO and CO₂

C-C bond formation is one of the key transformations in organic synthesis. Some C-C bond reactions involve the introduction of a molecule of carbon monoxide (CO)[38] or carbon dioxide (CO_2)[39] into substrates such as olefins, alkynes, alkyls and epoxides giving a wide variety of products. These processes include reactions such as hydroformylation, hydrocarboxylation, hydroesterification, carbonation, carboxylation and copolymerisation (Scheme 1.1) to obtain aldehydes, carboxylic acids, esters, polyketones, polycarbonates, cyclic carbonates, pyrones, lactames and other cyclic products. In this work we studied the copolymerisation reactions, which give as products polyketones and polycarbonates.
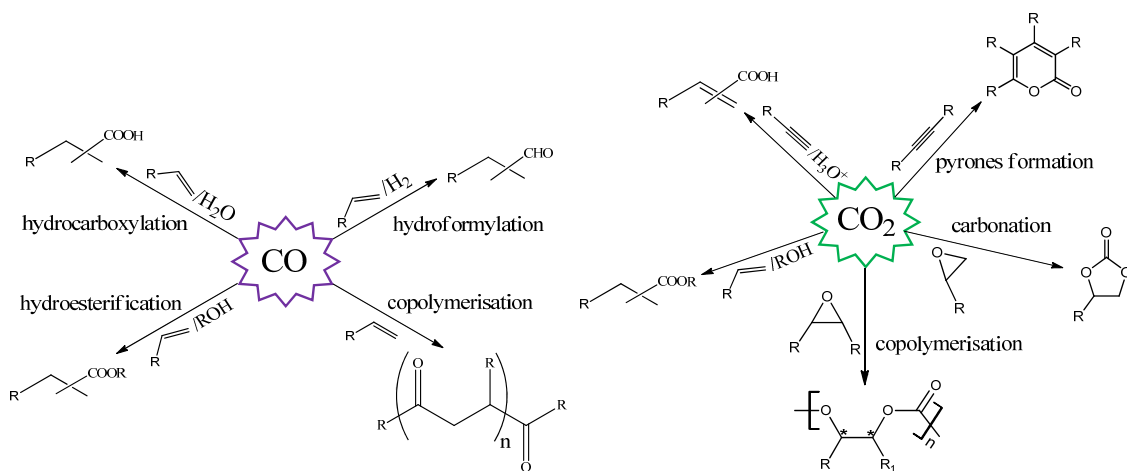
Scheme 1.1. C-C bond formation using CO and CO_2.

In the next sections we will focus on the copolymerisation reaction using CO or CO_2 as C_1 building block with olefins or epoxides, respectively.

1.4.1 Copolymerisation of CO/ vinyl arenes

Over the past years, the palladium catalyzed alternating copolymerisation of vinyl arenes and carbon monoxide yielding perfectly alternated polyketones (Scheme 1.2) has been the focus of great attention for four primary reasons. First, the monomers of most polyketones are readily available. Second, due to the carbonyl functionality in the polymer backbone, polyketones are photodegradable. Third, the carbonyl backbone also provides a possible mode for biodegradation. Finally, it is possible to introduce new functionality into the polymer chain by post-polymerization reactions with the carbonyl group.[40] Special interest has been devoted to palladium (II) based complexes with heterocyclic sp^2 nitrogen donor chelating ligands and weakly coordinating anions X (like OTs^-, OTf^-, BF_4^-, PF_6^- and tetraarylborates).[40c,41] The fine tuning of the palladium catalyst, mainly achieved by ligand variation, allows the control of the stereochemistry of the synthesized macromolecule[42] and the regiochemistry of the polyketone.[43] The family of 2,2'-bipyridine (bpy), 1,10-phenantroline (phen)[44] and pyridine-imidazoline[45] are ligands highly efficient in terms of productivity and molecular weight of the synthesized copolymers.
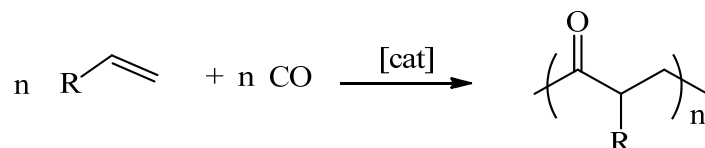
Scheme 1.2. Alternating copolymerisation of α-olefins with CO (R = H, CH$_3$, Ar).

The complexes generally used as precatalyst are mono [Pd(N-N)(CH$_3$)(L)][X] or dicationic compounds [Pd(N-N)$_2$][X]$_2$ characterized by the presence of one molecule of bidentate ligand, one methyl and one monodentate Lewis base (e.g. acetonitrile) or two molecules of bidentate ligands, respectively.[42a-c,46] The solvents commonly used are dichloromethane, methanol and 2,2,2-trifluoroethanol (TFE). In particular, it has been reported that, when the copolymerisation was carried out in TFE in place of methanol, the decomposition to inactive palladium was avoided due to its lower nucleophilicity allowing the synthesis of polyketones in high productivity and high molecular weight.[44e] Moreover, the influence of various counterions has also been investigated, with the result that the catalytic activity decreased in the order BArF$^-$ (B[3,5-

General Introduction

$(CF_3)_2C_6H_3]_4) > SbF_6^- / PF_6^- > BF_4^- > OTf^-$ (triflate) $>> BPh_4^-$. The strength of the interionic interactions has been shown to have a negative effect on the productivity of the catalyst.[44a]

1.4.1.1 *Ligands used*

The copolymerisation of styrene and its derivatives with CO requires the use of palladium (II) catalysts with N,N- or P,N-donor chelating ligands. Low molecular weight oligomers are in fact generally obtained with palladium catalysts stabilized by chelating diphosphines. The palladium nitrogen modified catalysts are long life catalysts compared to phosphorus modified catalysts, since β-H elimination does not prevail over propagation to polymer. In the following sections we will describe the different N,N- or P,N-donor ligands used in palladium catalysed CO/α-olefins copolymerisation and the results obtained as well as the effect in catalysis of the ligand's modification.

a) Nitrogen-donor ligands

Ligands containing sp^2-hybridized nitrogen atom, particularly when the N-atom is part of an aromatic system are the most applied in copolymerisation of CO/ vinyl arenes. Acetonitrile is also commonly used in copolymerisation, due to its lability, which lead to its replacement by the substrate.

In general nitrogen ligands in organometallic chemistry can form strong σ bonds to the metal centre and π interactions are also possible with ligands containing sp^2-hybridized N-donors. The strength of the M-N bond will be much more affected by steric effects than that of the corresponding M-P bonds. The N-donors, generally, in low-spin complexes are less thermodynamically stable and more kinetically labile than their analogous with P-donors. The strength of M-C bonds is directly related to the electron density of the metal centre. In this way, the organometallic complexes with N-ligands exhibit high reactivity.[41a]

The most effective catalytic systems are cationic palladium complexes with sp^2 nitrogen-chelating ligands (Figure 1.5) such as bipyridines (bpy, **6**),[42b,44b,44d,47-50] phenantrolines (phen, **7**),[42b,44c,44b,47-52] bisoxazolines (**8** and **9**),[53] pyridine-oxazoline (**10**, X=O and no R³),[54] pyridine-imidazoline (**10**, X=N, and **11**),[45,46a-b] pyridine-imine (**12**),[55] α-diimines (**13** and **14**)[42d,46c] or chiral diketimines (**15**)[56] and weakly coordinating anions.[41c]

Among these ligands, bpy and phen (**6** and **7**, respectively, Figure 1.5) provide very effective catalysts. The use of 2,2'-bipyridine and 1,10-phenantroline was reported for the first time by Shell, using palladium catalytic system for CO/styrene.[47] The first well-defined precatalyst was reported by Brookhart et al. in 1994, using a monocationic complex [Pd(CH$_3$)(NCCH$_3$)(N-N)][BArF] (N-N = **6** or **7,** Figure 1.5).[42b] Milani *et al.* found that dicationic bischelated complexes of general formula [Pd(N-N)$_2$][X]$_2$ efficiently catalysed the CO/styrene copolymerisation in methanol with no addition of acid or co-catalyst and in the presence of benzoquinone, despite they decomposed easily to palladium metal.[48]
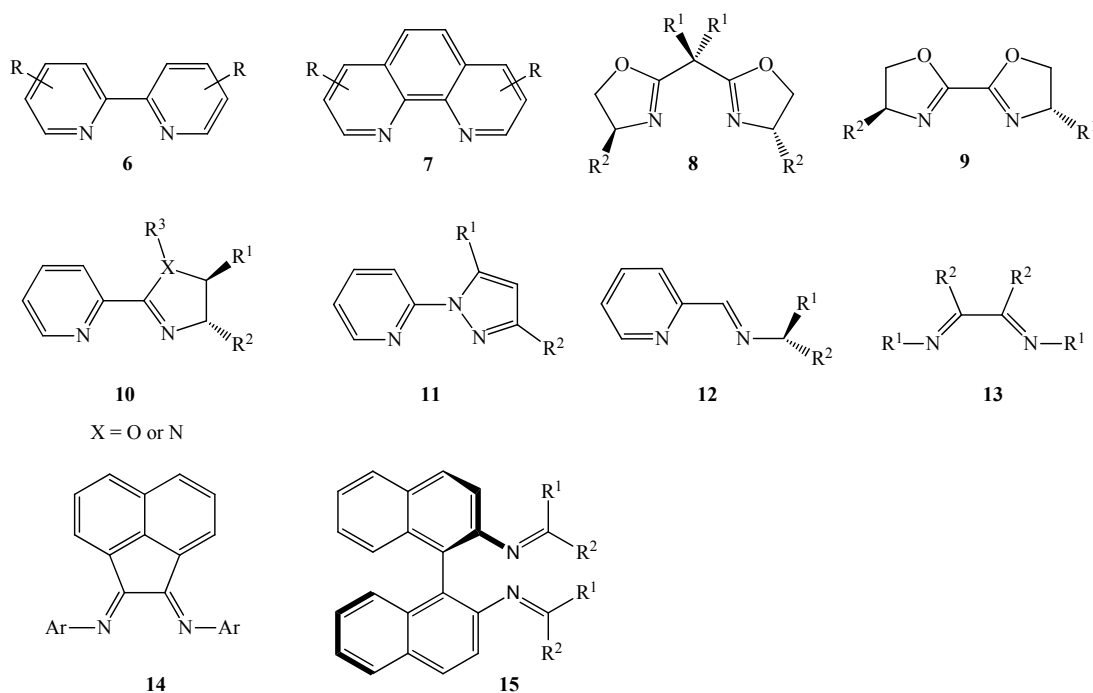
Figure 1.5. Nitrogen-donor ligands used in CO/vinyl arenes copolymerisation.

The analysis of the effect of the N,N-donor ligand showed that the bpy complex and phen derivative have similar activities. However, in the presence of 1,4-benzoquinone (BQ) the two catalysts showed different productivities, bpy showing higher activity due to the different stability of the corresponding active species.[44b] Moreover, studies of the substituent's effect, showed that methyl substituents in the 5,5' positions of bpy and the mono-substituted in 5 show slightly higher productivities (up to 11.5 kg CP/g Pd, in 14 h) and molecular weights (up to M$_w$ = 167000) compared to the non-substituted bpy.[44d] A similar observation was found with phen substituted in position 3 by an alkyl group (3-*R*-phen) the productivity and molecular weight values increased on increasing the bulkiness of the substituents.[44c,51] However, complexes

General Introduction

with phenanthroline substituted in position 2 and 9[52] and bipyridine in 6-[49] were inactive due to the presence of sterical demanding group in the *ortho* position. On the other hand, it was found that the addition of [(N-N)H][PF$_6$] as co-catalyst increased the productivity one order of magnitude. This effect was attributed both to the acidic function, as co-catalyst, and its capability to provide an additional stability to the active species, due to a ligand exchange reaction.[50]

The most significant result with catalyst containing C$_2$-symmetrical bisoxazolines (**8** and **9**, Figure 1.5) was that copolymers were obtained with highly isotactic microstructure (all stereogenic centres have the same configuration).[53] Nevertheless, they showed rather poor catalytic activity due to the quite fast decomposition of the catalyst to inactive palladium black.

Despite the chiral nature of the pyridine-dihydrooxazole ligands **10** (X=O and no R^3, Figure 1.5), all the copolymers synthesized show a prevailing syndiotactic microstructure (the stereogenic centres show alternated configuration) and was found that the nature of the group in position 5 (R^2) played a crucial role in this reaction. Moreover, catalyst stability was enhanced upon addition of free ligand.[54]

Pyridine-imidazoline ligands **10** (X=N, Figure 1.5) were characterized by the presence of different groups on the *sp^3*-nitrogen atom that were found to affect the stereochemistry of the complexes synthesized as well as their catalytic behaviour. Surprisingly, different tacticity were observed when *R,R*-ligand or *R,S*-ligand were used, showing syndiotactic copolymers with *R,R*-ligands and less basic *R,S*-ligands, and atactic (randomly distribution of configuration of the stereogenic centres) copolymer with basic *R,S*-ligands.[45,46b]

C$_s$-symmetry ligands with pyrazole moiety (**11**, Figure 1.5)[46a] showed again the important influence of the presence of substituents in the proximity of the nitrogen-donor atom. With these systems they were synthesized copolymers with syndiotactic microstructure. Even more, using Pd(II) pyridine-imine ligands (**12**, Figure 1.5)[55] was found that the syndiotacticity decreased with increasing the substituent's size.

α-Diimines (**13** and **14**, Figure 1.5)[42d,46c] with steric hindrance above and below the square planar coordination plane were used to demonstrate that polymerization required a free apical position on the palladium to produce regioregular copolymers, since with these substituents only small amount of atactic polyketones was formed.

Finally, highly syndiotactic copolymers with moderate productivities and high molecular weights were obtained with chiral diketimine ligands (**15**, Figure 1.5).[56]

b) Phosphorus-Nitrogen ligands

In P,N-donor ligands, the soft and hard nature of phosphorus and nitrogen are known to bind in a unique way, in which the phosphorus moiety acts only as a weak π-acceptor and the nitrogen moiety as a good σ-donor. The two binding modes are electronically different, which can lead to regioselectivity. They can act as hemilabile ligands by reversible dissociation of one arm of the ligand and thus favouring the formation and stabilization of intermediate species.[57] Owing to the different stereoelectronic properties of the two coordination sites they may induce selective processes, allowing control over the reactivity of the metal centre.

There are few P,N ligands tested in CO/α-olefins copolymerisation. The best results were obtained in CO/styrene or its derivatives copolymerisation. For example, Consiglio and Gsponer[58] reported the best results in terms of productivities for CO/styrene copolymerisation with the catalytic system $[Pd(\textbf{16b})(H_2O)_2][OTf]_2$ (Figure 1.6, productivity 84.8 g CP/g Pd·h and M_n = 13000, at 320 bars CO, 50ºC, with 40 equivalents of benzoquinone). The copolymer formed with this system presented unsaturated end-groups as a consequence of chain termination through β-H elimination. Ligands **17**,[59] **18**,[60] and **19**[61] (Figure 1.6) were applied in palladium catalysed CO/ethylene copolymerisation with moderate productivities (up to 357 g CP/g Pd in 6 h) with $[Pd(CH_3)(NCCH_3)(\textbf{17b'})][SbF_6]$.

When we focus on CO/styrene copolymerisation, the main studies are related to understand the stereoselectivity of the reaction.[62] Consiglio *et al.*[43] have reported that the nature of the phosphorus substituent in phosphine-oxazoline hybrid ligands **20** (Figure 1.6) strongly affects the stereoregularity of the CO/styrene polyketone. The regularity was found to decrease in the order of the phosphorus substituent phenyl > *p*-anisyl > *o*-anysil > *o*-tolyl (**20b**, **d-f**, Figure 1.6). Steric factors have been claimed to be more important than electronic factors in controlling the regioselectivity. It has been suggested, in fact, that the enantioface discrimination is determined within a complex showed in Figure 1.7 for which they assumed a site-selective coordination of the olefin and a secondary insertion for the incoming styrene unit. Steric repulsion between the

General Introduction

substituent R of the ligand and the Ph group of the substrate determines enantioface selection during chain growth.
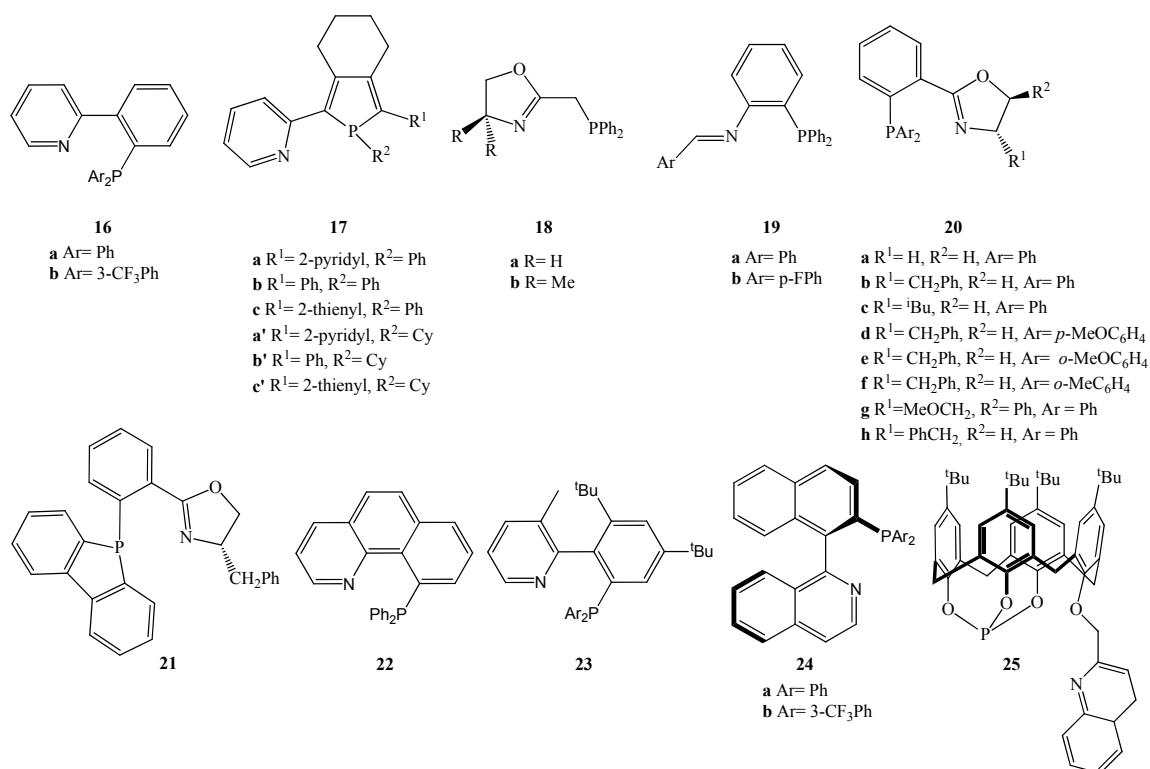
Figure 1.6. P-N reported ligands in CO/α-olefins copolymerisation.
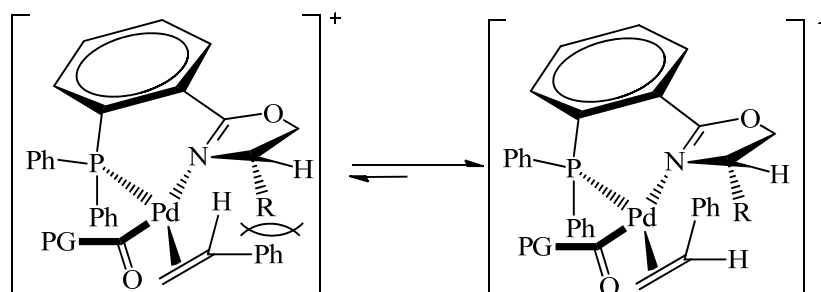
Figure 1.7. Representation of the olefin insertion in palladium complex with ligand **20**. GP = growing polymer chain.

In order to gain further insight into the factors responsible for the stereoregulation in CO/styrene copolymerisation, Consiglio and co-workers[54b] compared several P,N-donor palladium catalysts with its analogous complexes containing N,N-donor ligands. They used phosphino-oxazoline ligands L-L = **20g-h** in [Pd(L-L)(H$_2$O)$_2$][OTf]$_2$ (Figure 1.6). When P,N ligands were used a copolymer with *ll*-triad (isotactic) was obtained, while in the case of palladium complexes with the analogous pyridine-oxazoline ligands *uu*-triad (syndiotactic) were found. Therefore, the

isotactic selectivity observed with ligands **20g-h** was attributed to a pronounced site selective coordination, the olefins coordinate *trans* to the phosphorus atom.

The enantioselective terpolymerisation of ethene, styrene and CO has been achieved using [Pd(Me)(MeCN)(**21**)][OTf] (Figure 1.6).[63] They found a high enantioface selective catalytic system during styrene insertion independently of the last olefin unit.

As well, the catalytic systems studied with ligands **16**, **22-24** (Figure 1.6)[58] showed different stereoregulation yielding syndiotactic, isotactic and completely atactic copolymers, respectively. These differences in the enantioface discrimination behaviour were attributed to differences in the dihedral angle in the coordinated atropoisomeric ligands.

In a recent example a calyx[4]-based P,N-ligand **25** (Figure 1.6) was used for the palladium (II) catalysed CO/α-olefins copolymerisation.[64] Again, moderate productivities were shown (17 g CP/g Pd) in the CO/ethene copolymerisation, but the copolymerisation of CO with styrene did not lead to polyketones formation.

1.4.1.2 *Mechanism*

The first exhaustive mechanistic interpretation of the CO/ethene copolymerisation in methanol was reported by Drent et al. in 1991 (Scheme 1.3) using cationic palladium complexes with diphosphine ligands.[40,65] However, some of the kinetic and thermodynamic studies carried out in the following years have been done with dinitrogen ligands, in particular bpy, phen and bis(arylimino)acenaphtene (Ar-Bian).[66]

The proposed mechanism (Scheme 1.3) comprises two competing cycles (**A** and **B**) connected by two termination steps. The experimental conditions are the responsible to favour cycle **A** or cycle **B**. Cycle **A** initiates (**I**) with the insertion of CO in a Pd-OMe bond that generated a Pd-carbomethoxy complex, followed by alternating insertion of ethene and CO. Cycle **A** lead to copolymers with either keto-ester, diester or unsaturated olefin terminal structure. Depending on the termination step: protonolysis (**H**) of the Pd-alkyl intermediate give a keto-ester (**II**), the methanolysis (**M**) of the Pd-acyl group produce a diester (**III**) and the β-H elimination (**β**) of the Pd-acyl group give a unsaturated olefin (**IV**). On the other hand, cycle **B** initiates with the insertion of ethene in a Pd-H bond forming Pd-alkyl complex, followed by alternating insertion of

General Introduction

CO and ethene. This cycle leads also to keto-ester (**II**) by methanolysis (**M**) of a Pd-acyl bond. Moreover, via protonolysis (**H**) of Pd-alkyl bond are obtained diketones (**IV**) and it can be also formed unsaturated ketones (**VI**) by β-H elimination (**β**) of the Pd-alkyl.

Methanolysis (**M**) and β-H elimination (**β**) are competitive termination steps, and the experimental conditions favour one of both termination mechanisms.

Some catalytic experiments carried out at different conditions have shown palladium-hydride as the most probable initiator and methanolysis as the main termination step, when methanol is the solvent.[40]
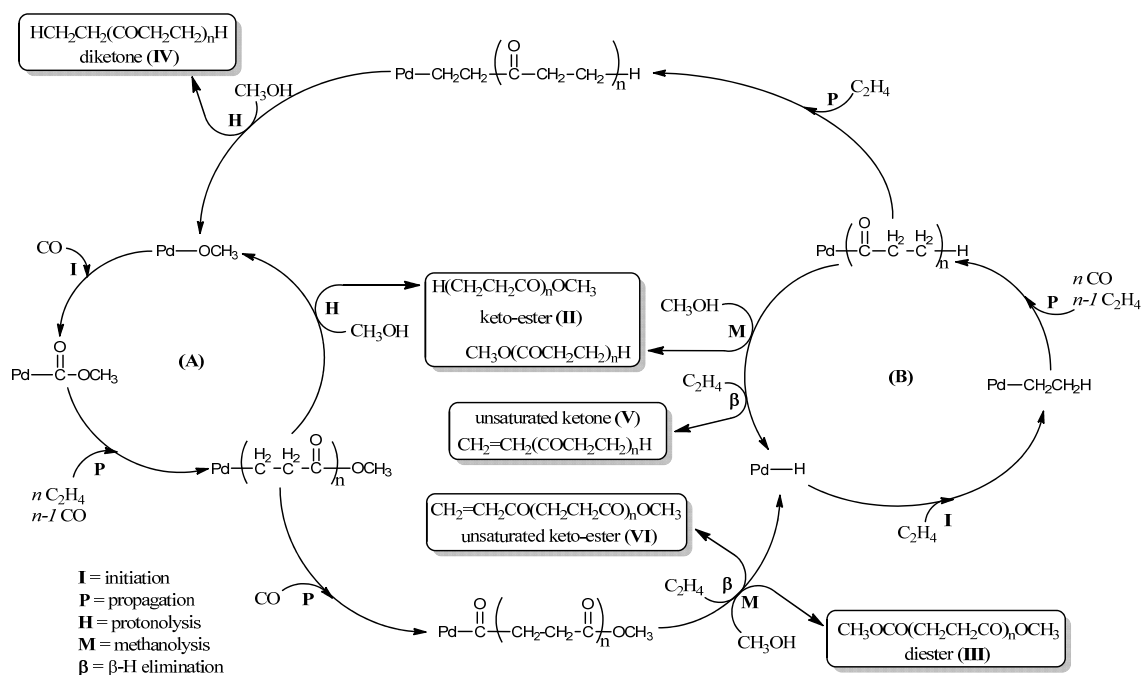
Scheme 1.3. Mechanism proposed for the copolymerisation of CO/alkenes.

The general features of the reaction mechanism discussed for the ethene copolymerisation are also valid for the CO/styrene copolymerisation with some differences explained in detail below.[40,41b,67]

a) Initiation and termination steps

The initiation and termination mechanisms can be determined by matrix-assisted laser desorption/ionization time-of-flight (MALDI-TOF) mass spectrometry, studying the copolymer end-groups. The initiation and termination steps are strongly dependent on the olefin co-monomer, on the bidentate ligand present in the palladium coordination sphere and on the reaction medium.[41c,44b,68]

The end groups of the polyketones synthesized in methanol indicates the presence of the initiation through the Pd-carbomethoxy pathway and the termination through an ester end-group. On the contrary, when the copolymers were obtained in a fluorinated alcohol, TFE, complete suppression of alcoholysis was achieved, β-hydrogen elimination being the only effective termination process, however, initiation through the insertion of TFE in Pd-H can be present.[68]

i. The role of oxidant promoter

The copolymerisation catalysts generally show a higher activity in the presence of added oxidants like quinones such as 1,4-benzoquinone (BQ) or 1,4-naphthoquinone (NQ). In copolymerisation reactions involving nitrogen ligands without an oxidant, Pd-H species drops out of the catalytic cycle by decomposition to Pd(0), which immediately precipitates as palladium black. It is known that the role of BQ is oxidizing the intermediate Pd(0) complexes to active Pd(II) species (Scheme 1.4).[40c]
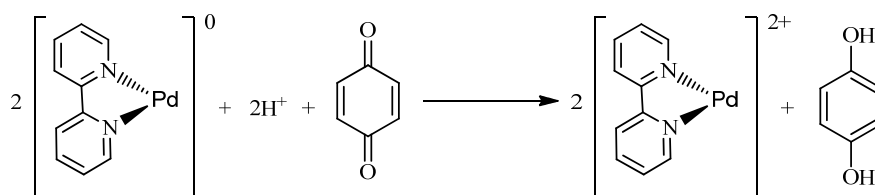
Scheme 1.4. The role of oxidant promoter.

In some cases the addition of an oxidant has as well negative effects, reducing the length of the polymeric chains because the hydroquinone (HQ) formed can produce alcoholisis.[68] Moreover, when bpy and phen containing catalyst are used in the presence of BQ, carbon monoxide become inhibiting: the productivity increases of almost 3 times when the CO pressure is decrease from 40 to 10 bars. Whereas, when no oxidant is present, CO is important for the catalyst stability and to obtain polyketones of high molecular weight.[41c,44b]

b) Propagation step

The propagation steps are identical in both ethene and styrene copolymerisation reactions and consist of two alternating reactions: migratory insertion of CO into the palladium-alkyl bond and migratory insertion of the olefin into the resulting palladium-acyl bond (Scheme 1.5). Propagation errors, like double carbonylation or double olefin insertion, are oddly observed. The propagation species consist of a cationic Pd(II)

General Introduction

complex stabilized by a bidentate nitrogen ligand containing the coordinated monomer and the growing chain in a reactive *cis*-arrangement forced by the *cis*-coordination of the chelating ligand. Carbon monoxide insertion is thought to be rapid and reversible,[69] while olefin insertion is the slowest (rate-determining) step in polyketones formation (species c_1 in Scheme 1.5).[66c,70]

In the propagation steps the species responsible for the regiochemistry and stereochemistry control are formed for alkenes different than ethene. The palladium intermediate present after the insertion of the olefin into the Pd-acyl bond is a five-membered metallacycle originated through the interaction with palladium of the growing chain and the last inserted carbonyl group (species d in Scheme 1.5). This metallacycle is considered to be responsible for the perfect alternation of the growing chain.[40] On the other hand, the palladium intermediated formed after the insertion of carbon monoxide into the Pd-alkyl bond is a six-membered metallacycle deriving from the interaction with palladium and the second last inserted carbonyl group of the growing chain (species b in Scheme 1.5), which is considered to be responsible for the efficient stereochemical control in CO/vinyl arenes copolymerisation.[71]
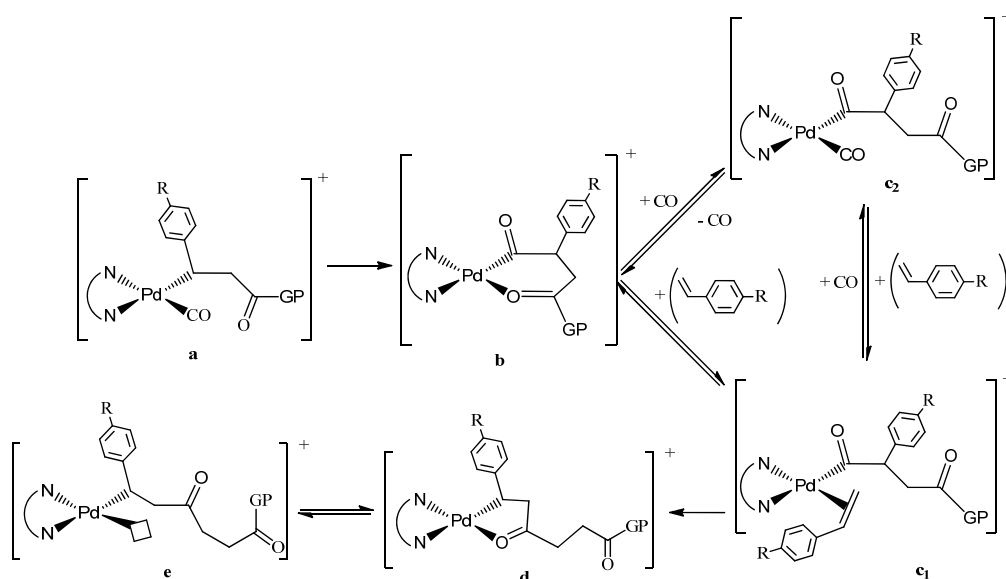
Scheme 1.5. Copolymerisation of CO/arenes propagation step. GP = Growing Polymer.

18

i. <u>Regiochemistry</u>

The olefin insertion into the polymer chain can take place in three different arrangements: head-to-head, head-to-tail and tail-to-tail (Figure 1.8*a*). If the chain growths with the same regioselectivity, primary (1,2-mode) or secondary (2,1-mode), the polymer should consist of solely head-to-tail units. The 2,1-insertion isomer could be stabilized by allylic coordination and the 1,2-isomer by β-aryl coordination (Figure 1.8 *b* and *c*).[42a]
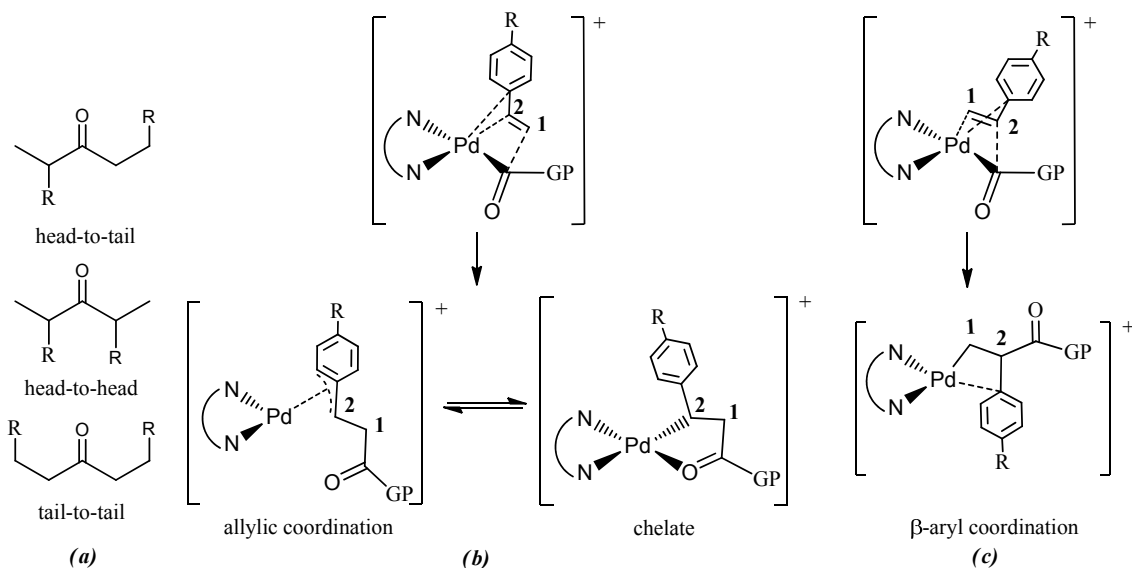
Figure 1.8. *(a)* regioselectivity of propagation (3 different arrangements) *(b)* 2,1-insertion isomers and *(c)* 1,2-insertion isomer.

Brookhart[42b,42a] has shown that after the 2,1-insertion, the product exists as a rapidly exchanging mixture of allylic (η^3-π-benzyl derivate) and chelated structure (Figure 1.8b) demonstrating that allylic coordination is quite strong, but chelated structure predominate over allylic coordination when N,N-donor ligands are used (at -80ºC in a ratio 3:1, respectively).[42a,66a] The η^3-π-benzyl derivative might be responsible for the fact that the copolymerisation does not proceed when complexes with diphosphine ligands are used, since it is suggested that the Pd-styryl intermediate formed is so strongly stabilized by η^3-π-benzyl (due to a better π back donation from Pd to CO) that this inhibits CO insertion and the η^3-π-benzyl species proceeded by β-H elimination leading the final product (E-1,5-diphenylpent-1-en-3-one).[72,73]

In the case of styrene, the olefin insertion takes place with a 2,1-mechanism and head-to-tail arrangement with all the N,N-donor ligands studied, while in the case of aliphatic olefins, regioregular and regioirregular polyketones can be obtained depending

General Introduction

on the nature of P,P-donor ligand.[40] Possibly, steric hindrance between the acyl group and the phenyl group in the 1,2-insertion transition state blocks the 1,2-regiochemistry. It could also be that interaction between the palladium atom and the phenyl ring during the insertion provides a lower energy insertion pathway.[40] However, two examples were found in the literature, where the styrene insertion takes place in a predominant 1,2-mechanism. It was firstly observed by Consiglio and co-workers using phosphine-oxazoline ligands (**20** and **21**, Figure 1.6)[43,63] and later by Nozaki *et al.*[46d] using the monocationic palladium (*R,S*)-BINAPHOS (complex **26a**, Figure 1.9).

26 **a** Ar = 3-((CH$_2$)$_2$-C$_6$F$_{13}$)C$_6$H$_4$
         b Ar = C$_6$H$_5$
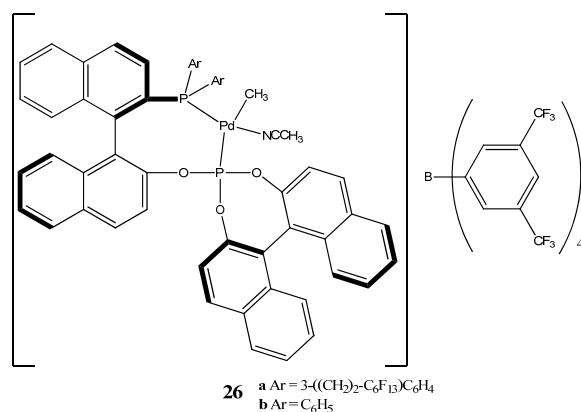
Figure 1.9. Monocationic palladium (*R,S*)-BINAPHOS complex (**26**).

ii. <u>Stereochemistry</u>

The stereochemistry of vinyl arenes insertion along the chain determines the copolymer tacticity: isotactic, syndiotactic or atactic (Figure 1.10). The relationship between two or three units in the copolymers is named *u* and *l*, for *unlike* and *like*, respectively. *Unlike* means that two subsequent centres have different absolute configurations, thus they form a *syndiotactic* polymer, while *like* means that they have the same configuration and thus they form an *isotactic* polymer.[67] The tacticity of the copolymers with olefin containing monomers is determined by the integration of the signals due to the *ipso* carbon atom for the CO/styrene polyketones and to the metylenic carbon atom both for the CO/methylstyrene and CO/*tert*butylstyrene copolymers in the ^{13}C NMR spectra (Figure 1.10b).

Two factors may be responsible for the control of the stereochemistry of copolymers. On one hand, the enantioselective environment created by the chiral ligand may control the stereoregularity of the vinyl arene insertion, which is known as *enantiosite control*, and this may lead to isotactic polymers. On the other hand, the

growing polymer chain, which is also chiral because of its successive stereogenic carbon centres, may lead to control the insertion of styrene. This control is known as *chain-end control*, and it can produce syndiotactic polymers.[62]
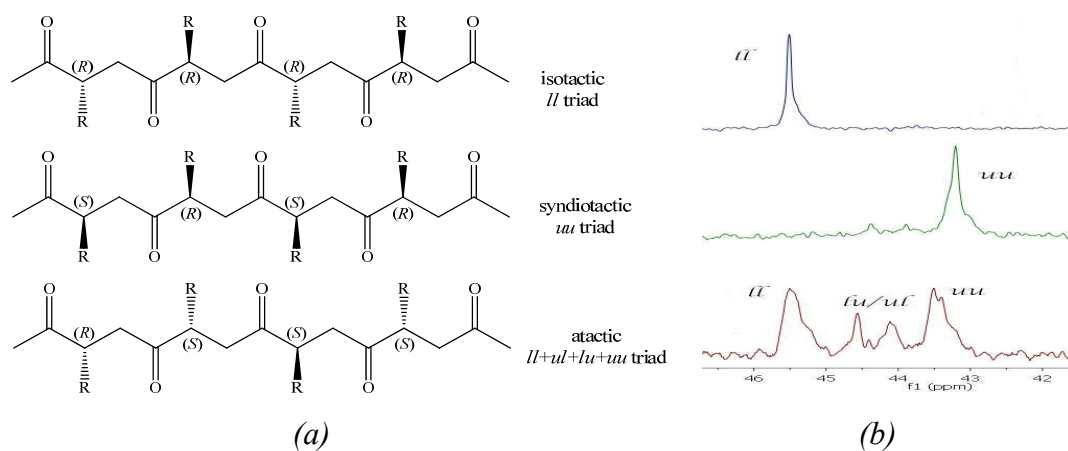
Figure 1.10. *(a)* Tacticity of CO/vinyl arenes copolymers. R = Ph or derivatives. *(b)* ^{13}C NMR spectra of methylene carbon atom-region of CO/TBS copolymers.

The symmetry of the ligand can play an important role in the stereochemistry of the copolymer. When C_2 (no enantiopure) and C_{2v} symmetric ligands are used, completely stereoregular syndiotactic copolymers can be obtained, for example α-diimine, 2,2'-bipyridine and 1,10-phenantroline ligands.[46c,74,75] Isotactic copolymers can be formed, if chiral C_2 symmetrical ligands are present and the site control is more effective than control by the chain-end.[56] For example, if enantiomerically pure C_2-symmetrical bisoxazoline ligands[42b,76] are present in the catalytic complex, only one enantiomer of the polymer may be obtained. However, in the case of C_1 and C_s ligands the relative influence of the enantiosite control and chain-end control cannot be predicted *a priori* and these ligands led to isotactic,[43a,54a,76,77] syndiotactic[51,54a,74] or even atactic copolymers.[43]

From the results reported in the literature,[68,76,78,79] it is clear that the control of the stereochemistry in the CO/α-olefins copolymerization reaction is not only related to the symmetry of the N-N ligand present in the palladium coordination sphere, but it is affected by other factors, such as the reaction medium, the anion, the nature of the precatalyst, and the ligand/palladium ratio.

General Introduction

1.4.1.3 *Copolymerisation of CO/alkenes in scCO$_2$*

Copolymerisation CO/vinyl arenes has scarcely been studied using scCO$_2$ as solvent, in contrast to other carbonylation reactions such as hydroformylation of 1-alkenes and vinyl arenes, which has been extensively studied in this medium.[15,80] There are only few examples described, which are shown below.

In 2000, Klaüi *et al.*[81] studied the first example of CO/ethylene copolymerisation in supercritical carbon dioxide. They used a catalytic system with nickel (II) associated to N,O-donor perfluorinated ligands (**27**, Figure 1.11) affording alternated copolymer in a yield of 11 kg CP / g Ni in 16 h.

27

R= Me, Ph, CF$_3$, C$_3$F$_7$, C$_7$F$_{15}$, OMe
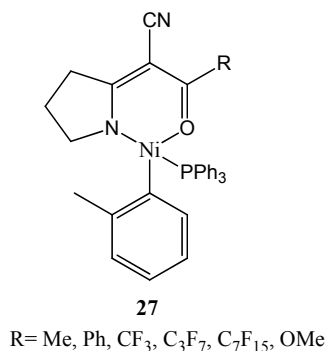
Figure 1.11. Nickel catalytic system for CO/ethene copolymerisation in scCO$_2$.

Later, Nozaki *et al.*[82] studied the copolymerisation of CO and ω-perfluoroalkyl-1-alkenes with a palladium(II) complex with (*R,S*)-BINAPHOS (**26a, b**, Figure 1.9 Figure 1.12) in CH$_2$Cl$_2$ and in scCO$_2$. They observed a 3% yield in perfluorinated copolymer (**28**, Figure 1.12) using the palladium catalytic system (**26b**, Figure 1.9) in scCO$_2$.

28
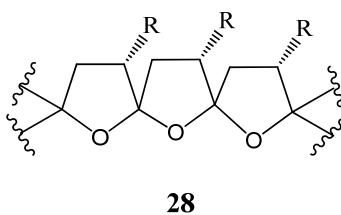
28a	R = CF$_3$
28b	R = CH$_2$C$_4$F$_9$
28c	R = CH$_2$C$_6$F$_{13}$
28d	R = CH$_2$C$_8$F$_{17}$
28e	R = CH$_2$CH$_2$C$_4$F$_9$
28f	R = CH$_2$CH$_2$C$_6$F$_{13}$

Figure 1.12. CO/perfluoralkyl-1-alkenes copolymers.

There is only one example of CO/*tert*-butylstyrene (TBS) copolymerisation in scCO$_2$. Giménez *et al.*[23] studied the reaction using perfluorinated bipyridines and phenanthrolines as ligands with a palladium system [Pd(CH$_3$)(NCCH$_3$)(N-N)][BArF] (**29**, Figure 1.13). They obtained better polydispersities (M$_w$/M$_n$ = 1.2) than in the organic solvents, with productivities up to 234 g CP/g Pd in 24 h and good molecular weight (M$_w$ = 87820).
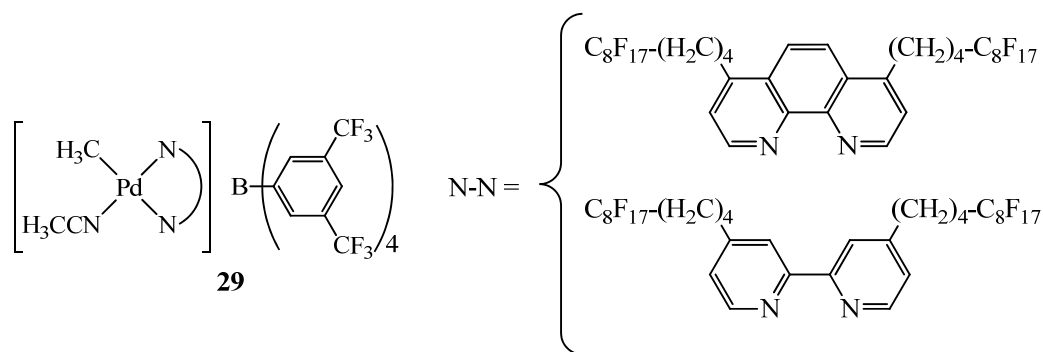
Figure 1.13. Palladium catalytic system for CO/TBS copolymerisation.

In this context, we found interesting the development of new copolymerisation catalysts adapted to be used in supercritical carbon dioxide.

1.4.2 Copolymerisation of epoxides and CO$_2$

In the recent years, polycarbonates became indispensable polymeric material, since they display promising characteristics. They have good biodegradability, they are highly transparent to visible light and have better light transmission characteristics than many kinds of glass, are hard, and moreover, they could be employed to develop other polymers.[83,84] For example, due to its properties polycarbonates are applied to eye-wear lenses, CDs manufacture, impact resistant sheets, electronic and automotive goods. Some important commercialized products are Makrolon® (Bayer) and Lexan® (General Electrics). The annual consumption for polycarbonates in 2002 was estimate to be in two million tones,[84,85] with an increasing foresight of *ca* 9% in the future years. The industrial production of polycarbonates involves the polycondensation of phosgene and diols (most commonly bisphenol A, Scheme 1.6).[86] It is well known that phosgene, however, is notorious for its high toxicity and corrosiveness. Since polycarbonate reduce environmental impact with its biodegradability properties, the development of synthetic procedures that reduce energy consumption, the use of renewable resources and avoiding the use of hazard products would lead to a completely green process.[87]

General Introduction
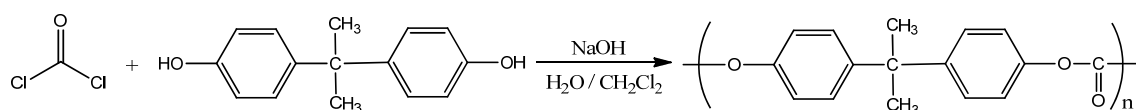
Scheme 1.6. Polycondensation reaction of phosgene and bisphenol A.

Carbon dioxide has been considered an attractive C_1 building block for producing *polycarbonates* (Scheme 1.7) by copolymerisation with epoxides because is an inexpensive, non-toxic and non-flammable gas.[83] Furthermore, since it is a *green house effect gas* the development of processes devoted to transform it could be an efficient way to reuse it. However, the thermodynamic stability of carbon dioxide has hampered its utility as a reagent for chemical synthesis. To overcome this limitation, reactions require the use of catalysts.[86] Nevertheless, the polycarbonate synthesis can lead to the formation of sub-products such as cyclic carbonates or the formation of ether linkage, due to the non-alternating introduction of CO_2.
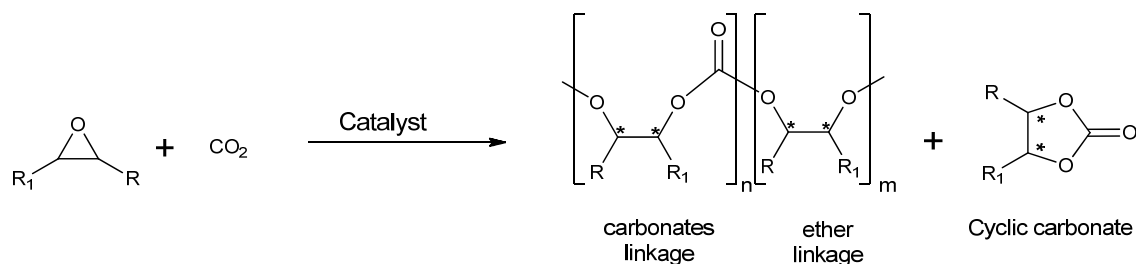
Scheme 1.7. General reaction of polycarbonates synthesis.

The first remarkable discovery was made by Inoue and co-workers in 1969, when they found that a mixture of $ZnEt_2$ and H_2O was active for catalysing the alternating copolymerisation of propylene oxide (PO) and CO_2, setting up the epoxides-CO_2 coupling chemistry.[86c,88] As a result, a significant amount of recent studies have been focused on the discovery and development of new catalysts and ligands for this process. Some example of these catalytic systems are based on alkoxides,[89] salen,[90] β-diiminates,[91] porphyrins[92] and pyridines[93,94] chelating ligands combined with active metals such as Al, Cr, Co, Mg, Li, Zn, Cu and Cd.[86] Studies have shown that large differences in catalytic efficacy result from the organic ligands coordinated to these metals, especially in the case of zinc.[86]

1.4.2.1 *Mechanism*

Epoxide-CO_2 copolymerisation mechanism is generally accepted to proceed by two main steps (Scheme 1.8*a*): the insertion of CO_2 into a metal alkoxide and the ring-opening of epoxide by backside attack of the resulting carbonate. Hence, most catalyst (polymerization initiators) are metal alkoxide or metal carboxylate species that are similar to the catalytic intermediates. A competitive mechanism starting with the growing polymer can explain the formation of cyclic species, which are common by-products (Scheme 1.8*b*). The enthalpically disfavoured consecutive insertion of two molecules of CO_2 to give dicarbonate linkages has not been reported.[83,86b]
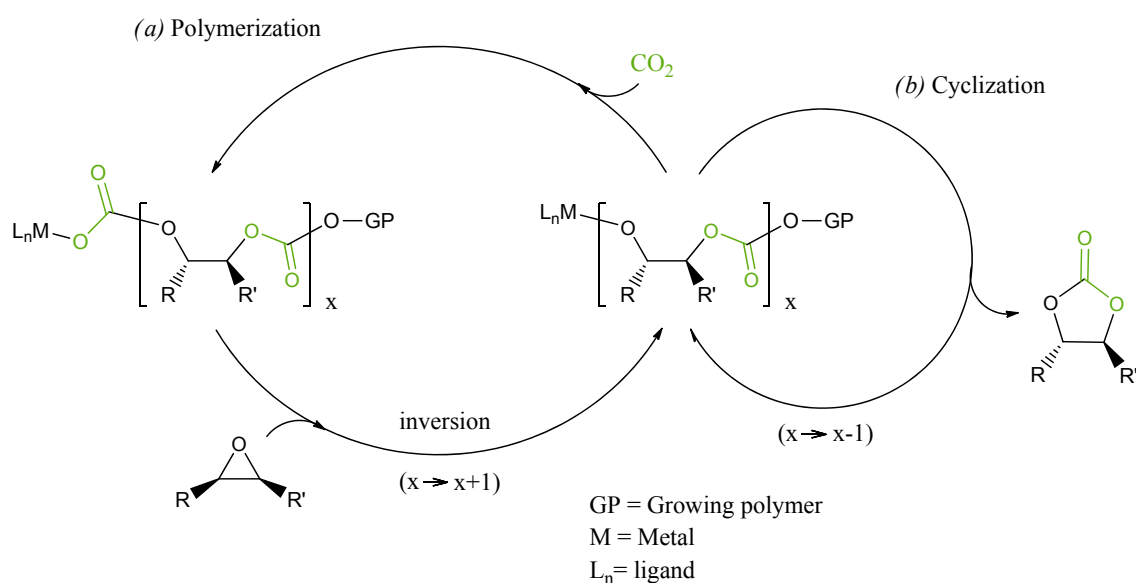
Scheme 1.8. The basic mechanism of epoxide-CO_2 copolymerisation and the formation of cyclic carbonates.[83,86b]

a) Regiochemistry

In the copolymerisation of carbon dioxide and unsymmetrically aliphatic epoxides, epoxide ring-opening is typically favoured at the least-hindered C-O bond, although cleavage is normally observed at both C-O bonds, giving regioirregular polymers.[83,86b]

b) Stereochemistry

In the copolymerisation of carbon dioxide and alicyclic epoxides, such as cyclohexene oxide, C-O bond cleavage typically occurs with inversion of configuration at the site of attack (bimolecular nucleophilic substitution, S_N2 type mechanism) generating *trans* 1,2 diol units (ring opened product). There are examples of stereocontrol by site- control mechanisms using chiral metal catalysts.[83,86b] In this case three different copolymers can be obtained: syndiotactic (*RSRSRS*), isotactic (*RRRR* o *SSSS*) and atactic (irregular distribution). As well as for the CO/vinyl arenes copolymerisation, the copolymer chain tacticity is determined by ^{13}C NMR spectroscopy analysing the carbonate region (δ 150 – 160 ppm). The model epoxide used is normally cyclohexene oxide (CHO). Three different carbonate ^{13}C resonances were observed at δ 153.7, 153.3 and 153.1 ppm, which were assigned to syndiotactic, atactic and isotactic, respectively.
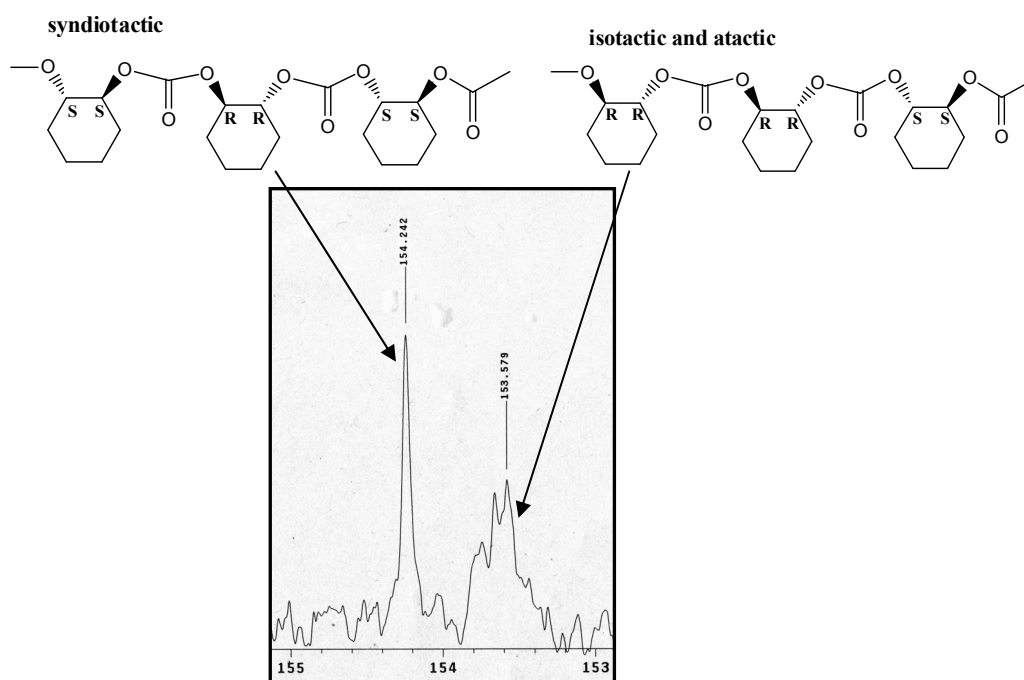
Figure 1.14. ^{13}C NMR spectrum of the carbonate region in a polychyclohexene carbonate (PCHC).

c) Polymer-cyclic selectivity

It is proposed that the formation of cyclic species is due to a backbiting mechanism (Scheme 1.9*a*) of a metal-alkoxide into an adjacent carbonate linkage, with the result of the *trans*-cyclic carbonate.[86a] Moreover, if halogens are presents, the *cis-*

cyclohexene carbonate can also be formed by a double inversion of the CHO carbon centre. As described by Kisch, first the nucleophilic attack of the halogen takes place and further attack of the metal-alkoxide gives the *cis*-cyclic carbonate (Scheme 1.9*b*).[95,96]

The percentage of polymer typically increases at lower reaction temperatures. Systems can be tuned to favour cyclic-species or polymer formation depending on the catalyst, additives, CO_2 pressure, epoxide concentration, and temperature.[83,86b]

The presence of cyclic species is analysed by FTIR, ^{1}H and ^{13}C NMR spectroscopy. Normally in CHO/CO_2 copolymerisation, FTIR is used only to determine if there is cyclic species, which show in methylene chloride a $v(CO_2)$ stretching vibration at 1803 cm^{-1} and 1793 cm^{-1} (*trans* and *cis* isomer, respectively) while the asymmetric $v(CO_2)$ stretching vibration of the polycarbonate linkage was observed at 1750 cm^{-1}. The percentage of polycarbonate selectivity versus cyclic carbonate was calculated from the relative intensities of the ^{1}H NMR signals of the methylene protons next to the carbonate linkage, δ 4.60 ppm for polycyclohexanecarbonate and δ 3.9 and 4.7 ppm for *trans*- and *cis*-cyclic cyclohexane carbonate, respectively.[97]
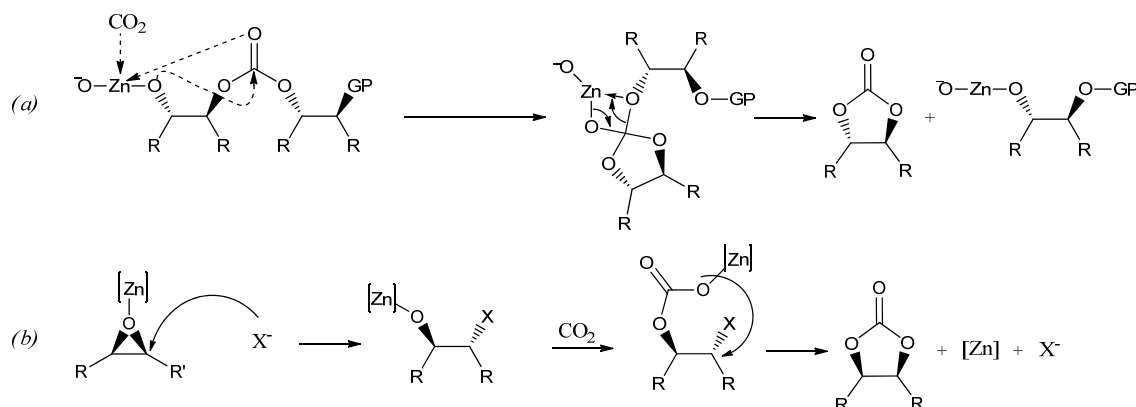
Scheme 1.9. *a) Trans*-cyclic carbonate formed by backbiting mechanism.[86a] *b)* Proposed mechanism for *cis*-cyclic carbonate formation, where X$^-$ is an halogen atom.[95]

d) Polymer degradation

The degradation of the growing polycarbonate chain leads to low molecular weight polymers and low intrinsic viscosity. It was suggested to occur via polymer degradation (Scheme 1.10) and by backbiting mechanism (Scheme 1.9*a*).

General Introduction

The polymer degradation mechanism was reported by Kuran and Listos for the degradation of polypropylene carbonate with a catalysts containing active phenolatozinc species.[98] The presence of high concentrations of catalyst resulted in the incorporation of the fenolate moiety into the chain as an end group of the polymer (Scheme 1.10).
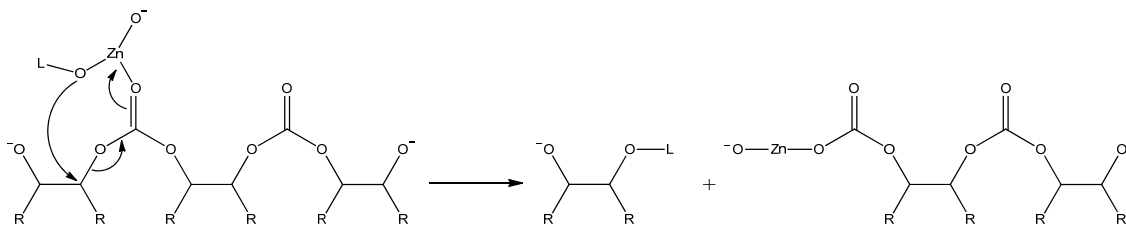
Scheme 1.10. Polymer degradation.

e) <u>Ether and dicarbonate linkages</u>

The presence of ether linkage as a result of consecutive epoxide enchainment can be observed in some aliphatic polycarbonates (Scheme 1.7). The polycarbonate and polyether linkages in a polymer can be determined by ^{1}H NMR. The percentage of carbonate linkage in the purified polymer was calculated from the relative intensities of the ^{1}H NMR signals in polycyclohexanecarbonate of the methylene protons next to the carbonate linkage ($\delta = 4.60$ ppm) and ether linkage ($\delta = 3.45$ ppm).[97]

Most systems can be tuned to favour CO_2 incorporation by catalyst selection, CO_2 pressure, epoxide concentration, and polymerization temperature.

1.4.2.2 *Zinc as catalyst*

Darensbourg and Holtcamp reported in 1995 the first discrete zinc complexes for the alternating copolymerisation of epoxides and CO_2.[89a] Based on this discovery different families of zinc catalytic systems were developed.

a)   The first family was the zinc dimeric phenolates, studied by Darensbourg *et al.*[89] (**30**, Figure 1.15), which promoted CO_2/CHO copolymerisation efficiently. At temperature of 80 ºC and 55 bars, this catalyst exhibits a productivity of 790 g PCHC/ g Zn (averaged productivity = 16.5 g PCHC/g Zn·h). Investigations on the steric influence and electronic density of *O*-aryl substituents were performed illustrating that bulky *ortho* substituents were not essential for high copolymerisation rates and electron-withdrawing groups resulted in higher activities (F > Cl > Br). This was related with the

increasing of the complex electrophilicitiy (the ability of the Zn to activate the epoxide).[89c,89d] Moreover, these ligands were likely to act as polymerization initiators. In combination to the monomeric zinc phenoxide complexes, the addition of phosphine derivates were studied.[89,99] The presence of phosphine ligands such as PCy_3 inhibited the homopolymerisation of CHO to polyether.

b)   The second group was the single-site β-diiminate (BDI) zinc catalysts, reported by Coates and co-workers[91] (**31** and **32**, Figure 1.15). The combination of the unsymmetrical ligand geometries and the electron withdrawing cyano substituent in **32** (Figure 1.15) yielded high active catalysts (an extremely high TOF of 2290 mol CHO consumed/mol Zn·h, estimated 5.0 kg PCHC/g Zn·h),[91d] polymers with narrow polydispersities (M_w/M_n = 1.1), although the molecular weights were moderate (M_n≈22000 g/mol). A positive effect was also observed with the introduction of electron withdrawal substituents in the ligands.[91e]

c)   The third family had as general structure $[L^nZn_2(OX)_n]$ (where X = Et, Ac and n = 1, 2) and L was based on N,N,O-Schiff base ligands (**33** and **34**, Figure 1.15).[100] Catalysts **33a** exhibited good activities (TOF = 142 mol CHO consumed/mol Zn·h, estimated 309 g PCHC/g Zn·h) under moderate conditions (only 20 bar of CO_2 and 80ºC), without any observation of ether linkage (M_n up to 21000 g mol^{-1} and with low polydispersity ratios, 1.3).[100a]

d)   The fourth family comprised the anilido-aldimine zinc complexes (**35**, Figure 1.15).[101] Complexes **35** showed high activity at diluted conditions ([Zn]/[CHO] = 1:16800). For example, complex **35d** exhibited high TON (up to 2980 mol CHO/mol Zn, estimated 6.5 kg PCHC/g Zn, in 15h, average TOF= 200 mol CHO/mol Zn·h, estimated. 434.8 g PCHC/g Zn·h) and the highest molecular weight polymers reported (M_n up to 284000), although, they presented some ether linkage (91% carbonate linkage) and broad molecular weight distribution (M_w/M_n = 1.7). This broad polydispersities could be related with high copolymerisation temperature (85-75ºC).[91e] This high activity at such low concentration of CHO was attributed to the fact that this kind of complexes favour an active dimeric species. In contrast to the mononucleating β-diketiminate ligands (**31** and **32**), which needed high zinc concentration to form dimeric active species. As was expected the introduction of fluorine atoms in the anilido ring (**35h**)[101b] gave the highest TOF (2860 mol CHO/mol Zn·h, 6.2 kg PCHC/g Zn·h).

General Introduction

33a-h R = Me

a Ar = Ph
b Ar = 4-MePh
c Ar = 3-MePh   **33i** Ar = Ph, R = NO$_2$
d Ar = 4-MeOPh   **33j** Ar = Ph, R = ^{t}Bu
e Ar = 4-PhPh
f Ar = 4-CF$_3$Ph
g Ar = 3,5-(CF$_3$)$_2$Ph
h Ar = ClPh

34

L^{n}Zn$_2$(OAc)$_2$

X = OAc

a n = 1, R = ^{t}Bu
b n = 2, R = Me
c n = 3, R = OMe

35a-g X = H

	a	b	c	d	e	f	g
R	^{i}Pr	Me	Me	Me	Et	Et	^{i}Pr
R'	^{i}Pr	Me	Me	^{i}Pr	Me	^{i}Pr	Et

35h X = F; R = Me; R' = ^{i}Pr
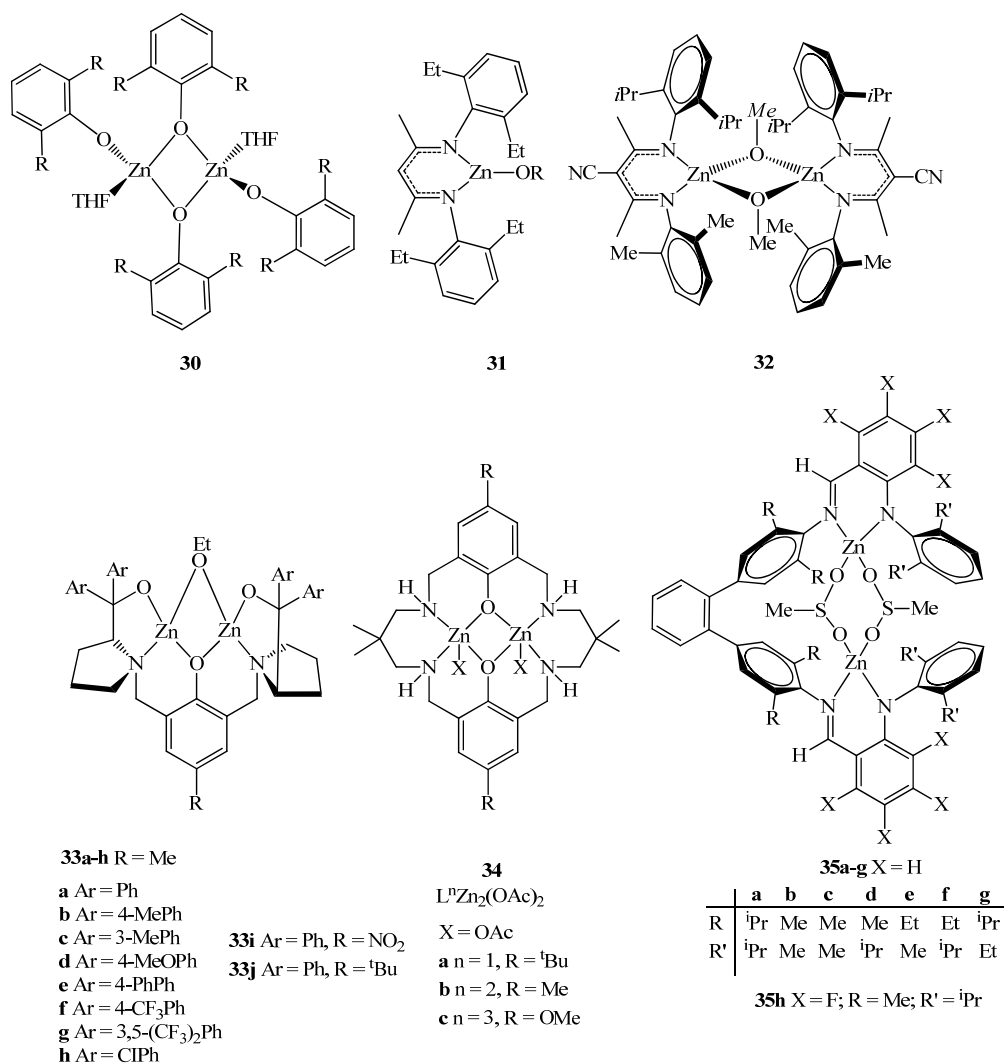
Figure 1.15. Example of copolymerisation zinc catalysts.

Coates and co-workers[91e] performed mechanistic studies on Zn-β-diiminate (BDI) catalytic systems and based on their results they proposed the mechanism shown in Scheme 1.11a. This mechanism depends on the precatalyst used. It was observed that BDI zinc acetates reacted at the beginning with CHO, while BDI zinc alkoxides reacted with CO$_2$. The molecular weight of the copolymer formed was determined by the ratio of CHO to Zn.

The zinc alkoxide monomer (**A**) or dimer (**A$_2$**) inserted CO$_2$ to yield either carbonate complexes (**B** in equilibrium with **B$_2$**) or an alkoxide/carbonate dimer (**AB**). **B$_2$** inserted CHO to yield **AB**, which subsequently reacted with CO$_2$ to complete one full catalytic cycle. **A$_2$**, **A**, and **AB** compounds did not react with CHO, and **B** and **B$_2$** did not react with CO$_2$. Moreover, the dimeric mechanism was proposed to exhibit an epoxide ring-opening transition state (Scheme 1.11b), where one zinc moiety

30

coordinated and activated the epoxide and the second zinc moiety delivered the carbonate propagating species to the back side of the *cis*-epoxide ring in a concerted fashion. *In situ* FTIR spectroscopy revealed zero-order dependence in CO_2 and first-order dependence in CHO. Thus, the insertion of CHO into a zinc carbonate was the rate-determining step. This mechanism suggests that various dimeric zinc complexes are the effective catalysts, although it can not be ruled out the possibility of a small contribution from a monometallic mechanism.
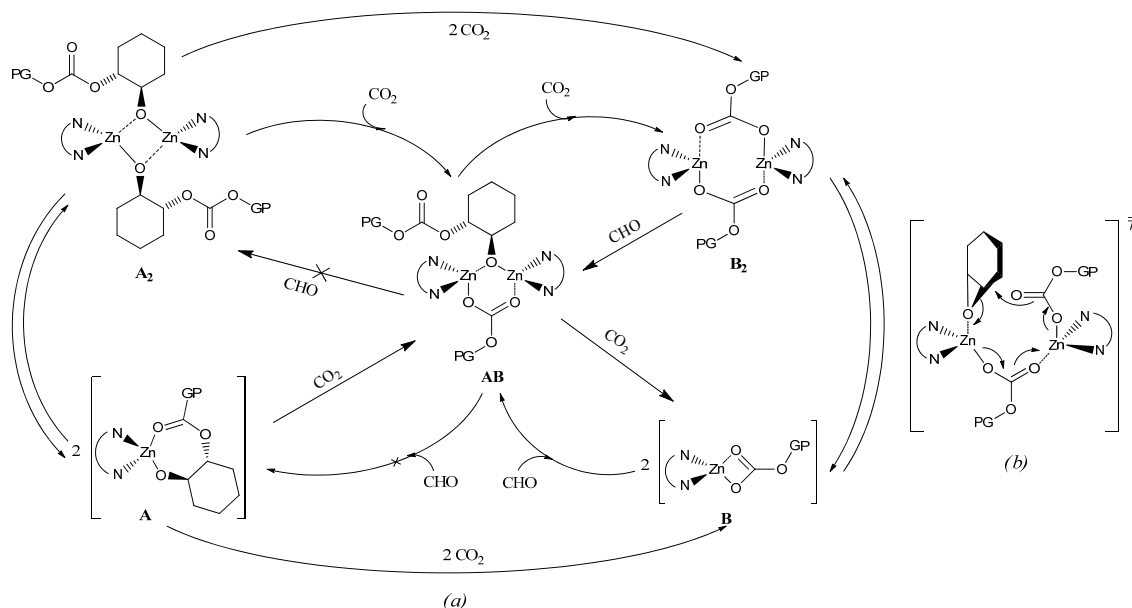
Scheme 1.11. Proposed *(a)* mechanism of copolymerisation *(b)* epoxide ring-opening transition state (CHO = cyclohexene oxide; GP = polymer chain).

e) Based on the necessity of two zinc metal centres for the copolymerisation reaction, some double metal complexes were proposed for the CHO/CO_2 copolymerisation (Figure 1.16). These compounds are double metal cyanide (DMC) with general formula $Zn_{1or3}[M(CN)_{4or6}]_{1or2} \cdot xZnX_2 \cdot yH_2O \cdot z$[complexing agent] and different compositions depending on the preparation methods. They were formed by reaction of ZnX_2 (X = Cl⁻, Br⁻ or I⁻), $K_3M(CN)_6$ (M = Co^III, Fe^III, Cr^III or Ir^III) or $K_2Ni(CN)_4$ and an organic complexing agent such as alcohols or ethers.[102] While most of these double metal compounds behave as heterogeneous catalysts, Zn-Fe cyanide complexes **36** and **37** (Figure 1.16) have a defined structure and presented different behaviour in copolymerisation.[102a] While complex **36** surprisingly provided exclusively the *cis* cyclic cyclohexene carbonate, complex **37** presented moderate activity for copolymer formation with 88% of carbonate linkage.[102a] Another example

General Introduction

was Zn-Ni double metal cyanide Zn[Ni(CN)$_4$], which was found to be moderate active in CHO/CO$_2$ copolymerisation, giving between 5.6 and 22.5 g PCHC/g of complex and low CO$_2$ incorporation (only 30% carbonate linkage).[102c] The newest DMC found is a Zn-Co species, with the typical formula Zn[Co(CN)$_6$]. This catalyst presented very high activity for alternating copolymerisation of cyclohexene oxide and carbon dioxide (TOF 3815 mol CHO consumed/ mol Zn·h^{-1} and 24.0 kg PCHC / g Zn). The PCHC formed was atactic with M$_n$ 10000 g·mol^{-1}, broad polydispersities (2.0 - 3.0) and presented low carbonate linkage (44-47%).[102d]

36

[CpFe(μ–CN)$_2$ZnI(THF)]$_2$(μ–dppp)

37

[CpFe(PPh$_3$)(μ–CN)$_2$Zn(2,6-OC$_6$H$_3$(*tert*-butyl)$_2$(THF)]$_2$
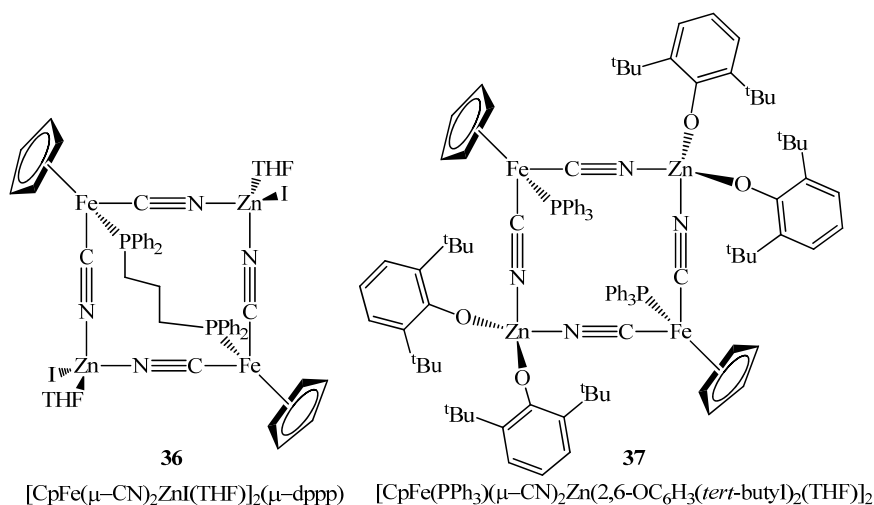
Figure 1.16. Example of double metal cyanide complexes for CHO/CO$_2$ copolymerisation.

a) <u>Asymmetric cyclohexene oxide-CO$_2$ copolymerisation</u>

When the ring-opening of a *meso*-epoxide proceeds with inversion at one of the two carbon centres with control of the absolute stereochemistry (by a chiral catalyst) optically active aliphatic polycarbonate with an (*R,R*)- or (*S,S*)-*trans*-1,2-diol unit can be formed. This microstructure can affect polymer properties[103] and this kind of copolymerisation are a potential route to obtain chiral building blocks.[104] Cyclohexene oxide (CHO), a *meso* molecule, is a model substrate for asymmetric alternating copolymerisation using chiral catalysts.

Nozaki *et al.*[105] described an active chiral catalytic system formed with the amino-alcohol ligand *(S)*-**38** (Figure 1.17) and ZnEt$_2$ that gave good results in terms of yield and enantiomeric excess in the copolymerisation CO$_2$/CHO. The polycarbonates contained a 100% of carbonate linkages (PCHC) and the hydrolysis of the polycarbonate produced the corresponding *trans*-cyclohexane-1,2-diol with 73%

enantiomeric excess. ^{13}C NMR spectroscopic studies of model polycarbonate oligomers afforded spectral assignments for isotactic dyads (153.7 ppm) and syndiotactic dyads (153.3-153.1 ppm).[106] In more recent literature, Nozaki *et al.* isolated the presumed intermediates consisting of a dimer (*(S,S)*-**38a**, Figure 1.17), which was structurally characterized by X-ray diffraction.[107] When the copolymerisation was attempted with *(S,S)*-**38a** and 0.2-1.0 equivalents EtOH were added, enantioselectivities increased up to 80% *ee* and better control of molecular weight and polydispersity resulted. End-group analysis by MALDI-TOF mass spectrometry and ^{1}H NMR spectroscopy revealed that in the absence of EtOH, signals assignable to the amino alcohol-initiated polymerization were identified. This was further confirmed by end-group analysis using ^{1}H NMR spectroscopy.[105-107] In 2005,[108] an exhaustive investigation of the dimeric zinc catalysts **38a** showed that the enantiomeric excess and activity obtained depended on the chiral structure of the dimeric complex. When racemic mixture of **38** was used, the copolymerisation had lower activity (29% yield). This was found to be due to the formation of a heterochiral zinc dimer *(R,S)*-**38a**, which was found to be more stable than its counterpart *(S,S)*-**38a** and consequently less active for copolymerisation.
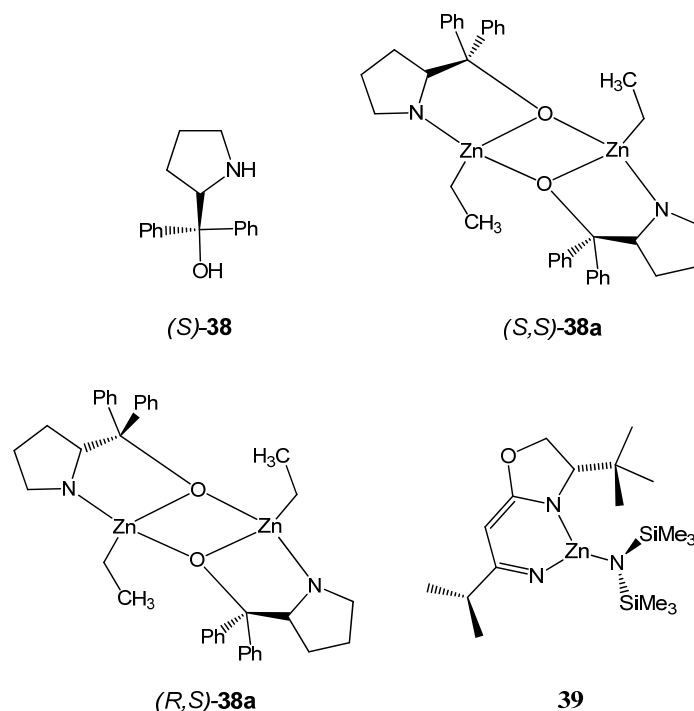
Figure 1.17. Chiral ligand and zinc catalysts for the asymmetric copolymerisation of CHO and CO_2.

General Introduction

In 2000, Coates and co-workers developed C_1-symmetric imine-oxazoline ligated zinc bis(trimethylsilyl)amido compound (**39**, Figure 1.17) for the steroselective, alternating copolymerisation of CHO and CO_2.[104] **39** was found to exhibit high enantioslectivity (*RR:SS* ratio=86:14; 72% *ee*). The resultant PCHC possessed 100% carbonate linkage and a M_n of 14700 g/mol with M_w/M_n of 1.35.

More recently, in 2005, the Trost's dinuclear zinc complex **33a** (Figure 1.15) was reported to exhibit good activity in the CO_2/CHO copolymerisation reaction, affording PCHC as the only product (>99% yield), with high M_n of 44100 g mol^{-1} and a relatively narrow polidispersity of 1.82 (M_w/M_n). Neverthless, the enantioselectivity only afforded a 18% ee with an *S,S* configuration of the cyclohexane-1,2-diol units.[100a]

1.4.2.3 *Copolymerisation of CO₂ and epoxides in scCO₂*

The copolymerisation of CO_2 has been also studied using compressed carbon dioxide (liquid or scCO$_2$) as a reactant and solvent.[14]

The first example was reported by Stevens *et al.*,[109] who performed the copolymerisation of ethylene oxide and CO_2 in the presence of polyhydric alcohols (for example ethylene glycol or glycerol) under supercritical conditions. However, the polymers formed had low molecular weight (up to 5000) and large sections of polyether linkage with only 3 to 10 % carbonate units.

In 1995, Darensbourg *et al.*[110] reported a zinc glutarate heterogeneous catalyst for propylene oxide (PO) and CO_2 copolymerisation, which presented a productivity between 8.0 and 34.8 g PC/ g Zn, high selectivity to carbonate linkage (up to 98%) and molecular weight (M_w up to 153000), although some cyclic carbonate (between 2-14%) was found.

Other example of zinc catalyst soluble in scCO$_2$ was reported by Beckman *et al.*[111] The catalytic system was based in ZnO and fluorinated derivative of maleic anhydride **40** (Figure 1.18) and produced alternating copolymer from carbon dioxide and cyclohexene oxide at supercritical conditions. The best results are summarized in entry 1 (Table 1.2). The average M_w obtained was in the range of 50000-180000. A very careful study of phase behaviour during the reaction revealed that the cyclohexene oxide-CO_2 binary system was the best choice for the effective copolymerisation because of favourable mass transfer and high reactant concentration in the same phase containing the catalyst.
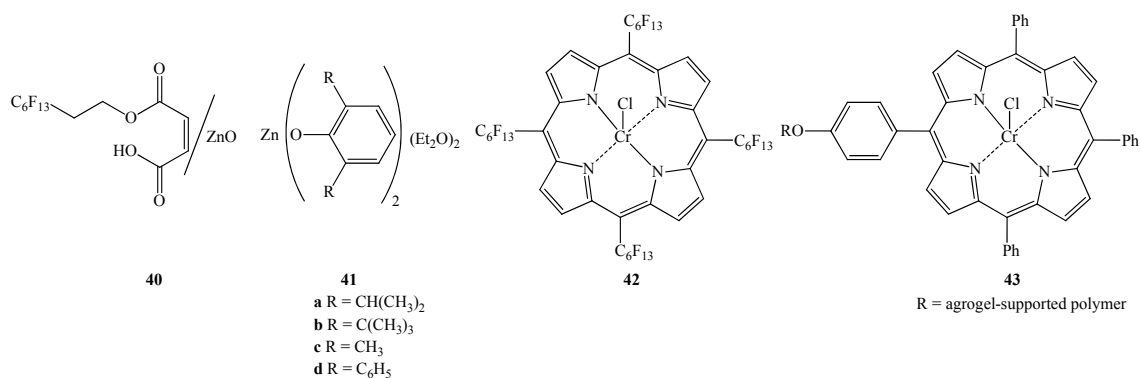
Figure 1.18. Catalytic systems for CHO/CO_2 copolymerisation in compressed CO_2.

When a CO_2 soluble monomeric bulky phenoxy Zn(II) catalyst (**41**, Figure 1.18)[89c,89] was used as an initiator, the copolymerisation of CO_2 and CHO at 80ºC and 50 bar produced over 400 g PCHC/g Zn (**41a**, R=CH(CH$_3$)$_2$, Figure 1.18). They observed that the catalytic activity was strongly influenced by the structure of the catalyst and the reaction conditions. The catalytic system **41c** containing isopropil groups showed the best result (entry 2, Table 1.2). In attempt to increase the productivity, the catalytic system **41d** was tested in scCO$_2$ but the productivity did not improve (entry 3 and 4, Table 1.2).

The chromium porphyrin complex with pentafluorophenyl substituents in the *meso*-position (**42**, Figure 1.18) were used in supercritical carbon dioxide as catalyst by Holmes and co-workers.[92b] **42** was found to be soluble in both liquid and scCO$_2$ at high pressures (70-215 bars) and moderate to high temperatures (20-80ºC). The best result from this system is shown in entry 5 (Table 1.2). The results were strongly temperature- and pressure-dependent. At low temperatures and at low CO_2 pressure, only oligomeric polyether formation was observed, while at higher temperatures or pressure, a significant decrease in yield and molecular weight was observed. It was found that depolymerisation processes led to significant weight loss.

The related similar chromium porphyrin catalyst (**43**, Figure 1.16)[112] was supported in a polymer. Under scCO$_2$ conditions this catalytic system showed > 90% carbonate introduction, low polydispersities (1.2 – 1.7), low molecular weights (M_n between 2200 – 7100) and better productivities than the previous chromium soluble porphyrin (**42**) up to 5.5 kg polymer /g chromium (entry 6, Table 1.2). Moreover, they successfully recycled the catalyst, although a decrease in molecular weight and productivity was observed.

Table 1.2. Copolymerisation of CO_2 and CHO catalyzed by Cr and Zn complexes in liquid CO_2 and $scCO_2$.

Entry	Cat.	Medium, bars	Temp. (^{o}C)	Time (h)	g PCHC/g M (g PCHC/g M h) [a]	M_w (M_w/M_n) [b]
1[111]	**40**	$scCO_2$, 136	110	24	457 (19)	109000 (6.4)
2[89c]	**41c**	CO_2, 50	80	69	1441 (21)	173000 (4.5)
3[89a,c]	**41d**	CO_2, 50	80	69	602 (9)	45000 (2.5)
4[89a,c]	**41d**	$scCO_2$, 139	80	69	357 (5)	n.r.
5[92b]	**42**	$scCO_2$, 230	110	18	3900 (217)	3930 (1.2)
6[112]	**43**	$scCO_2$, 170	90	24	5500 (229)	4290 (1.3)

[a] Average value calculated from the reported data. [b] determined by GPC relative to polystyrene standards. n.r. = not reported. M = metal used.

1.5   References

[1]   Anastas, P. T.; Warner, J. C.; *Green Chemistry: Theory and practice*, Oxford University Press, **1998**, New York (USA).

[2]   Anastas, P. T. (Ed.) and Crabtree R.H. (Ed.) *Handbook of Green Chemistry-Green Catalysis Vol. 1: Homogeneous Catalysis*, WILEY-VCH, **2009**, Weinheim (Deutschland).

[3]   Cole-Hamilton, D.J. and Tooze, R.P. *Catalyst separation, recovery and recycling*, Springer, **2006**, Dordrecht (The Netherlands).

[4]   Keim, W. *Green Chem.* **2003**, *5*, 105-111.

[5]   *(a)* Blanchard, L.A., Hâncu, D., Beckman, E.J. and Brennecke, J.F. *Nature* **1999**, *399*, 28-29. *(b)* Wasserscheid, P. and Keim, W. *Angew. Chem. Int. Ed.* **2000**, *39*, 3772-3798.

[6]   Pollet, P.; Hart, R.J.; Eckert, C.A. and Liotta, C.L. *Acc. Chem. Res.* **2010**, *43*, 1237-1245.

[7]   Jessop, P. G. and Leitner, W. *Chemical synthesis using supercritical fluids*, VCH, **1999**, Weinheim (Deutschland).

[8]   Jessop, G.P.; Ikariya, T. and Noyori, R. *Chem. Rev.* **1999**, *99,* 475-493.

[9]   Wu, B. C.; Klein, M. T.; Sandler, S. I., *Ind. Eng. Chem. Res.*, **1991**, *30*, 822-828.

[10] Sovová, H.; Procházka, J., *Ind. Eng. Chem. Res.*, **1993**, *32*, 3162-3169.

[11] *(a)* Sassiat, P. R.; Mourier, P.; Caude, M. H.; Rosset, R. H. *Anal. Chem.*, **1987**, *59*, 1164-1170. *(b)* Liong, K. K.; Wells, P. A.; Foster, N. R., *Ind. Eng. Chem. Res.*, **1992**, *31*, 390-399. *(c)* Catchpole, O. J., King, M. B., *Ind. Eng. Chem. Res.*, **1994**, *33*, 1828-1827.

[12] *(a)* Kaupp, G. *Angew. Chem. Int. Ed. Engl.* **1994**, *33*, 1452-1455. *(b)* Jessop, P. G.; Ikariya, T.; Noyori, R. *Science*, **1995**, *269*, 1065-1069.

[13] Leitner, W. *Acc. Chem. Res.* **2002**, *35*, 746 − 756.

[14] DeSimone, J. M.; Tumes, W. (Eds.), *Green Chemistry using liquid and supercritical carbon dioxide,* Oxford University Press, **2003**, New York (USA).

[15] Jessop, P.G. *J. Supercrit. Fluids* **2006**, *38*, 211-231.

[16] *(a)* Kainz, S.; Koch, D.; Baumann, W. and Leitner, W. *Angew. Chem. Int. Ed. Engl.* **1997**, *36*, 1628-1630. *(b)* Koch, D. and Leitner, W. *J. Am. Chem. Soc.* **1998**, *120*, 13398-13404. *(c)* Osswald, T.; Schneider, S.; Wang S. and Bannwarth, W. *Tetrahedron Letters* **2001**, *42*, 2965–2967 *(d)* Giménez-Pedrós, M.; Masdeu-Bultó, A.M.; Bayardon, J. and Sinou, D. *Catal. Lett.* **2006**, *107*, 205-208. *(e)* Tortosa-Estorach, C. and Masdeu-Bultó, A.M. *Catal. Lett.* **2008**, *122*, 76–79. *(f)* Tortosa-Estorach, C.; Orejón, A.; Ruíz, N.; Masdeu-Bultó, A.M. and Laurenczy, G. *Eur. J. Inorg. Chem.* **2008**, 3524–3531.

[17] *(a)* Lagalante, A.F.; Hansen, B.N.; Bruno, T.J. and Sievers, R.E *Inorg. Chem.* **1995**, *34*, 5781-5785. *(b)* Hu, Y.; Chen, W.; Xu, L. and Xiao, J. *Organometallics* **2001**, *20*, 3206-3208.

[18] *(a)* Jessop, P.G.; Hsiao, Y.; Ikariya, T. and Noyori, R. *J. Am.Chem. Soc.* **1996**, *118*, 344-355. *(b)* Back, I. and Cole-Hamilton, D.J. *Chem. Commun.* **1998**, 1463-1464. *(c)* Early, T.R.; Gordon, R.S.; Carroll, M.A.; Holmes, A.B.; Shute, R.E. and McConvey, I.F. *Chem. Commun.* **2001**, 1966-1967. *(d)* Sellin, M. F.; Bach, I.; Webster, J. M.; Montilla, F.; Rosa, V.; Avilés, T.; Poliakoff, M.; Cole-Hamilton, D. J. *J. Chem. Soc., Dalton Trans.* **2002**, 4569-4576.

[19] *(a)* Rathke, J.W.; Klingler, R.J. and Krauser, T.R. *Organometallics* **1991**, *10*, 1350-1355. *(b)*Warzinski, R.P.; Lee, C-H. and Holder, G.D. *J. Supercrit. Fluids* **1992**, *5*, 60-71.*(c)* Montilla, F.; Clara, E.; Avilés, T.; Casimiro, T.; Aguiar Ricardo, A and Nunes da Ponte, M. *J. Organomet. Chem.* **2001**, *626*, 227-232. .

[20] *(a)* Montilla, F.; Rosa, V.; Prevett, C.; Avilés, T.; Nunes da Ponte, M.; Masi, D.: Mealli, C. *Dalton Trans*. **2003**, 2170-2176. *(b)* Montilla, F.; Galindo, A.; Rosa, V.; Avilés, T. *Dalton Trans*. **2004**, 2588-2592. *(c)* Montilla, F.; Galindo, A.; Andrés, R.; Córdoba, M.; de Jesús, E. and Bo, C. *Organometallics* **2006,** *25,* 4138-4143. *(d)* Rodríguez, L-I.; Rossell, O.; Seco, M.; Orejón, A. and Masdeu-Bultó, A.M. *J. Organomet. Chem.* **2008**, *693*, 1857-1860. *(e)* Rodríguez, L-I.; Rossell, O.; Seco, M.; Orejón, A. and Masdeu-Bultó, A.M. *J. Supercrit. Fluids* **2011**, *55*, 1023-1026.

[21] *(a)* Bhanage, B.M.; Ikushima, Y.; Shirai, M. and Arai, M. *Chem. Commun.* **1999**, 1277-1278. *(b)* Jacobson, G.B.; Lee, C.T.; Jr., Johnston, K.P. and Tumas, W. *J. Am. Chem. Soc.* **1999**, *121*, 11902-11903. *(c)* Bonilla, R.J.; James, B.R. and Jessop, P.G. *Chem. Commun.* **2000**, 941-942. *(d)* Tortosa-Estorach, C.; Ruíz, N. and Masdeu-Bultó, A.M. *Chem. Commun.* **2006**, 2789-2791. *(e)* Tortosa-Estorach, C.; Giménez-Pedrós, M.; Masdeu-Bultó, A.M.; Sayede, A.D. and Monflier, E. *Eur. J. Inorg. Chem.* **2008**, 2659–2663.

[22] Beckman, E.J. *J. Supercrit. Fluids* **2004**, *28*, 121-191.

[23] Giménez-Pedrós, M.; Tortosa-Estorach, C.; Bastero, A.; Masdeu-Bultó, A. M.; Solinas, M.; Leitner, W. *Green Chem.* **2006**, *8*, 875-877.

[24] *(a)* Franciò, G. and Leitner, W. *Chem. Commun.* **1999**, 1663-1664. *(b)* Berthod, M.; Mignani, G. and Lemaire, M. *Tetrahedron: Asymmetry* **2004**, *15*, 1121–1126.

[25] Wu, X.-W.; Oshima, Y. and Koda, S. *Chem. Lett.* **1997**, 1045-1046.

[26] Bastero, A.; Franciò, G.; Leitner, W.; Mecking, S. *Chem. Eur. J.* **2006**, *12*, 6110-6116.

[27] *(a)* Palo, D.R. and Erkey, C. *Organometallics*, **2000**, *19*, 81-86. *(b)* Hâncu, D. and Beckman, E.J. *Green Chem.* **2001**, *3*, 80-86.

[28] *(a)* Burk, M.J.; Feng, S.G.; Gross, M.F. and Tumas, W. *J. Am. Chem. Soc.* **1995**, *117*, 8277-8278. *(b)* Cole-Hamilton, D.J. *Adv. Synth. Catal.* **2006**, *348*, 1341-1351.

[29] Kainz, S., Brinkmann, A., Leitner, W. and Pfaltz, A. *J. Am. Chem. Soc.* **1999**, *121*, 6421-6429.

[30] Nishikido, J., Kamishima, M., Matsuzawa, H. and Mikami, K. *Tetrahedron* **2002**, *58*, 8345-8349.

[31] He, L.N., Yasuda, H. and Sakakura, T. *Green Chem.* **2003**, *5*, 92-94.

[32] *(a)* Brown, R.A., Pollet, P., McKoon, E., Eckert, C.A., Liotta, C.L. and Jessop, P.G. *J. Am. Chem. Soc.* **2001**, *123*, 1254-1255. *(b)* Bösman, A., Franciò, G., Janssen, E., Solinas, M., Leitner, W. and Wasserscheid, P. *Angew. Chem. Int. Ed.* **2001**, *40*, 2697-2699. *(c)* Heldebrant, D.J. and Jessop, P.G. *J. Am. Chem. Soc.* **2003**, *125*, 5600-5601. *(d)* Solinas, M., Pfaltz, A., Cozzi, P.G. and Leitner, W. *J. Am. Chem. Soc.* **2004**, *126*, 16142-16247.

[33] McCarthy, M., Stemmer, H. and Leitner, W. *Green Chem.* **2002**, *4*, 501-504.

[34] Sowden, R.J., Sellin, M.F., De Blasio, N. and Cole-Hamilton, D.J. *Chem. Commun.* **1999**, 2511-2512.

[35] van den Broeke, L.J.P., Goetheer, E.L.V., Verkerk, A.W., de Wolf, W., Deelman, B.-J., van Koten, G. and Keurentjes, J.T.F. *Angew. Chem. Int. Ed.* **2001**, *40*, 4473-4474.

[36] *(a)* Jessop, P.G. and Subramaniam, B. *Chem. Rev.* **2007**, *107*, 2666-2694. *(b)* Akien, G.R. and Poliakoff, M. *Green Chem.*, **2009**, *11*, 1083–1100.

[37] Musie, G.; Wei, M.; Subramaniam, B. and Busch, D.H. *Coord. Chem. Rev.* **2001**, *219-221*, 789-820.

[38] Colquhoun, H.M.; Thompson, D.J. and Twigg, M.V. *Carbonylation*, Plenum Press, **1991**, New York (USA).

[39] *(a)* Braunstein, B.; Matt, D. and Nobel, D. *Chem. Rev.* **1988**, *88,* 747-764. *(b)* Leitner, W. *Coord. Chem. Rev.* **1996**, *153*, 257-284. *(c)* Okiaki, B. and Endo, T. *Prog. Polym. Sci.* **2005**, *30,* 183–215. *(d)* Riduan, S.N. and Zhang, Y. *Dalton Trans.*, **2010**, *39*, 3347-3357.

[40] *(a)* Sen, A. *Acc. Chem. Res.* **1993**, *26*, 303-310. *(b)* Drent, E. and Budzelaar, P.H.M. *Chem. Rev.* **1996**, *96*, 663-681. *(c)* Bianchini, C. and Meli, A. *Coord. Chem. Rev.* **2002**, *225*, 35–66. *(d)* Mark, H.F. (Ed.) *Encyclopedia of polymer science and technology*, John Wiley & Sons, **2003**, Hoboken (USA). *(e)* García Suárez, E. J.; Godard, C.; Ruiz, A.; Claver, C. *Eur. J. Inorg. Chem.* **2007**, 2582-2593.

[41] *(a)* Togni, A.; Venanzi, L. M. *Angew. Int. Ed. Engl.* **1994**, *33*, 497-526. *(b)* Sen, A., *Catalytic Synthesis of alkene-carbon monoxide copolymers and cooligomers*, Kluwer Academic Publishers, **2003**, Dordrecht (The Netherlands). *(c)* Durand, J.; Milani, B. *Coord. Chem. Rev.* **2006**, *250*, 542-560.

[42] *(a)* Brookhart, M.; Rix, F. C.; De Simone, J. M.; Barborak, C. J. *J. Am. Chem. Soc.* **1992**, *114*, 5894-5895. *(b)* Brookhart, M.; Wagner, M. I.; Balavoine, G. G. A.; Haddou, H. A. *J. Am. Chem. Soc.* **1994**, *116*, 3641-3642. *(c)* Brookhart, M.; Wagner, M. L. *J. Am. Chem. Soc.* **1996**, *118*, 7219-7220. *(d)* Carfagna, C.; Formica, M.; Gatti, G.; Musco, A.; Pierleoni, A. *Chem. Commun.* **1998**, *10*, 1113-1114.

[43] *(a)* Sperrle, M.; Aeby, A.; Consiglio, G.; Pfaltz, A. *Helv. Chim. Acta,* **1996**, *79*, 1387-1392. *(b)* Aeby, A.; Gsponer, A.; Consiglio, G. *J. Am. Chem. Soc.,* **1998**, *120*, 11000-11001.

[44] *(a)* Macchioni, A.; Bellachioma, G.; Cardaci, G.; Travaglia, M.; Zuccaccia, C.; Milani, B. Corso, G.; Zangrando, E.; Mestroni, G.; Carfagna, C.; Formica, M. *Organometallics* **1999**, *18*, 3061-3069. *(b)* Milani, B.; Corso, G.; Mestroni, G.; Carafagna, C.; Formica, M.; Seraglia, R. *Organometallics* **2000**, *19*, 3435-3441. *(c)* Scarel, A.; Milani, B.; Zangrando, E.; Stener, M.; Furlan, S.; Fronzoni, G.; Mestroni, G.; Gladiali, S.; Carfagna, C.; Mosca, L. *Organometallics* **2004**, *23*, 5593-5605. *(d)* Soro, B.; Stoccoro, S.; Cinellu, M. A.; Minghetti, G.; Zucca, A.; Bastero, A.; Claver, C. *J. Organomet. Chem.* **2004**, *689*, 1521-1529. *(e)* Scarel, A.; Durand, J.; Franchi, D.; Zangrando, E.; Mestroni, G.; Milani, B.; Gladiali, S.; Carfagna, C.; Binotti, B.; Bronco, S.; Gragnoli, T. *J. Organomet. Chem.* **2005**, *690*, 2106-2120. *(f)* Durand, J.; Zangrando, E.; Carfagna, C.; Milani, B. *Dalton Trans.* **2008**, 2171-2182.

[45] Bastero, A.; Claver, C.; Ruiz, A.; Castillón, S.; Daura, E.; Bo, C.; Zangrado, E. *Chem. Eur. J.* **2004**, *10*, 3747-3760.

[46] *(a)* Bastero, A.; Ruiz, A.; Reina J.A.; Claver, C.; Guerrero, A. M., Jalon, F. A.; Manzano, B. R. *J. Organomet. Chem.* **2001**, *619*, 287-292. *(b)* Bastero, A.; Ruiz, A. Claver, C. and Castillon, S. *Eur. J. Inorg. Chem.*, **2001**, *12*, 3009-3011. *(c)* Carfagna, C.; Gatti, G.; Martini, D.; Pettinari, C. *Organometallics*, **2001**, *20*, 2175-2182. *(d)* Nozaki, K.; Komaki, H.; Kawashima, Y.; Hiyama, T.; Matsubara, T. *J. Am. Chem. Soc.,* **2001**, *123*, 534-544.

[47] Drent, E. *Eur. Pat. Appl.* 229408, **1986**.

[48] Sommazzi, A.; Garbassi, F.; Mestroni, G.; Milani, B. *US Patent* 5310871, **1994.**

[49] Stoccoro, S., Alesso, G., Cinellu, M.A., Minghetti, G., Zucca, A., Bastero, A., Claver, C. and Manassero, M. *J. Organomet. Chem.* **2002**, *664*, 77-84.

[50] Santi, R., Romano, A.M., Garrone, R., Abbondanza, L., Scalabrini, M. and Bacchilega, G. *Macromol. Chem. Phys.* **1999**, *200*, 25-30.

[51] Milani, B., Scarel, A., Mestroni, G., Gladiali, S., Taras, R., Carfagna, C. and Mosca, L. *Organometallics* **2002**, *21*, 1323-1325.

[52] Milani, B., Alessio, E., Mestroni, G., Sommazzi, A., Garbassi, F., Zangrando, E., Bresciani-Pahor, N. and Randaccio, L. *J. Chem. Soc., Dalton Trans.* **1994**, 1903-1911.

[53] Binotti, B., Carfagna, C., Gatti, G., Martini, D., Mosca, L. and Pettinari, C. *Organometallics* **2003**, *22*, 1115-1123.

[54] *(a)* Aeby, A. and Consiglio, G. *Inorg. Chim. Acta* **1999**, *296*, 45-51. *(b)* Gsponer, A., Schmid, T.M. and Consiglio, G. *Helv. Chim. Acta* **2001**, *84*, 2986-2995.

[55] Jiang, Z., Adams, S.E. and Sen, A. *Macromolecules* **1994**, *27*, 2694-2700.

[56] Reetz, M.T., Haderlein, G. and Angermund, K. *J. Am. Chem. Soc.* **2000**, *122*, 996-997.

[57] Espinet, P. and Soulantica, K. *Coord. Chem. Rev.* **1999**, *193–195*, 499–556.

[58] Gsponer, A. and Consiglio, G. *Helv. Chim. Acta*, **2003**, *86*, 2170-2172.

[59] Sauthier, M., Leca, F., Toupet, L. and Réau, R. *Organometallics*, **2002**, 1591-1602.

[60] Braunstein, P., Fryzuk, M.D., Le Dall, M., Nand, F., Rettig, S.J. and Speiser, F. *J. Chem. Soc. Dalton Trans.* **2000**, 1067-1074.

[61] Reddy, K.R., Chen, C.-L., Liu, Y.-H., Peng, S.-M., Chen, J.-T. and Liu, S.-T. *Organometallics*, **1999**, *18*, 2574-2576.

[62] Milani, B. and Masdeu-Bultó, A.M. *Ligand Chirality in Palladium Catalysed Polyketone Synthesis*, in: Palyi, G.; Zucchi, C. and Cagliot (Eds.), L., *Organometallic Chirality*, Modena (Italy), Enrico Mucchi Editore S.R.L; **2008**, 161-203.

[63] *(a)* Aeby, A.; Bangerter, F.; Consiglio, G. *Helv. Chim. Acta* **1998**, *81*, 764-769. *(b)* Aeby, A. and Consiglio, G. *J. Chem. Soc. Dalton Trans.* **1999**, 655-656.

[64] Marson, A.; Ernsting, J.E.; Lutz, M.; Spek. A.L; van Leeuwen, P.W.N.M. and Kamer, P.C.J. *Dalton Trans.*, **2009**, 621–633.

[65] Drent, E., van Broekhoven, J.A.M. and Doyle, M. *J. Organomet. Chem.* **1991**, *417*, 235-251.

[66] *(a)* van Asselt, R., Gielens, E.G.C., Rulke, E.R., Vrieze, K. and Elsevier, C.J. *J. Am. Chem. Soc.* **1994**, *116*, 977-985. *(b)* Markiens, B.A., Kruis, D., Rietveld, M.H.P., Verkerk, K.A.N., Boersma, J., Kooijman, H., Lakin, M.T., Spek, A.L. and van Koten, G. *J. Am. Chem. Soc.* **1995**, *117*, 5263-5274.*(c)* Rix. F.C., Brookhart, M. and White, P.S. *J. Am. Chem. Soc.* **1996**, *118*, 4746-4764.

[67] van Leeuwen, P.W.N.M, *Homogeneous Catalysis: Understanding the art*, Kluwer Academic Publishers, **2004**, Dordrecht (the Netherlands).

[68] Scarel, A.; Durand, J.; Franchi, D.; Zangrando, E.; Mestroni, G.; Carfagna, C.; Mosca, L.; Seraglia, R.; Consiglio, G.; Milani, B. *Chem. Eur. J.* **2005**, *11*, 6014-6023.

[69] Brumbaugh, J.S. and Sen, A. *J. Am. Chem. Soc.* **1988**, *110*, 803-816.

[70] *(a)* Rix. F.C. and Brookhart, M. *J. Am. Chem. Soc.* **1995**, *117*, 1137-1138. *(b)* Rix. F.C., Brookhart, M. and White, P.S. *J. Am. Chem. Soc.* **1996**, *118*, 2436-2448.

[71] Consiglio, G. and Milani, B. *Stereochemical aspects of cooligomerization and copolymerization*, in: Sen A. (Ed.), *Catalytic Synthesis of Alkene-Carbon Monoxide Copolymers and Cooligomers*, Dordrecht (the Netherland), Kluwer Academic, **2003**, 189-215.

[72] Milani, B.; Paronetto, F. and Zangrando, E. *J. Chem. Soc., Dalton Trans.* **2000**, 3055-3057.

[73] Crascall, L.E. and Spencer, J.L. *J. Chem. Soc., Dalton Trans.*, **1992**, 3445-3452.

[74] Sen, A. and Jiang, Z. *Macromolecules* **1993**, *26*, 911-915.

[75] Milani, B., Anzilutti, A., Vicentini, L., Sessanta o Santi, A., Zangrando, E., Geremia, S. and Mestroni, G. *Organometallics* **1997**, *16*, 5064-5075.

[76] Gsponer, A.; Milani, B.; Consiglio, G. *Helv. Chim. Acta*, **2002**, *85*, 4074-4078.

[77] Nozaki, K., Sato, N. and Takaya, H. *J. Am. Chem. Soc.* **1995**, *117*, 9911-9912.

[78] Sirbu, D.; Consilio, G.; Milani, B.; Kumar, P. G. A.; Pregosin, P.S.; Gischig, S. *J. Organomet. Chem.,* **2005**, *690,* 2254-2262.

[79] Binoti, B.; Carfagna, C.; Zuccaccia, C.; Macchioni, A. *Chem. Commun.*, **2005**, 92-94.

[80] Bektesevic, S., Kleman, A.M., Marteel-Parrish, A.E. and Abraham, M.A. *J. Supercrit. Fluids*, **2006**, *38*, 232-241.

[81] Klaüi, W.; Bongards, J. and Reiβ, G.J. *Angew. Chem. Int. Ed.* **2000**, *39*, 3894-3896.

[82] Nozaki, K.; Shibahara, F.; Elzner, S. and Hiyama, T. *Can. J. Chem.* **2001**, *79*, 593-597.

[83] Coates, W.G. and Jeske, R.C. *Homogeneous catalyst design for the Synthesis of aliphatic polycarbonates and polyesters*, in: Anastas, P. T. (Ed.) and Crabtree R.H. (Ed.) *Handbook of Green Chemistry-Green Catalysis Vol. 1: Homogeneous Catalysis*, Weinheim (Deutschland), WILEY-VCH, **2009**, 343-373.

[84] *(a)* Allen, G. (Ed.) *Comprehensive Polymer Science,* Pergamon Press, **1989**, Oxford (UK); *(b)* Fried, J.R. *Polymer Science and Technology*, Prentice Hall, **1995**, Englewood Cliffs (USA).

[85] China Chemical Reporter, 16 Mayo 2002, [on line, http://goliath.ecnext.com/coms2/gi0199-1790647/Bright-prospect-for-the-polycarbonate.html]; Visit date: 28/01/2010.

[86] *(a)* Darensbourg, D. J. and Holtcamp, M. W. *Coord. Chem. Rev.*, **1996**, *153*, 155-174. *(b)* Coates, G. W.; Moore, D. R. *Angew. Chem. Int. Ed.* **2004**, *43*, 6618-6639. *(c)* Sugimoto, H. and Inoue, S. *J. Polym. Sci. Part A: Polym. Chem.* **2004**, *42*, 5561-5573. *(d)* Darensbourg, D.J.; Mackiewicz, R.M.; Phelps, A.L. and Billodeaux, D.R. *Acc. Chem. Res.*, **2004**, *37*, 836-844. *(e)* Zevenhoven, R.; Eloneva, S. and Teir, S. *Catal. Today* **2006**, *115*, 73-79. *(f)* Darensbourg, D.J. *Chem. Rev.* **2007**, *107*, 2388-2410.

[87] Anastas, P.T. and Williamson, T.C. *Green Chemistry: Designing Chemistry for Environment*, American Chemical Society, **1994**, Washington DC (USA).

[88] *(a)* Inoue, S., Koinuma, H. and Tsuruta, T. *J. Polym. Sci., Part B: Polym. Lett.* **1969**, *7*, 287-292. *(b)* Inoue, S., Koinuma, H. and Tsuruta, T. *Macromol. Chem.* **1969**, *130*, 210-220.

[89] *(a)* Darensbourg, D. J.; Holtcamp, M. W. *Macromolecules,* **1995**, *28,* 7577-7579. *(b)* Darensbourg, D. J.; Niezgoda, S. A.; Draper,J. D.; Reibenspies, J. H. *J. Am. Chem. Soc.* **1998**, *120,* 4690-4698. *(c)* Darensbourg, D. J.; Holtcamp, M. W.; Struck, G. E.; Zimmer, M. S.; Niezgoda, S. A.; Rainey, P.; Robertson, J. B.; Draper, J. D.; Reibenspies, J. H. *J. Am. Chem. Soc.* **1999**, *121,* 107-116. *(d)* Darensbourg, D. J.;Wildeson, J. R.; Yarbrough, J. C.; Reibenspies, J. H. *J. Am. Chem. Soc.* **2000**, *122,* 12487-12496. *(e)* Koning, C. E.; Wildeson, J.; Parton, R.;

General Introduction

Plum, B.;Steeman, P.; Darensbourg, D. J. *Polymer*, **2001**, *42,* 3995-4004.*(f)* Dinger, M. B.; Scott, M. J. *Inorg. Chem.* **2001**, *40,* 1029-1036.

[90] *(a)* Darensbourg, D.J. and. Yarbrough, J..C. *J. Am. Chem. Soc.*, **2002**, *124*, 6335-6342. *(b)* Cohen, C.T.; Thomas, C.M.; Peretti, K.L.; Lobkovsky, E.B. and Coates, G.W. *Dalton Trans.*, **2006**, 237-249. *(c)* Nakano, K.; Nakamura, M. and Nozaki, K. *Macromolecules* **2009**, *42*, 6972–6980.

[91] *(a)* Cheng, M.; Lobkovsky, E. B.; Coates, G. W. *J. Am. Chem. Soc.* **1998**, *120*, 11018-11019. *(b)* Cheng, M.; Moore, D. R.; Reczek, J. J.; Chamberlain, B. M.; Lobkovsky, E. B.; Coates, G. W. *J. Am. Chem. Soc.* **2001**, *23*, 8738-8749. *(c)* Allen, S.D.; Moore, D. R.; Lobkovsky, E. B.; Coates, G. W. *J. Am. Chem. Soc.* **2002**, *124*, 14284-14285. *(d)* Moore, D. R.; Cheng, M.; Lobkovsky, E. B.; Coates, G. W. *Angew. Chem. Int. Ed.,* **2002**, *41*, 2599-2602. *(e)* Moore, D. R.; Cheng, M.; Lobkovsky, E. B.; Coates, G. W. *J. Am. Chem. Soc.* **2003**, *125*, 11911-11924.

[92] *(a)* Kruper, W.J. and Dellar, D.V. *J. Org. Chem.* **1995**, *60*, 725-727. *(b)* Mang, S.; Cooper, A.I.; Colclough, M.E.; Chauhan, N. and Holmes, A.B. *Macromolecules*, **2000**, *33*, 303-308. *(c)* Inoue, S. *J. Polym. Sci. Part A: Polym. Chem.* **2000**, *38*, 2861-2871.

[93] Kim, H.S; Kim, J.J.; Lee, B.G.; Jung, O.S.; Jang, H.G. and Kang, S.O. *Angew. Chem. Int. Ed.,* **2000**, *39*, 4096-4098.

[94] Kim, H.S; Kim, J.J.; DeukLee, S.; Lah, M.S.; Moon, D. and Jang, H.G. *Chem. Eur. J.*, **2003**, *9*, 678-686.

[95] Dümler, W.; Kisch, H. *Chem. Ber.* **1990**, *123*, 277-283.

[96] Darensbourg, D. J.; Fang, C. C.; Rodgers, J. L. *Organometallics*, **2004**, *23*, 924-927.

[97] Darensbourg, D.J.; Lewis, S.J.; Rodgers, J.L. and Yarbrough, J.C. *Inorg. Chem.* **2003**, *42*, 581-589.

[98] Kuran, W. and Listos, T. *Macromol. Chem. Phys.*, **1994**, *195*, 1011-1015.

[99] Darensbourg, D. J.;Zimmer, M. S.; Rainey, P.; Larkins, D. L. *Inorg. Chem.* **2000**, *39,* 1578-1585.

[100] *(a)* Xiao, Y.; Wang, Z. and Ding, K. *Chem. Eur. J.* **2005**, *11*, 3668-3678. *(b)* Kember, M.R.; White, A.J.P. and Williams, C.K. *Inorg. Chem.* **2009**, *48*, 9535-9542.

[101] *(a)* Lee, B.Y.; Kwon, H.Y.; Lee, S.Y.; Na, S.J.; Han, S.; Yun, H., Lee, H. and Park, Y-W. *J. Am. Chem. Soc.* **2005**, *127*, 3031-3037. *(b)* Bok, T.; Yun, H. and Lee, B.Y. *Inorg. Chem.*, **2006**, *45*, 4228-4237.

[102] *(a)* Darensbourg, D.J.; Adams, M.J.; Yarbrough, C.J. and Phelps, A.L. *Inorg. Chem.* **2003**, *42*, 7809-7818. *(b)* Yi, M.J.; Byun, S-H.; Ha, C-S.; Park, D-W and Kim, I. *Solid State Ionics*, **2004**, *172*, 139-144. *(c)* Chen, S.; Xiao, Z. and Ma, M. *J. Appl. Polym. Sci.* **2008**, *107*, 3871-3877. *(d)* Sun, X-K.; Zhang, X-H.; Liu, F. Chen. S.; Du, B-Y.; Wang, Q.; Fan, Z-Q. and Qi, G-R. *J. Polym. Sci., Part A: Polym. Chem.* **2008**, *46*, 3128-3139. *(e)* Lee, I.K.; Ha, J.Y.; Cao, C.; Park, D-W., Ha, C-S. and Kim, I. *Catal. Today*, **2009**, *148*, 389-397.

[103] Nakano, K., Kosaka, N., Hiyama, T. and Nozaki, K. *Dalton Trans.* **2003**, 4039-4050.

[104] Cheng, M., Darling, N.A., Lobkovsky, E.B. and Coates, G.W. *Chem. Commun.* **2000**, 2007-2008.

[105] Nozaki, K; Nakano, K; Hiyama, T. *J. Am. Chem. Soc.* **1999**, *121*, 11008-11009.

[106] Nakano, K., Nozaki, K. and Hiyama, T. *Macromolecules*, **2001**, *34*, 6325-6332.

[107] Nakano, K; Nozaki, K; Hiyama, T. *J. Am. Chem. Soc.* **2003**, *125*, 5501-5510.

[108] Nakano, K., Hiyama, T. and Nozaki, K. *Chem. Comm*, **2005**, 1871-1873.

[109] Stevens, H.C. *US Patent*, **1963**, *3248415*. Pittsburg Plate Glass Company.

[110] Darensbourg, D.J.; Stafford, N.W. and Katsurao, T. *J. Mol. Catal. A: Chem.* **1995**, *104*, L1-L4.

[111] Super, M., Berluche, E., Costello, C. and Beckman, E. *Macromolecules* **1997**, *30*, 368-372.

[112] Stamp, L.M.; Mang, S.A.; Holmes, A.B.; Knights, K.A.; de Miguel, Y.R. and Mc Convey, I.F. *Chem. Commun.* **2001**, 2502-2503.

Chapter - 2

Objectives

2.1 Objectives

The aim of this thesis is to study two aspects of the CO_2 uses. In the first part the use of CO_2 as solvent will be explored. The objective of this part is the development of new catalysts designed to be used in compressed carbon dioxide (liquid or supercritical, $scCO_2$) and to promote the CO/vinyl arenes copolymerisation in this medium. The second objective is the use of carbon dioxide as C_1 building block in the preparation of polycarbonates by the copolymerisation of CO_2 and epoxides with new efficient catalysts.

The specific aims are:

Part 1. Preparation of new catalysts for CO/vinyl arenes soluble in compressed carbon dioxide:

a) The development of new modified bipyridine ligands containing perfluorinated chains in 4,4'- or 5,5'- position of the aromatic ring (**L1-L3**, Figure 2.1). Most of the examples in the literature introduce the fluorinated chains as a perfluoroalkyl group. In this work, the introduction of the perfluorinated chain through an ester function will be explored. These ligands could be easily prepared and synthesised. The ligands will be used to synthesise palladium (II) complexes such as bischelated complexes $[Pd(\textbf{N-N})_2]^{2+}$ and monocationic complexes $[Pd(CH_3)(NCCH_3)(\textbf{N-N})][X]$. The coordination chemistry of these ligands to other metals is as well an object of study. The Pd(II) complexes will be the focus of the catalytic study using carbon dioxide as a medium.

b) To explore the new possibilities of a catalytic systems with P,N-donor ligands, a semi equivalent bpy ligand containing a low-coordinated "soft" phosphorus and a "hard" nitrogen heteroatom (**L4**, Figure 2.1). To synthesise and characterize palladium (II) complexes, bischelated complex and monocationic complexes ($[Pd(\textbf{L4})_2]^{2+}$ and $[Pd(CH_3)(NCCH_3)(\textbf{L4})]^+$, respectively). The coordination chemistry of this ligand towards other metals and its reactivity will be also studied. The activity of the Pd(II) complexes in copolymerisation of CO/α-olefins will be studied.

L1 5,5'- R'=Me; R= $(CH_2)_4C_8F_{17}$
L2 4,4'- R',R = $COO(CH_2)_3C_8F_{17}$
L3 5,5'- R',R = $COO(CH_2)_3C_8F_{17}$

L4
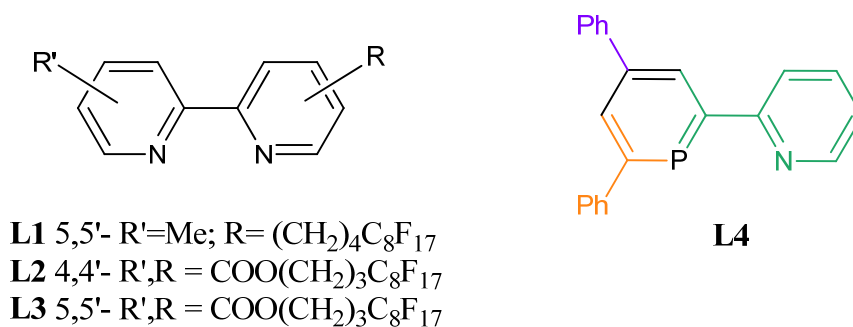
Figure 2.1. Bipyridine ligands (**L1-L3**) and 2-(2-pyridyl)-4,6-diphenylphosphinine ligand (**L4**) for palladium catalysed CO/α-olefins copolymerisation.

Part 2. Carbon dioxide as C_1 building block in the copolymerisation of CO_2 and epoxides:

a) To investigate the catalytic activity of Zn(II) precatalytic systems with chiral amino-alcohol ligands (Figure 2.2) in the asymmetric alternating copolymerisation of epoxides/CO_2.

b) To study the Zn-catalysed epoxide/CO_2 copolymerisation with a family of tridentate Schiff-base ligands N,N,O, (E)-2,4-di-tert-butyl-6-(((pyridin-2-ylmethyl)imino)methyl)phenol ligand (Figure 2.2).

chiral aminoalcohols

N,N,O-donor ligand
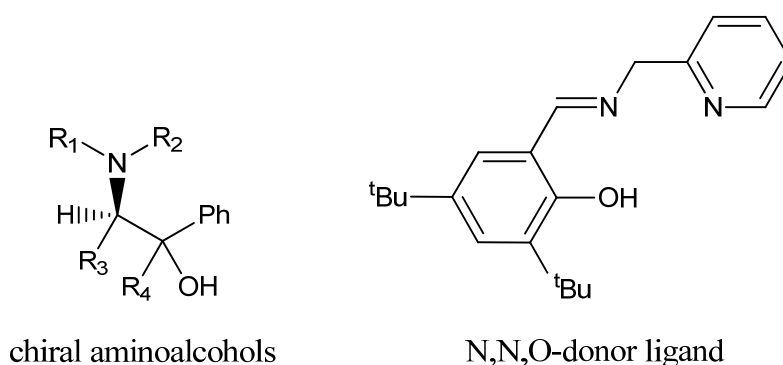
Figure 2.2. Chiral amino-alcohol and tridentate N,N,O ligand for zinc catalysed epoxides/CO_2 copolymerisation.

PART - 1

CO2 as Solvent

Chapter - 3

New Efficient Dicationic Palladium(II) Complexes for the CO/Vinyl Arenes Copolymerisation in Compressed Carbon Dioxide and 2,2,2-Trifluoroethanol

New palladium complexes with perfluorinated 2,2′-bipyridine ligands have been prepared to be used as catalytic systems for CO/4-tert-butylstyrene (TBS) and CO/styrene (ST) copolymerisation in compressed carbon dioxide and 2,2,2-trifluoroethanol. Polyketones with high molecular weights (up to M_w = 222000 for CO/TBS and up to M_w = 692000 for CO/ST) and low polydispersities (M_w /M_n = 1.3-3.3) have been obtained. MALDI-TOF analysis of the copolymer end groups revealed that the main initiation and termination steps involved the insertion of the alkene into the Pd-H bond and the β-H-elimination on the Pd-alkyl bond, respectively. Rhodium (I) complexes were also prepared to analyse electronic properties and the X-ray structure [Rh(cod)(NN)][PF₆] (NN = L3 and L3′) were obtained.
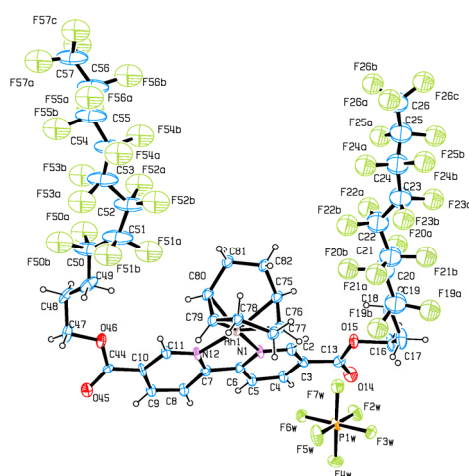
Dicationic Pd(II) complexes for CO/vinyl arenes in compressed CO₂ and TFE

3.1 Introduction

The carbon monoxide/vinyl arenes copolymerisation, leading to perfectly alternating polyketones (Scheme 3.1), is an interesting reaction,[1-6] due to the unusual properties of the synthesized polymers (as thermoplastics) and to the presence of the carbonyl functionality that allows further functionalisation along the polymer backbone.[2,7]
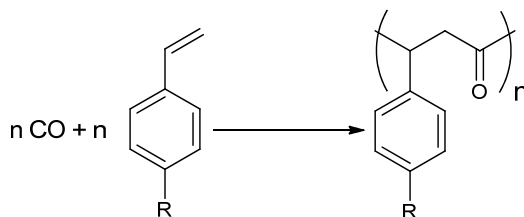
Scheme 3.1. Alternating copolymerisation of vinyl arenes with carbon monoxide (R = H, CH_3, *tert*-butyl).

It is well known from the literature that for the CO/vinyl arene copolymerisation the best performing catalysts are based on palladium (II) complexes with nitrogen-donor ligands belonging to the family of 2,2'-bipyridine (bpy) or 1,10-phenanthroline (phen)[8] or pyridine-imidazoline.[9] In particular, it has been reported that, when the copolymerisation was carried out in 2,2,2-trifluoroethanol (TFE) the dicationic bischelated Pd-complexes of general formula [Pd(3-R-phen)₂][PF₆]₂ (3-R-phen = 3-alkyl substituted phen) generated very productive catalysts (up to 12.0 kg CO/ST CP/g Pd in 72 h; kg CP/g Pd = kilograms of copolymer per gram of palladium) for the synthesis of high molecular weight copolymers (up to Mw = 300000).[10]

During the last years, the use of compressed carbon dioxide as a medium for catalysed reactions has represented an environmental friendly alternative to traditional solvents, since it is non-toxic and non-flammable.[11] Most of the examples of polymerisation reactions carried out in compressed CO_2 dealt with free radical polymerisation.[12-15] The catalytic polymerisation in this medium has been less studied.[16] Also, carbon dioxide can be used at low pressures dissolved in a solvent forming carbon dioxide expanded liquid (CXL).[17] The advantage of this medium is that the low polarity of CO_2 can be tuned with the appropriated solvent, thus increasing the solubility of the products in it, and that milder conditions than with supercritical

carbon dioxide ($scCO_2$) can be used. Using CXL, the activities observed in some hydroformylation[18] and oxidation[19] reactions were higher than using net liquids or $scCO_2$.

In 2006, in the group it was reported the first example of an active catalytic system for the CO/4-*tert*-butylstyrene (TBS) copolymerisation in $scCO_2$ based on a monocationic palladium complexes with perfluorinated phenantroline and bipyridine ligands (**A** and **B**, Figure 3.1), [Pd(Me)(NCMe)(N-N)][BArF] (N-N = **A** and **B**, BArF = B[3,5-$(CF_3)_2C_6H_3$]$_4$), achieving a productivity of 234 g CP/g Pd in copolymers of higher molecular weight (M_w = 87800) and narrower polydispersities (M_w/M_n = 1.2) than in organic solvents.[20]
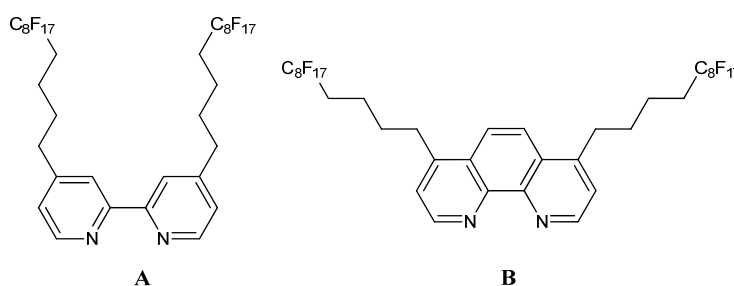
Figure 3.1. Perfluorinated nitrogen chelating ligand **A** and **B**.

More recently, the dicationic complexes [Pd(N-N)$_2$][X]$_2$ (N-N = **A** and **B**, X = $BArF^-$, PF_6^-, BF_4^-) were prepared and their catalytic activity in the CO/TBS copolymerisation in compressed CO_2 was studied. The optimum catalytic conditions were found with [Pd(**A**)$_2$][BArF]$_2$ showing high productivity (1.4 kg CP/g Pd) and molecular weight (Mw = 161800) at 30 bars CO, 70 bars of CO_2, 60°C during 24h.[21] This is in agreement with the results reported in the literature, were bischelated catalyst precursors [Pd(N-N)$_2$][X]$_2$ provided higher productivity and molecular weight than monochelated systems.[8c,10a]

As discussed in Chapter 1, Soro *et al.*[22] reported that [Pd(N-N)$_2$][BArF]$_2$ complexes containing bpy ligands substituted by methyl groups in 5 or 5,5' positions generated more productive catalysts than those containing the unsubstituted bpy. Therefore, we extended the series of perfluorinated bpy to the new ligands **L1-L3** (Figure 3.2) bearing equal or different substituents in 4,4'- or 5,5'- positions and prepared the bischelated catalyst precursors [Pd(N-N)$_2$][X]$_2$ (N-N = **L1-L3**; X = $BArF^-$) and studied their catalytic activity in the CO/vinyl arene copolymerisation in compressed CO_2. For comparison purposes, complexes with model ligands **A'** and **L1'-**

Dicationic Pd(II) complexes for CO/vinyl arenes in compressed CO₂ and TFE

L3' (Figure 3.2) were also prepared. The coordination chemistry of these ligands was also studied.
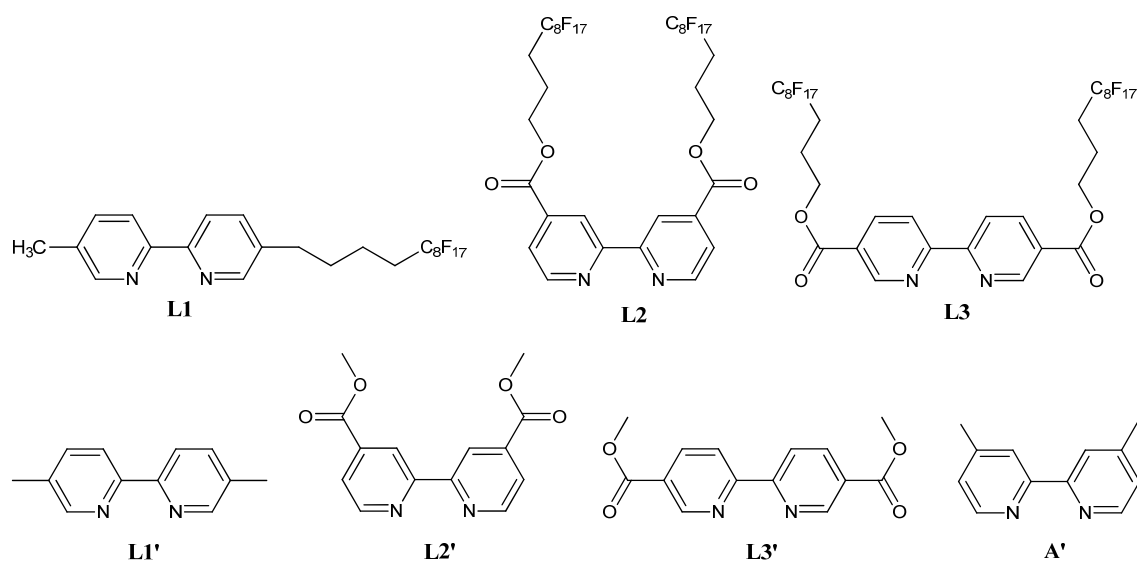
Figure 3.2. Perfluorinated nitrogen chelating ligand **L1-L3** and model ligands **A'**, **L1'**-**L3'**.

3.2 Results and Discussion

3.2.1 Synthesis of ligands L1-L3

The synthesis of the 5,5'-disubstituted analogous of **A** was attempted following the same methodology as for ligands **A** and **B** based on C-alkylation of the corresponding dimethyl-2,2'-bipyridine,[20,23] however the non-symmetrical 5-[4-(perfluorooctyl)butyl]-5'-methyl-2,2'-bipyridine was isolated (**L1**, Figure 3.2). All the attempts to obtain the disubstituted compound were unsuccessful. These difficulties prompted us to synthesise a new family of bipyridine ligands introducing the perfluorinated chain through an ester function (**L2** and **L3**, Figure 3.2).

The new family of bipyridines was obtained in a three-step reaction from 4,4'- and 5,5'-dimethyl-2,2'-bipyridine, which were initially oxidized with sodium dichromate to the corresponding bis(carboxylic) acids following a described method (Scheme 3.2).[24] Afterwards, the acid derivatives were transformed into the corresponding acyl chlorides, which were reacted with the desired perfluorinated alcohol giving the perfluorinated bipyridines **L2** and **L3** as a cream powder, the last step being a variation

of the procedure described by Garelli and Vierling.[25] While **L2** was soluble in most organic solvents, **L3** was only soluble in toluene at 80ºC. This fact may account for the higher yield of **L3**, being its precipitation from the reaction medium the driving force of the synthetic procedure.

$Rf = C_8F_{17}(CH_2)_3-$

i) $Na_2Cr_2O_7 / H_2SO_4$; ii) $SOCl_2$; iii) $Rf(CH_2)_3OH/ NEt_3/ CH_2Cl_2$

L2 = 4,4'-COORf
L3 = 5,5'-COORf
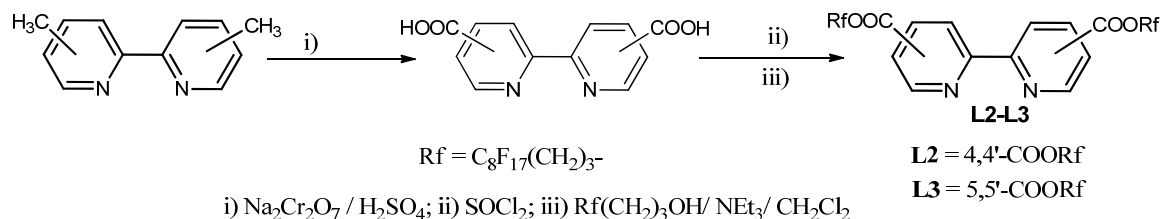
Scheme 3.2. Synthetic pathway for ligands **L2** and **L3**.

Bipyridines **L1-L3** were characterised by NMR, FTIR spectroscopy and mass spectrometry. The ^{1}H and ^{13}C NMR spectra of **L2** and **L3** showed the pattern corresponding to a C_2 symmetric molecule, i.e. three different broad signals at the ^{1}H NMR aromatic region (δ 7.9-9.3 ppm) indicating the two equivalent bipyridine rings. As expected, the signal of the methylenic protons α to the carboxylic group appeared downfield, (δ 4.0 and 4.5 ppm), while the resonances of the β and γ methylenic groups were between δ 1.7-2.3 ppm. As a general trend, the ^{1}H NMR peaks of the aromatic protons of **L3** were downfield shifted with respect to those of **L2**, likely due to the different experienced electron-withdrawing effect as a function of the substituent position. The presence of the ester group was confirmed by the C-O stretching frequency ν(CO) at 1731 and 1716 cm^{-1} for **L2** and **L3**, respectively.

In the aliphatic region of the ^{1}H NMR spectrum of **L1** both the signals of the hydrocarbon chain attached to the fluorinated tail (δ 1.70-2.70 ppm) and the signal of the methyl group (δ 2.40 ppm) were present, while in the aromatic region only three well separated multiplets were observed. In the ^{13}C NMR spectrum separated singlets for all the aromatic carbons, which were related to the corresponding protons in the ^{1}H-^{13}C-HSQC spectrum, could be observed thus confirming the non-symmetric structure of the ligand.

Dicationic Pd(II) complexes for CO/vinyl arenes in compressed CO₂ and TFE

3.2.2 Palladium complexes

The dicationic bischelated palladium complexes [Pd(N-N))₂][X]₂ (N-N = **L1-L3**, Scheme 3.3) with X = BArF¯ (BArF = 3,5-(trifluoromethyl)phenyl borate) as counterion were synthesized following a two-step procedure starting from Na₂[PdCl₄], which reacted with one equivalent of the corresponding ligand to get the neutral complexes [PdCl₂(N-N)] (**L1a-L3a**, N-N = **L1-L3,** Scheme 3.3).[22,26] These complexes were handled with sodium tetrakis 3,5-(trifluoromethyl)phenyl borate sodium salt and another equivalent of the ligand to obtain the desired dicationic derivatives **L1b-L3b**. The driving force for the last step was the formation of NaCl, which is insoluble in dichloromethane, where the desired products are soluble.

$$Na_2[PdCl_4] \xrightarrow{MeOH} [PdCl_2(N\text{-}N)] + 2\ NaCl$$

$$[PdCl_2(N\text{-}N)] \xrightarrow[\text{NaBArF}]{CH_2Cl_2} [Pd(N\text{-}N)_2][BArF]_2 + 2\ NaCl$$
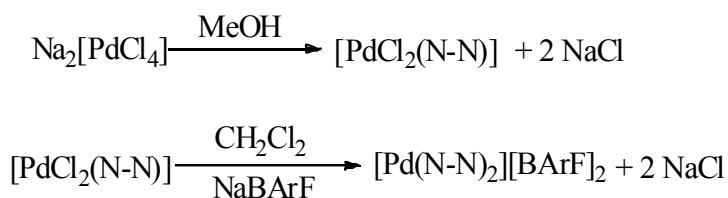
N-N	[PdCl₂(N-N)]	[Pd(N-N)₂][BArF]₂
L1	**L1a**	**L1b**
L2	**L2a**	**L2b**
L3	**L3a**	**L3b**

Scheme 3.3. Synthetic pathway for the palladium complexes **L1a-L3a** and **L1b-L3b**.

Complexes **L1a-L3a** were isolated in good yield as light brown or yellow solids. They were not soluble in common organic solvents and were characterized by FTIR spectroscopy and mass spectrometry (MALDI-TOF), which confirmed the formation of mononuclear species.

Complexes **L1b-L3b** were isolated as pale brownish foams and fully characterized by mass spectrometry, NMR and FTIR spectroscopy.

The ¹H NMR spectrum of **L1b** showed separated signals in the aliphatic region, while the aromatic protons gave one signal for H[6,6'] and one overlapped multiplet for H[3,3'] and H[4,4'] (see experimental section for atom numbering). For this complex, *syn* and *anti* isomers can be expected according to the relative coordination of the two non

symmetric bpy ligands. On the basis of the NMR analysis it was not possible to identify either if one isomer or both of them were present.

The ^{1}H NMR spectrum in CDCl$_3$ at room temperature of **L2b** showed two sets of rather broad signals with different intensity both for the aromatic protons and for the methylenic group bonded to the oxygen atom (Figure 3.3c), while the other methylenic protons gave one broad resonance. The assignment of the signals was based on COSY experiment (see Supplementary Information, SI). No signals due to free ligand were present and all the signals, with the exception of that due to H$^{5,5'}$, were upfield shifted with respect to the same signals in the free ligand. These NMR data indicated the presence of two species, **I** and **II,** in ratio 1:1 at room temperature. In each of them, both the two ligands bonded to palladium and the two halves of each ligand were equivalent.

(1)   (2)
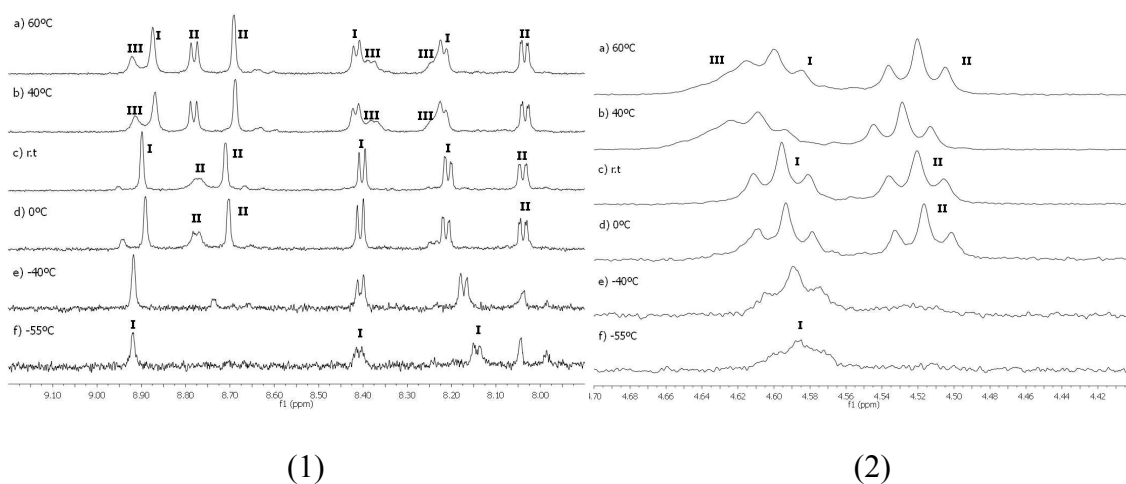
Figure 3.3. Variable temperature ^{1}H NMR spectra in CDCl$_3$ of **L2b** (1) aromatic region, (2) -O-CH$_2$- region at (a) 60ºC, (b) 40ºC, (c) room temperature, (d) 0ºC, (e) -40ºC, (f) -55ºC.

NMR experiments at variable temperature from -55ºC to 60ºC were performed (Figure 3.3a-f). At the lowest temperature reached, only the set of broad signals corresponding to species **I** was observed. On the other hand, increasing the temperature above 25ºC did not affect the ratio of species **I** and **II**. However, at 40ºC a new species **III** appeared, in a ratio 1.0:1.0:0.5. A NOESY experiment performed at room temperature evidenced that the two species were in exchange. The NMR spectrum of **L3b** at room temperature showed also two sets of signals in the aromatic and methylenic regions.

One possible hypothesis is that the two observed species were due to the two conformers *twist* or *bow-step* (Figure 3.4) arising from a geometrical distortion from ideal square planar geometry. These two conformers were observed in solid state for analogous bischelated compounds $[Pd(N-N)_2]^{2+}$ with bpy, phen and their alkyl substituted derivatives in 4,4'- and 5,5'-position;[8c,27] while in solution an average situation was always observed.

(a)   (b)
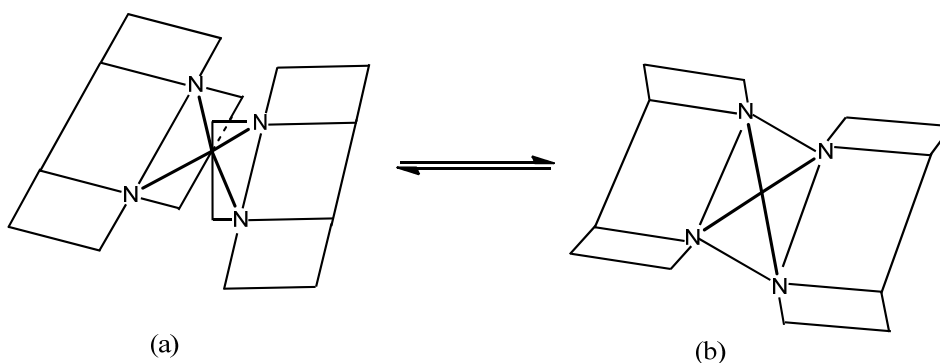
Figure 3.4. Conformational geometries of $[Pd(N-N)_2]^{2+}$ cations *(a) twist* conformation, *(b) bow-step* conformation.

Another possibility to take into account is that the signals were due to different relative positions of the carbonyl group in the bipyridine ligands. To confirm this point, the analogous complexes with the model ligands **A'** and **L2'** (Figure 3.2), $[Pd(A')_2][BArF]_2$[28] and $[Pd(L2')_2][BArF]_2$ were prepared. In the ^{1}H NMR spectrum of $[Pd(A')_2][BArF]_2$ only one set of signals was observed at room temperature (Figure 3.5a), while signals of three species were observed for $[Pd(L2')_2][BArF]_2$ in a ratio 1.0:0.2:0.3 (Figure 3.5b). This experiment points towards the relative disposition of the carbonyl groups being the responsible of the formation of different species.

To confirm this point a theoretical study was performed in collaboration with the Quantum Chemistry group of our department (Dra. M.M. Reguero). DFT calculations were run, using the B3LYP functional and a 6-31Gd basis set with *LANL2DZ* (Los Alamos National Laboratory 2 double z) pseudo potentials for the palladium atom. The optimized geometries of the *twist* and *bow-step* conformers and of all the possible symmetric isomers of the $[Pd(A')_2]^{2+}$, $[Pd(L2')_2]^{2+}$ and $[Pd(L3')_2]^{2+}$ cations were obtained (Figure 3.6).
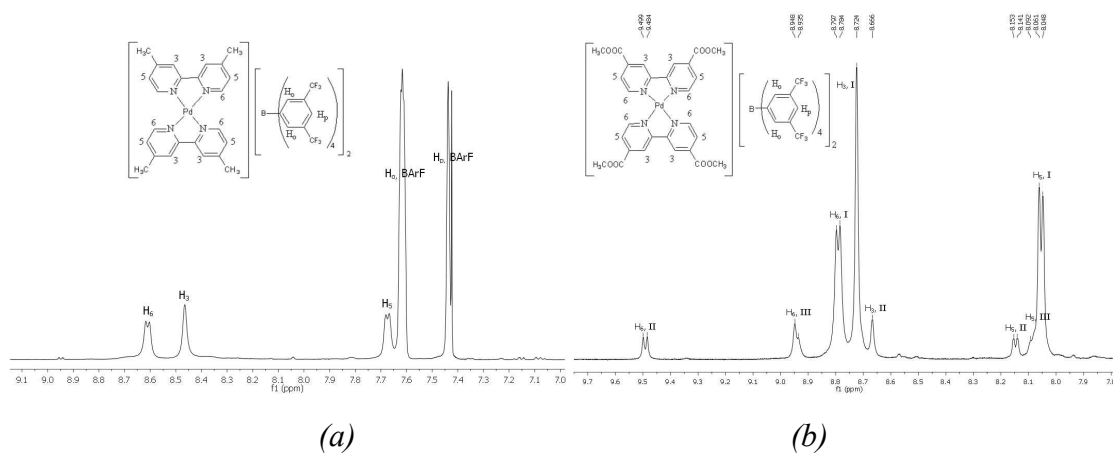
Figure 3.5. Aromatic region of the ^{1}H NMR spectra at room temperature of *(a)* [Pd(**A'**)$_2$][BArF]$_2$ (CDCl$_3$/acetone-d$_6$) *(b)* [Pd(**L2'**)$_2$][BArF]$_2$ (CDCl$_3$).
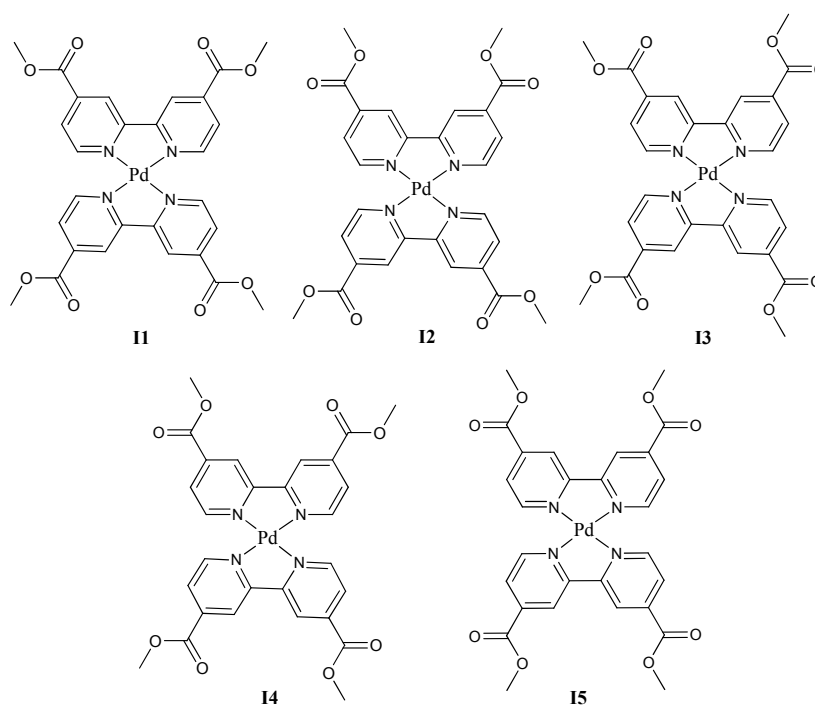
Figure 3.6. Relative positions of the carbonyl groups in complex [Pd(**L2'**)$_2$]$^{2+}$.

The relative energies of the stable species found are collected in Table 3.1. For each compound, energies are relative to the most stable isomer. Assuming a Boltzmann distribution, the relative populations of all the minima of each compound have also been calculated an included in Table 3.1.

The initial analysis was performed on [Pd(**A'**)$_2$]$^{2+}$ cation, where only one *twist* and one *bow-step* isomer are possible. For [Pd(**A'**)$_2$]$^{2+}$, the *twist* conformation was substantially more stable than the *bow-step* one, so it is expected that only this

Dicationic Pd(II) complexes for CO/vinyl arenes in compressed CO₂ and TFE

conformer will be populated. This is in agreement with the obtained NMR spectra,[28] where only one set of signals was observed (Figure 3.5a) and in agreement with crystal structure reported for $[Pd(\mathbf{A'})_2][OTf]_2$ $(OTf = CF_3SO_3)$.[28a]

Table 3.1. Relative energies (kcal mol^{-1}) and populations of the optimized minima located for all the isomers of the $[Pd(\mathbf{A'})_2]^{2+}$ (in gas state), $[Pd(\mathbf{L2'})_2]^{2+}$ and $[Pd(\mathbf{L3'})_2]^{2+}$ (in CHCl$_3$ solution) cations. Magnitudes relative to the most stable isomer in each compound.

$$[Pd(\mathbf{A'})_2]^{2+}$$

Twist		Bow-step	
Energy	Population	Energy	Population
0.00	1.00	2.63	0.012

$[Pd(\mathbf{L2'})_2]^{2+}$ $\qquad\qquad\qquad$ $[Pd(\mathbf{L3'})_2]^{2+}$

Isomer	Twist		Isomer	Twist	
	Energy	Population		Energy	Population
I1	0.00	1.00	I1	0.00	1.00
I2	0.84	0.24	I2	1.23	0.13
I3	0.90	0.22	I3	1.32	0.11
I5	1.76	0.05	I4	1.51	0.08
I4	9.08	0.00	I5	2.71	0.01

For $[Pd(\mathbf{L2'})_2]^{2+}$ and $[Pd(\mathbf{L3'})_2]^{2+}$ calculations showed that also the *bow-step* conformation was less stable than the *twist* one. The relative populations calculated predict that no signal will be observed for the *bow-step* conformers (see SI). For a better comparison between DFT calculation and NMR experiments it was introduced the solvent (CHCl$_3$) as a variable in the DFT calculations and only *twist* isomers were analysed for $[Pd(\mathbf{L2'})_2]^{2+}$ and $[Pd(\mathbf{L3'})_2]^{2+}$ cations. The possible isomers are represented in Figure 3.6 and the results are shown in Table 3.1. Regarding the relative disposition of the carbonyl group, comparing the five possible isomers of *twist*-$[Pd(\mathbf{L2'})_2]^{2+}$ (Figure 3.6), there are 3 isomers (I1-I3) with sizable populations that could give place to signals in a relative ratio 1.0:0.24:0.22. The intensities predicted theoretically are in qualitative agreement with the experimental results (1.0:0.2:0.3). Unfortunately the precision of the

level of theory used in these calculations does not allow obtaining more detailed information, but it definitely rules out the presence of *bow-step* conformers.

On the other hand, for *twist*-$[Pd(\mathbf{L3'})_2]^{2+}$ similar results were obtained, but the theoretical calculations predicted that 3 isomers (I1, I2 and I3) would be observed in a ratio 1.0:0.13:0.11 and an isomer I4 would be at a relative ratio 0.08. This is in qualitative agreement with the ratio observed in the ^{1}H NMR spectrum of $\mathbf{L3'b}$ in which three species were detected in a ratio 1.0:0.2:0.2 (Figure 3.8). In I1 (Figure 3.7a), the confronted substituents are =O, which generate the smallest steric repulsion and give place to a distinctive signal. The reason of the small stability of the other isomers seem to arise from the steric repulsion generated by the $-OCH_3$ group when this is oriented towards the other bpy ligand. In fact, the most unstable isomer is I5 (Figure 3.7b), which has the four $-OCH_3$ groups confronted two by two. I4 has only two $-OCH_3$ groups confronted, and consequently it is the second more stable. In both Isomer-3 and I4 the steric repulsion is produced by two couples of =O and $-OCH_3$ confronted. I2, I3 and I4 have very similar stabilities, so then, is difficult to predict which two of them will give place the two different signals observed.

(a)   **(b)**
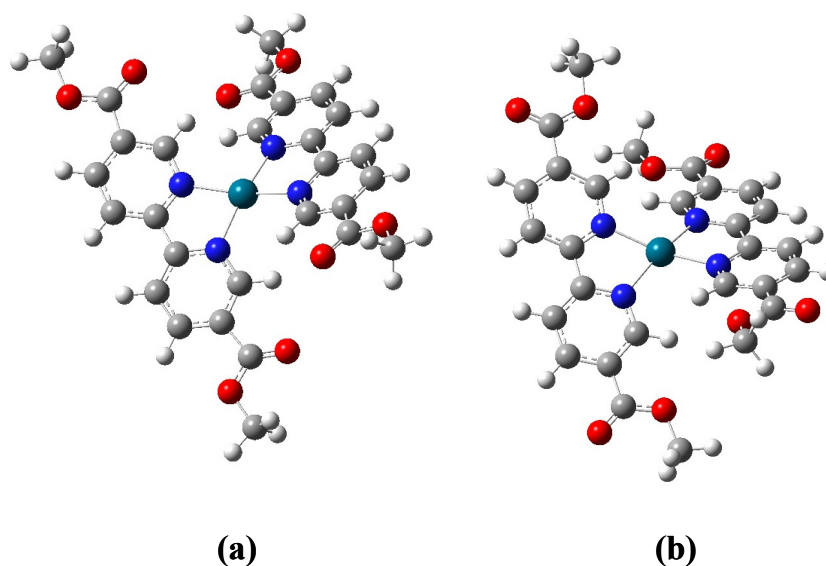
Figure 3.7. Geometries optimized at the B3LYP level for *(a)* Isomer-1 of the twist conformation of $[Pd(\mathbf{L3'})_2]^{2+}$ cation and *(b)* Isomer-5 of the twist conformation of $[Pd(\mathbf{L3'})_2]^{2+}$ cation.

Dicationic Pd(II) complexes for CO/vinyl arenes in compressed CO$_2$ and TFE
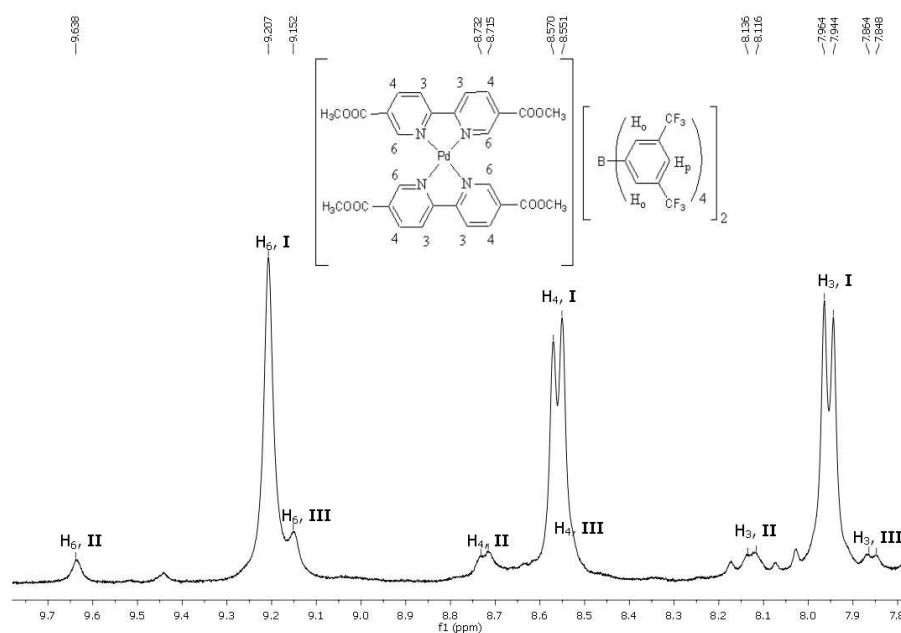
Figure 3.8. Aromatic region of the ^{1}H NMR spectra at room temperature of [Pd(**L3'**)$_2$][BArF]$_2$, **L3'b** (CDCl$_3$, 400MHz).

To sum up, the new species observed in the ^{1}H NMR spectra of bischelated complexes **L2b**, **L3b**, **L2'b** and **L3'b** were attributed to the relative position of the carbonyl groups. DFT calculations with model complexes **L2'b** and **L3'b** confirmed this hypothesis.

3.2.3 Rhodium complexes

Rhodium carbonyl complexes [Rh(CO)$_2$(N-N)][PF$_6$] were synthesized in order to study the coordination ability of the ligands and their electronic properties through the variation of the CO stretching frequency. The carbonyl species were obtained in a two-step reaction involving the initial isolation of the cationic complexes [Rh(cod)(N-N)][PF$_6$] (cod = 1,5-cyclooctadiene, **L1c-L3c**, Scheme 3.4),[9,21,29] which have been fully characterised.

For comparison purposes, analogous Rh-complexes with the non fluorinated ligands **L1'**- **L3'**[30,31] (Scheme 3.4) were also prepared following the described methods.[32]

$$[Rh(cod)_2][PF_6] \xrightarrow{CH_2Cl_2} [Rh(cod)(N-N)][PF_6] \xrightarrow[CH_2Cl_2]{CO} [Rh(CO)_2(N-N)][PF_6]$$
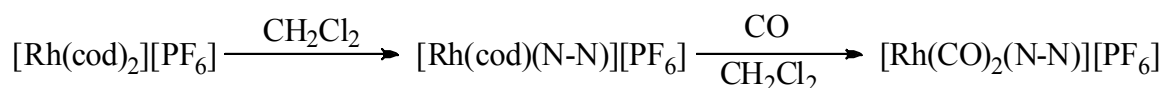
N-N	[Rh(cod)(N-N)]PF$_6$	[Rh(CO)$_2$(N-N)$_2$]PF$_6$
L1	L1c	L1d
L2	L2c	L2d
L3	L3c	L3d
L1'	L1'c	L1'd
L2'	L2'c	L2'd
L3'	L3'c	L3'd

Scheme 3.4. Synthesis of rhodium complexes with ligands **L1-L3** and **L1'-L3'**.

Single crystals of **L3'c** and **L3c**, suitable for X-ray analysis, were obtained by recrystallization from chloroform/diethyl ether after one week at room temperature (Figure 3.9 and Figure 3.10, respectively). The Rh(I) atom adopts the usual square-planar coordination geometry with the nitrogen atoms of the bipyridine ligand and the centre of the double bonds of the cod ligand on the side of the square plane. For complex **L3c**, the average Rh-C distance (2.101 Å) is a slightly shorter in comparison to the value for **L3'c** (2.138Å) and [Rh(bpy)(cod)]$^+$ complex known from the literature (average 2.135Å).[33] Similar Rh-N bond distances were found in both complexes. The bite angle of the ligand **L3**, 77.8(6)º, is smaller than those found in [Rh(bpy)(cod)]$^+$ (78.61º) and [Rh(cod)(phen)]$^+$ (79.80º) or than of **L3'** in **L3'c** (79.08(15)º). It should be noted that in complex **L3c** the fluorinated tails are on the same side of the square-planar plane and the carbonyl groups are in a relative *cis* position, while in complex **L3'c** the methyl and the carbonyl groups are in a *trans* relative position.

Dicationic Pd(II) complexes for CO/vinyl arenes in compressed CO₂ and TFE
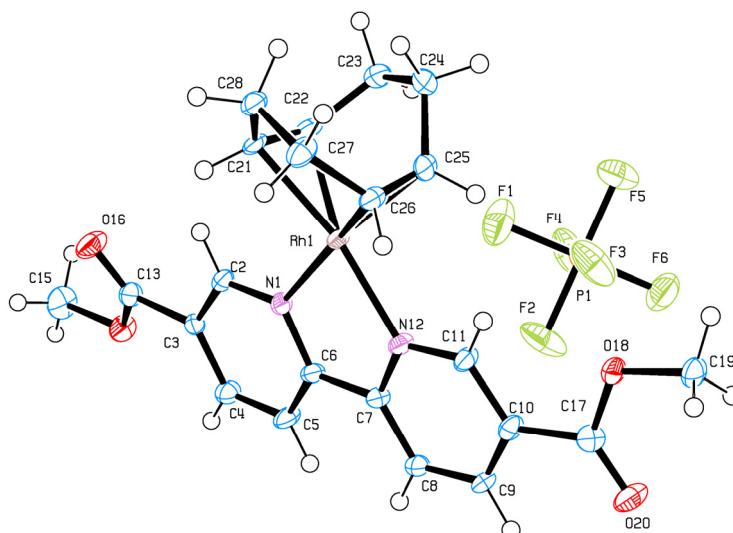
Figure 3.9. ORTEP drawing (25% probability) of complex [Rh(cod)(**L3'**)]PF$_6$ (**L3'c**). Selected bond lengths [Å] and angles [º]: Rh1-N1: 2.093(4), Rh1-N12: 2.081(4), Rh1-C21: 2.142(4), Rh1-C22: 2.124(5), Rh1-C25: 2.154(5), Rh1-C26: 2.135(5), N12-Rh1-N1: 79.08(15), C26-Rh1-C21: 81.81(18), C22-Rh1-C25: 81.54(19), C22-Rh1-C26: 97.89(19), C21-Rh1-C25: 89.21(19).
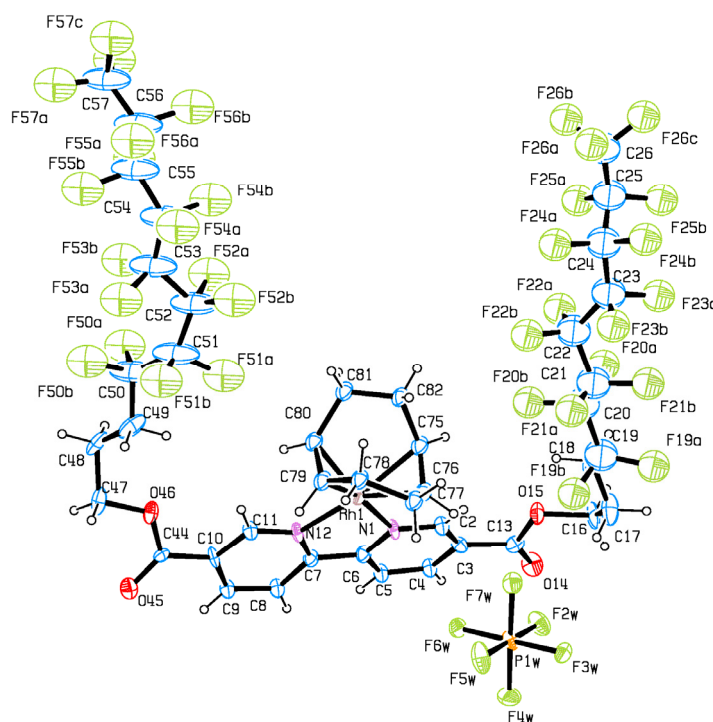
Figure 3.10. ORTEP drawing (25% probability) of complex **L3c**. Selected bond lengths [Å] and angles [º]: Rh1-N1: 2.109(16), Rh1-N12: 2.119(14), Rh1-C75: 2.16(2), Rh1-C76: 2.013(9), Rh1-C79: 2.14(2), Rh1-C80: 2.09(2), N1-Rh1-N12: 77.8(6), C76-Rh1-C79: 83.2(8), C80-Rh1-C75: 82.6(8), C76-Rh1-C80: 100.3(8), C79-Rh1-C75: 88.8(7).

By bubbling carbon monoxide through dichloromethane solutions of **L1c-L3c**, the corresponding dicarbonyl species (**L1d-L3d**) were formed and precipitated adding diethyl ether to the solution. Their characterisation by FTIR, NMR spectroscopy and mass spectrometry confirmed the formation of the complexes. The ^{1}H NMR spectra were performed in solution without further purification, therefore the signals of the free cod were observed. The complexes **L2d** and **L3d** presented solvatochromism as also reported for iron (II) complexes with bpy derivatives:[34] their solutions were yellow, while **L2d** was mauve and **L3d** was green in solid state.

All these complexes presented in the IR spectra two stretching frequencies ν(CO), typical of *cis* arrangement of the two-coordinated carbonyl groups (Table 3.2).[29] For comparison purposes are also considered the rhodium carbonyl complexes with ligands **A** and its analogous non fluorinated **A'** ([Rh(CO)$_2$(**A**)]PF$_6$ and [Rh(CO)$_2$(**A'**)]PF$_6$, respectively).[21] No significant differences in the ν(CO) were observed between complexes with perfluorinated (**A**, **L1-L3)** and the corresponding non-fluorinated ligands (**A'**, **L1'-L3'**) suggesting that the methylenic fragments between the fluorinated chain and the pyridine ring buffer the electron-withdrawing effect of the fluorinated chain itself. Slightly higher ν(CO) values were observed for complexes **L2d** and **L3d** with respect to the ones observed for [Rh(CO)$_2$(**A**)]PF$_6$ and **L1d**, in agreement with the electron-withdrawing effect of the ester group. The position of the substituents does affect neither the ν(CO) frequency values. On the basis of this analysis, it should be expected that the new dicationic palladium complexes with perfluorinated substituents have electronic properties similar to the non fluorinated ones, with a slight differences of electron densities between the two families with and without ester function.

Dicationic Pd(II) complexes for CO/vinyl arenes in compressed CO₂ and TFE

Table 3.2. IR ν(CO) data for **L1d-L3d**, $[Rh(CO)_2(A)]PF_6$ and model complexes $[Rh(CO)_2(A')]PF_6$ and **L1'd-L3'd** in CD_2Cl_2.[a]

Entry	Complex	ν(CO) (cm^{-1})	
1[21]	$[Rh(CO)_2(A)]PF_6$	2098.6	2040.7
2[21]	$[Rh(CO)_2(A')]PF_6$	2099.5	2042.5
3	**L1d**	2099.9	2042.3[b]
4	**L1'd**	2098.4	2039.8
5	**L2d**	2104.4	2048.1
6	**L2'd**	2101.2	2045.8
7	**L3d**	2104.8	2046.2
8	**L3'd**	2102.6	2046.4

[a] in situ complexes measurements, free cod observed in ^{1}H NMR. [b] Also a peak at 2003 cm^{-1} was observed.

3.2.4 Catalysis

3.2.4.1 CO/4-tert-butylstyrene copolymerisation

The dicationic Pd(II) complexes **L1b-L3b** were tested as catalysts for alternating CO/4-*tert*-butylstyrene (TBS) copolymerisation. In a previous study of the catalytic activity from dicationic palladium (II) complexes with ligands **A** and **B**, it was found that at conditions of liquid expanded carbon dioxide the productivity in the copolymers was very high.[21] We consider that since the substrate (2.2 mL) is occupying more than 5% of the total volume (11 mL) the conditions can be considered as a liquid expanded carbon dioxide. Therefore, the present study was performed at these conditions.

L1b-L3b complexes were soluble in liquid carbon dioxide at room temperature and 70 atm forming brownish solutions. The catalytic reactions were performed using 2.2×10^{-3} mmol of the dicationic palladium complex placed in an 11 mL autoclave. The presence of small amounts of 2,2,2-trifluoroethanol provided better results. Therefore, after purged with vacuum, the substrate TBS ([TBS]/[Pd] = 4843) and trifluoroethanol ([TFE]/[Pd] = 300) were introduced in the reactor. The system was pressurised with CO (P_{CO} = 30 atm) and carbon dioxide (up to 70 atm aprox. $\delta_{(CO2)}$ = 0.11 g/mL, when used) and heated up to the desired temperature (T = 60 °C). After the proper time, the reaction

was quenched by cooling down the reactor and venting the gases. The polymers were isolated by precipitation with methanol. The results are collected in Table 3.3.

We observed an increase of productivity going from **L1b**, $[Pd(A)_2][BArF]_2$ to the ester containing systems **L2b** and **L3b** (entries 1-4, Table 3.3). This indicates that the introduction of the ester group had a remarkable positive effect on the activity of the catalyst, likely due to its electron-withdrawing feature, which decreases the electron density on palladium, as evidenced by the studies on the rhodium complexes. The catalyst **L2b** provided homopolymer, which may be due to catalyst decomposition, since palladium black was observed at the end of the reaction. Catalyst containing ligand **L3** was thus far the best performing, both in terms of productivity (6.15 kg CP/g Pd) and molecular weight (M_w 222000) although the polydispersity was high (4.3). This result is in agreement with the literature data on palladium catalyst containing 5-substituted bpys[22] and on 3-substituted phenanthrolines,[10a] suggesting that the presence of substituents in *meta* position with respect to the nitrogen donor is relevant for achieving excellent performing catalysts.

The copolymers obtained with catalysts **L1b** and **L3b** were syndiotactic as expected for bpy based systems (example of syndiotacticity, Figure 3.11).[8c]
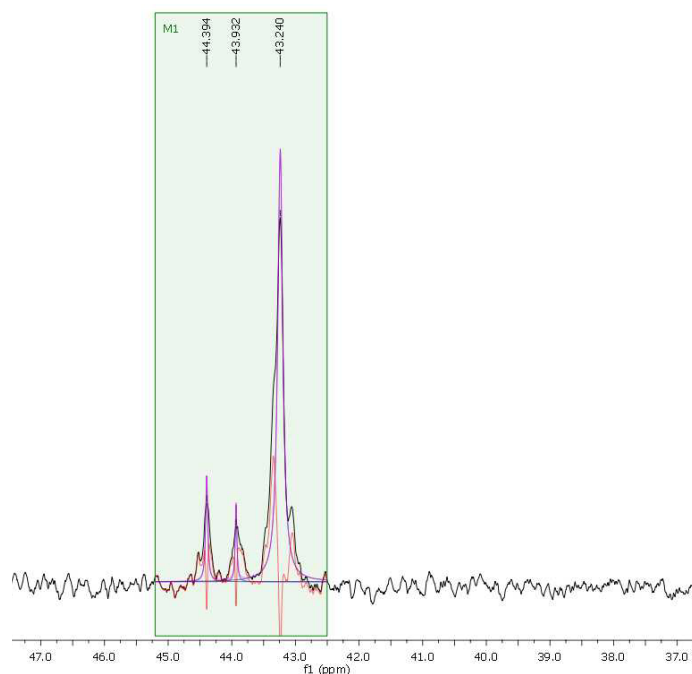
Figure 3.11. ^{13}C NMR spectra in $CDCl_3$ at room temperature, region of methylenic carbon atom, of: CO/TBS polyketone synthesized with **L1b** (entry 2, Table 3.3).

Dicationic Pd(II) complexes for CO/vinyl arenes in compressed CO$_2$ and TFE

Following this trend the complex **L3'b** showed a productivity of almost 5.5 kg CP/g Pd, close to the one obtained with **L3b**, suggesting that the major contribution to the improved productivity might be related to the electron properties of the ester group and only a minor part might be associated to the fluorinated tails (entry 5, Table 3.3). In addition, a decrease in molecular weight was observed comparing to system **L3b**.

When complex **L3b** was applied, it was observed through the reactor windows that, after 6 h of reaction, the precipitation of the copolymer avoided the magnetic bar to stir limiting the mass and gas transfer processes. Actually, in the case of catalyst **L3b** the values of productivity per hour on the isolated polyketones at 6 h were higher than those obtained at 24 h (532 g CP/g Pd·h in entry 6 *versus* 256 g CP/g Pd·h entry 5, Table 3.3).

For comparison, complexes **L1b-L3b** were tested in TFE as a solvent under the same conditions (entries 7-9, Table 3.3): a decrease in the productivity of more than one order of magnitude was observed for complex **L3b**. Polyketones of lower molecular weight than in liquid expanded CO$_2$ were produced.

Table 3.3. CO/TBS copolymerisation with precatalysts **L1b-L3b** and **L3'b**.[a]

Entry	Catalyst	Time (h)	Productivity (g CP/gPd)	Productivity[b] (gCP/gPd·h)	% uu	Mw (Mw/Mn)[c]
1[21]	[Pd(**A**)$_2$][BArF]$_2$	24	1379	57	-	167000 (1.9)
2	**L1b**	24	466	19	93	187700 (3.3)
3[d]	**L2b**	24	1535	64	-	-
4	**L3b**	24	6155	256	73	222000 (4.3)
5	**L3b**	6	3197	532	76	214600 (3.1)
6	**L3'b**	24	5490	228	84	197200 (3.2)
7[e]	**L1b**	24	491	20	98	68000 (1.9)
8[e]	**L2b**	24	303	13	97	34100 (1.6)
9[e]	**L3b**	24	222	9	94	25100 (2.0)

[a] Reaction conditions: 2.42·10^{-3}mmol catalyst, V$_{vessel}$ = 11 mL, TBS V = 2.2 mL ([TBS]/[Pd] = 4843), TFE V = 52μl ([TFE]/[Pd] = 300), P$_{CO}$ = 30 atm, P$_{CO2}$ = 70 atm; aprox. density 0.11 g/mol, T = 60 ºC, time = 24 h; [b] average productivity; [c] determined by GPC versus polystyrene standards; [d] homopolymer formed, 53%. [e] 2.42·10^{-3}mmol catalyst, solvent TFE V = 30mL, TBS V = 5.9 mL ([TBS]/[Pd] =4843).

In a direct comparison for CO/*tert*butylstyrene copolymerisation with the best literature results,[22] the catalytic system **L3b** in liquid expanded CO_2 showed a slightly lower productivities (532 g CP/g Pd·h) than the most active catalyst in TFE ([Pd(**L1'**)$_2$][BArF]$_2$,[22] 823 g CP/g Pd·h), but with better molecular weight (M_w = 215000 *vs.* 167000) and comparable polydispersities (3.1 *vs.* 3.2).

3.2.4.2 CO/styrene copolymerisation

Complexes **L1b-L3b** were also found to be active catalysts for the CO/styrene copolymerisation (Table 3.4). In agreement with the literature data,[10a] the CO/ST productivities were, in general, lower than those obtained for the CO/TBS copolymerisation and we observed partial decomposition of the catalyst to palladium black at the end of the reaction .

When the copolymerisations were carried out in liquid expanded CO_2, the trend of the productivities was analogous to that observed for the TBS as comonomer, being complex **L3b** the most productive (entries 1-3, Table 3.4). Again the catalyst with the non-fluorinated ligand, **L3'b**, showed a productivity very similar to that of **L3b**, however the fluorinated tails had a remarkable positive effect on the Mw (entry 3 *vs.* entry 4, Table 3.4).

Two series of experiments were performed in trifluoroethanol by using reaction conditions analogous to those of liquid expanded CO_2 in one case, and analogous to those reported in the literature, in the other.[10] For the first series very low productivities were obtained together with the decomposition of the catalyst to inactive palladium black (entries 5-7, Table 3.4). For the second series, the increased [styrene]/[Pd] ratio to the a higher value of 48000 (obtained by increasing the amount of the vinyl arene) resulted in the complete suppression of the catalyst decomposition and in higher values of productivity, that in any case remained lower than those obtained in liquid expanded CO_2 (entries 8-10, Table 3.4). Moreover, on going from TFE to liquid expanded CO_2 there was a remarkable increase in the Mw in liquid expanded CO_2.

Dicationic Pd(II) complexes for CO/vinyl arenes in compressed CO₂ and TFE

Table 3.4. CO/styrene copolymerisation with precatalysts **L1b-L3b** and **L3'b**.[a]

Entry	Catalyst	Solvent	Productivity (g CP/gPd)	% uu	Mw (Mw/Mn)[b]
1	**L1b**	CO_2	415	92	n.d.
2	**L2b**	CO_2	1432	97	n.d.
3	**L3b**	CO_2	2294	93	692600 (1.3)
4	**L3'b**	CO_2	2235	95	374200 (1.4)
5[c]	**L1b**	TFE	147	94	n.d.
6[c]	**L2b**	TFE	313	94	n.d.
7[c]	**L3b**	TFE	10	-	n.d.
8[d]	**L1b**	TFE	1249	-	n.d.
9[d]	**L2b**	TFE	955	-	n.d.
10[d]	**L3b**	TFE	2004	-	518500 (1.4)

[a] Reaction conditions: $2.42 \cdot 10^{-3}$ mmol catalyst, V_{vessel} = 11 mL, styrene V = 1.3 mL ([styrene]/[Pd] = 4843), P_{CO} = 30 atm, T = 60 ºC, time = 24 h; [b] determined by GPC versus polymethylmetacrylate standards. [c] TFE V = 30mL, styrene V = 3.7 mL ([styrene]/[Pd] =4843). [d] $5.4 \cdot 10^{-3}$ mmol Pd, styrene V = 30mL, TFE V = 20 mL ([styrene]/[Pd] = 48000), P_{co} = 30 atm, T = 50 ºC, time = 24 h.

Comparing the results obtained with **L3b** in the CO/styrene copolymerisation with the best literature results with the same kind of catalysts,[10] the catalytic system **L3b** in liquid expanded CO_2 showed comparable productivities (2.3 kg CP/g Pd) than the most active catalyst in TFE ([Pd(3-tmp-phen)₂][PF₆]₂, 3-tmp-phen = (*S*)-3-(1,2,2-trimethylpropyl)-1,10-phenanthroline; 2.7 kg CP/g Pd), with better molecular weight (M_w = 693000 *vs.* 206000) and lower polydispersities (1.3 *vs.* 1.5). Moreover, the polyketones obtained presented high stereoregularity (% uu >90%).

In conclusion, we achieved a new catalytic system (**L3b**) highly active, with high stereoregularity and long living in CO/TBS and in CO/ST copolymerisation and the most important in green and sustainable medium.

3.2.4.3 *Mechanism of the reaction*

From the results reported in the literature,[35-40] is clearly observed that MALDI techniques have been successfully applied in polymer analysis for the determination of the end groups, which are determined from their mass by subtracting the appropriate number of monomer units (and the mass of the cation) from the mass of a given molecular ion. Moreover, the use of a MALDI-TOF instrument with high mass resolution lead to a more accurate end groups determination by the isotope distribution for each ionic species. The MALDI analysis evidenced that the nature of the end groups depends on the olefin comonomer, the catalytic system and the reaction medium. Therefore, to elucidate the reactions involved in the initiation and termination steps of the catalytic cycle, the end-groups characterization of the polyketones obtained from CO/TBS and CO/ST were performed by MALDI-TOF analysis. The copolymers were characterized by several series of peaks that according to the mechanism could provide fragments containing chains a-d (Scheme 3.5) cationized with K^+ or Na^+. The macromolecules differ from the end-groups, while the repetitive unit (132 Da in ST and 188 Da in TBS) is that expected for this kind of copolymerisation reaction.

The MALDI-TOF mass spectra of the polymers CO/TBS formed at the best conditions in liquid expanded CO_2 were analyzed and compared with the ones obtained in TFE. The mass spectra of the polymers obtained with catalysts **L1b** (see SI) and **L3b** (Figure 3.12a) revealed that the main fragment in both solvents corresponded to a species, in which the initiation step involved the insertion of the alkene into the Pd-H bond and termination by β-H elimination (chain a). Therefore, TFE would not be involved in the initiation.[35] Nevertheless, the MALDI-TOF of the polyketones prepared in TFE (Figure 3.12b) showed also the peak corresponding to chain containing trifluoroethanol as a initiator (chain b, Scheme 3.5). Hence, the fluorinated alcohol did not rise to termination through alcoholysis, as it was observed in the literature,[35,41] and β-H elimination should be the main chain transfer process. There were no substantial differences between the composition of the polymers obtained with precatalyst **L1b** and **L3b** in the same medium. Minor peaks that may correspond to a double carbonylation were also observed in CO_2 (chain c + C=O).

Dicationic Pd(II) complexes for CO/vinyl arenes in compressed CO₂ and TFE
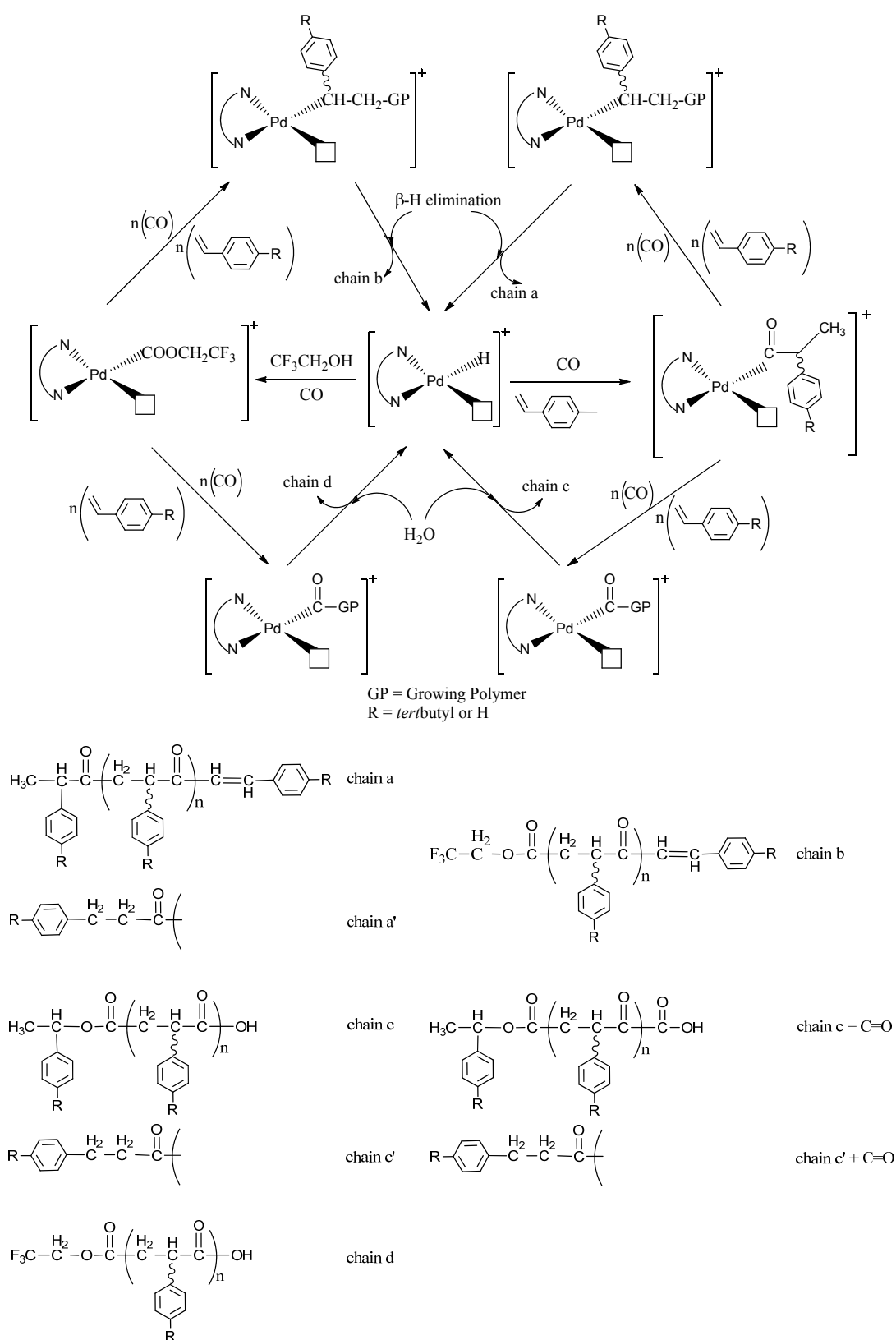
Scheme 3.5. The proposed catalytic cycles and chain end groups.

(a)

(b)
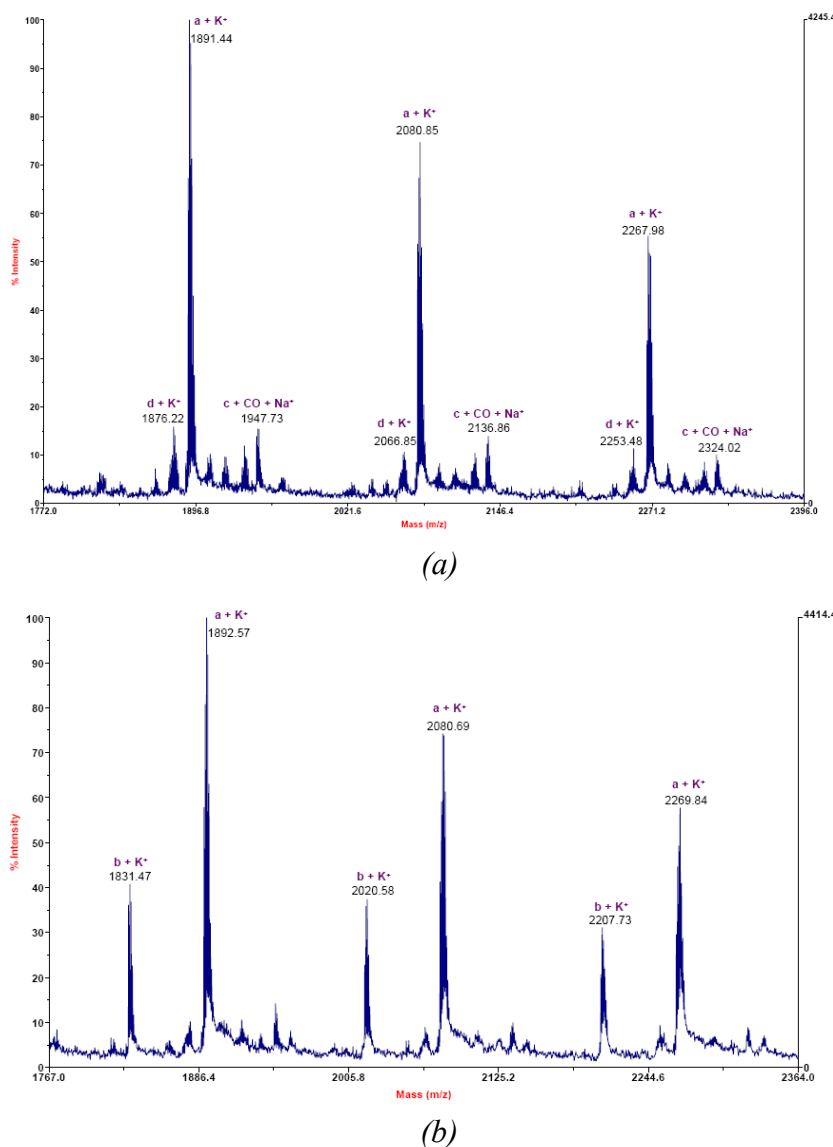
Figure 3.12. MALDI-TOF mass spectra of the CO/TBS polyketone synthesis using **L3b** as catalyst *(a)* in liquid expanded CO_2 (entry 4 Table 3.3), *(b)* in TFE (entry 9, Table 3.3).

In the case of the polymers obtained with styrene as comonomer, the mass spectra of the polyketones obtained with precatalysts **L2b** in liquid expanded CO_2 and TFE showed also the signal corresponding to chain a (Figure 3.13a and b). In liquid expanded CO_2 the mass spectra showed also peaks corresponding to double carbonylation termination mechanism (chain c + CO) with relative high intensity (Figure 3.13a). When the catalysis was run in TFE as solvent, contribution of chain b, which involves trifluoroethanol as an initiator, was also observed (Figure 3.13b).

Dicationic Pd(II) complexes for CO/vinyl arenes in compressed CO₂ and TFE
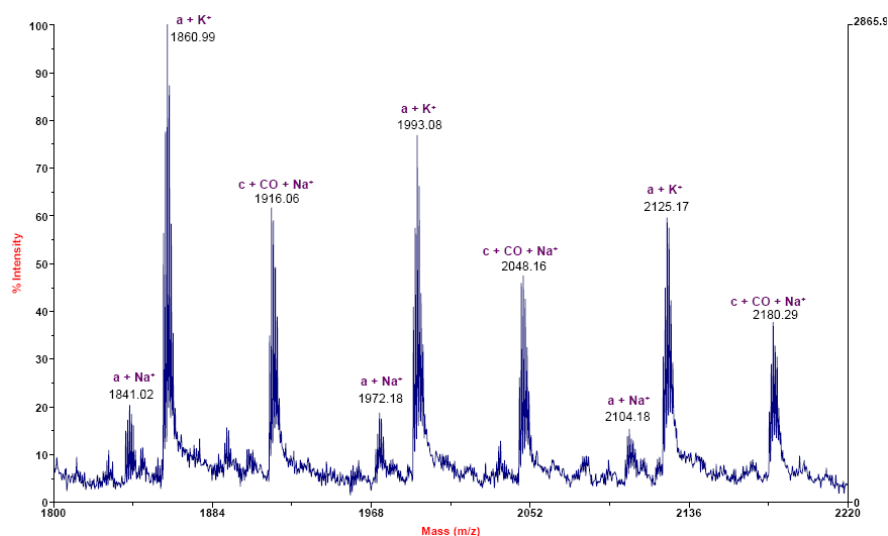
(a)
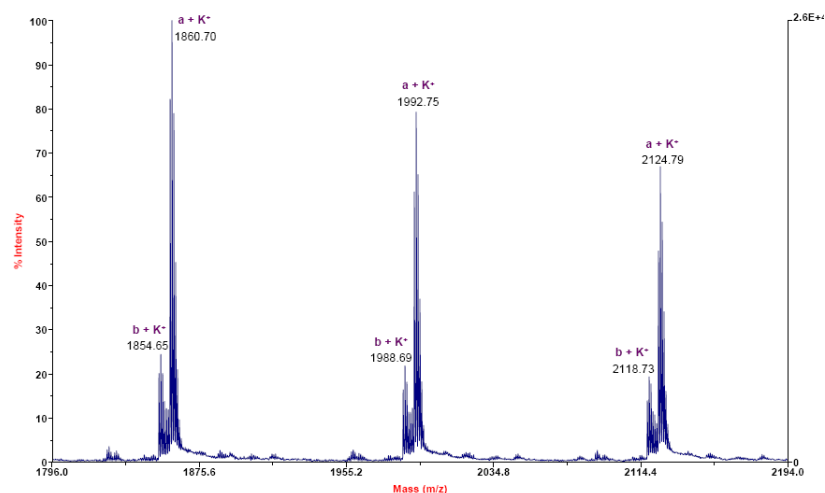
(b)

Figure 3.13. MALDI-TOF mass spectra of the CO/ST polyketone synthesis using **L2b** as catalyst (entry 2 Table 3.4), *(a)* in liquid expanded CO_2; *(b)* in TFE (entry 6 Table 3.4).

In conclusion, according to the mass spectra of the polyketones obtained with TBS in liquid expanded CO_2 the mechanism does not involve the trifluroethanol as an initiator but probably as a stabilising agent. When a less reactive substrate ST is used species with double carbonylation increased considerably when liquid expanded CO_2 was used.

3.3 Conclusion

We have synthesised a new family of perfluorinated bipyridine ligands (**L1-L3**) and studied their coordination chemistry towards palladium (II) and rhodium (I) complexes. Palladium complexes **L2b** and **L3b** showed different species in solution attributed to the different disposition of the carbonyl group in the ester function. The rhodium (I) complexes with these nitrogen ligands (**L1-L3c-d**) have been prepared and characterised by NMR, FTIR and MALDI-TOF. The FTIR spectroscopy studies of the Rh-carbonyl derivatives show that the perfluorinated ligands have similar electronic properties than the non perfluorinated ones due to the insulation effects of alkyl chains with a slightly differences between both families with and without ester function. Finally, the carbon monoxide/4-*tert*-butylstyrene copolymerisation and CO/styrene copolymerisation catalysed with palladium dicationic complexes containing perfluorinated ligands has been successfully achieved using compressed CO_2 as a solvent, productivities up to 6.1 kg CP·g Pd^{-1}, 222000 of molecular weight and 90% of stereoregularity in CO/TBS have been obtained with catalyst precursor **L3b**. These results demonstrate that CO_2 can be used as a green and sustainable medium for this reaction.

3.4 Experimental section

General Comments. Commercial available $Na_2[PdCl_4]$ (Johnson Matthey), ligands **A'** and **L1'** (Sigma-Aldrich) and methanol (Merck) were used without further purification for synthetic and spectroscopic purposes. **L2'**[30,31] and **L3'**[30,31] were prepared following the procedure described by Shan *et al*.[30] 2,2,2-Trifluoroethanol and dichloromethane (Alfa-Aesar) were purified by distillation with CaH_2 and stored under inert atmosphere. Carbon monoxide (CP grade, 99.0%) was supplied by Westfalen and Air Liquide. Carbon dioxide (CO_2, CP grade 5.3 and SCF grade 99.995 %) was supplied by Praxair and Air Products. **IR spectra** (range 4000-400 cm^{-1}) were recorded on a Midac Grams/386 spectrometer in KBr pellets or dichloromethane solution (when indicated). **NMR spectra** were recorded at 400 MHz Varian, with tetramethylsilane (^{1}H NMR and ^{13}C NMR) and fluoroform (^{19}F) as the internal standards. **MALDI-TOF measurements of complexes and polymers** were performed on a Voyager-DE-STR (Applied Biosystems, Franingham, MA) instrument equipped with a 337 nm nitrogen laser. All spectra were acquired in the positive ion reflector mode. 2,5-

Dicationic Pd(II) complexes for CO/vinyl arenes in compressed CO₂ and TFE

dihydroxybenzoic acid (DHB) was used as matrix for complexes. The matrix was dissolved in MeOH at a concentration of 10 mg·mL^{-1}. The complex was dissolved in CH$_2$Cl$_2$ (50 mg·L^{-1}). The matrix and the samples were premixed in the ratio 2:1 (Matrix:sample) and then the mixture was deposited (1 µL) on the target. For each spectrum 100 laser shots were accumulated. Ditranol was used as matrix for polymers (25 mg/mL in THF + 1 mg/mL KTFA). Copolymers (5 mg) were dissolved in CHCl$_3$ (1 mL) and a portion (5 µL) of this solution was added to 3 times the volume of the matrix solution (15 µL). About 1 µL of the resulting solution was deposited on the stainless steel sample holder and allowed to dry before introduction into the mass spectrometer. Three independent measurements were made for each sample. **Molecular weight measurements of TBS polyketones:** The molecular weights (Mw) of copolymers and the molecular weight distributions (Mw/Mn) were determined by gel permeation chromatography versus polystyrene standards. Measurements were made in THF on a Millipore-Waters 510 HPLC Pump device using three-serial column system (MZ-Gel 100Å, MZ-Gel 1000 Å, MZ-Gel 10000 Å linear columns) with UV-Detector (ERC-7215) and IR- Detector (ERC-7515a). The software used to get the data was NTeqGPC 5.1. Samples were prepared as follow: 5 mg of the copolymer was solubilised with 2 mL of tetrahydrofuran (HPLC grade) stabilised with toluene (HPLC grade). **Molecular weight measurements of ST polyketones:** The molecular weights (Mw) of styrene copolymers and the molecular weight distributions (Mw/Mn) were determined by gel permeation chromatography versus polymethylmethacrylate (PMMA) standards in the Servei de Recursos Cientifics from the University of Barcelona. Measurements were made in hexafluoroisopropanol (HFIP) on a Alliance-Waters 2695 HPLC Pump device using PSS PFG analytical 1000 Å rigid column with IR- Detector (Water-2414). The software used to get the data was Empower supplied by Water. Samples were prepared as follow: 2.0 mg of the copolymer was solubilised with 2 mL of hexafluoroisopropanol (HPLC grade).

Copolymerisation reactions in CO$_2$ as solvent. The catalytic experiments were performed in an 11 mL stainless steel autoclave. The catalyst was weight and introduced into the purged autoclave. Then a solution of substrate and the alcohol was added under argon atmosphere. The autoclave was pressurized with CO and CO$_2$ and heated to the temperature desired. After reaction time, the autoclave cooled down and depressurised

and the product was redissolved in 5 mL of CH_2Cl_2. The copolymer was precipitated by pouring the reaction solution into rapidly stirred methanol (70 mL). The polymer was filtered, washed with methanol and dried.

Copolymerisation reactions in TFE as solvent. Copolymerization reactions were carried out in a 100 mL Bergoff reactor equipped with a magnetic stirrer at 30 atmosphere of CO. After introduction of the catalyst precursor **L1b – L3b** ($2.2 \cdot 10^{-4}$ M or $5.4 \cdot 10^{-3}$ mmol catalyst) into the purged autoclaved, the solvent and substrate were added under argon atmosphere. The autoclave was pressurized with carbon monoxide and heated to the desired temperature. After the 24 hours, the reactor was vented out and the reaction mixture was poured into stirred methanol (100 mL). The polymer was filtered off, washed with methanol and dried under vacuum.

^{13}C NMR CO/*tert*-butylstyrene: (100.5 MHz, CDCl$_3$, 298 K): δ 208.0–206.5 (broad, CO), 150.0, 149.8, 134.6, 134.3 (C$_{ipso}$), 128.2, 125.8, 125.6 (C$_{arom}$), 52.9 (CH), 44.5-43.0 (broad, CH$_2$), 34.5 (C$_{tertbutyl}$) and 31.5 (CH$_3$); CO/styrene: (100.5 MHz, HFIP + CDCl$_3$, 298 K) δ 209.5–210.4 (broad, CO), 136.5, 136.1, 135.8, 135.3 (C$_{ipso}$), 129.4,128.3, 128.0 (C$_{arom}$), 53.5 (CH) and 42.3–44.5 (broad, CH$_2$).

3.4.1 Synthesis of ligands and complexes

5-[4-(perfluorooctyl)butyl]-5'-methyl-2,2'-bipyridine (L1).
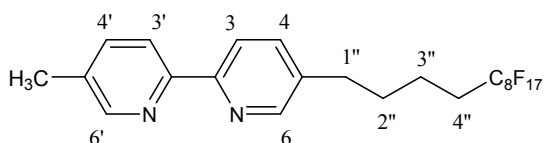
A solution of n-butyllithium 1.6 M in hexane (6 mL, 9.5 mmol, 3.5 eq) was added, via a syringe, to a solution of diisopropylamine (1.47 mL, 20.5 mmol) in tetrahydrofuran (3 mL) at -78°C. The solution was stirred for 10 min. at -78 °C and 5,5'-dimethyl-2,2'-bipyridine (0.5 g, 2.7 mmol) in 40 mL of tetrahydrofuran was then added drop wise. The dark brown solution was stirred at -78 °C for 1h. Then, 3-perfluorooctyl-1-iodopropane (3.77 g, 6.42 mmol) in 25 mL of tetrahydrofuran was added slowly via syringe at -78 °C. The brown solution was stirred for 5h at -78 °C and at room temperature overnight. The solvent was removed under reduced pressure, washed with

Dicationic Pd(II) complexes for CO/vinyl arenes in compressed CO₂ and TFE

60 mL of water and purified by soxhlet extraction in methanol. The methanol fraction was evaporated to obtain the product as a light-brown solid, 0.81 g (Yield 46 %).

HR MASS MALDI-TOF calc for $(C_{23}H_{17}F_{17}N_2)$ *m/z*: 644.1115 $[M^+]$, found *m/z*: 644.6413 $[M^+]$.

^{1}H NMR (300 MHz, CDCl$_3$): δ 1.71 (4H, m, $(CH_2)^{2'',3''}$), 2.11 (2H, m, $(CH_2)^{4''}$), 2.40 (3H, s, CH$_3$), 2.73 (2H, t, $(CH_2)^{1''}$, $J = 7.35$ Hz), 7.64 (1H, d, $(CH)^{4'}$, $J = 8.1$ Hz), 7.65 (1H, d, $(CH)^4$, $J = 8.1$ Hz), 8.24 (1H, d, $(CH)^{3'}$, $J = 8.1$ Hz), 8.28 (1H, d, $(CH)^3$, $J = 8.1$ Hz), 8.51 (2H, s, $(CH)^{6,6'}$); ^{13}C NMR (75.43 MHz, CDCl$_3$): δ 18.6 (CH$_3$), 20.3 $(C^{3''}H_2)$, 30.9 $(C^{2''}H_2)$, 31.1 $(C^{4''}H_2)$, 32.9 $(C^{1''}H_2)$, 110-120 (CF$_2$ – CF$_3$), 120.6 (C^4H), 120.7 (C^4H), 137.3 $(C^{3'}H)$, 134.0 $(C^{2'})$, 138.0 (C^3H), 137.6 (C^2), 149.6 $(C^{6'}HN)$, 150.1 (C^6HN), 153.8 $(C^{4'})$, 154.5 (C^4); ^{19}F NMR (376.3 MHz, CDCl$_3$): δ -126.58 (CF$_2$), -123.97 (CF$_2$), -123.19 (CF$_2$), -122.40 (CF$_2$), -122.2 (CF$_2$), -114.82 (CF$_2$), -81.19 (CF$_3$).

4,4'-bis[3-(perfluorooctyl)propanoxy]-carbonyl-2,2'-bipyridine (L2).
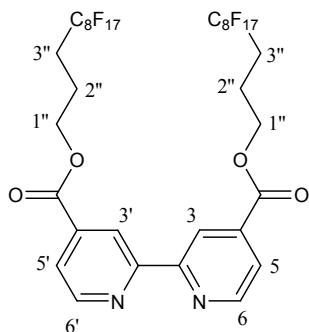
2,2'-bipyridine-4,4'-dicarboxylic acid[24] (525 mg, 2.15 mmol) was suspended in tionyl chloride (8 mL, 43 mmol, 20 eq) and refluxed (78°C) under nitrogen until complete solubilisation of the diacid (about 24 h). The excess of tionyl chloride was removed by reducing pressure. The resulting white powder was dissolved in dry dichloromethane (10 mL) and was added drop wise to a solution of 3-(perfluorooctyl)propanol (2.6 g, 5.4 mmol, 2.5 eq) in dry dichloromethane (30 mL) and triethylamine (1.2 mL, 8.6 mmol, 4 eq).[25] The mixture was refluxed for 6 h and stirred at room temperature for 12 h. After removal of dichloromethane, the obtained powder was washed with water, filtered under suction, recrystallised from dichloromethane and washed three times with pentane to afford a pale-white powder, 0.57 g (Yield 23 %). The pentane solution was

evaporated and the non reacted perfluorinated alcohol was recovered and recrystallised with dichloromethane and hexane (0.96 g).

HR MASS MALDI-TOF calc for ($C_{34}H_{18}F_{34}N_2O_4$) *m/z*: 1164.0718 [M^+], found *m/z*: 1164.4781 [M^+]. IR $\nu(COO^-)$ 1731 cm^{-1}.

^{1}H NMR (400 MHz, CDCl$_3$): δ (ppm) 2.18 (4H, m, $(CH_2)^{3''}$), 2.30 (4H, m, $(CH_2)^{2''}$), 4.49 (4H, t, $(CH_2)^{1''}$, $^3J_{H-H}$ = 6Hz), 7.90 (2H, d, $(CH)^{5,5'}$, $^3J_{H5-H6}$ = 4Hz), 8.88 (2H, d, $(CH)^{6,6'}$, $^3J_{H6-H5}$ = 4Hz), 8.96 (2H, s, $(CH)^{3,3'}$); ^{13}C NMR (100.57 MHz, CDCl$_3$): δ (ppm) 20.3 (s, $C^{3''}H_2$), 28.1 (s, $C^{2''}H_2$), 64.5 (s, $C^{1''}H_2$), 110-120 ($CF_2 - CF_3$), 120.7 (s, $C^{3,3'}H$), 123.4 (s, $C^{5,5'}H$), 138.5 (s, $C^{4,4'}$), 150.4 (s, $C^{6,6'}HN$), 156.7 (s, $C^{2,2'}$), 165.2 (s, CO); ^{19}F NMR (376.3 MHz, CDCl$_3$): δ (ppm) -126.5 (CF_2), -123.7 (CF_2), -123.1 (CF_2), -122.3 (CF_2), -122.1 (CF_2), -114.7 (CF_2), -81.1 (CF_3).

5,5'-bis[3-(perfluorooctyl)propanoxy]-carbonyl-2,2'-bipyridine (L3).
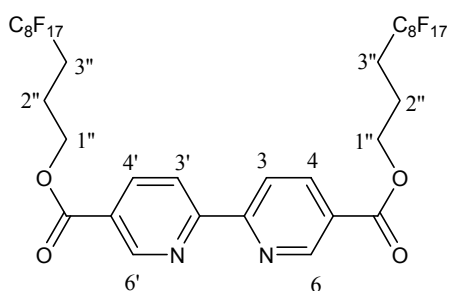
L3 was prepared following the same procedure as **L2** affording a white powder, 1.42 g (Yield 52 %); perfluorinated alcohol recovered (0.65 g).

HR MASS MALDI-TOF calc for ($C_{34}H_{18}F_{34}N_2O_4$) *m/z*: 1165.0796 [$M^+ + H^+$], found *m/z*: 1165.1724 [$M^+ + H^+$]. IR $\nu(COO^-)$ 1716 cm^{-1}.

^{1}H NMR (400 MHz, *d*-Toluene, 80°C): δ (ppm) 1.71 (4H, m, $(CH_2)^{3''}$), 1.91 (4H, m, $(CH_2)^{2''}$), 3.99 (4H, t, $(CH_2)^{1''}$, $^3J_{H-H}$ = 6.2Hz), 8.13 (2H, d, $(CH)^{3,3'}$, $^3J_{H3-H4}$ = 8Hz), 8.54 (2H, d, $(CH)^{4,4'}$, $^3J_{H4-H3}$ = 8Hz) 9.29 (2H, s, $(CH)^{6,6'}$); ^{19}F NMR (376.3 MHz, *d*-Toluene, 80°C): δ (ppm) -126.5 (CF_2), -123.6 (CF_2), -123.5 (CF_2), -123.0 (CF_2), -122.2 (CF_2), -122.9 (CF_2), -114.3 (CF_2), -81.1 (CF_3).

[PdCl$_2$(NN)](L1a-L3a). A solution of the desired ligand **L1-L3** (0.22 mmol) in 4 mL of tetrahydrofuran was added to a solution of Na$_2$[PdCl$_4$] (46.1 mg, 0.17 mmol) in 4 mL of methanol. The orange solution was stirred for 1h and a solid was formed. The complex

Dicationic Pd(II) complexes for CO/vinyl arenes in compressed CO₂ and TFE

was filtered off and washed with water, methanol and diethyl ether. The complex was dried at reduced pressure.

[PdCl₂(L1)] (L1a). Cream powder (Yield 99 %).

HR MASS MALDI-TOF calc for $(C_{23}H_{17}Cl_2F_{17}N_2Pd)$ *m/z*: 752.0315 [M⁺-2Cl], 897.8637 [M⁺-2H⁺+2K⁺], found *m/z*: 752.8941 [M⁺-2Cl], 897.8487 [M⁺-2H⁺+2K⁺].

[PdCl₂(L2)] (L2a). Pale yellow solid (Yield 99%).

HR MASS MALDI-TOF calc for $(C_{34}H_{18}Cl_2F_{34}N_2O_4Pd)$ *m/z*: 1269.9766 [M⁺-2Cl], 1417.8244 [M⁺-2H⁺+2K⁺], found *m/z*: 1270.4787 [M⁺-2Cl], 1417.0913 [M⁺-2H⁺+2K⁺]. IR (KBr) ν(COO⁻) 1736 cm⁻¹

[PdCl₂(L3)] (L3a). Pale yellow powder (Yield 91 %).

HR MASS MALDI-TOF calc for $(C_{34}H_{18}Cl_2F_{34}N_2O_4Pd)$ *m/z*: 1382.8920 [M⁺+2H⁺+K⁺], 1493.8615 [M⁺+K⁺+CF₃COO⁻], found *m/z*: 1382.8939 [M⁺+2H⁺+K⁺], 1493.9546 [M⁺+K⁺+CF₃COO⁻]. IR (KBr) ν(COO⁻) 1716 cm⁻¹

[PdCl₂(L2')] (L2'a) . Yellow-cream fine powder (Yield 82%).

HR MASS MALDI-TOF calc for $(C_{14}H_{12}Cl_2N_2O_4Pd)$ *m/z*: 527.8468 [M⁺+ 2K⁺], 565.9281 [M⁺+3H⁺+CF₃COO⁻], found *m/z*: 526.1460 [M⁺+ 2K⁺], 566.1768 [M⁺+3H⁺+CF₃COO⁻], IR (KBr) 1730 cm⁻¹ ν(COO⁻).

[PdCl₂(L3')] (L3'a). Pale yellow fine powder (Yield 99%).

HR MASS MALDI-TOF calc for $(C_{14}H_{12}Cl_2N_2O_4Pd)$ *m/z*: 445.8882 [M⁺], 527.8469 [M⁺+ 2·K⁺], found *m/z*: 445.1522 [M⁺], 526.1670 [M⁺+ 2·K⁺]. IR (CH₂Cl₂) 1724 cm⁻¹ ν(COO⁻), IR (KBr) 1726 cm⁻¹ ν(COO⁻).

[Pd(N-N)₂][BArF]₂ (L1b-L3b). To a suspension of [PdCl₂(N-N)] (**L1a-L3a**) (0.072 mmol) in 20 mL of dichloromethane, a solution of the ligand (**L1-L3** (0.076 mmol) and sodium tetrakis 3,5-(trifluoromethyl)phenyl borate (128.4 mg, 0.145 mmol) in 10 mL of dichloromethane were added slowly. The mixture was heated for 1h at 40ºC. The product was filtered off over celite and the solvent was removed under reduced

pressure. The product obtained as an oil was triturated in pentane and a solid was obtained.

[Pd(L1)$_2$][BArF]$_2$ (L1b). Pale brown solid (Yield 53 %)

HR MASS MALDI-TOF calc for (C$_{110}$H$_{58}$B$_2$F$_{82}$N$_4$Pd) *m/z*: 1397.1521 [M$^+$-2BArF], found *m/z*: 1397.3773 [M$^+$-2BArF].

^{1}H NMR (400 MHz, CD$_2$Cl$_2$): δ (ppm) 1.63 (4H, m, (CH$_2$)$^{2''}$), 1.71 (4H, m, (CH$_2$)$^{3''}$), 2.13 (4H, m, (CH$_2$)$^{4''}$), 2.40 (6H, s, CH$_3$), 2.72 (4H, m, (CH$_2$)$^{1''}$), 7.55 (8H, br, H^{para} BArF), 7.73 (16H, br, H^{orto} BArF), 7.90-8.00 (4H, m, CH$^{4',4,3',3}$), 8.51 (2H, d, CH$^{6,6'}$, $^4J_{\text{H-H}}$ = 8 Hz); ^{19}F NMR (376.3 MHz, DMSO-*d*): δ (ppm) -126.2 (CF$_2$), -123.5 (CF$_2$), -122.9 (CF$_2$), -122.2 (CF$_2$), -113.7 (CF$_2$), -80.7 (CF$_3$), - 62.0 (CF$_3$, BArF).

[Pd(L2)$_2$][BArF]$_2$ (L2b). Pale brown solid (Yield 92 %).

HR MASS MALDI-TOF calc for (C$_{132}$H$_{60}$B$_2$F$_{116}$N$_4$O$_8$Pd) *m/z*: 2434.0499 [M$^+$-2BArF], found *m/z*: 2434.2235 [M$^+$-2BArF]. IR ν(COO$^-$) 1742 and 1713 cm^{-1}

^{1}H NMR (400 MHz, 298 K, CDCl$_3$): ratio I:II = 1:1; δ (ppm) 2.17 (16H, m, (CH$_2$)$^{2'',3''}$, **I** and **II**), 4.51 (4H, t, (CH$_2$)$^{1''}$, $^3J_{\text{H-H}}$ = 6.4Hz, **II**), 4.57 (4H, t, (CH$_2$)$^{1''}$, $^3J_{\text{H-H}}$ = 6.2Hz, **I**), 8.03 (2H, dd, CH^5, $^3J_{\text{H5-H6}}$ = 5.6Hz, $^4J_{\text{H5-H3}}$ = 1.6Hz, **II**), 7.46 (16H, br, H^{para} BArF), 7.66 (32H, br, H^{orto} BArF), 8.20 (2H, dd, CH^5, $^3J_{\text{H5-H6}}$ = 5.2Hz, $^4J_{\text{H5-H3}}$ = 1.6Hz, **I**), 8.52 (2H, d, CH^6, $^3J_{\text{H6-H5}}$ = 5.2Hz, **I**), 8.70 (2H, d, CH^3, $^4J_{\text{H3-H5}}$= 1.6Hz, **II**), 8.77(2H, d, CH^6, $^3J_{\text{H6-H5}}$ = 5.6Hz, **II**), 8.77(2H, s, CH^3, **I**); ^{19}F NMR (376.3 MHz, CDCl$_3$): δ (ppm) -127.5 (CF$_2$'), -126.7 (CF$_2$), -124.6 (CF$_2$'), -123.9 (CF$_2$), -123.2 (CF$_2$), -123.2 (CF$_2$'), -122.5 (CF$_2$'), -122.2 (CF$_2$), -115.5 (CF$_2$'), -114.8 (CF$_2$), -82.4 (CF$_3$'), -81.2 (CF$_3$), -63.4 (CF$_3$', BArF), -62.9 (CF$_3$, BArF).

[Pd(L3)$_2$][BArF]$_2$ (L3b). Pale brown solid (Yield 61%).

HR MASS MALDI-TOF calc for (C$_{132}$H$_{60}$B$_2$F$_{116}$N$_4$O$_8$Pd) *m/z*: 2434.0499 [M$^+$-2BArF], found *m/z*: 2434.2408 [M$^+$-2BArF]. IR ν(COO$^-$) 1741.5 and 1718 cm^{-1}.

^{1}H NMR (400 MHz, 298 K, CDCl$_3$): ratio I:II = 1:1; δ (ppm) 2.08 (16H, m, (CH$_2$)$^{2'',3''}$ **I** and **II**), 2.25 (16H, m, (CH$_2$)$^{2''-3''}$ 4.42 (8H, t, (CH$_2$)$^{1''}$, $^3J_{\text{H-H}}$ = 6.2 Hz, **II**), 4.52 (8H, t, (CH$_2$)$^{1''}$, $^3J_{\text{H-H}}$ = 9.6 Hz, **II**) 7.48 (16H, br, H^{para} BArF), 7.68 (32H, br, H^{orto} BArF), 7.82 (2H, d, CH^3, $^3J_{\text{H3-H4}}$ = 8Hz, **II**), 7.96 (2H, m, CH^3, **I**), 8.52 (4H, d, CH^4, $^3J_{\text{H4-H3}}$ = 8Hz,

Dicationic Pd(II) complexes for CO/vinyl arenes in compressed CO_2 and TFE

II), 8.63 (4H, d, CH^4, $^3J_{H4-H3}$ = 8Hz, **I**), 9.15 (4H, s, CH^6, **II**) 9.20 (4H, s, CH^6, **I**); ^{19}F NMR (376.3 MHz, CDCl$_3$): δ (ppm) -126.7 (CF_2), -123.9 (CF_2), -123.3 (CF_2), -122.5 (CF_2), -122.3 (CF_2), -114.9 (CF_2), -81.3 (CF_3), -62.9 (CF_3, BArF).

[Pd(L2')$_2$][BArF]$_2$ (L2'b). Pale orange solid (Yield 57%).

HR MASS MALDI-TOF calc for ($C_{92}H_{48}B_2F_{48}N_4O_8Pd$) *m/z*: 650.0635 [$M^+$ - 2·BArF], found *m/z*: 650.2218 [M^+ - 2·BArF]. IR (CH$_2$Cl$_2$) 1740 cm^{-1} $v(COO^-)$, (KBr) 1742 cm^{-1} $v(COO^-)$.

^1H NMR (400 MHz, 298 K, CDCl$_3$): ratio I:II:III = 1.0:0.2:0.3; δ (ppm) 4.02 (24H, s, CH_3, **I** and **III**), 4.07 (12H, s, CH_3, **II**), 7.45 (24H, br, BArF), 7.65 (48H, br, BArF), 8.05 (4H, d, $(CH)^5$, $^3J_{H5-H6}$ = 5.2Hz, **I** and **II**), 8.09 (4H, br, $(CH)^5$, **III**), 8.15 (4H, d, $(CH)^5$, $^3J_{H5-H6}$ = 4.8Hz, **II**), 8.66 (4H, s, $(CH)^3$, **II**), 8.72 (4H, s, $(CH)^3$, **I**), 8.79 (4H, d, $(CH)^6$, $^3J_{H6-H5}$ = 5.2 Hz, **I**), 8.94 (4H, d, $(CH)^6$, $^3J_{H6-H5}$ = 5.2 Hz, **III**), 9.49 (4H, d, $(CH)^6$, $^3J_{H6-H5}$ = 4.8 Hz, **II**); ^{19}F NMR (376.3 MHz, CDCl$_3$): δ (ppm) -62.8 (CF_3, BArF).

[Pd(L3')$_2$][BArF]$_2$ (L3'b). Mustard solid (Yield 49%).

HR MASS MALDI-TOF calc for ($C_{92}H_{48}B_2F_{48}N_4O_8Pd$) *m/z*: 650.0635 [$M^+$-2·BArF], found *m/z*: 650.2895 [M^+-2·BArF]. IR (CH$_2$Cl$_2$) 1739 cm^{-1} $v(COO^-)$, (KBr) 1742 cm^{-1} $v(COO^-)$.

^1H NMR (400 MHz, 298 K, CDCl$_3$): ratio I:II:III = 1.0:0.2:0.2; δ (ppm) 3.94 (12H, s, CH_3, **I**), 3.97 (12H, s, CH_3, **III**), 4.02 (12H, s, CH_3, **II**), 7.86 (4H, d, $(CH)^3$, $^3J_{H3-H4}$ = 6.4 Hz, **III**), 7.92 (4H, d, $(CH)^3$, $^3J_{H3-H4}$ = 8.0 Hz, **I**), 8.13 (4H, d, $(CH)^3$, $^3J_{H3-H4}$ = 8.4 Hz, **II**), 8.56 (4H, d, $(CH)^4$, $^3J_{H4-H3}$ = 8.0Hz, **I** and **III**), 8.72 (4H, d, $(CH)^4$, $^3J_{H4-H3}$ = 8.4 Hz, **II**), 9.15 (4H, s, $(CH)^6$, **III**), 9.20 (4H, d, $(CH)^6$, **I**), 9.64 (4H, s, $(CH)^6$, **II**); ^{19}F NMR (376.3 MHz, CDCl$_3$): δ (ppm) -62.8 (BArF).

[Rh(cod)(N-N)][PF$_6$] (L1c-L3c, L1'c-L3'c). The N-ligand (**L1-L3, L1'-L3'**) (0.03 mmol) was added to a solution of the complex [Rh(cod)$_2$]PF$_6$ (13.96 mg, 0.03 mmol) in 2 mL of anhydrous dichloromethane. The solution changed from burgundy to orange. Then it was stirred for 5 minutes. Diethyl ether was added to the solution to afford the corresponding solid, which was filtered off, washed with cold diethyl ether and dried under vacuum.

[Rh(cod)(L1)](PF$_6$) (L1c). Brown solid (Yield 90%).

HR MASS MALDI-TOF calc for (C$_{31}$H$_{29}$F$_{23}$N$_2$PRh) *m/z*: 855.1109 [M$^+$-PF$_6$], 871.1296 [M$^+$-2H$^+$+NH$_4^+$], found *m/z*: 855.4879 [M$^+$-PF$_6$], 871.4982 [M$^+$-2H$^+$+NH$_4^+$].

^{1}H NMR (400 MHz, CDCl$_3$): δ (ppm) 1.53 (m, 2H, (CH$_2$)$^{4''}$), 1.65 (m, 4H, (CH$_2$)$^{3'',2''}$) 2.10 (d, 4H, (CH$_2$)^{COD}, *J* = 8Hz), 2.36 (s, 3H, CH$_3$), 2.65 (m, 4H, (CH$_2$)^{COD}), 2.67 (t, 2H, (CH$_2$)$^{1''}$, $^3J_{H-H}$ = 8.4Hz), 4.49 (m, 4H, (CH)^{COD}), 7.43 (s, 2H, (CH)$^{6,6'}$), 7.90 (d, 1H, (CH)^4, $^3J_{H4-H3}$ = 8Hz), 7.93 (d, 1H, (CH)$^{4'}$, $^3J_{H4'-H3'}$ = 8.4Hz), 8.16 (d, 1H, (CH)^3, $^3J_{H3-H4}$ = 8Hz), 8.20 (d, 1H, (CH)$^{3'}$, $^3J_{H3'-H4'}$ = 8.4Hz); ^{19}F NMR (376.3 MHz, CDCl$_3$): δ (ppm) -126.5 (CF$_2$), -123.9 (CF$_2$), -123.1 (CF$_2$), -122.4 (CF$_2$), -122.1 (CF$_2$), -114.7 (CF$_2$), -81.1 (CF$_3$), -73.5 (PF$_6$, $^1J_{P-F}$ = 715 Hz).

[Rh(cod)(L2)](PF$_6$) (L2c). Brown-orange solid (Yield 24%).

HR MASS MALDI-TOF calc for (C$_{42}$H$_{30}$F$_{40}$N$_2$O$_4$PRh) *m/z*: 1375.0712 [M$^+$-PF$_6$], found *m/z*: 1375.5528 [M$^+$-PF$_6$]. IR ν(COO$^-$) 1741 cm^{-1} (ATR).

^{1}H NMR (400 MHz, CDCl$_3$): δ (ppm) 2.22 (m, 8H, (CH$_2$)$^{3''}$ overlapped (CH$_2$)^{COD}), 2.29 (m, 4H, (CH$_2$)$^{2''}$), 2.64 (m, 4H, (CH$_2$)^{COD}), 4.56 (t, 4H, (CH$_2$)$^{1''}$, $^3J_{H-H}$ = 6.4Hz), 4.69 (m, 4H, (CH)^{COD}), 8.01 (d, 2H, (CH)^3, $^3J_{H3-H4}$ = 5.6Hz), 8.19 (d, 2H, (CH)^4, $^3J_{H4-H3}$ = 5.6Hz), 8.80 (s, 2H, (CH)^6); ^{19}F NMR (376.3 MHz, CDCl$_3$): δ (ppm) -126.6 (CF$_2$), -123.7 (CF$_2$), -122.4 (CF$_2$), -122.2 (CF$_2$), -114.6 (CF$_2$), -81.2 (CF$_3$), -73.5 (PF$_6$, $^1J_{P-F}$ = 715 Hz).

[Rh(cod)(L3)](PF$_6$) (L3c). Salmon solid (Yield 32%).

HR MASS MALDI-TOF calc for (C$_{42}$H$_{30}$F$_{40}$N$_2$O$_4$PRh) *m/z*: 1374.0634 [M$^+$-H$^+$-PF$_6$], 1391.0899 [M$^+$ -PF$_6$-2H$^+$+NH$_4^+$], found *m/z*: 1374.4410 [M$^+$-H$^+$-PF$_6$], 1391.7397 [M$^+$ -PF$_6$-2H$^+$+NH$_4^+$]. IR ν(COO$^-$) 1731 cm^{-1} (ATR).

^{1}H NMR (400 MHz, CDCl$_3$): δ (ppm) 2.20 (m, 12H, (CH$_2$)$^{2'',3''}$ overlapped (CH$_2$)^{COD}), 2.65 (m, 4H, (CH$_2$)^{COD}), 4.49 (t, 4H, (CH$_2$)$^{1''}$, $^3J_{H-H}$ = 5.6Hz), 4.64 (m, 4H, (CH)^{COD}), 8.32 (s, 2H, (CH)^6), 8.69 (d, 2H, (CH)^4, $^3J_{H4-H3}$ = 8Hz), 8.74 (d, 2H, (CH)^3, $^3J_{H3-H4}$ = 8Hz); ^{19}F NMR (376.3 MHz, CDCl$_3$): δ (ppm) -126.5 (CF$_2$), -123.7 (CF$_2$), -123.1 (CF$_2$), -122.3 (CF$_2$), -122.1 (CF$_2$), -114.7 (CF$_2$), -81.1 (CF$_3$), -73.2 (PF$_6$, $^1J_{P-F}$ = 715 Hz).

Dicationic Pd(II) complexes for CO/vinyl arenes in compressed CO$_2$ and TFE

[Rh(L1')(cod)][PF$_6$] (L1'c). Schocking orange (Yield 89%).

HR MASS MALDI-TOF calc for (C$_{20}$H$_{24}$F$_6$N$_2$PRh) *m/z*: 395.0989 [M$^+$-PF$_6$], 582.0951 [M$^+$ +Na$^+$+NH$_4$$^+$ +H$^+$], found *m/z*: 395.3448 [M$^+$-PF$_6$], 582.4246 [M$^+$ +Na$^+$+NH$_4$$^+$ +H$^+$].

^{1}H NMR (300 MHz, CDCl$_3$): δ (ppm) 2.16 (4H, m, (CH$_2$)^{COD}), 2.42 (3H, s, CH$_3$-bpy), 2.63 (4H, br, (CH$_2$)^{COD}), 4.55 (4H, m, (CH$_2$)^{COD}), 7.49 (2H, br, (CH)^6), 7.98 (2H, d, (CH)^3, $^3J_{H3-H4}$ = 8.0Hz), 8.25 (2H, d, (CH)^4, $^3J_{H4-H3}$ = 8.0 Hz); ^{19}F NMR (376.3 MHz, CDCl$_3$): δ (ppm) -73.1 (PF$_6$, $^1J_{P-F}$ = 715 Hz).

[Rh(L2')(cod)][PF$_6$] (L2'c). Burgundy solid (Yield 91%).

HR MASS MALDI-TOF calc for (C$_{22}$H$_{24}$F$_6$N$_2$O$_4$PRh) *m/z*: 483.0786 [M$^+$-PF$_6$], found *m/z*: 483.3046 [M$^+$-PF$_6$]. IR (CH$_2$Cl$_2$) 1740 cm^{-1} ν(COO$^-$), (KBr) 1727 cm^{-1} ν(COO$^-$).

^{1}H NMR (400 MHz, CDCl$_3$): δ (ppm) 2.13 (m, 4H, (CH$_2$)^{COD}), 2.57 (m, 4H, (CH$_2$)^{COD}), 4.02 (6H, s, CH$_3$), 4.65 (m, 4H, (CH)^{COD}), 7.97 (2H, d, (CH)^6, $^3J_{H6-H5}$ = 6.0Hz), 8.14 (2H, dd, (CH)^5, $^3J_{H5-H6}$ = 6.0Hz, $^4J_{H5-H3}$ = 1.2Hz), 8.67 (2H, d, (CH)^3, $^4J_{H3-H5}$ = 1.2Hz); ^{19}F NMR (376.3 MHz, CDCl$_3$): δ (ppm) -73.8 (PF$_6$, $^1J_{P-F}$ = 715 Hz).

[Rh(L3')(cod)][PF$_6$] (L3'c). Brown solid (Yield 94%).

HR MASS MALDI-TOF calc for (C$_{22}$H$_{24}$F$_6$N$_2$O$_4$PRh) *m/z*: 483.0786 [M$^+$-PF$_6$], found *m/z*: 483.2176 [M$^+$-PF$_6$]. IR (CH$_2$Cl$_2$) 1739 cm^{-1} ν(COO$^-$), (KBr) 1729 cm^{-1} ν(COO$^-$).

^{1}H NMR (400 MHz, CDCl$_3$): δ (ppm) 2.21 (4H, m, (CH$_2$)^{COD}), 2.66 (4H, m, (CH$_2$)^{COD}), 4.01 (6H, s, CH$_3$), 4.65 (4H, m, (CH)^{COD}), 8.32 (2H, s, (CH)^6), 8.70 (2H, d, (CH)^3, $^3J_{H3H-4}$ = 8.8Hz), 8.77 (2H, dd, (CH)^4, $^3J_{H4-H3}$ = 8.8Hz, $^4J_{H4-H6}$ = 1.4Hz); ^{19}F NMR (376.3 MHz, CDCl$_3$): δ (ppm) -73.6 (PF$_6$, $^1J_{P-F}$ = 715 Hz).

[Rh(CO)$_2$(N-N)][PF$_6$] (L1d-L3d, L1'd-L3'd). To a solution of [Rh(cod)(N-N)]PF$_6$ (**L1c-L3c, L1'c-L3'd**) (7.5 mmol) in 3 mL of dichloromethane was bubbled CO during 5 minutes. The solution changes to yellow colour indicating the formation of carbonyl species. Then diethyl ether was added to the solution to afford the corresponding solid, which was filtered off, washed with cold diethyl ether and dried under vacuum.

[Rh(L1)(CO)$_2$][PF$_6$] (L1d). Deep red solid (Yield 65 %).

HR MASS MALDI-TOF calc for (C$_{25}$H$_{19}$F$_{23}$N$_2$O$_2$PRh) *m/z*: 803.0068 [M$^+$ -PF$_6$], 972.9764 [M$^+$+Na$^+$], found *m/z*: 803.1718 [M$^+$-PF$_6$], 972.2365 [M$^+$+Na$^+$]. IR (CH$_2$Cl$_2$) 2099.9, 2042.3 and 2003 cm^{-1} ν(CO).

^{1}H NMR (400 MHz, CD$_2$Cl$_2$): δ (ppm) 1.75 (m, 4H, (CH$_2$)$^{2'',3''}$), 2.18 (m, 2H, (CH$_2$)$^{4''}$), 2.53 (s, 3H, CH$_3$), 2.84 (t, 2H, (CH$_2$)$^{1''}$, $^3J_{H-H}$ = 7.6 Hz), 8.12 (s, 2H, (CH)$^{6,6'}$), 8.21 (d, 1H, (CH)^4, $^3J_{H4-H3}$ = 8.8Hz), 8.24 (d, 1H, (CH)$^{4'}$, $^3J_{H4'-H3'}$ = 8.8Hz), 8.44 (s, 1H, (CH)^3), 8.46 (s, 1H, (CH)$^{3'}$); ^{19}F NMR (376.3 MHz, CD$_2$Cl$_2$): δ (ppm) -126.8 (CF$_2$), -124.2 (CF$_2$), -123.4 (CF$_2$), -122.5 (CF$_2$), -122.4 (CF$_2$), -115.0 (CF$_2$), -81.5 (CF$_3$), -73.4 (PF$_6$, $^1J_{P-F}$ = 715 Hz).

[Rh(L2)(CO)$_2$][PF$_6$] (L2d). Mauve solid (Yield 74 %).

HR MASS MALDI-TOF calc for (C$_{36}$H$_{20}$F$_{40}$N$_2$O$_6$PRh) *m/z*: 1471.9626 [M$^+$+2H$^+$], 1563.9217 [M$^+$+4Na$^+$], found *m/z*: 1471.7712 [M$^+$+2H$^+$], 1563.7707 [M$^+$+4Na$^+$]. IR (CH$_2$Cl$_2$) 2104.4, 2048.1cm^{-1} ν(CO), 1741 cm^{-1} ν(COO$^-$).

^{1}H NMR (400 MHz, CD$_2$Cl$_2$): δ (ppm) 2.13-2.27 (m, 8H, (CH$_2$)$^{3'',2''}$), 4.50 (t, 4H, (CH$_2$)$^{1''}$, $^3J_{H-H}$ = 6.4Hz), 8.20 (dd, 2H, CH^5, $^3J_{H5-H6}$ = 5.6Hz, $^4J_{H5-H3}$ = 1.6Hz), 8.78 (d, 2H, (CH)^3, $^4J_{H3-H5}$ = 1.6Hz), 8.83 (d, 2H, (CH)^6, $^3J_{H6-H5}$ = 5.6Hz) ^{19}F NMR (376.3 MHz, CD$_2$Cl$_2$): δ (ppm) -126.6 (CF$_2$), -123.7 (CF$_2$), -122.4 (CF$_2$), -122.3 (CF$_2$), -81.2 (CF$_3$), -73.5 (PF$_6$, $^1J_{P-F}$ = 715 Hz).

[Rh(L3)(CO)$_2$][PF$_6$] (L3d). Green bottle solid (Yield 55 %).

HR MASS MALDI-TOF calc for (C$_{36}$H$_{20}$F$_{40}$N$_2$O$_6$PRh) *m/z*: 1471.96266 [M$^+$+2H$^+$], 1563.9217 [M$^+$+4Na$^+$], found *m/z*: 1471.7712 [M$^+$+2H$^+$], 1563.7707 [M$^+$+4Na$^+$]. IR (CH$_2$Cl$_2$) 2104.8, 2046.2cm^{-1} ν(CO), 1738 cm^{-1} ν(COO$^-$).

^{1}H NMR (400 MHz, CDCl$_3$): δ (ppm) 2.20 (m, 4H, (CH$_2$)$^{3''}$), 2.28 (m, 4H, (CH$_2$)$^{2''}$), 4.54 (t, 4H, (CH$_2$)$^{1''}$, $^3J_{H-H}$ = 5.6Hz), 8.73 (d, 2H, (CH)^3, $^3J_{H3-H4}$ = 8Hz), 8.86 (d, 2H, (CH)^4, $^3J_{H4-H3}$ = 8Hz), 9.18 (d, 2H, (CH)^6); ^{19}F NMR (376.3 MHz, CDCl$_3$): δ (ppm) -126.5 (CF$_2$), -123.7 (CF$_2$), -123.1 (CF$_2$), -122.3 (CF$_2$), -122.1 (CF$_2$), -114.7 (CF$_2$), -81.2 (CF$_3$), -73.1 (PF$_6$, $^1J_{P-F}$ = 715 Hz).

Dicationic Pd(II) complexes for CO/vinyl arenes in compressed CO$_2$ and TFE

[Rh(L1')(CO)$_2$][PF$_6$] (L1'd). Ocher-colored solid (Yield 56 %).

HR MASS MALDI-TOF calc for (C$_{14}$H$_{14}$F$_6$N$_2$O$_2$PRh) *m/z*: 343.9948 [M$^+$-PF$_6$-2H$^+$], 512.9644 [M$^+$+Na$^+$], found *m/z*: 343.0752 [M$^+$-PF$_6$-2H$^+$], 512.1781 [M$^+$+Na$^+$]. IR (CH$_2$Cl$_2$) 2108, 2056 cm^{-1} ν(CO).

^{1}H NMR (300 MHz, CD$_2$Cl$_2$): δ (ppm) 2.53 (3H, s, CH$_3$-bpy), 8.10 (2H, d, (CH)^4, $^3J_{H5\text{-}H6}$ = 8.4Hz), 8.17 (2H, d, (CH)^3, $^3J_{H6\text{-}H5}$ = 8.0Hz), 8.46 (2H, s, (CH)^6). ^{19}F NMR (376.3 MHz, CD$_2$Cl$_2$): δ (ppm) -73.1 (PF$_6$, $^1J_{P\text{-}F}$ = 715 Hz).

[Rh(L2')(CO)$_2$][PF$_6$] (L2'd). Orange brownish solid (Yield 63 %).

HR MASS MALDI-TOF calc for (C$_{16}$H$_{14}$F$_6$N$_2$O$_6$PRh) *m/z*: 518.9410 [M$^+$-COOCH$_3$], 562.9308 [M$^+$-CH$_3$], 563.9387 [M$^+$+H$^+$-CH$_3$], found *m/z*: 519.2269 [M$^+$-COOCH$_3$], 563.2351 [M$^+$-CH$_3$], 564.2559 [M$^+$+H$^+$-CH$_3$]. IR (CH$_2$Cl$_2$) 2114, 2050 ν(CO), 1732 ν(COO$^-$) cm^{-1}.

^{1}H NMR (400 MHz, CDCl$_3$): δ (ppm) 4.11 (6H, s, CH$_3$), 8.26 (2H, dd, (CH)^5, $^3J_{H5\text{-}H6}$ = 5.6Hz, $^4J_{H5\text{-}H3}$ = 2.0Hz), 8.84 (2H, d, (CH)^3, $^4J_{H3\text{-}H5}$ = 2.0Hz), 8.89 (2H, dd, (CH)^6, $^3J_{H5\text{-}H6}$ = 5.6Hz, $^5J_{H6\text{-}H3}$ = 1.2Hz); ^{19}F NMR (376.3 MHz, CDCl$_3$): δ (ppm) -73.3 (PF$_6$, $^1J_{P\text{-}F}$ = 715 Hz).

[Rh(L3')(CO)$_2$][PF$_6$] (L3'd). Shocking yellow solid (Yield 84%).

HR MASS MALDI-TOF calc for (C$_{16}$H$_{14}$F$_6$N$_2$O$_6$PRh) *m/z*: 518.9410 [M$^+$-COOCH$_3$], 562.9308 [M$^+$-CH$_3$], 563.9387 [M$^+$+H$^+$-CH$_3$], found *m/z*: 519.2293 [M$^+$-COOCH$_3$], 563.2365 [M$^+$-CH$_3$], 564.2627 [M$^+$+H$^+$-CH$_3$]. IR (CH$_2$Cl$_2$) 2108, 2044 cm^{-1} ν(CO) 1733 cm^{-1} ν(COO$^-$).

^{1}H NMR (400 MHz, CDCl$_3$): δ (ppm) 4.07 (6H, s, CH$_3$), 8.78 (2H, d, (CH)^3, $^3J_{H3\text{-}H4}$ = 8.4Hz), 8.89 (2H, dd, (CH)^4, $^3J_{H4\text{-}H3}$ = 8.4Hz, $^4J_{H4\text{-}H6}$ = 1.6Hz), 9.18 (2H, s, (CH)^6); ^{19}F NMR (376.3 MHz, CDCl$_3$): δ (ppm) -73.1 (PF$_6$, $^1J_{P\text{-}F}$ = 715 Hz).

3.4.2 X-ray crystallography

Diffraction data for the structures reported were carried out on a Bruker Appex-II CCD diffractometer system with Mo Kα radiation (λ = 0.71073 Å). Cell refinement, indexing and scaling of the data sets were carried out using programs Apex-II (Bruker AXS, 2005). All the structures were solved by *SIR97* [42]and refined by Shelxl97 and the molecular graphics with *ORTEP-3* for Windows.[43] Crystal data and details of structure

refinements are reported in Table 3.5. All the calculations were performed using the *WinGX* publication routines.[44]

Table 3.5. Crystallographic data and details of structure refinements for compounds **L3c** and **L3'c**.

	L3c	L3'c
Molecular formula	$C_{42}H_{30}F_{40}N_2O_4PRh$	$C_{22}H_{24}F_6N_2O_4PRh$
Molecular weight	1520.56	628.31
Crystal system	Monoclinic	Monoclinic
Space group	$P2_1/n$	$C2/c$
Shape and colour	Prism, colourless	Prism, colourless
Temp. (K)	100	100
Radiation (λ, Å)	Mo $K\alpha$ ()	Mo $K\alpha$ ()
a (Å)	21.8355 (15)	26.7982 (12)
b (Å)	10.5880 (5)	11.4909 (6)
c (Å)	25.1135 (17)	14.8735 (8)
β (º)	115.278 (2)	94.895 (2)
Volume ($Å^3$)	5250.1 (6)	4563.4 (4)
Z	4	8
D_c (Mg·m^{-3})	1.924	1.829
F (000)	2992	2528.0
Crystal dimensions (mm)	0.75 x 0.39 x 0.01	0.18 x 0.1 x 0.04
μ (Mo $K\alpha$) (mm^{-1})	0.54	0.90
θ_{max} (º)	21.1	26.0
Reflections collected	29682	21504
Unique reflections	5689	4482
$R_{int.}$	0.142	0.070
Observed [$I > 2\sigma(I)$]	3373	3357
Parameters	594	339
R$_1$ [$I > 2\sigma(I)$]	0.146	0.045
wR$_2$	0.385	0.114
$\Delta\rho$ (e/ $Å^3$)	2.05, -1.31	1.55, -0.59

Dicationic Pd(II) complexes for CO/vinyl arenes in compressed CO₂ and TFE

3.5 Supporting Information Available

Characterisation analysis of all complexes (NMR spectra, IR spectra and MALDI-TOF), characterisation of polymers by NMR spectroscopy and MALDI-TOF mass spectrometry, CIF files giving crystallographic data for **L3c** and **L3'c** are available in the supporting information as an electronic file.

3.6 References

[1] *(a)* Sen, A. *Acc. Chem. Res.* **1993**, *26*, 303-310. *(b)* Sen, A. (Ed.) in *Catalytic synthesis of alkene-carbon monoxide copolymers and cooligomers*, Kluwer Academic Publishers, **2003**, Dordrecht (the Netherland).

[2] Drent, E.; Budzelaar, P. H. M. *Chem. Rev.* **1996**, *96*, 663-681.

[3] Nozaki, K.; Hiyama, T. *J. Organomet. Chem.* **1999**, *576*, 248-253.

[4] Bianchini, C.; Meli, A. *Coord. Chem. Rev.* **2002**, 225, 35-66.

[5] García Suárez, E. J.; Godard, C.; Ruiz, A.; Claver, C. *Eur. J. Inorg. Chem.* **2007**, 2582-2593.

[6] Durand, J.; Milani, B. *Coord. Chem. Rew.* **2006**, *250*, 542-560.

[7] Sen, A.; Jiang, Z.; Chen, J. T. *Macromolecules.* **1989**, *22*, 2012-2014.

[8] *(a)* Drent, E. *Eur. Pat. Appl.* **1986**, *229*, 408. *(b)* Brookhart, M.; Rix, F. C.; DeSimone, J, M. *J. Am. Chem. Soc.* **1992**, *114*, 5894-5895. *(c)* Milani, B.; Anzilutti, A.; Vicentini, L.; Sessanta, A.; Zangrado, E.; Geremia, S.; Mestroni, G. *Organometallics* **1997**, *16*, 5064-5075. *(d)* Sommazzi, A.; Garbassi, F.; Mestroni, G.; Milani, B. *US Patent* 5,310,871, **1994.**

[9] Bastero, A.; Claver, C.; Ruiz, A.; Castillón, S.; Daura, E.; Bo, C.; Zangrado, E. *Chem. Eur. J.*, **2004**, *10*, 3747-3760.

[10] *(a)* Scarel, A.; Milani, B.; Zangrando, E.; Stener, M.; Furlan, S.; Fronzoni, G.; Mestroni, G.; Gladiali, S.; Carfagna, C.; Mosca, L. *Organometallics* **2004**, *23*, 5593-5605. *(b)* Milani, B.; Scarel, A.; Mestroni, G.; Gladiali, S.; Taras, R.; Carfagna, C.; Mosca, L. *Organometallics* **2002**, *21*, 1323-1325.

[11] Leitner, W., *Acc. Chem. Res.* **2002**, *35*, 746-756.

[12] Kendall, J. L.; Canelas, D. A; Young, J. L.; DeSimone, J. M. *Chem. Rev.* **1999**, *99*, 543-563.

[13] Kemmere M. F.; Meyre, T. *Supercritical carbon dioxide in polymer*, Weinheim : Wiley-VCH, **2005.**

[14] Cooper, A. I., *J. Mater. Chem.;* **2000**, 10, 207-234.

[15] Erdmenger, T.; Guerrero-Sanchez, C.; Vitz, J.; Hoogenboom, R.; Schubert, U. S. *Chem. Soc. Rev.* **2010**, *39*, 3317-3333.

[16] *(a)* Hori, H.; Six, C.; Leitner, W. *Macromolecules* **1999**, *32*, 3178-3182. *(b)* de Vries, T. J.; Duchateau, R.; Vorstmana, M. A. G.; Keurentjes, J. T. F. *Chem. Commun.*, **2000**, 263-264. *(c)* Kläui, W.; Bongards, J.; Reiβ, G. J. *Angew. Chem. Int. Ed.*, **2000**, *39*, 3894-3896. *(d)* de Vries, T. J.; Kemmere, M. F.; Keurentjes, J. T. F. *Macromolecules* **2004**, *37*, 4241-4246. *(e)* Bastero, A.; Franció, G.; Leitner, W.; Mecking, S. *Chem. Eur. J.* **2006**, *12*, 6110-6116. *(f)* Guironnet, D.; Gottker-Schnetmann, I.; Mecking, S. *Macromolecules* **2009**, *42*, 8157-8164.

[17] Jessop, P. G.; Subramaniam, B. *Chem. Rev.* **2007**, *107*, 2666-2694.

[18] Jin, H.; Subramaniam, B. *Chem. Eng. Sci.* **2004**, *59*, 4887-4893.

[19] Wei, M.; Musie, G. T.; Busch, D.H.; Subramaniam, B. *J. Am. Chem. Soc.,* **2002**, *124*, 2513-2517.

[20] Giménez-Pedrós, M.; Tortosa-Estorach, C.; Bastero, A.; Masdeu-Bultó, A. M.; Solinas, M.; Leitner, W. *Green Chemistry* **2006,** *8*, 875-877.

[21] Tortosa-Estorach, C. *PhD. Thesis*, Universitat Rovira i Virgili, **2007**, Tarragona, Spain.

[22] Soro, B.; Stoccoro, S.; Cinellu, M.A.; Minghetti, G.; Zucca, A.; Bastero, A.; Claver. C. *J. Organomet. Chem.* **2004**, *689*, 1521-1529.

[23] Quici, S.; Cavazzini, M.; Ceragioli, S.; Montanari, F.; Pozzi, G. *Tetrahedron Lett.* **1999**, *40*, 3647-3650.

[24] *(a)* Oki A.R.; Morgan, R. J. *Synthetic Commun.* **1995**, *25*, 4093-4097; *(b)* Donnici, C. L.; Filho, D. H. M.; Moreira, L.L.C.; Teixeira dos Reis, G.; Cordeiro, E.S.; Ferreira de Oliveira, I. M.; Carvalho, S.; Paniago, E. B. *J. Braz. Chem. Soc.* **1998**, 9, 455-460.

[25] Garelli, N.; Vierling P. *J. Org. Chem.* **1992**, *57*, 3046-3051.

[26] Stoccoro, S.; Alesso, B.; Cinellu, M. A.; Minghetti, G.; Zucca, A.; Bastero, A.; Claver, C.; Manassero, M. *J. Organomet. Chem.* **2002**, 664, 77-84.

Dicationic Pd(II) complexes for CO/vinyl arenes in compressed CO₂ and TFE

[27] Geremia, S.; Randaccio, L.; Mestroni, G.; Milani, B. *J. Chem. Soc. Dalt. Trans.* **1992**, 2117-2118.

[28] *(a)* Synthesis of [Pd(**A'**)Cl$_2$] and [Pd(**A'**)$_2$][CF$_3$SO$_3$]$_2$ is described in: Wehman, P.; Dol, G.C.; Moorman, E.R.; Kamer, P.C.J. and van Leeuwen, P.W.N.M. *Organometallics*, **1994**, *13*, 4856-4869. *(b)* Synthesis of [Pd(**A'**)$_2$][PF$_6$]$_2$ is described in: 8c. *(c)* Synthesis of [Pd(**A'**)Cl$_2$] and [Pd(**A'**)$_2$][B(C$_6$F$_5$)$_4$]$_2$ is described in: Foley, S.R.; Stockland Jr., R.A.; Shen, H. and Jordan R.F. *J. Am. Chem. Soc.* **2003**, *125*, 4350-4361.

[29] Claver, C.; Marco, E.; Oro, L. A.; Royo, M.; Pastor, E. *Transition Met. Chem.* **1982**, *7*, 246-249.

[30] Shan, B.-Z.; Zhao, Q.; Goswami, N.; Eichhorn, D. M. and Rillema, D.P. *Coord. Chem. Rev.*, **2001**, *211*, 117-144.

[31] Case, F. H. *J. Am. Chem. Soc.* **1946**, *68*, 2574-2577.

[32] Ribeiro, P. E. A.; Donnici, C. L.; dos Santos, E. N. *J. Organomet. Chem.* **2006**, *691*, 2037-2043.

[33] Felix, A.; Guadalupe, A.R.; Huang, S.D. *Krist. Z. New. Cryst. Struct.*, **1999**, *214*, 463-464.

[34] Gameiro, P.; Pererira, E.; Garcia, P.; Breia, S.; Burgess, J. and de Castro, B. *Eur. J. Inorg. Chem.* **2001**, 2755-2761.

[35] Milani, B.; Corso, G.; Mestroni, G.; Carfagna, C.; Formica, M.; Seraglia, R. *Oranometallics*, **2000**, *19*, 3435-3441.

[36] Nozaki, K.; Komaki, H.; Kawashima, Y.; Hiyama, T.; Matsubara, T. *J. Am. Chem. Soc.*, **2001**, *123*, 534-544.

[37] Milani, B.; Scarel, A.; Durand, J. and Mestroni G. *Macromolecules*, **2003**, *36*, 6295–6297.

[38] Scarel, A.; Durand, J.; Franchi, D.; Zangrando, E.; Mestroni, G.; Carfagna, C.; Mosca, L.; Seraglia, R.; Consiglio, G.; Milani, B. *Chem. Eur. J.* **2005**, *11*, 6014-6023.

[39] Durand, J.; Scarel, A.; Milani, B.; Seraglia, R.; Gladiali, S.; Carfagna, C. and Binotti, B. *Helv. Chim. Acta* **2006**, 89, 1752-1771.

[40] Axet,M.R.; Amoroso, F.; Bottari, G.; D'Amora, A.; Zangrando, E.; Faraone, F.; Drommi, D.; Saporita, M.; Carfagna, C.; Natanti, P.; Seraglia, R. and Milani, B. *Organometallics* **2009**, *28*, 4464–4474.

[41] Van Leeuwen, P. W. N. M.; Zuideveld, M. A.; Swennenhuis, B. H. G.; Freixa, Z.; Kamer, P. C. J.; Goubitz, K.; Fraanje, J.; Lutz, M. and Spek, A. L. *J. Am. Chem. Soc.* **2003**, *125*, 5523-5539.

[42] Altomare, A.; Burla, M.C.; Camalli, M.; Cascarano, G.L.; Giacovazzo, C.; Guagliardi, A.; Moliterni, A.G.G.; Polidori, G. and Spagna, R. *J. Appl. Cryst.* **1999**, *32*, 115-119.

[43] Ortep-3 for Windows - A Version of ORTEP-III with a Graphical User Interface (GUI). L. J. Farrugia, *J. Appl. Crystallogr.* **1997**, *30*, 565-566.

[44] WinGX Suite for Single Crystal Small Molecule Crystallography. L. J. Farrugia, *J. Appl. Cryst.* **1999**, *32*, 837-838.

Chapter - 4

Perfluorinated Cationic Palladium (II) Complexes as Catalysts for CO/Vinyl Arenes Copolymerisation in Conventional and Green Media.

*New monochelated palladium complexes [Pd(CH₃)(NCCH₃)(N-N)][X] with ligands N-N= **L1-L3** and X= PF₆⁻, OTs⁻ and BArF⁻ as counterions have been synthesised. They were characterized by multinuclear (^1H, ^{19}F and ^{15}N) and multidimensional NMR spectroscopy. The interionic structure was investigated by pulsed gradient spin-echo diffusion method (PGSE), ^{19}F-^1H HOESY and ^1H-^1H NOESY NMR spectroscopy. In solution, PF₆⁻ and OTs⁻ appear to be localized close to the acetonitrile ligand and shifted to the bipyridine ring trans to the Pd-CH₃ bond. The new palladium complexes were active catalysts in CO/vinyl arenes copolymerisation and it was found that the order of the catalytic activity depend on the counterion used. In 2,2,2-trifluoroethanol the order of the activity was: PF₆⁻ > OTs⁻ ≈ BArF⁻, while in liquid expanded CO₂ the highest results were obtained with complexes containing BArF⁻. Polyketones with high molecular weights (up to 200000 with CO/TBS and up to 914000 with CO/ST), low polydispersities (1.3-2.5 M_w/M_n) and high syndiotacticity (up to 96% in CO/TBS and 93% in CO/ST) were obtained. The mechanism was analysed by studying the initiation and end groups of the copolymers by MALDI-TOF mass spectrometry analysis.*

$$n\, CO + n$$ (with R = H or *tert*-butyl) → (CO₂ or TFE as medium)

R = H or *tert*-butyl   X⁻ = BArF⁻, PF₆⁻ or OTs⁻
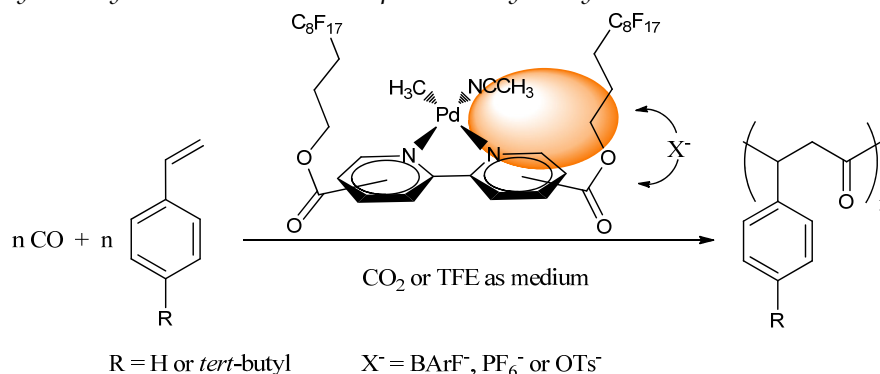
This work has been done in collaboration with Dra. B. Milani (Università degli study di Trieste, Italy)

Cationic Pd(II) complexes for CO/vinyl arenes in TFE and CO₂

4.1 Introduction

As we have discussed in Chapter 1 and 3, the bischelated palladium (II) complexes $[Pd(N-N)_2][X]_2$ lead to higher productivities in alternating copolymerisation of vinyl arenes and carbon monoxide (Scheme 4.1)[1] compared to its counterpart monochelated palladium (II) complexes $[Pd(CH_3)(NCCH_3)(N-N)][X]$, however they need higher energies (pressure and temperature), making the catalysis greener when monochelated complexes are used.[2] On the other hand, the monochelated catalytic systems in organic solvents generate a rather unstable active species, which easily decomposes to inactive palladium metal. This decomposition was avoided using 2,2,2-trifluoroethanol (TFE)[3] due to its lower nucleophilicity and 1,4-benzoquinone (BQ) allowing the synthesis of CO/styrene polyketones in high productivity and high molecular weight with the system $[Pd(CH_3)(NCCH_3)(F_4-phen)](PF_6)$ (F_4-phen = 5,5,6,6-tetrafluoro-5,6-dihydro-1,10-phenanthroline; up to $M_w = 1000000$) at mild catalytic conditions.[4]

$$n \, CO + n \quad \xrightarrow{[Pd]}$$
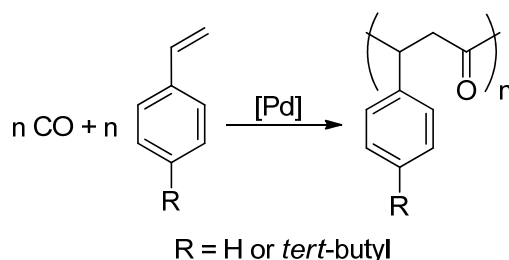
R = H or *tert*-butyl

Scheme 4.1. Palladium catalyzed alternating copolymerisation of CO/vinyl arenes..

Concerning the use of compressed carbon dioxide with this kind of catalysts, in our group they were reported some studies in the field of CO/*tert*-butylstyrene copolymerisation reaction catalyzed by palladium complexes of general formula $[Pd(CH_3)(NCCH_3)(N-N)][BArF]$ in scCO₂ media, where N-N was **A** and **B** and BArF = $B[3,5-(CF_3)_2C_6H_3]_4$ (Figure 4.1.), which showed high solubility in scCO₂ in catalytic conditions.[5] These palladium complexes catalyzed the copolymerisation reaction leading to the desired polyketones (Scheme 4.1, R = *tert*-butyl) with better productivity (up to 234 g CP/g Pd), molecular weight ($M_w = 87000$) and polydispersity ($M_w/M_n = 1.2$) than in organic solvent.
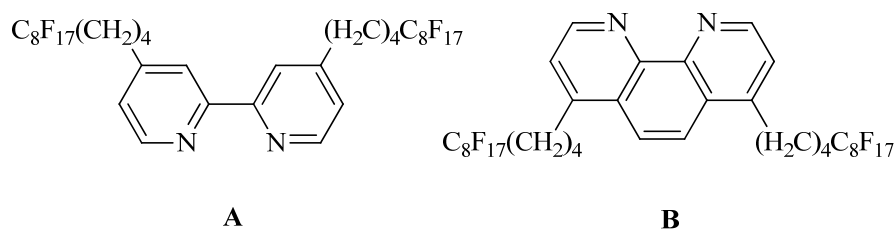
Figure 4.1. Ligands used in CO/*tert*-butylstyrene copolymerisation.

In Chapter 3, we presented the preparation of the catalyst precursors [Pd(N-N)$_2$][BArF]$_2$ with new perfluorinated ligands (**L1-L3** Figure 4.2) and their application in the CO/4-*tert*-butylstyrene (TBS) and styrene (ST) copolymerisation. These catalytic systems proved to be effective in copolymerisation CO/TBS reaction affording up to 6.1 kg CP/g Pd, 222000 of molecular weight and between 73-98 % of stereoregularity and in copolymerisation CO/ST reaction affording up to 2.3 kg CP/g Pd, 693000 of molecular weight and between 92-97 % of syndiotactic triads.
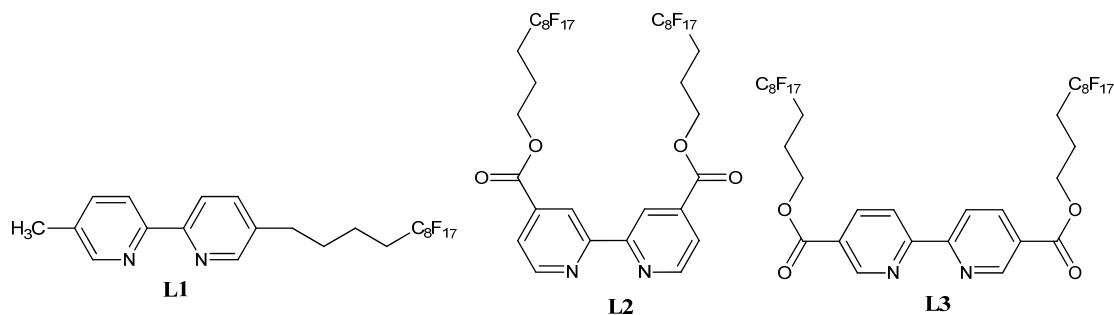
Figure 4.2. New perfluorinated ligands used in Pd-catalyzed CO/vinyl arenes copolymerisation.

In this chapter we present the preparation and characterisation of cationic complexes [Pd(CH$_3$)(CH$_3$CN)(**L1-L3**)][X], (X = PF$_6^-$, OTs$^-$ and BArF$^-$). The catalytic activity of these systems in CO/vinyl arenes (styrene and *tert*-butylstyrene, Scheme 4.1) copolymerisation was studied comparing conventional (TFE) and green solvent (compressed CO$_2$), where the effect of the amount of oxidant, counterion and amount of substrate were studied.

Cationic Pd(II) complexes for CO/vinyl arenes in TFE and CO$_2$

4.2 Results and Discussion

4.2.1 Synthesis of the cationic complexes

The cationic palladium complexes [Pd(CH$_3$)(NCCH$_3$)(**L1-L3**)]X (**Ia-c**, **IIa-c** and **IIIa-c**, Scheme 4.2) with different counterions X =, PF$_6^-$ (**a**), OTs$^-$ (**b**)) were synthesized following a two-steps procedure reported in the literature[6] starting from [Pd(CH$_3$)Cl(cod)] (cod = 1,5-cyclooctadiene), which reacted with one equivalent of the corresponding ligand to get the neutral complexes [Pd(CH$_3$)Cl(**L1-L3**)] (**I**, **II** and **III**, Scheme 4.2). These complexes handled with the corresponding salt and acetonitrile to obtain the monochelated complexes.[3b] The driving force for the last step is the formation of AgCl, which is insoluble in dichloromethane while the complexes **Ia-b**, **IIa-b** and **IIIa-b** are soluble in the reaction medium.

This procedure failed for the synthesis of complexes [Pd(CH$_3$)(NCCH$_3$)(**L1-L3**)](BArF) **Ic-IIIc**, which were obtained by counterion exchange reaction[7] from complexes **Ib-IIIb** by reaction with NaBArF. The driving force of this reaction was the formation of the NaOTs salt, which is more insoluble in dichloromethane than NaBArF (Scheme 4.2).

[Pd(CH$_3$)(Cl)(cod)] + N-N $\longrightarrow$ [Pd(CH$_3$)(Cl)(N-N)] $\xrightarrow{\text{AgX}}$ [Pd(CH$_3$)(NCCH$_3$)(N-N)][X]

L1, L2, L3   **I, II, III**   AgCl   **I, II, III**

X = (**a**) PF$_6$, (**b**) OTs

[Pd(CH$_3$)(NCCH$_3$)(N-N)][OTs] $\xrightarrow{\text{NaBArF}}$ [Pd(CH$_3$)(NCCH$_3$)(N-N)][BArF]

Ib, IIb, IIIb   NaOTs   **Ic**, **IIc**, **IIIc**
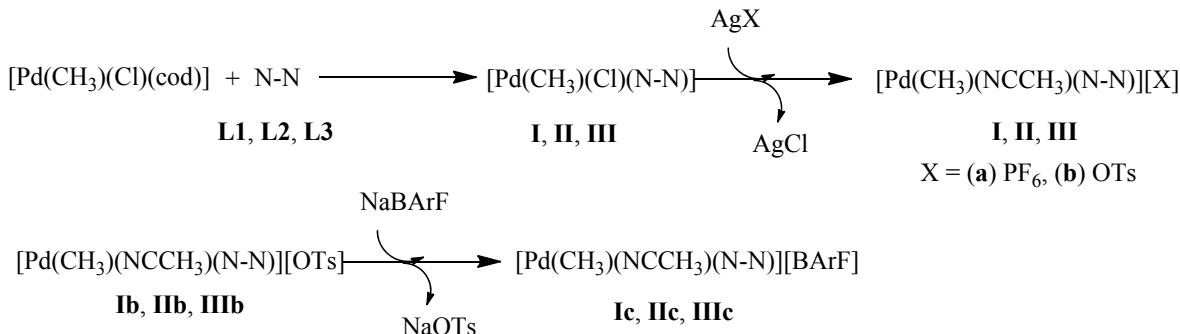
N-N	[Pd(CH$_3$)Cl(N-N)]	[Pd(CH$_3$)(CH$_3$CN)(N-N)][X]
L1	I	Ia-c
L2	II	IIa-c
L3	III	IIIa-c

Scheme 4.2. Synthesis of complexes **I-III** and **Ia-c**, **IIa-c** and **IIIa-c**. X= PF$_6^-$ (**a**), OTs$^-$ (**b**) or BArF$^-$ (**c**).

The complexes **I-III** and **Ia-c**, **IIa-c** and **IIIa-c** were isolated as pale yellow or pale brown solids and fully characterized by infrared spectroscopy (IR), mass spectrometry (MALDI-TOF) and mono- and bidimensional ^{1}H, ^{15}N and ^{19}F NMR

spectroscopy, except complex **III**, which was not soluble enough for the NMR spectra and was only characterized by mass spectrometry and IR.

The assignation of the signals corresponding to the protons of the bipyridine ligand was made in basis of 2D-COSY and 1D-NOESY NMR experiments, where a correlation between H^6 and Pd-CH$_3$ was observed (see for example Figure 4.3 and Supplementary information for details).

The ^{1}H NMR spectra of neutral complexes **I** and **II** were in agreement with the coordination of the N-N ligands in a non symmetric chemical environment. For these complexes the singlet signal due to the methyl bonded to palladium falls in the range between 0.8-1.2 ppm. The bipyridine ligand resonances generally occurs *ca.* 0.2-0.3 ppm downfield from free ligand values. Moreover, the protons from the donor ring *cis* to the chloride are marked by downfield shifts in agreement with literature values.[8]
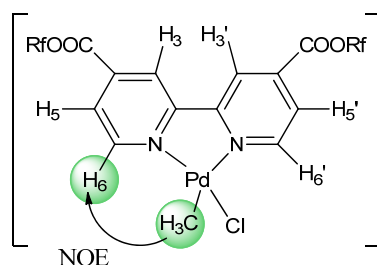
Figure 4.3. Assignments of the protons in complex **II**.

When proton assignments were done in complex **I**, it was observed that metylenic protons bonded to pyridine (py) ring gave correlation both in 2D-COSY and 1D-NOESY NMR spectra with both H^4, H^6 and $H^{4'}$, $H^{6'}$. This was attributed to a mixture of *cis* and *trans* isomers (respect to the Pd-CH$_3$ position, Figure 4.4), which in the NMR timescale were observed as the average situation between both isomers.
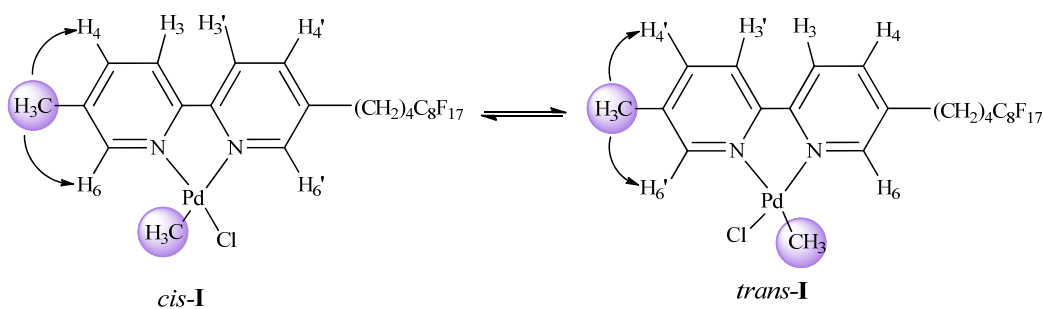
Figure 4.4. Assignment of the protons in *cis*-**I** and *trans*-**I** complex.

Cationic Pd(II) complexes for CO/vinyl arenes in TFE and CO$_2$

The ^{1}H NMR spectra of the cationic complexes **Ia-c**, **IIa-c** and **IIIa-c**, showed the signals of the coordinated acetonitrile (δ 2.35-2.60 ppm; free acetonitrile δ 2.10 ppm[9]) and the singlet due to the methyl group bonded to palladium (δ 0.90-1.25 ppm). Unexpectedly, the ^{1}H NMR spectra of these complexes depended on the counterion, which suggested the presence of an interaction between the ions. For example, the aromatic region of the ^{1}H NMR of complexes **Ia-c**, **IIa-c** and **IIIa-c** showed that the proton signals of the bipyridine ring *trans* to Pd-CH$_3$ (*trans*-py ring) were shifted depending on the counterion (Figure 4.5, Figure 4.7 and Figure 4.8). This suggested that the interaction could take place selectively with this ring. However, there was no evidence of counterions coordination.

Complexes **Ia-c** showed broad signals probably due to an exchange between *cis/trans* isomers (Figure 4.5). The 1D-NOESY NMR experiments of complex **Ib** confirmed the formation of both geometric isomers (1:1), being proton H[6] and H[6'] different in *cis* and *trans* isomer (X= OTs⁻, Figure 4.5). The exchange could produce free CH$_3$CN, which was detected in the ^{1}H NMR spectra (see SI). Complex **Ic** presented a complex ^{1}H NMR spectrum, that became simpler at -80 ºC, although signals corresponding to H[3] and H[4] continued overlapped (Figure 4.6).

Figure 4.5. ^{1}H NMR spectra in the aromatic region of complexes **Ia-c** (CD$_2$Cl$_2$, 500MHz).
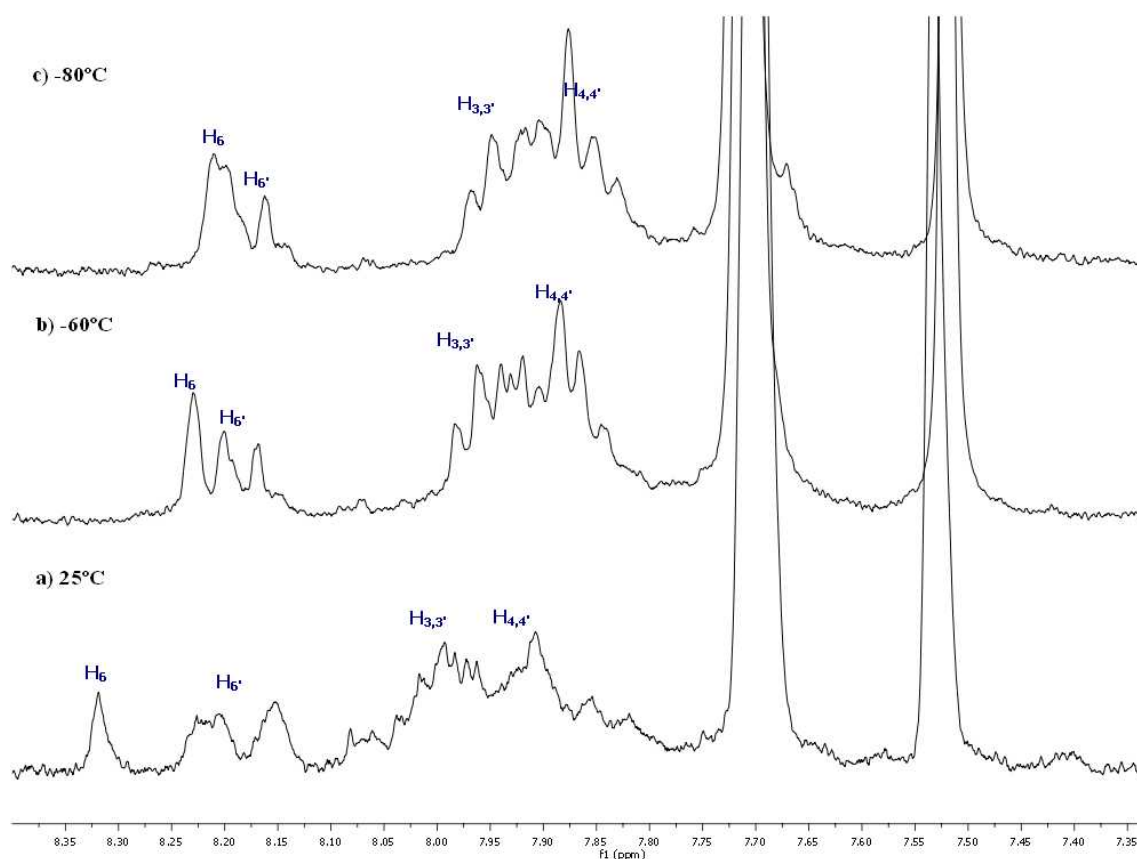
Figure 4.6. Variable ^{1}H NMR spectra in the aromatic region of complex **Ic** (CD$_2$Cl$_2$, 400MHz); a) 25ºC, b) -60ºC, c) -80ºC.

The chemical shifts of the aromatic protons in the ^{1}H NMR spectra of complexes **IIa-c** were also very different between them (Figure 4.7). In the case of complex **IIb**, all the aromatic signals were quite broad suggesting that may be equilibrium between the species with free and coordinated acetonitrile. Nevertheless, variable temperature NMR experiment failed, since the complex precipitated at low temperature.

Similar trends were observed with the complexes **IIIa-c**. Although in the complexes **IIIa** and **IIIc** the chemical shift of the H$^{6'}$ were closer than for complex **IIIb** (Figure 4.8).

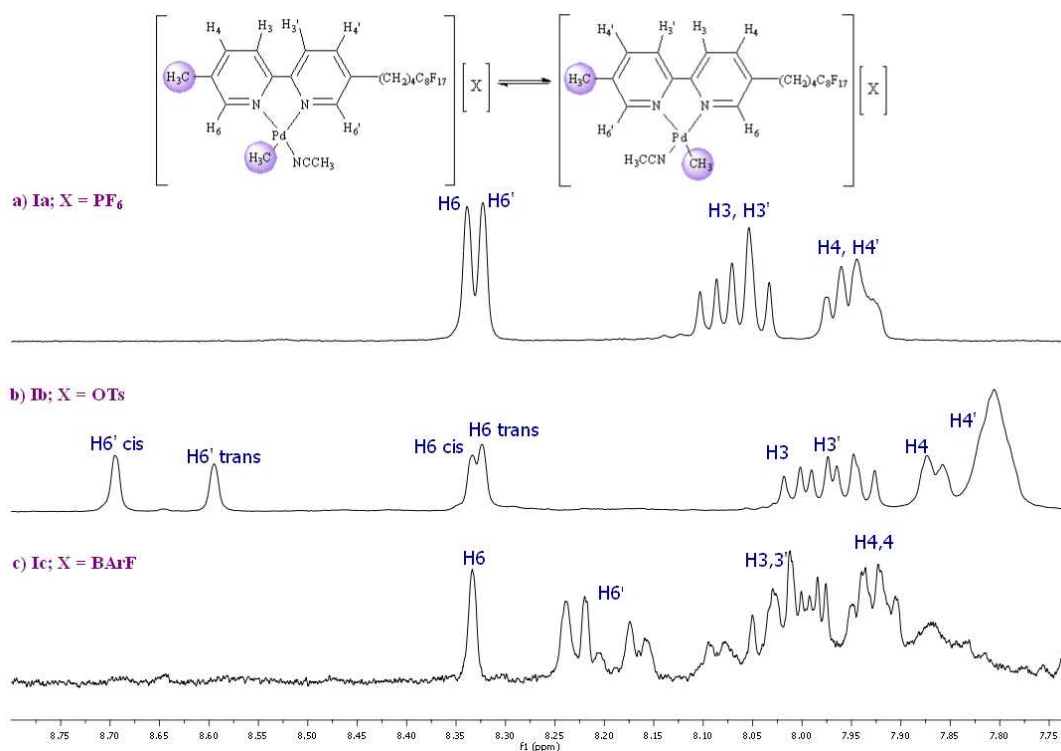*Cationic Pd(II) complexes for CO/vinyl arenes in TFE and CO₂*

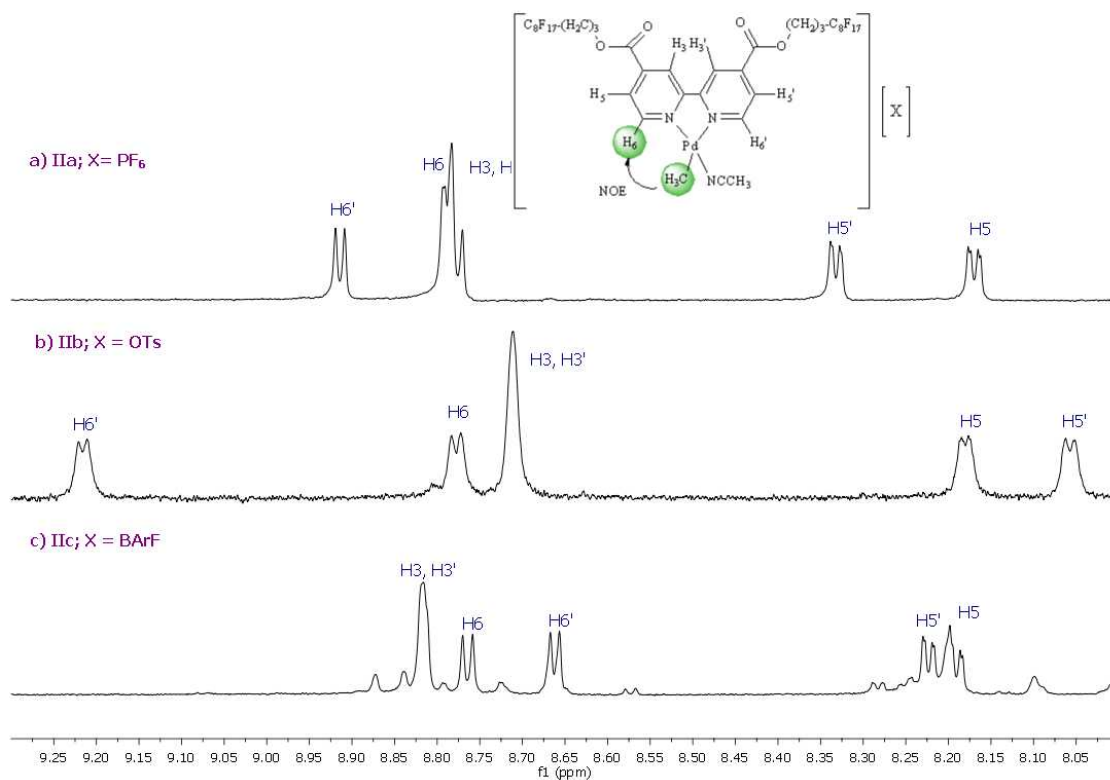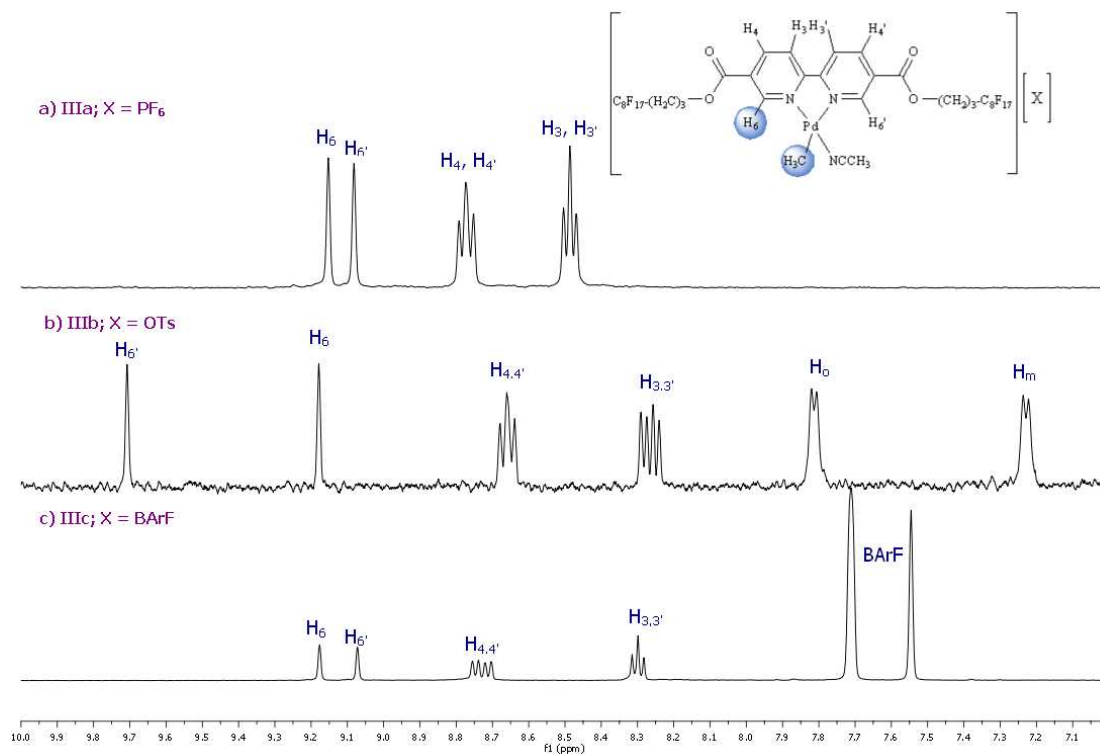**Figure 4.7.** ¹H NMR spectra in the aromatic region of complexes **IIa-c** (CD₂Cl₂, 500MHz).

Figure 4.8. ¹H NMR spectra in the aromatic region of complexes **IIIa-c** (CD₂Cl₂, 500MHz).

<u>^{15}N NMR spectroscopy</u>

^{15}N-^{1}H HMBCAD NMR experiments at natural abundance of the ^{15}N isotope were performed to obtain more evidence of the coordination mode of the ligands as chelates. For this kind of experiments the range of expected scalar coupling $^nJ(^{15}N,^1H)$ is required. For similar ligands the reported values of scalar coupling $^2J(^{15}N,^1H)$ were in the range 5-12 Hz.[6] Data was first obtained running at several input values in this range of $^2J(^{15}N,^1H)$ for ligands **L1** and **L2** to obtain the reference chemical shifts for free ligands (entries 1 and 6, Table 4.1). Unfortunately, **L3** was not soluble enough to perform the experiment.

Similar series of experiments was run for the first complex of each series at different values of $^2J(^{15}N,^1H)$, and the obtained $^2J(^{15}N,^1H)$ was later used for the other complexes of the same family. Once obtained the $^2J(^{15}N,^1H)$, the ^{15}N chemical shifts of N*cis* (N *cis* to Pd-CH$_3$) and N*trans* of compounds **I**, **Ia-c**, **IIa**, **IIb** and **IIIa-c** were attributed by their correlations with H^6 and H$^{6'}$, respectively, in the ^{15}N-^{1}H HMBCAD spectra. Additionally, a $^3J(^{15}N,^1H)$ was expected for Pd-NCCH$_3$, therefore signals for this ligand were observed in some of the NMR spectra of the complexes. The ^{15}N NMR data and the difference with free ligand ($\Delta\delta = \delta$complex $- \delta$ligand) have been compiled in Table 4.1. Complexes **II**, **IIb** and **III** were not soluble enough to perform these experiments.

Signals of ligand **L2** appeared deshielded with respect to **L1**, which correlated with increasing the electronegativity of the substituent.[10] If ^{15}N chemical shifts are compared between ligand and complex, we observed the expected shielding effect exerted by the metal *d* electrons.[10]

All ^{15}N resonances fall within the expected chemical shift ranges, which were in agreement with the results reported by B. Milani *et al.* for similar complexes.[6] The nuclei N*cis* presented ^{15}N chemical shifts between -148 and -166 ppm, but the resonance of N*trans* was found at higher frequencies, around -110 and -122 ppm. This was related with the *trans* influence of the methyl ligand.[11] The difference of the chemical shift between coordinated and free ligand obtained were in agreement with the reported $\Delta\delta$ values, -75 to -90 for N*cis* and -40 to -50 for N*trans* values.[6,12] The ^{15}N chemical shift for Pd-NCCH$_3$ obtained appeared between -204 and -207 ppm and the $\Delta\delta$ values were obtained using the ^{15}N chemical shift -137.1 ppm from free acetonitrile.[13]

Cationic Pd(II) complexes for CO/vinyl arenes in TFE and CO$_2$

In complexes with ligand **L1**, all ^{15}N chemical shifts were identified for **Ia**, while for **Ib** and **Ic** [15]N signal corresponding to Pd-NCCH$_3$ and/or N*trans* were not detected. This may be attributed to the lability of Pd-N bond and/or the equilibrium between *cis* and *trans* [15]N nucleus and/or the fact that the $^3J(^{15}N,^1H)$ falls out the expected range.[11b] Similar observations were found for complex **IIIb**, where only N*trans* could be observed.

To sum up, almost all complexes studied presented the expected ^{15}N chemical shift values for chelated N-ligands complexes and in most of them it was also found the ^{15}N chemical shift from coordinated acetonitrile ($\Delta\delta$ between -67 and -70 ppm). No evidences of monocoordination of the N,N-ligands were obtained.

Table 4.1. [15]N chemical shifts in ligands, neutral and cationic complexes. [a]

Entry	Compound	Chemical Shift (ppm)		
		N*cis*	N*trans*	NCCH$_3$
1	**L1**	-76.8	-76.7	-
2	**I**	-149.5 (-72.7)	-116.6 (-39.9)	-
3	**Ia**	-159.2 (-82.4)	-121.1 (-44.4)	-204.7 (-67.6)
4	**Ib**	-162.4 (-85.6)	-115.9 (-39.2)	n.f.
5	**Ic**	-165.9 (-89.1)	n.f.	n.f.
6	**L2**	-61.6		-
7	**IIa**	-148.9 (-87.3)	-111.9 (-50.3)	-207.6 (-70.5)
8	**IIc**	-149.3 (-87.7)	-111.5 (-49.9)	-204.3 (-67.2)
9	**IIIa**	-156.6	-119.0	-205.6 (-68.5)
10	**IIIb**	n.f.	-135.0	n.f.
11	**IIIc**	-155.9	-118.2	-204.8 (-67.7)

[a] Concentration 10mM; solvent: CD$_2$Cl$_2$, 400 MHz NMR spectra. $\Delta\delta$ (δ coordinated-δ free) values in parenthesis. n.f. = not found.

Rhodium complexes

In an attempt to elucidate if Rh(I) complexes would present similar behaviour in the ^{1}H NMR with the different counterions than Pd(II) complexes, we synthesised the rhodium (I) cyclooctadiene complexes [Rh(**L1**)(cod)][X], where X was PF$_6^-$ (**Ia'**), OTs$^-$ (**Ib'**) and BArF$^-$ (**Ic'**), following the same procedure described in Chapter 3.[14] The ^{1}H NMR spectrum showed also differences depending on the counterion used (Figure 4.9).
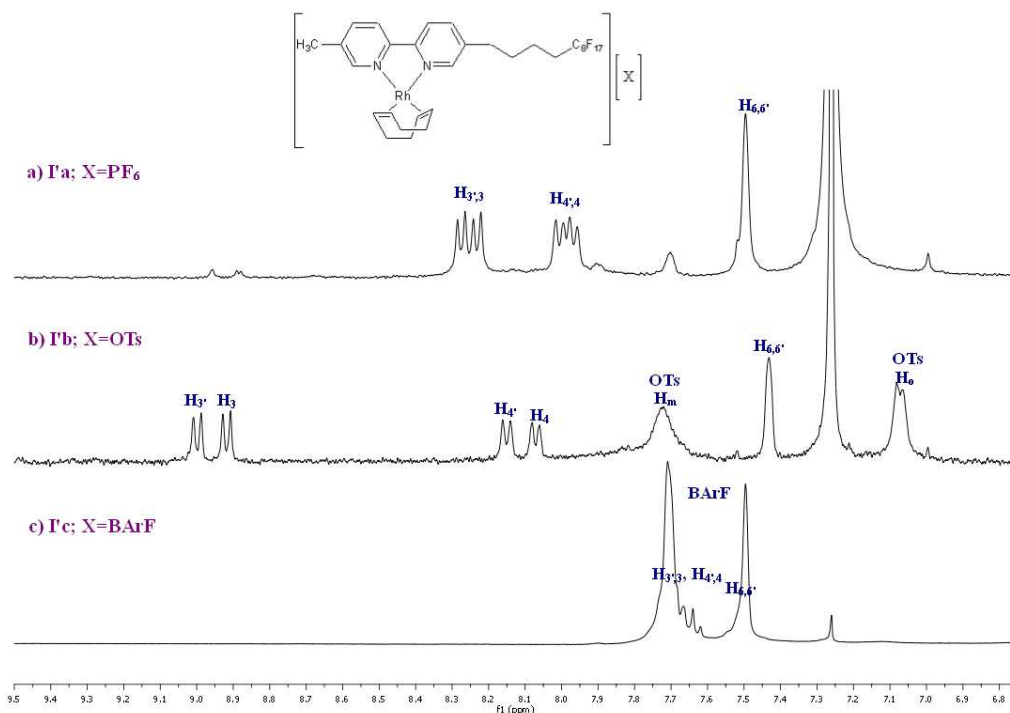
Figure 4.9. ^{1}H NMR spectra in the aromatic region of rhodium (I) complexes **Ia'-c'** (CDCl₃, 400MHz).

In conclusion, the monochelated complexes of general formula [Pd(CH₃)(NCCH₃)(**L1-L3**)][X], where X is PF_6^-, OTs^- or $BArF^-$ (**Ia-c**, **IIa-c** and **IIIa-c**), were synthesised and characterised by IR, MALDI-TOF spectrometry and ^{1}H, ^{15}N and ^{19}F NMR spectroscopy. Unexpected counterion dependence was observed in the ^{1}H NMR spectra, indicating that it may be an interaction between the counterion and the *trans*-py ring. Hetero- and homonuclear overhauser experiments ([1]H-^{19}F HOESY and ^{1}H-^{1}H NOESY) and NMR diffusion measurements were performed to confirm the existence of these interionic contacts.

4.2.1.1 *Ion Pairing studies (Diffusion Data and Overhauser Studies)*

NMR diffusion methods (pulse gradient spin-echo, PGSE) in combination with hetero-nuclear Overhauser spectroscopy are a useful and complete methodology to analyse the existence and degree of ion pairing.[15,16] In fact, in the recent literature there are a large number of studies about the counterion localization and the degree of ion pairing.[15-27] Therefore [1]H-^{1}H NOESY and [1]H-^{19}F HOESY experiments were done for palladium (II) complexes in order to assign the position of the counterion X⁻, and PGSE experiments were performed to obtain an estimation of the degree of ion pairing in CD₂Cl₂.

```
UNIVERSITAT ROVIRA I VIRGILI
CARBON DIOXIDE AS SOLVENT AND C1 BUILDING BLOCK IN CATALYSIS
Ariadna Campos Carrasco
ISBN:/DL:T. 1023-2011
```

Cationic Pd(II) complexes for CO/vinyl arenes in TFE and CO$_2$

a) ^{1}H-^{1}H NOESY and ^{1}H-^{19}F HOESY NMR experiments

First of all ^{1}H-^{1}H NOESY NMR spectra in CD$_2$Cl$_2$ were examined for complexes containing BArF$^-$ and OTs$^-$. No correlation was observed in the ^{1}H-^{1}H NOESY NMR spectra for complexes with BArF$^-$ **Ic**, **IIc** and **IIIc**. These results are in agreement with the literature[20,21,27] and supported by the fact that BArF$^-$ is a weak coordination anion[27,28] and its size makes difficult to have ion pairs.[21,29]

The analogous spectra for complex with OTs$^-$, **Ib**, showed one cross-peak connecting the aromatic protons of the tosylate to the palladium acetonitrile and three cross-peaks between the methyl group of the tosylate and the aromatic protons of the *trans*-py ring (H$^{6'trans}$, H$^{6cis/6trans}$ and H$^{3'}$, Figure 4.10a). Then, it was confirmed the interaction between tosylate – *trans*-py ring and tosylate – acetonitrile ligand. However, in **IIb** the tosylate protons interacted with the methylenic protons of the perfluorinated chain (specifically (CH$_2$)$^{3''}$, Figure 4.10b) and not with pyridine ring or coordinated acetonitrile suggesting that the perfluorinated chains, which are surrounding the metal centre, would avoid the OTs$^-$ approximation to the palladium centre and py ring. The perfluorinated chain may adopt a similar *syn* structure than the one observed in crystal structure of [Rh(cod)(**L3**)][PF$_6$] (Chapter 3). Complex **IIIb** was not soluble enough for running ^{1}H-^{1}H NOESY experiment.
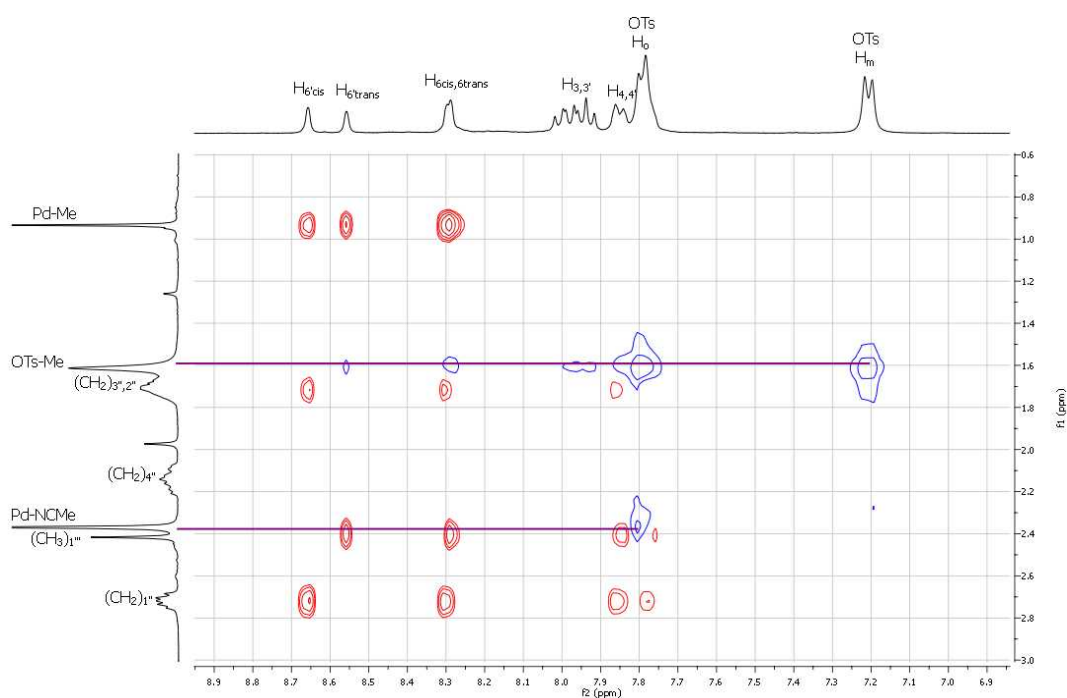
Figure 4.10a. ^{1}H-^{1}H NOESY NMR spectra in CD$_2$Cl$_2$ of complex [Pd(CH$_3$)(NCCH$_3$)(**L1**)][OTs] **Ib**.
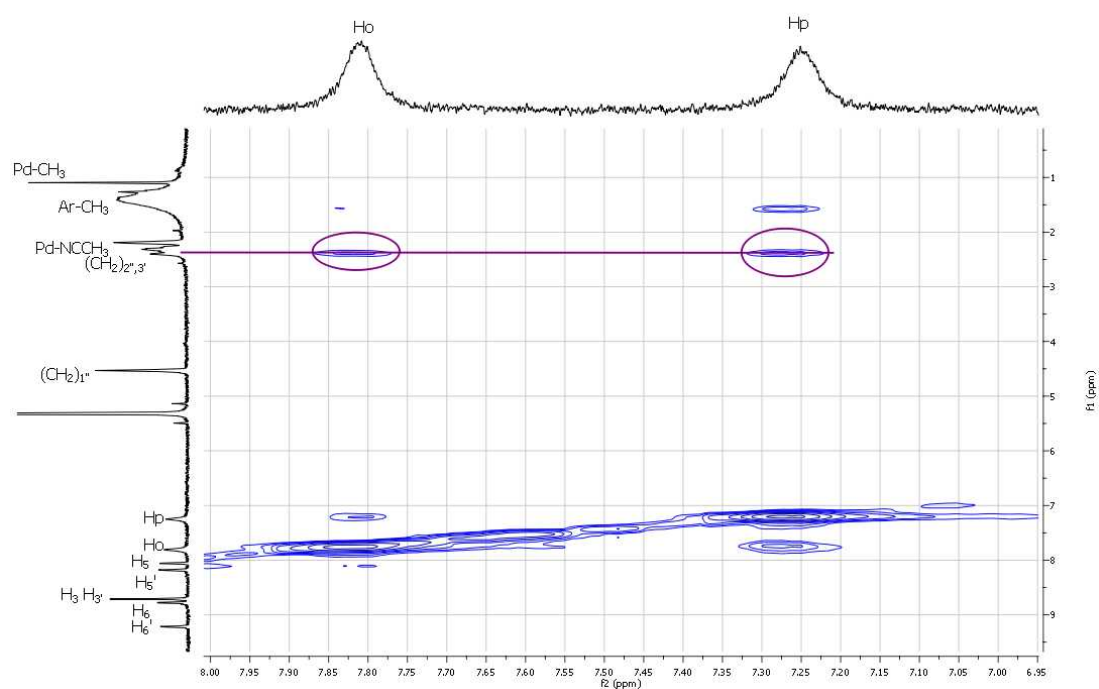
Figure 4.10b. ^{1}H-^{1}H NOESY NMR spectra in CD_2Cl_2 of complex [Pd(CH$_3$)(NCCH$_3$)(**L2**)][OTs] **IIb**.

For the complexes containing PF$_6^-$ as counterion ^{1}H-^{19}F HOESY methods were used. In the ^{1}H-^{19}F HOESY spectra for **Ia**, **IIa** and **IIIa** appeared cross-peaks between PF$_6$ and the aromatic protons (see spectra for **IIa** as an example, Figure 4.11) and the cross-peak bonded to acetonitrile. This suggested that PF$_6^-$ anion take up selective positions shifted to *trans*-py ring and close to the acetonitrile ligand (Figure 4.11). This type of selective behaviour for an anion is not unusual,[20,23,30] and similar observation was previously reported by Macchioni and co-workers.[30b] This behaviour might be related with its small volume which permited it to get close to the palladium atom, where the positive charge of the complex is located.[30b]

Cationic Pd(II) complexes for CO/vinyl arenes in TFE and CO₂
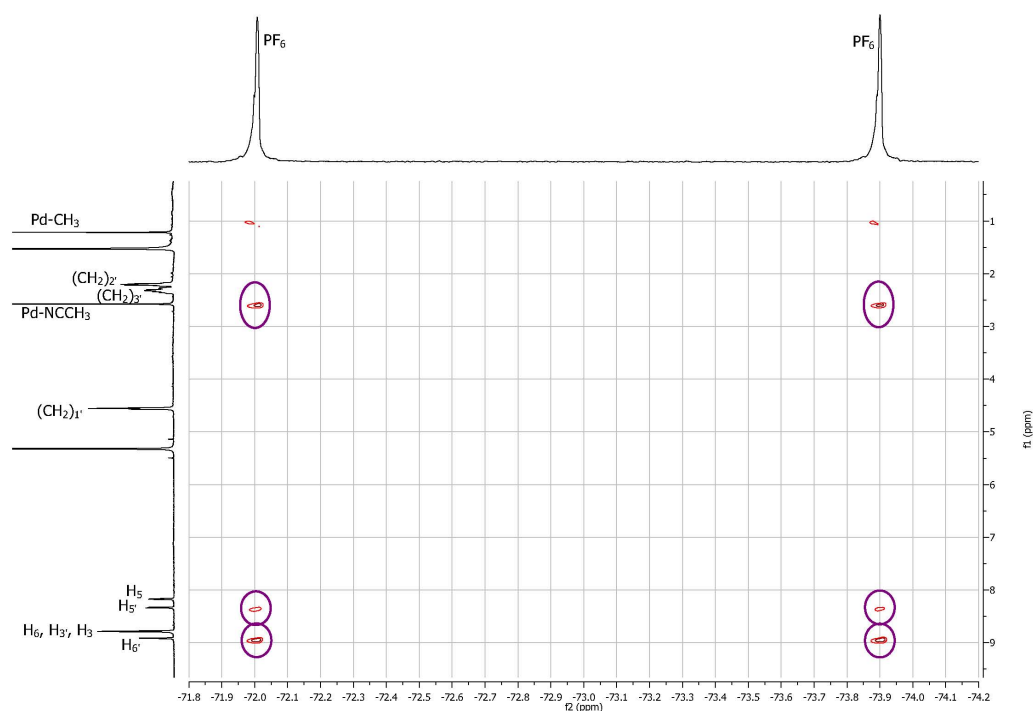
Figure 4.11. ^{1}H-^{19}F HOESY NMR spectra in CD_2Cl_2 of complex $[Pd(CH_3)(NCCH_3)(\textbf{L2})][PF_6]$ **IIa**.

In summary, homo- and heteronuclear NMR experiments showed evidences, in complexes **Ia-b**, **IIa-b** and **IIIa**, of interionic contact probably located in the proximity of the *trans*-py ring and Pd-NCCH$_3$ (Figure 4.12). In fact, the analysis of the acetonitrile proton signals showed a shielding effect in complexes with OTs⁻ respect to PF$_6$⁻ attributed to the proximity of the aromatic ring of the counterion.[19] This effect was more pronounced for compound **IIb**, in which the acetonitrile protons exhibited the strongest interionic contact since the proton signal was more shielded with respect to the same signal of complex **IIa** (Δδ up to 0.18 ppm).
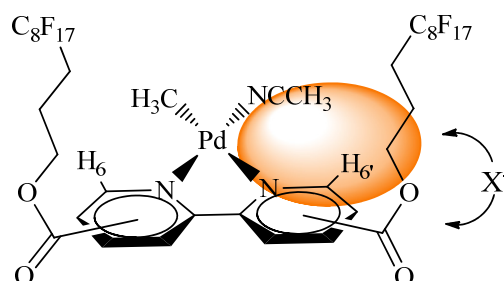
Figure 4.12. Representation of the counterion localization in solution deduced from NMR measurements for complexes with counterion X⁻ = PF$_6$⁻ and OTs⁻.

b) Pulsed gradient spin-echo (PGSE) NMR diffusion measurements

A pulse gradient spin-echo (PGSE) NMR diffusion measurement allows estimating the degree of ion pairing and the molecular volume. PGSE experiment is based on a spin-echo sequence and two pulsed field gradients separated by a waiting time, Δ.[15] This kind of NMR experiments consists on the repetition of this sequence increasing the gradient strength, G, giving different NMR spectra with different intensity of the signals. The variation of intensity in the NMR signals produced between both pulses is related to the diffusion of the species. The representation of the observed intensity changes, $ln(I/I_o)$, in front of G^2, affords the diffusion coefficient, D (see eq. 1), as the straight line slope according to equation 1. The larger the substance is, the smaller the absolute value of the slope becomes.[25]

$$\ln(I/I_o) = -\gamma_x \cdot \delta^2 \cdot G^2 \cdot \left(\Delta - \frac{\delta}{3}\right) \cdot D \tag{1}$$

γ_x = gyromagnetic ratio of the x nucleus
δ = length of the gradient pulse
G = gradient strength
Δ = delay between the midpoints of the gradients.
D = diffusion coefficient.

Once obtained the diffusion coefficient D is possible to found the hydrodynamic radii, r_H, via the Stoke-Einstein equation (see eq. 2), where k is the Boltzmann constant, η is the viscosity of the solvent, and T is the temperature.

$$r_H = \frac{kT}{6\pi\eta D} \tag{2}$$

The r_H and D values are used to determine the amount of interaction between cation-anion. In a normal experiment, the r_H value found for the anion is compared with the r_H data from the literature measured in MeOH, which provides an estimation of the real hydrodynamic radii without ion pairing, solvatation and hydrogen bonding. The higher the value of the experimental r_H in comparison with the literature r_H value is, the higher amount of ion pairing between anion-cation becomes. Even more, the comparison between the diffusion coefficients (D_{cation} and D_{anion} values) will also give information on the degree of interaction between both ions. The smaller difference between both D values is, the higher degree of ion pairing becomes.

In our experiments we obtained the PGSE data from a DOSY (diffusion ordered spectroscopy), a 2D spectrum, where the chemical shift is found in x-axis and the diffusion coefficient in y-axis (Figure 4.13). The DOSY spectrum is split up in the different 1D NMR spectra and integrated separately to avoid non consistent data and more accurate results.
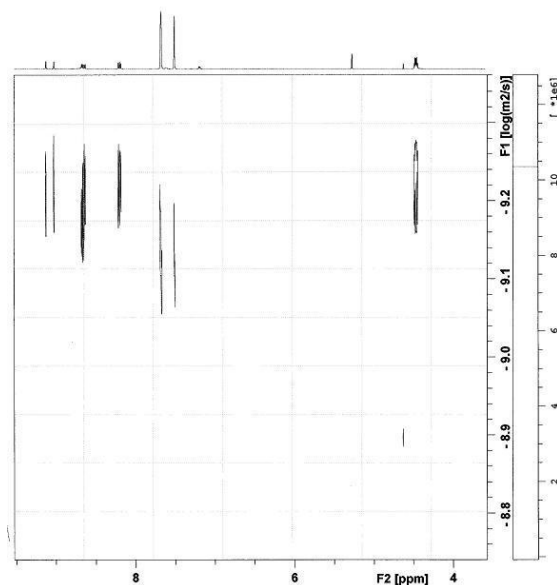
Figure 4.13. Example of DOSY spectrum from complex **IIa** (entry 7, Table 4.2).

Diffusion constants, *D*, were only obtained by the ^{1}H NMR diffusion measurements for the anion (BArF$^-$ and OTs$^-$) and cation, since its signals were separated and well resolved[20-22,30a] (Table 4.2). In the literature there are also other nucleus diffusion measurements (for example ^{19}F, ^{31}P or ^{35}Cl),[15-26] but unfortunately we did not found the optimised conditions for ^{31}P diffusion measurements and ion pairing was not determined for complexes with PF$_6^-$. The NMR spectra were recorded in CD$_2$Cl$_2$, since it is know that this solvent promote ion pairing in various transition metals with different counterions.[16,19-21]

In the literature it was found the typical value for hydrodynamic radii of BArF$^-$ in methanol, which is *ca.* 6.1-6.3 (entry 1, Table 4.2).[20,24,26] However the r_H value for OTs$^-$ anion was not found. Therefore we recorded the PGSE NMR spectra of AgOTs in CD$_3$OD, which provided a diffusion-based r_H of OTs$^-$ 4.4 Å (entry 2, Table 4.2). This experimental r_H obtained was used as estimation of the real hydrodynamic radii.

The *D* value and r_H for the neutral complexes [Pd(CH$_3$)(**L1-L2**)Cl] (**I-II**) have also been obtained as a reference value of hydrodynamic radii (r_H 5.41 and 7.27 Å,

respectively; entries 3 and 4, Table 4.2) in CD_2Cl_2 and in the absence of strong solvatation and/or ion-pairing effects.[22]

Table 4.2. Diffusion Coefficients (D, $10^{-10}m^2s^{-1}$) and Hydrodynamic Radii (r_H)[a]

Entry	Compound		D	r_H[b] (Å)
1[20,24,26]	**NaBArF**	BArF⁻	-	6.1-6.3
2	**AgOTs**[c]	OTs⁻	9.29	4.42
3	**I**[d]	-	9.75	5.41
4	**II**[d]	-	7.10	7.42
5	**Ib**	Cation	8.76	6.04
		OTs⁻	8.96	5.88
6	**IIb**	Cation	7.43	7.09
		OTs⁻	7.75	6.80
7	**Ic**	Cation	6.51	8.09
		BArF⁻	7.37	7.15
8	**IIc**	Cation	7.44	7.08
		BArF⁻	8.30	6.35
9	**IIIc**	Cation	7.15	7.37
		BArF⁻	8.25	6.39

[a] Concentration 2mM and recorded at 300K, using ^{1}H signals. [b] $\eta(CD_2Cl_2)$ = 0.414 x 10^{-3} kg·s⁻¹.[15] [c] Concentration 5mM and recorded in CD_3OD at 300K; $\eta(CD_3OD)$ = 0.526 x 10^{-3} kg·s⁻¹.[15] [d] Concentration 5mM.

Concerning the complexes containing OTs⁻, the obtained r_H value for complex **Ib** (entry 5, Table 4.2) indicated that both, cation and anion, diffuse at very similar rate (r_H OTs⁻ = 5.9 Å and $r_H$cation = 6.0 Å), as can be observed in Figure 4.14a, where both cation and OTs⁻ are represented by the same slope.[23] Furthermore, OTs⁻ anion is known to have a diffusion-based r_H values in methanol 4.4 Å, and the experimental r_H for **Ib** is considerably high. These results pointed to almost 100% ion pairing.

While the hydrodynamic radius was not so different between the cation of **IIb** and the neutral species **II**, the r_H value for the anion OTs⁻ (entry 6, Table 4.2) was considerably high (r_H value 6.8 Å) compared to the literature r_H value, therefore evidenced high amount of interaction but smaller than in complex **Ib**. Unfortunately low solubility of complex **IIIb** avoided the measurement of r_H value. These results confirmed the evidences of ionic interaction obtained from the [1]H-^{1}H NOESY experiments, for complexes containing OTs⁻ as counterion.

Cationic Pd(II) complexes for CO/vinyl arenes in TFE and CO₂

For complexes with BArF⁻ anion, **Ic**, **IIc** and **IIIc** the diffusion coefficient of the anions were different pointing to different translation ratios for both cation and anion. We found in **Ic** a r_H value for anion of 7.15 Å a slightly higher than the typical value of BArF⁻ in methanol (entry 7 *vs.* entry 1, Table 4.2), which could be consistent with the presence of some interactions and moreover, the volume of the cation increased with respect to the neutral complex, **I** (r_H value 8.1 Å *vs.* 5.4 Å; entry 7 *vs.* 3, Table 4.2, respectively). Nevertheless, the lack of contact from BArF⁻ and the cation in the ¹H-¹H NOESY experiments confirms that there was no interaction.[18,22]

Complexes **IIc** and **IIIc** had the same behaviour. The hydrodynamic radii were not so different between all cations and are very similar than the neutral species (in the case of **IIc**). In **IIc** and **IIIc** BArF⁻ has a *D*-value of up to 8.3 and r_H value of 6.3-6.4 Å (entry 8 and 9, Table 4.2), which indicated no interactions, in keeping with the results from the ¹H-¹H NOESY NMR measurements. Figure 4.14b clearly showed different diffusion for cation and BArF⁻, since both had different slopes.

As we observed in the literature,[18] changing the structure of the bipyridine substituents, for example as a monosubstituted perfluorinated ligand **L1**, modifies the amount of ion pairing under the same conditions. While in **Ib** (OTs⁻) had almost 100% ion pairing, in the case of **IIb** and **IIIb** the degree of ion pairing were smaller.
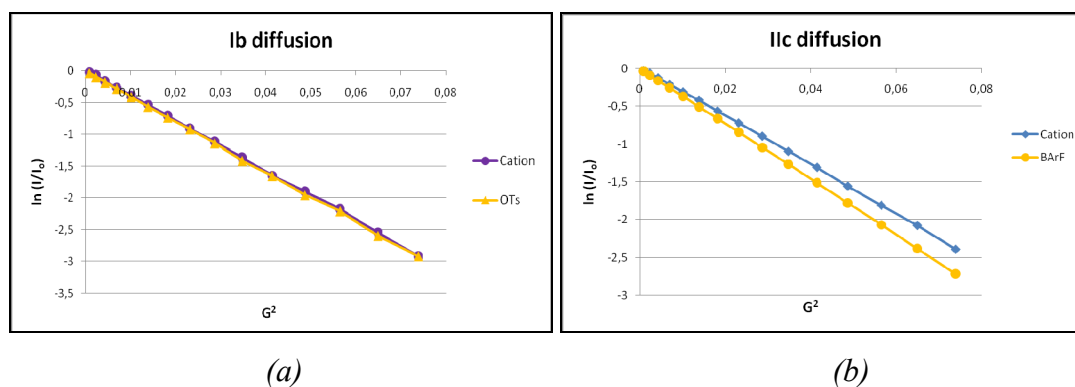

(a)   *(b)*

Figure 4.14. Plot of ¹H ln(*I/I*ₒ) *vs.* arbitrary units proportional to the square of the gradient amplitude *(a)* on complex **Ib** *(b)* on complex **IIc**.

4.2.2 CO/Styrene and *tert*-butylstyrene copolymerisation

4.2.2.1 *CO/Styrene copolymerisation in TFE*

Firstly, we studied the catalytic activity of complexes **Ia-c**, **IIa-c** and **IIIa-c** in the copolymerisation of CO/styrene using an organic solvent 2,2,2-trifluoroethanol at reference conditions reported in the literature:[31] 1 atm of CO pressure, 30°C, $4.1 \ 10^{-4}$ M catalyst and 10 ml of styrene. We analyzed the effect of the ligands, the addition of benzoquinone (BQ) as oxidant and the counterion used. The results obtained are represented in Figure 4.15 and Figure 4.17.

Initially we studied the catalytic activity of complexes with PF_6^- as counterion (**Ia-IIIa**). All the complexes tested gave good results in terms of productivity (up to 4.65 kg CP/g Pd), syndiotacticity (up to 93%) and molecular weight (up to M_w = 580000, SI) (Figure 4.15). At these conditions, the best result (4.65 kg CP/g Pd) was obtained with the catalytic system **IIa**, which contained ligand **L2** at a ratio of [BQ]/[Pd] = 5.
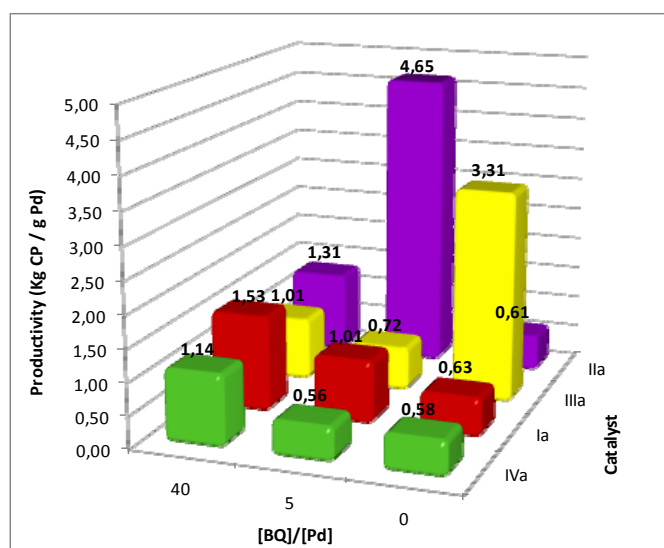
Figure 4.15. Representation of the productivity in front of the amount of BQ using ST as substrate. Catalytic conditions: $1.27 \ 10^{-5}$ mol catalyst, styrene V = 10 mL ([ST]/[Pd] = 6823), TFE V = 20 mL, P_{co} = 1 atm, T(°C) = 30 °C, time = 24h.

In most of the conditions studied, the productivities obtained with the cationic complexes **Ia-IIIa** were higher than the ones obtained with the non fluorinated 2,2-bipiridine (bpy) [Pd(CH$_3$)(NCCH$_3$)(**bpy**)][PF$_6$] (**IVa**) (*ca* 0.5 kg CP/g Pd). We speculated that the presence of the perfluorinated electronwithdrawing tails increased

Cationic Pd(II) complexes for CO/vinyl arenes in TFE and CO$_2$

the stability of these systems. In fact no decomposition of the catalyst was observed with complexes **Ia-IIIa**, while palladium metallic was observed at the end of the reaction in the case of using complex **IVa**.

a) Effect of benzoquinone (BQ)

As it was described in the introductory chapter, the role of 1,4-benzoquinone (BQ) is the stabilization of the intermediate hydride species by oxidizing Pd(0) to Pd^{2+}, which can then immediately re-enter the catalytic cycle.[1b,32] The catalytic experiments without BQ showed different behaviour depending on the catalytic system used. For instance, **Ia** and **IIa** showed moderate activity (0.61-0.63 kg CP/g Pd), while **IIIa** exhibited the highest activity for this catalytic system (3.31 kg CP/g Pd), high molecular weight (M$_w$ = 486000) and low polydispersity (1.3).

An increase in the amount of BQ (BQ/Pd = 5 and 40) produced an increase in the productivity for system **Ia** up to 1-1.5 kg CP/g Pd. In all the cases using BQ as oxidant, no decomposition of the complex was observed. These results were in agreement with the ones obtained by Milani *et al.* with non symmetrical Ar-BIAN ligands, which showed the best results with the highest amount of benzoquinone.[31,33]

In the case of catalytic systems **IIa** and **IIIa** an inhibiting effect of BQ was observed, since increasing the amount of BQ did not increase the productivity as expected. Similar inhibitory effect of BQ was reported in the literature[31,34] and was attributed to a competitive effect between HQ (producing alcoholisis of the growing chain) and propagation step. Therefore, the reaction slowed down and decreased the productivity. Nevertheless, in our case in the MALDI-TOF mass analysis we did not found clear evidences of this as we will discuss below.

The ^{13}C NMR spectra analysis of the CO/styrene copolymers synthesized with catalyst **IIa** showed a syndiotactic microstructure, the content of the *uu* triad was 93%, the remaining 7% corresponded to the *ul* and *lu* triads (see one example, Figure 4.16).
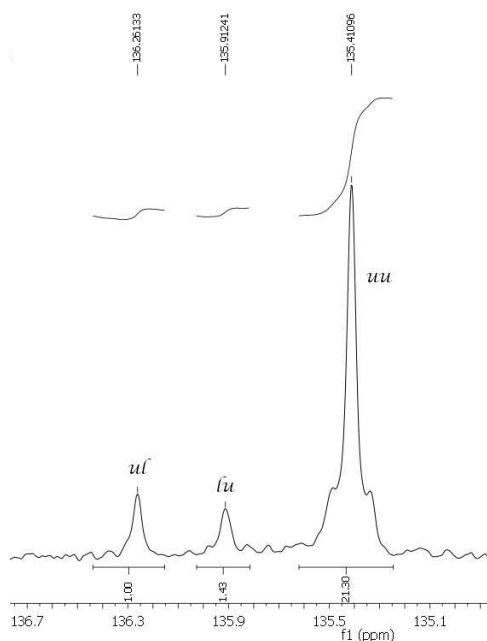
Figure 4.16. ^{13}C NMR spectra in HFIP + CDCl$_3$ at room temperature, region of *ipso* carbon atom, of: CO/styrene polyketone synthesized with **IIa**.

b) Effect of the counterion

The effect of the counterion with the complexes **Ia-c**, **IIa-c** and **IIIa-c** at BQ/Pd = 5 and at the same catalytic conditions was studied in TFE. The order of productivity found was X = PF$_6^-$ > OTs$^-$ ≈ BArF$^-$ (Figure 4.17). The systems with OTs$^-$ (**Ib-IIIb**) showed decomposition of the complex, while in the case of BArF$^-$ (**Ic-IIIc**) and PF$_6^-$ (**Ia-IIIa**) no decomposition was observed. The order of activity found is in contrast with the results reported by Macchioni *et al.* with complexes [Pd(η^1,η^2-C$_8$H$_{12}$OMe)bpy]X (bpy = 2,2'-bipyridine and C$_8$H$_{12}$OMe = cyclooctenylmethoxy group) in methylene chloride,[27] where the order of the catalytic activity of the complexes tested was related with the coordinating ability (X = BPh$_4^-$ << CF$_3$SO$_3^-$ < BF$_4^-$ < PF$_6^-$ < SbF$_6^-$ < BArF$^-$) and the best anion was the least strong coordinating one.

Cationic Pd(II) complexes for CO/vinyl arenes in TFE and CO₂
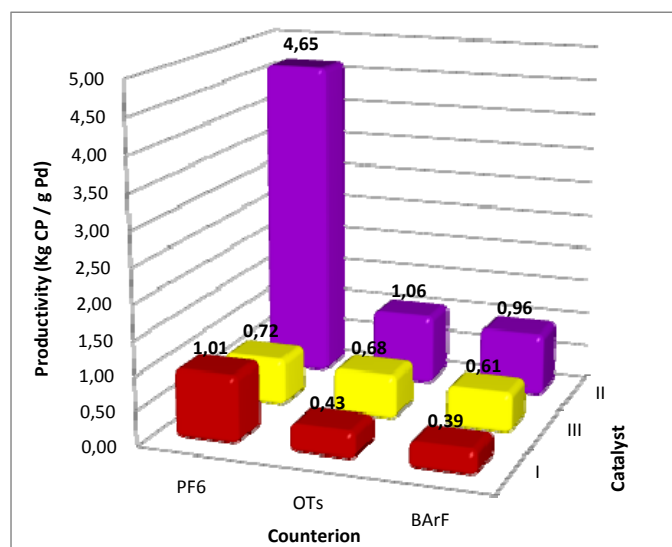
Figure 4.17. Representation of the productivity in front of the counterion used with complexes **Ia-c**, **IIa-c** and **IIIa-c**. Catalytic conditions: 1.27 10⁻⁵ mol catalyst, styrene V = 10 mL ([ST]/[Pd] = 6823), TFE V = 20 mL, p_{co} = 1 atm, T = 30ºC, time = 24 h and [BQ]/[Pd] = 5.

4.2.2.2 *CO/Styrene and CO/tert-butylstyrene in compressed carbon dioxide*

The catalytic activity of complexes **Ia-c**, **IIa-c** and **IIIa-c** in the copolymerisation of CO/styrene (ST) and *tert*-butylstyrene (TBS) using supercritical carbon dioxide (scCO₂) or liquid expanded CO₂ as solvent at reference conditions 5 atm of CO pressure, 37ºC, 4.1·10⁻⁴ M catalyst was studied.[5]

Initially we studied the catalytic activity in the CO/TBS copolymerisation of complexes with BArF⁻ as counterion (**Ic-IIIc**), since it is known to provide the most soluble systems in CO₂. The results obtained in supercritical conditions (250 atm of total pressure and 37ºC) are represented in Figure 4.18. Almost all the catalytic systems investigated presented better results than the model complex [Pd(CH₃)(NCCH₃)(**A**)][BArF] (**Vc**).[5] The catalytic systems with ligands containing a chain in position 5 gave better productivities (340 and 280 g CP/g Pd with **Ic** and **IIIc**, respectively) and molecular weight (75200 and 197900 with **Ic** and **IIIc**, respectively). The stereoregularity found in scCO₂ ranged between 85-90% *uu* triads, in syndiotactic copolymers.
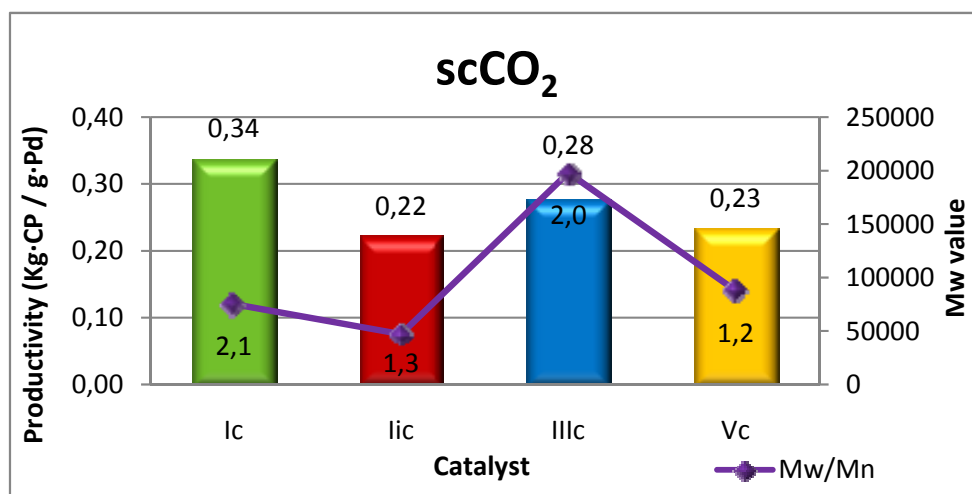
Figure 4.18. Representation of the productivity and molecular weight in front of the catalyst **Ic**, **IIc**, **IIIc** and [Pd(CH$_3$)(NCCH$_3$)(A)][BArF] (**Vc**),[5] with TBS in scCO$_2$. Catalytic conditions: 1.27·10^{-5} mol catalyst, [TBS] / [Pd] = 620, P$_{CO}$ = 5 atm, P$_t$ = 250 atm, T(ºC) = 37 ºC and time = 24h.

The catalytic study was focused on complex **IIIc** to optimise the conditions (Table 4.3). The CO$_2$ phase influence was investigated and it was found an increase in productivity of 2.6 times moving from scCO$_2$ to liquid CO$_2$ (entry 1 and 2, Table 4.3). This is in agreement with the results obtained with bischelated systems (Chapter 3).[35] A contribution of this improvement may be due to the increase of catalyst concentration, since the volume of the liquid phase is lower than the volume of the vessel. Moreover, as it was observed with bischelated systems, after 6h the magnetic stirring bar was blocked in the reactor. After 6h the productivity was high corresponding to an average TOF of 132 g CP/g Pd (entry 2 and 3, Table 4.3).

Increasing CO pressure from 5 to 10 bars (entry 3 *vs.* 4, Table 4.3), the productivity increased 1.2 times and molecular weight up to 1.6 times, in agreement with literature results.[2a] The increase in the amount of substrate had a positive effect in catalysis (entry 4 *vs.* 6 and *vs.* 9, Table 4.3). The addition of TFE (TFE/Pd = 300) did not promote any significant improvement in the productivity and a slight decrease in M$_w$ and high polydispersity were found (entry 7, 9 and 11 *vs.* 6, 8 and 10, Table 4.3), in contrast with the observed behaviour in the bischelated systems.[35]

Using [TBS]/[Pd] = 3100 the copolymer did not precipitate from the reaction mixture after 6 h and the reaction could be run for 24h. Nevertheless, small difference in

Cationic Pd(II) complexes for CO/vinyl arenes in TFE and CO$_2$

productivity was observed (entry 8 *vs.* 10, Table 4.3) indicating that complex **IIIc** achieved the maximum of catalytic activity after 6h.

At the best conditions found for CO/TBS, the copolymerisation CO/styrene was studied. We observed a decrease in productivity (entry 12, Table 4.3), in agreement with the results reported in previous chapter, but on the contrary the catalyst provided high M_w copolymers (long living character, $M_w = 914100$).

Table 4.3. Catalysis results with catalyst system **IIIc** in CO/vinyl arenes copolymerisation in CO_2 as solvent.[a]

Entry	P_{CO} (atm)	CO_2 Phase[b]	time (h)	[subs]/[Pd] molar ratio	g CP/ g Pd (g CP/g Pd·h)[c]	% uu	Mw (Mw/Mn)[d]
1[e]	5	scCO$_2$	24	620	276 (11)	85	197900 (2.03)
2	5	CO$_2$ liq.	24	620	736 (31)	83	82600 (2.12)
3	5	CO$_2$ liq.	6	620	660 (110)	84	78300 (1.93)
4	10	CO$_2$ liq.	6	620	789 (132)	82	102300 (1.66)
5	5	CO$_2$ liq.	6	1240	1049 (175)	84	85600 (1.73)
6	10	CO$_2$ liq.	6	1240	1212 (202)	86	141000 (1.77)
7[f]	10	CO$_2$ liq.	6	1240	1291 (215)	84	130900 (1.78)
8[g]	10	CO$_2$ liq.	6	3100	1554 (259)	85	149500 (2.40)
9[f,g]	10	CO$_2$ liq.	6	3100	1418 (236)	85	120700 (2.50)
10[g]	10	CO$_2$ liq.	24	3100	1705 (71)	83	144200 (2.17)
11[f,g]	10	CO$_2$ liq.	24	3100	1652 (69)	81	104600 (2.35)
12[f,h]	10	CO$_2$ liq.	24	3100	1092 (46)	84	914100 (1.24)

[a] Catalytic conditions: $1.27 \cdot 10^{-5}$ mol **IIIc**, [subs] = TBS, $P_t = 70$ atm, T(ºC) = 37 ºC. [b] Ocular observation through the reactor window. [c] Averaged values [d] Determined by GPC *vs.* polystyrene standards in TBS copolymers and *vs.* polymethylmetacrylate standards in ST copolymers. [e] Pt = 250 atm. [f] $V_{TFE} = 52$ μL ([TFE]/[Pd] = 300). [g] $P_t = 65$ atm to maintain liquid phase. [h] [subs] = Styrene.

a) Effect of the counterion

Catalysts **Ia-c**, **IIa-c** and **IIIa-c** were tested using the best catalytic conditions. Results are shown in Table 4.4 and Figure 4.19. Catalysts **Ia-c** presented no decomposition to Pd-black indicating high stability, but provided low productivity (entry 1-4, Table 4.4). This low productivity may be related with *cis/trans* equilibrium process observed by NMR spectroscopy. The catalyst **Ic** presented a long living character, since increasing the reaction time increased twice the activity, eight times the productivity and considerably the molecular weight (entry 3 *vs.* entry 4, Table 4.4). Even more, liquid expanded conditions were confirmed as the best conditions for the catalytic system **Ic**, being 2.3 times better than under $scCO_2$ conditions (entry 4, Table 4.4 *vs.* Figure 4.18).

On the other hand, for complexes with ligands **L2** and **L3**, catalysts **II-IIIa-c**, were found to be by far the most productive with the less coordinating anion (BArF⁻, **IIc** and **IIIc**, entry 7 and 10, Table 4.4). Complexes **IIb** and **IIIb** (containing OTs⁻) showed low productivity and formation of polyterbutylstyrene (entry 6 and 9, Table 4.4) probably due to decomposition. In contrast with the results observed in Chapter 3, the catalytic system containing ligand **L2** in the reported catalytic conditions was more active than complexes with **L3**.

The main differences between catalysts **IIa**, **IIc**, **IIIa** and **IIIc** were the stereoregularity values. Although both produce syndiotactic copolymers, higher degree of stereoregularity were obtained with **IIa** and **IIc** (up to 96% *uu* triads) than with **IIIa** and **IIIc** (76-85% *uu* triads). These results may be related with the position of the perfluorinated chains.[36] For complexes containing the 5,5'-substituted ligand **L3**, the counterion significantly affects the stereoregularity of the copolymers (the syndiotactic content triads) and seems to be related with the coordination ability of the anion.[37] While the use of BArF⁻ (**IIIc**) resulted in slightly higher percentage of the *uu*-triad (85%), catalyst **IIIa**, having more coordinating PF_6^- anion, afforded polyketone containing 76% *uu*-triad. The effect of the anion on the microstructure was instead negligible when comparison was made between catalysts **Ia-c** and **IIa-c**.

Cationic Pd(II) complexes for CO/vinyl arenes in TFE and CO₂

Table 4.4. CO/TBS copolymerisation results studying the effect of the counterion used in liquid expanded CO_2.[a]

Entry	Catalyst	(g CP/ g Pd)	(g CP/ g Pd) h⁻¹	% uu	Mw (Mw/Mn)[b]
1	**Ia**	393	66	89	44331 (1.21)
2	**Ib**	505	84	93	128170 (1.68)
3	**Ic**	094	16	90	117150 (1.71)
4[c]	**Ic**	791	33	89	167530 (2.16)
5	**IIa**	788	131	96	196130 (2.63)
6[d]	**IIb**	68	11	-	-
7	**IIc**	1664	277	93	125950 (1.98)
8	**IIIa**	0671	112	76	76721 (1.49)
9[e]	**IIIb**	121	20	-	-
10	**IIIc**	1554	259	85	149510 (2.40)

[a] Catalytic conditions: $1.27 \cdot 10^{-5}$ mol catalyst, [subs] = TBS, V_{TBS}= 2.55 mL ([TBS] / [Pd] = 3100), [TFE]/[Pd] = 0, P_{CO} = 10 atm, P_t = 65 atm, T(ºC) = 37 ºC, time = 6 h. [b] Determined by GPC *vs.* polystyrene standards. [c] time = 24h. [d] Homopolymer = 48%. [e] Homopolymer = 25%.

In summary, there are different factors affecting the productivity using compressed CO_2 in the catalysts studied (Figure 4.19). The productivity of catalysts **IIa-c** and **IIIa-c** presented counterion dependence, being the order X = BArF⁻ > PF₆⁻ >>> OTs⁻, which corresponds to the increasing ionic interaction. OTs⁻ containing complexes (**IIb** and **IIIb**) were unstable and lead to homopolymer formation. On the other hand, complexes **Ia-c** were less productive, which may be related with the existence of *cis*/*trans* equilibrium processes. The most productive catalytic system was **IIc** showing up to 1.7 kg CP/g Pd and the highest molecular weight copolymer was obtained with catalyst **IIa** (up to M_w 196000) and high syndiotacticity (up to 96% *uu* triads).
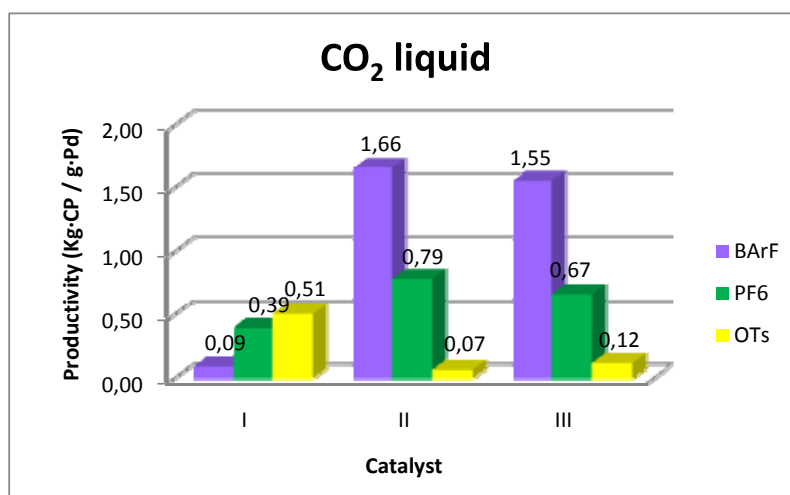
Figure 4.19. Representation of the productivity in front of the counterion used with complexes **I-IIIa-c** with TBS as substrate in liquid expanded CO_2. Catalytic conditions: $1.27 \cdot 10^{-5}$ mol catalyst, V_{TBS}= 2.55 mL ([TBS] / [Pd] = 3100), [TFE]/[Pd] = 0, P_{CO} = 10 atm, P_t = 65 atm, T(ºC) = 37 ºC, time = 6 h.

Some general conclusions can be extracted, although no direct comparison between the performance of the studied catalysts in TFE and compressed CO_2 due to the different characteristics of the substrates and technical problems related with the limitation of the reactor volume and stirring. Good productivities were obtained in compressed CO_2, nevertheless the absolute values of productivities were higher in TFE than in compressed CO_2. Comparing the productivities in the CO/ST copolymerisation obtained in both media, the highest results were obtained in TFE (3.31 *vs.* 1.09 kg CP/g Pd) but the concentration of substrate was very high. However, the most important conclusion drawn from the study is the potential of the compressed CO_2 as medium for this reaction.

4.2.2.3 *Initiation and termination steps study*

The initiation and termination mechanisms were determined by matrix-assisted laser desorption/ionization (MALDI) mass spectrometry of the copolymer end-groups. In base of previous results reported in the literature[31,38] and the observations discussed in Chapter 3 the catalytic cycle proposed is the same shown in the previous chapter. The copolymers were characterized by several series of peaks represented in Figure 4.20.

Cationic Pd(II) complexes for CO/vinyl arenes in TFE and CO₂
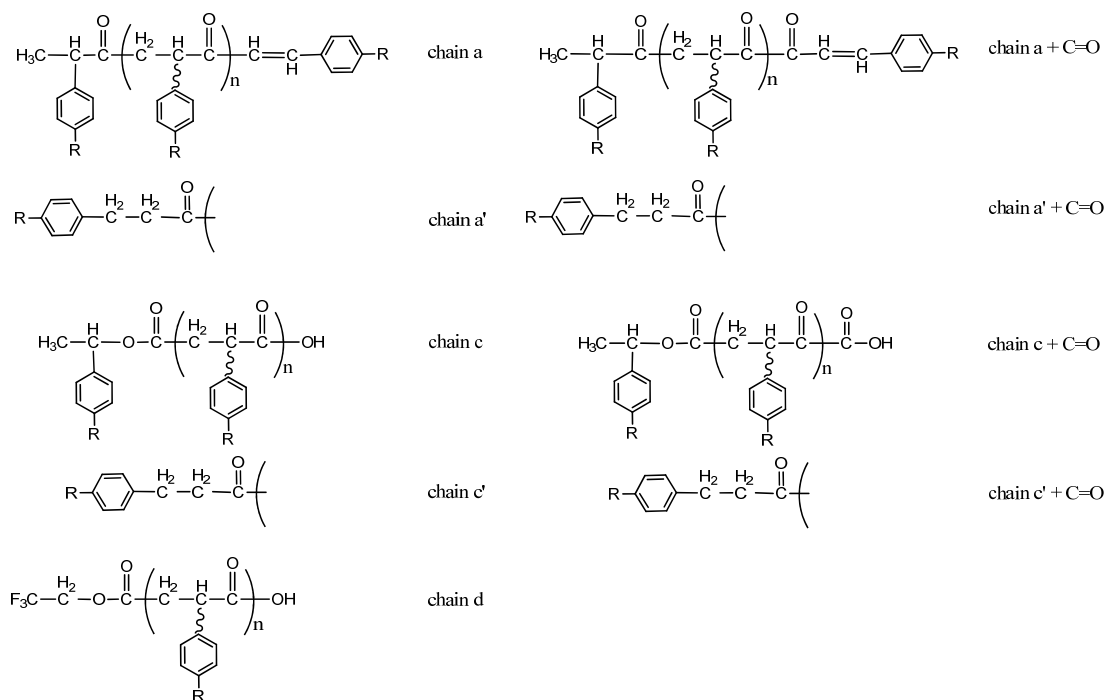
Figure 4.20. Polymeric chains presents in the CO/*tert*-butylstyrene (R= *tert*butyl) or styrene (R=H) polyketones.

MALDI-TOF mass spectra of the styrene/CO copolymers formed in TFE with [BQ]/[Pd]=5 (catalyst **IIIa**) and without BQ (catalyst **IIa**) were analyzed and compared. The mass spectra of polymers obtained without BQ revealed that the main fragment corresponded to a species in which the initiation step involved the insertion of styrene into the Pd-H bond and the termination by β-H elimination (chain a, Figure 4.20). When BQ was present the same mass spectrum was observed. However, the chain in which the initiation step involved the TFE and the termination the incorporation of the reduced BQ (HQ, chain e, Figure 4.21 and Figure 4.22a) could not be excluded since chain e and chain a give rise to a series of peaks whose differences in mass were too low to be distinguished with the instrumental set-up employed.[31] The incorporation of HQ in the end of the copolymer is a typical process taking place when the copolymerization is carried out in an alcoholic medium in the presence of the oxidant.[1b,31]
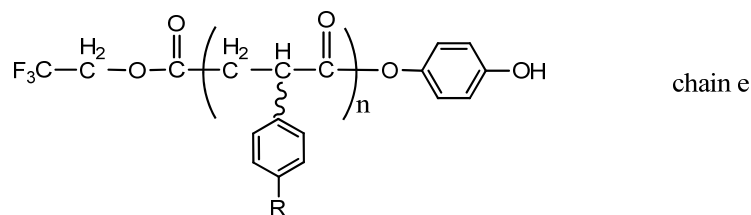
Figure 4.21. Polymeric chain in the CO/styrene (R=H) copolymer when BQ is used.

In the case of the styrene copolymers formed in liquid expanded CO_2, the mass spectra showed also as a main peak the one corresponding to chain a, however it also appeared peaks corresponding to end groups with double carbonylation followed by nucleophilic attack of water (chain c o c' + C=O),[39] with a high relative abundance (Figure 4.22b).
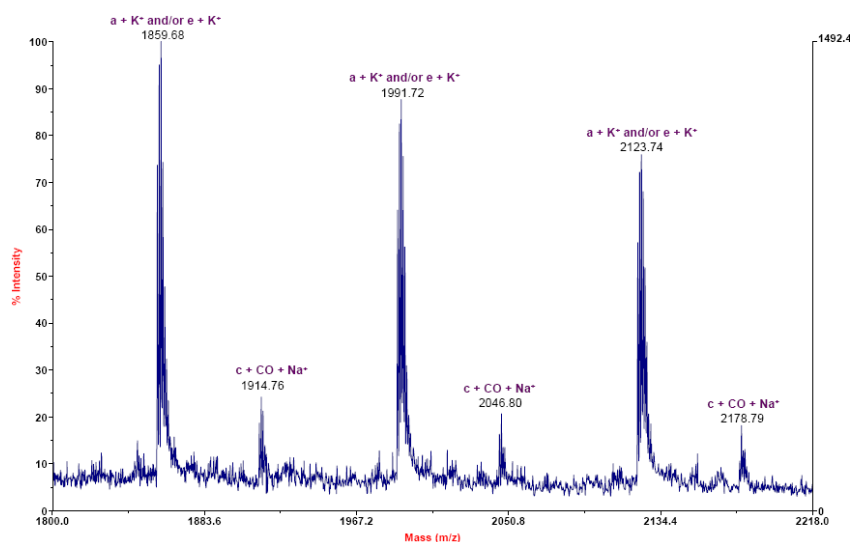
(a)
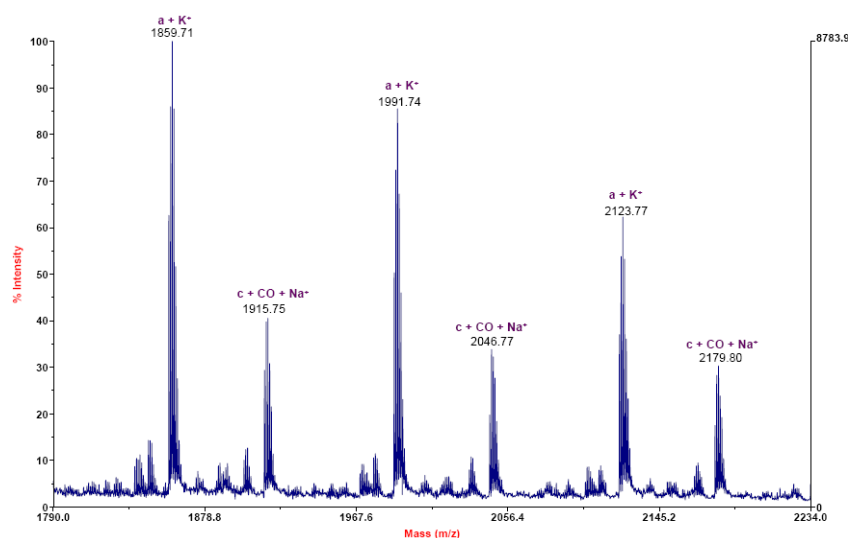
(b)

Figure 4.22. MALDI-TOF mass spectra of the CO/ST polyketones synthesis using *(a)* catalyst **IIIa** in TFE with BQ, Figure 4.15; *(b)* catalyst **IIIc** in liquid expanded CO_2, entry 13, Table 4.3.

The MALDI-TOF spectra of TBS copolymers formed in liquid expanded CO_2 presented fragments corresponding to chain a (Figure 4.23a). However other fragments were also observed if TFE was present, depending on the amount of substrate used or

Cationic Pd(II) complexes for CO/vinyl arenes in TFE and CO₂

the catalyst. For example, the addition of TFE (Figure 4.23b) yielded other minor fragments assigned to the initiation through TFE and termination by -OH (chain d), the initiation by TBS insertion to Pd-H and end groups by hydrolysis (chain c o c') and double carbonylation (chain c o c' + C=O).

(a)

(b)
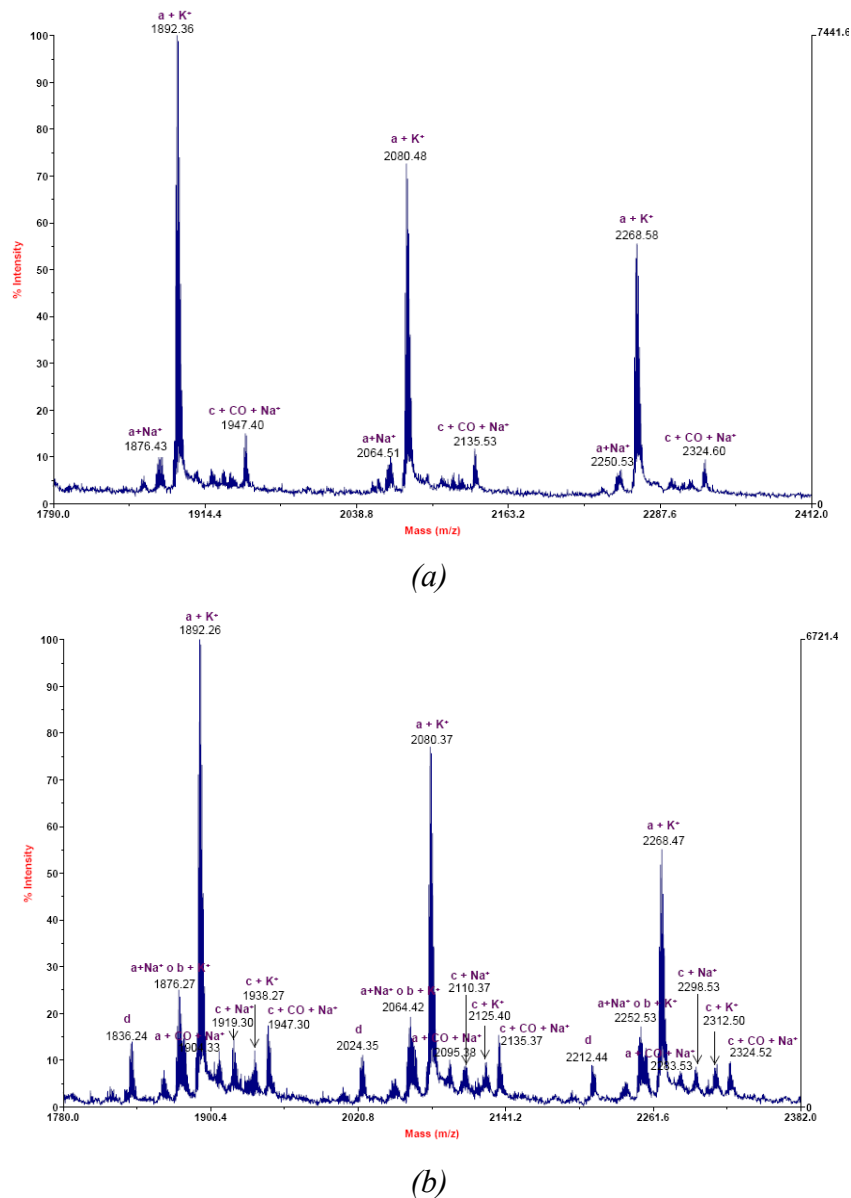
Figure 4.23. MALDI-TOF mass spectra of the CO/TBS polyketones syntheses using catalyst **IIIc** *(a)* in liquid expanded CO_2, entry 9, Table 4.3; *(b)* with addition of TFE in liquid expanded CO_2, entry 11, Table 4.3.

When the amount of substrate was reduced, the copolymers had a common initiator and multiple chain end groups ([TBS]/[Pd]=620, Figure 4.24a), maybe due to lower concentration of substrate. If PF_6^- was used as counterion instead of $BArF^-$, the relative abundance of chain c or c' +C=O increased and appeared the fragments

corresponding to termination by the nucleophilic attack of water (chain c o c', Figure 4.24b).

(a)

(b)
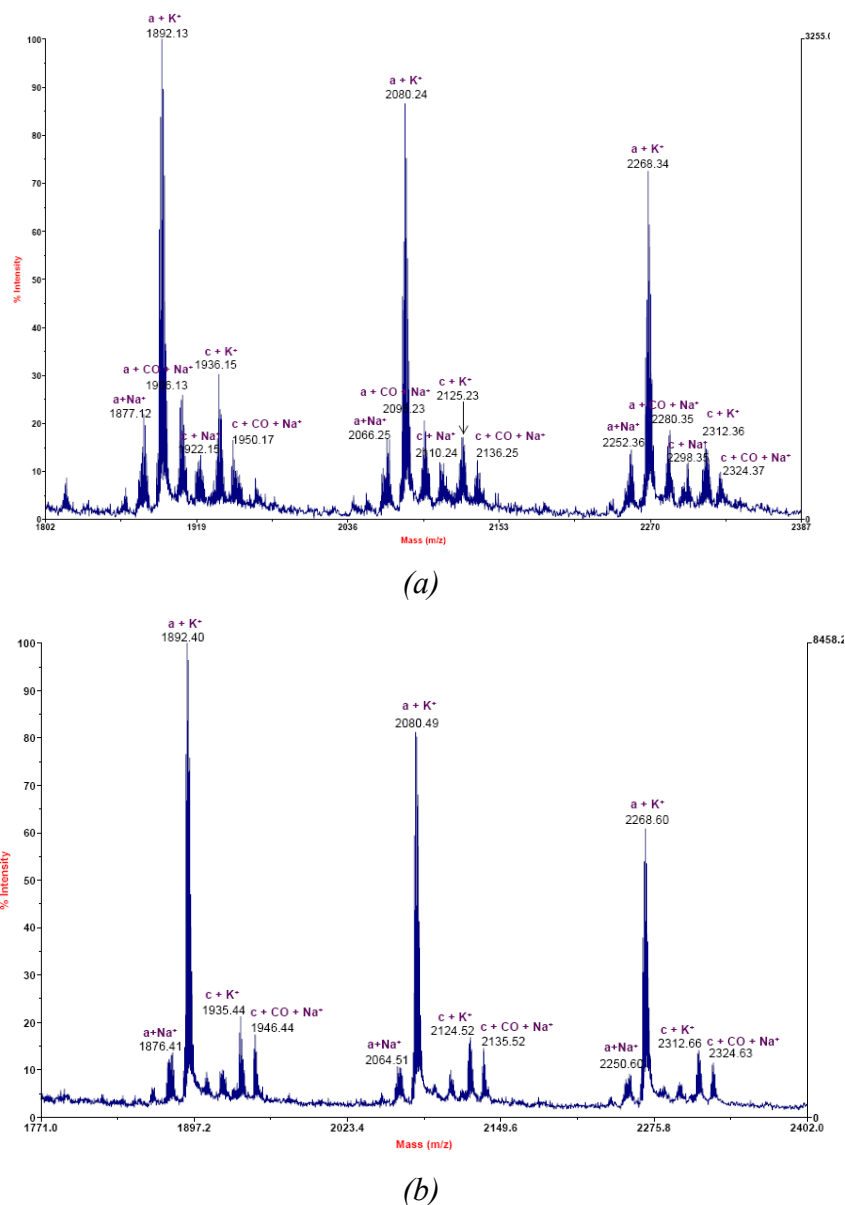
Figure 4.24. MALDI-TOF mass spectra of the CO/TBS polyketones syntheses in compressed CO_2 *(a)* using catalyst **IIIc** and [TBS]/[Pd]=620, entry 3, Table 4.3; *(b)* using catalyst **IIIa**, entry 8, Table 4.4.

In conclusion, the mass spectra of CO/ST polyketones showed as main mechanism the initiation through the alkene and the termination by β-H elimination in both mediums, however liquid expanded CO_2 increased the double carbonylation end group (c o c' + C=O). CO/TBS polyketones obtained with **IIIc** in liquid expanded CO_2

Cationic Pd(II) complexes for CO/vinyl arenes in TFE and CO₂

were selective to chain a, while when **IIIa** or TFE were used, multiple polymeric chains were present.

4.3 Conclusion

We synthesized and fully characterized new cationic palladium complexes with perfluorinated bipyridines. Their ^{1}H NMR spectra showed anion dependence, which was investigated by NMR measurements. The interionic structure of all complexes confirmed ion pairing in some of them by PGSE, ^{1}H-^{1}H NOESY and ^{19}F-^{1}H HOESY experiments. In solution, PF_6^- and OTs^- appeared to be localized close to the bipyridine ring *trans* to palladium methyl and acetonitrile, while $BArF^-$ did not show any significant interionic contact.

The catalytic activity of the complexes towards CO/vinyl arenes (ST and TBS) copolymerisation was tested. In TFE the best catalytic result in CO/ST copolymerisation was obtained with catalyst **IIa** (4.65 kg CP/g Pd, M_w up to 580000 and syndiotacticity up to 93%) using BQ.

In compressed CO_2, catalyst **IIIc** was used to optimise the catalytic conditions. The parameters studied were CO_2 phase, CO pressure, TFE addition, the amount of TBS and catalysis time. The increase in the CO pressure and TBS amount had a positive effect in the productivity, while addition of TFE had no significant effect. The most important parameter was CO_2 phase showing the best results in liquid expanded CO_2 (65 atm total pressure and 38ºC), which in combination with the increase of TBS and CO pressure lead to the optimised conditions. Under the optimised condition precatalyst **IIc** showed the best catalytic results (1.66 kg CP/g Pd in only 6h, M_w up to 126000 and syndiotacticity up to 93%). Unfortunately, **IIb** and **IIIb** showed homopolymer formation.

Finally, the initiation and end group's analysis in liquid expanded CO_2 showed that when ST was the substrate, the mechanism had two termination steps, the major one by β-H elimination and the minor by the double carbonylation followed by water attack. However, when TBS was used, almost only chain a (β-H elimination) was present.

4.4 Experimental Section

General Comments. Ligands **L1-L3** were prepared following Chapter 3 described procedures. Commercial available $Na_2[PdCl_4]$ (Johnson Matthey), methanol (Merck) and 2,2,2-trifluoroethanol (Sigma-Aldrich) were used as received. Dichloromethane used for the synthesis of complexes was purified through distillation over CaH_2 and stored under inert atmosphere. Carbon monoxide (CP grade 99.0 %) was supplied by Westfalen. Carbon dioxide (CO_2, CP grade 5.3 and SCF grade 99.995 %) was supplied by Praxair. **IR** spectra (range 4000 - 400 cm^{-1}) were recorded on a Midac Grams/386 spectrometer in KBr pellets or dichloromethane solution (when indicated). **NMR** spectra were recorded at 400 MHz Varian, with tetramethylsilane (^1H and ^{13}C), fluoroform (^{19}F) and nitromethane (^{15}N) as the internal standards. **PGSE Diffusion Measurements.** All the measurements were recorded by Dr. Miguel Angel Rodríguez from Servei de Recursos Científics of the University Rovira i Virgili, and were performed at 600.20 MHz frequency using an Avance III-600 MHz Bruker® spectrometer equipped with an inverse TCI 5 mm cryoprobe® with an actively shielded Z-gradient coil and a microprocessor controlled gradient unit. A line shape gradient was used, and its length was 2.00 ms. The gradient strength was increased by steps of 1 % (or 5 %) during the course of the experiment (long experiment (2h) 2 % - 97 % in steps of 1%; short experiment (20 min) 5 % - 95 % in steps of 5 %). For diffusion a double stimulated echo for convection compensation with bipolar gradients and LED (longitudinal eddy-current delay) was used.[40] The time between midpoints of the two gradients was 76.57 ms for a total diffusion time of 153.14 ms for all experiments. The experiments were carried out at set temperature of 300 K within the NMR probe. The diffusion spectra were processed using TopSpin software (version 2.1, Bruker®). Diffusion values were measured on 2 mM CD_2Cl_2 solutions. Cation diffusion rates were measured using the ^1H signal from the aromatic protons. Anion diffusion was obtained from the ^1H of the protons attached to aromatic ring in BArF and OTs. We estimated the experimental error in the D-values to be ± 2 %. All data leading to the reported D-values afforded lines whose correlation coefficients were > 0.999 and 7-18 points have been used for regression analysis. **HOESY.** ^{19}F-^1H HOESY spectra were measured at concentrations of 10 mM, in CD_2Cl_2, at 298 K with a 0.8 s mixing time. **MALDI-TOF measurements of complexes:** Voyager-DE-STR (Applied Biosystems, Franingham, MA) instrument equipped with a 337 nm nitrogen laser. All spectra were acquired in the

Cationic Pd(II) complexes for CO/vinyl arenes in TFE and CO_2

positive ion reflector mode. α-cyano-4-hydroxycinnamic acid (CHCA) was used as matrix. The matrix was dissolved in THF at a concentration of 10 mg·mL^{-1}. The complex was dissolved in $CHCl_3$ (50 mg·L^{-1}). The matrix and the samples were premixed in the ratio 1:1 (Matrix : sample) and then the mixture was deposited (1 μL) on the target. For each spectrum 100 laser shots were accumulated. **MALDI-TOF measurements of copolymers**: Voyager-DE-STR (Applied Biosystems, Franingham, MA) instrument equipped with a 337 nm nitrogen laser. All spectra were acquired in the positive ion reflector mode. Ditranol was used as matrix (25 mg/mL in THF + 1 mg/mL potassium 2,2,2'-trifluoroacetate, KTFA). Copolymers CO/TBS (5 mg) were dissolved in $CHCl_3$ (1 mL) and a portion (5 μL) of this solution was added to the same volume of the matrix solution Copolymers CO/ST (5 mg) were dissolved in hexafluoroisopropanol, HFIP (0.4 mL) and $CHCl_3$ (0.6 mL) and a portion (5 μL) of this solution was added to the same volume of the matrix solution. About 1 μL of the resulting solution was deposited on the stainless steel sample holder and allowed to dry before introduction into the mass spectrometer. Three independent measurements were made for each sample. **Molecular weight measurements of CO/TBS polyketones:** The molecular weights (Mw) of copolymers and the molecular weight distributions (Mw/Mn) were determined by gel permeation chromatography versus polystyrene standards. Measurements were made in THF on a Millipore-Waters 510 HPLC Pump device using three-serial column system (MZ-Gel 100Å, MZ-Gel 1000 Å, MZ-Gel 10000 Å linear columns) with UV-Detector (ERC-7215) and IR- Detector (ERC-7515a). The software used to get the data was NTeqGPC 5.1. Samples were prepared as follow: 5 mg of the copolymer was solubilised with 2 mL of tetrahidrofurane (HPLC grade) stabilised with toluene (HPLC grade). **Molecular weight measurements of CO/ST polyketones:** The molecular weights (Mw) of styrene copolymers and the molecular weight distributions (Mw/Mn) were determined by gel permeation chromatography versus polymethylmethacrylate (PMMA) standards in the Servei de Recursos Científics from the University of Barcelona. Measurements were made in hexafluoroisopropanol (HFIP) on a Alliance-Waters 2695 HPLC Pump device using PSS PFG analytical 1000 Å rigid column with IR- Detector (Water-2414). The software used to get the data was Empower supplied by Waters. Samples were prepared as follow: 2.0 mg of the copolymer was solubilised with 2 mL of hexafluoroisopropanol (HPLC grade).

Standard copolymerisation experiment in organic solvent. Copolymerisation reactions were carried out in a thermostated glass reactor equipped with a magnetic stirrer under CO atmosphere. After introduction of the catalyst precursor **Ia-c**, **IIa-c** and **IIIa-c** ($4.1 \cdot 10^{-4}$ M), benzoquinone, solvent (20 mL), and styrene (10 mL), carbon monoxide was bubbled for 10 min into the reaction mixture heated at 30ºC. The system was then closed and connected to a balloon containing CO. After the appropiate reaction time, the reaction mixture was poured into methanol (100 mL). The polymer was filtered off, washed with methanol and dried under vacuum. **Standard copolymerisation experiment in CO_2.** In an standard catalytic experiment, the catalyst precursor **Ia-c**, **IIa-c** and **IIIa-c** ($4.1 \cdot 10^{-4}$ M) was weight and introduced into a 11 mL stainless steel high pressure reactor equipped with thick-wall glass windows. Then the α-olefin (styrene or *tert*-butylstyrene) was introduced under argon. The autoclave was pressurized with CO and CO_2 and heated up to 37 ºC and stirred during the reaction time. After reaction time, the autoclave was cooled down to room temperature and was carefully vented. The copolymer was dissolved in CH_2Cl_2 (5 mL) and precipitated pouring the solution into 70 mL of rapidly stirred methanol. The product was filtered off, washed with MeOH and vacuum dried.

Safety warning. Experiments involving pressurized gases can be hazardous and must be conducted with suitable equipment and follwing appropriate safety conditions only.

^{13}C NMR CO/*tert*-butylstyrene: (100.5 MHz, CDCl$_3$, 298 K): δ 208.0–206.5 (broad, CO), 150.0, 149.8, 134.6, 134.3 (C_{ipso}), 128.2, 125.8, 125.6 (C_{arom}), 52.9 (CH), 44.5-43.0 (broad, CH_2), 34.5 ($C_{tertbutyl}$) and 31.5 (CH_3); CO/styrene: (100.5 MHz, HFIP + CDCl$_3$, 298 K) δ 209.5–210.4 (broad, CO), 136.5, 136.1, 135.8, 135.3 (C_{ipso}), 129.4, 128.3, 128.0 (C_{arom}), 53.5 (CH) and 42.3–44.5 (broad, CH_2).

4.4.1 Complexes synthesis

[Pd(CH$_3$)Cl(NN)] (I-III)

1.2 equivalents of the ligand (**L1-L3**) (0.214 mmol) were added to a solution of [Pd(CH$_3$)Cl(COD)] (47 mg, 0.178 mmol) in 7 mL dry dichloromethane at room temperature and under argon atmosphere. After 5 h stirring at room temperature, diethyl ether was added and the product precipitated as a yellow solid, which was filtered off, washed with diethyl ether and dried under vacuum.

Cationic Pd(II) complexes for CO/vinyl arenes in TFE and CO$_2$

[Pd(CH$_3$)Cl(L1)] (I)
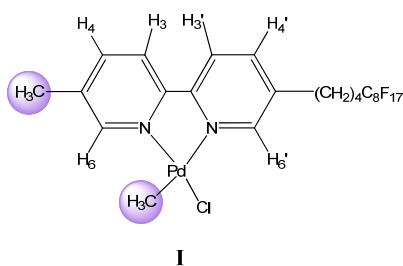
Pale brown solid (Yield 97 %).

MALDI-TOF calc. for ($C_{24}H_{20}ClF_{17}N_2Pd$) *m/z*: 840.9708 [M$^+$+K$^+$], 861.0209 [M$^+$+K$^+NH_4^+$]; found *m/z*: 841.1279 [M$^+$+K$^+$], 861.0731 [M$^+$+K$^+$NH$_4^+$].

^{1}H NMR (500 MHz, CD$_2$Cl$_2$): δ 0.89 (s, 3H, Pd-CH$_3$), 1.71-1.78 (m, 4H, (CH$_2$)$^{2'',3''}$), 2.15 (m, 2H, (CH$_2$)$^{4''}$), 2.46 (br, 3H, CH$_3$), 2.79 (m, 2H, (CH$_2$)$^{1''}$), 7.79 (d, 1H, (CH)^4, $^3J_{H3\text{-}H4}$ = 10Hz), 7.85 (d, 1H, (CH)$^{4'}$, $^3J_{H3'\text{-}H4'}$ = 5Hz), 7.95 (m, 2H, (CH)$^{3,3'}$), 8.45 (s, 1H, (CH)^6), 8.96 (psd, 1H, (CH)$^{6'}$). ^{19}F NMR (376.3 MHz, CD$_2$Cl$_2$): δ -79.6 (CF$_3$), -113.1 (CF$_2$), -120.5 (CF$_2$), -120.6 (CF$_2$), -121.4 (CF$_2$), -122.3 (CF$_2$), -124.9(CF$_2$). ^{15}N NMR (40 MHz, CD$_2$Cl$_2$): δ -149.5 (N*cis*), -116.6 (N*trans*).

[Pd(CH$_3$)Cl(L2)] (II)
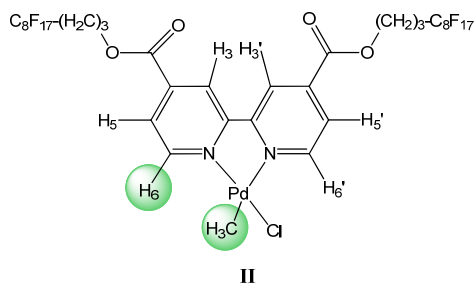
Bright yellow solid (Yield 94 %).

IR (KBr) 1732 cm^{-1} ν(COO$^-$). MALDI-TOF calc. for ($C_{35}H_{21}ClF_{34}N_2O_4Pd$) *m/z*: 1309.9678 [M$^+$-CH$_3$+3H$^+$], 1325.9992 [M$^+$+4H$^+$]; found *m/z*: 1309.9784 [M$^+$-CH$_3$+3H$^+$], 1325.9589 [M$^+$+4H$^+$].

^{1}H NMR (500 MHz, CDCl$_3$): δ 1.19 (s, 3H, Pd-CH$_3$), 2.21 − 2.29 (m, 8H, (CH$_2$)$^{3'',2''}$), 4.57 (br, 4H, (CH$_2$)$^{1''}$), 8.12 (pst, 2H, (CH)$^{5',5}$), 8.67 (s, 1H, (CH)^3), 8.71 (s, 1H, (CH)$^{3'}$), 8.93 (d, 1H, (CH)^6, $^3J_{H6\text{-}H5}$ = 5Hz), 9.48 (d, 1H, (CH)$^{6'}$, $^3J_{H6'\text{-}H5'}$ = 5Hz). ^{19}F NMR (376.3 MHz, CDCl$_3$): δ -81.1 (CF$_3$), -114.7 (CF$_2$), -122.2 (CF$_2$), -122.3 (CF$_2$), -123.2 (CF$_2$), 123.7 (CF$_2$), 126.6 (CF$_2$).

[Pd(CH$_3$)Cl(L3)] (III)

III
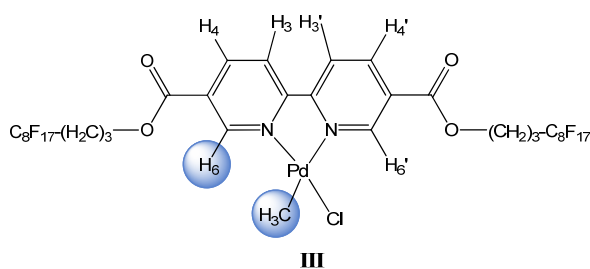
Bright yellow powder (Yield 99 %).

IR (KBr) 1717 cm^{-1} ν(COO$^-$). MALDI-TOF calc. for (C$_{35}$H$_{21}$ClF$_{34}$N$_2$O$_4$Pd) *m/z*: 1419.9295 [M$^+$-CH$_3$+CF$_3$COO$^-$], found *m/z*: 1419.1521 [M$^+$-CH$_3$+CF$_3$COO$^-$].

[Pd(CH$_3$)(NCCH$_3$)(NN)](Ia-IIIb)

1.2 equivalents of the salt, silver hexafluorophosphate or silver tosylate (6.6·10^{-2} mmol) dissolved in 1 mL of dry acetonitrile was added to a solution of [Pd (CH$_3$)(Cl)(**L1-L3**)] (**I-III**) (5.5·10^{-2} mmol) in 4 mL of dry dichloromethane, kept in dark, under magnetic stirring, at room temperature and in argon atmosphere. After 5 h the solution was filtered over celitte to remove the silver chloride salt. The solution was concentrated and diethyl ether was added giving a precipitate, which was filtered off, washed with diethyl ether and dried under vacuum.

[Pd(CH$_3$)(NCCH$_3$)(L1)][PF$_6$] (Ia)

Pale brown solid (Yield 84 %).

MALDI-TOF calc. for (C$_{26}$H$_{23}$F$_{23}$N$_3$PPd) *m/z*: 938.0223 [M$^+$-CH$_3$+2H$^+$], 954.0537 [M$^+$+3H$^+$], 974.0200 [M$^+$+Na$^+$]; found *m/z*: 938.7144 [M$^+$-CH$_3$+2H$^+$], 954.7755 [M$^+$+3H$^+$], 974.7293 [M$^+$+Na$^+$].

^{1}H NMR (500 MHz, CD$_2$Cl$_2$): δ 1.07 (s, 3H, Pd-CH$_3$), 1.72 (m, 2H, (CH$_2$)$^{3''}$), 1.78 (m, 2H, (CH$_2$)$^{2''}$), 2.17 (m, 2H, (CH$_2$)$^{4''}$), 2.48 (s, 3H, Pd-NCCH$_3$), 2.53 (s, 3H, (CH$_3$)$^{1'''}$), 2.80 (t, 1H, (CH$_2$)$^{1''}$, $^3J_{H-H}$ = 7.5Hz), 2.85 (t, 1H, (CH$_2$)$^{1''}$, $^3J_{H-H}$ = 7.5Hz), 7.96 (m, 2H, (CH)$^{4,4'}$), 8.07 (m, 2H, (CH)$^{3,3'}$), 8.32 (s, 1H, (CH)$^{6'}$), 8.34 (s, 1H, (CH)^6). ^{19}F NMR (376.3 MHz, CD$_2$Cl$_2$): δ -73.4 (PF$_6$, J_{P-F} = 712 Hz), -81.6 (CF$_3$), -115.0 (CF$_2$), -122.4 (CF$_2$), -122.6 (CF$_2$), -123.4 (CF$_2$), -124.2 (CF$_2$), -126.8 (CF$_2$). ^{15}N NMR (40 MHz, CD$_2$Cl$_2$): δ -204.7 (NCCH$_3$), -159.2 (N*cis*), -121.1 (N*trans*).

Cationic Pd(II) complexes for CO/vinyl arenes in TFE and CO$_2$

[Pd(CH$_3$)(NCCH$_3$)(L1)][OTs] (Ib)

Yellow brownish powder (Yield 74 %).

MALDI-TOF calc. for (C$_{33}$H$_{30}$F$_{17}$N$_3$O$_3$PdS) *m/z*: 938.0668 [M$^+$-NCCH$_3$+2H$^+$], 977.0778 [M$^+$]; found *m/z*: 938.7320 [M$^+$-NCCH$_3$+2H$^+$], 977.7690 [M$^+$].

^{1}H NMR (500 MHz, CD$_2$Cl$_2$): δ 0.94 (s, 3H, Pd-CH$_3$), 1.58 (s, 3H, CH$_3$-OTs), 1.67-1.74 (m, 4H, (CH$_2$)$^{3'',2''}$), 2.15 (m, 2H, (CH$_2$)$^{4''}$), 2.37 (s, 3H, (CH$_3$)$^{1'''}$), 2.42 (s, 3H, CH$_3$CN-Pd), 2.73 (m, 2H, (CH$_2$)$^{1''}$), 7.21 (d, 2H, *m*-CH-OTs, $^3J_{\text{Hm-Ho}}$ = 5Hz), 7.79 (br, 3H, *o*-CH-OTs, (CH)$^{4'}$ overlapped), 7.84 (d, 1H, (CH)^4, $^3J_{\text{H4-H3}}$ = 8.5Hz), 7.91-8.00 (m, 2H, (CH)$^{3,3'}$), 8.31 (psd, 2H, (CH)^{6cis,6trans}), 8.58 (s, 1H, (CH)$^{6'trans}$), 8.68 (s, 1H, (CH)$^{6'trans}$). ^{19}F NMR (376.3 MHz, CD$_2$Cl$_2$): δ -81.5 (CF$_3$), -115.1 (CF$_2$), -122.4 (CF$_2$), -122.6 (CF$_2$), -123.3 (CF$_2$), -124.1 (CF$_2$), -126.8 (CF$_2$). ^{15}N NMR (40 MHz, CD$_2$Cl$_2$): δ -162.4 (N*cis*), -115.9 (N*trans*).

[Pd(CH$_3$)(NCCH$_3$)(L2)][PF$_6$] (IIa)

Bright yellow solid (Yield 70 %).

IR (KBr) 1736 cm^{-1} ν(COO$^-$). MALDI-TOF calc. for (C$_{37}$H$_{24}$F$_{40}$N$_3$O$_4$PPd) *m/z*: 1439.0118 [M$^+$-PF$_6^-$+CF$_3$COO$^-$], 1473.0066 [M$^+$+2H$^+$]; found *m/z*: 1438.9903 [M$^+$-PF$_6^-$+CF$_3$COO$^-$], 1472.9887 [M$^+$+2H$^+$].

^{1}H NMR (500 MHz, CD$_2$Cl$_2$): δ 1.21 (s, 3H, Pd-CH$_3$), 2.20 (m, 4H, (CH$_2$)$^{2''}$), 2.32 (m, 4H, (CH$_2$)$^{3''}$), 2.58 (s, 3H, Pd-NCCH$_3$), 4.56 (t, 4H, (CH$_2$)$^{1''}$, $^3J_{\text{H-H}}$ = 5.5Hz), 8.17 (dd, 1H, (CH)^5, $^3J_{\text{H5-H6}}$ = 5.75Hz, $^4J_{\text{H5-H3}}$ = 1.25Hz), 8.33 (dd, 1H, (CH)$^{5'}$, $^3J_{\text{H5'-H6'}}$ = 5.5Hz, $^4J_{\text{H5'-H6'}}$ = 1.5Hz), 8.78 (m, 3H, (CH)$^{3, 3', 6}$), 8.91 (d, 1H, (CH)$^{6'}$, $^3J_{\text{H6'-H5'}}$ = 5.5Hz). ^{19}F NMR (376.3 MHz, CD$_2$Cl$_2$): δ -72.9 (PF$_6$, J_{P-F} = 712 Hz), -81.1 (CF$_3$), -114.5 (CF$_2$), -121.9 (CF$_2$), -122.2 (CF$_2$), -122.9 (CF$_2$), -123.6 (CF$_2$), 126.4 (CF$_2$). ^{15}N NMR (40 MHz, CD$_2$Cl$_2$): δ -207.6 (NCCH$_3$), -148.9 (N*cis*), -111.9 (N*trans*).

[Pd(CH$_3$)(NCCH$_3$)(L2)][OTs] (IIb)

Green brownish powder (Yield 72 %).

IR (KBr) 1729 cm^{-1} ν(COO$^-$). MALDI-TOF calc. for (C$_{44}$H$_{31}$F$_{34}$N$_3$O$_7$PdS) *m/z*: 1497.0381 [M$^+$], 1521.0361 [M$^+$+Na$^+$]; found *m/z*: 1497.1564 [M$^+$], 1521.1980 [M$^+$+Na$^+$].

^{1}H NMR (500 MHz, CD$_2$Cl$_2$): δ 1.09 (s, 3H, Pd-CH$_3$), 1.41 (br, 3H, CH$_3$-OTs), 2.19 (m, 4H, (CH$_2$)$^{3''}$), 2.31 (m, 4H, (CH$_2$)$^{2''}$), 2.40 (s, 3H, CH$_3$CN-Pd), 4.53 (s, 4H,

$(CH_2)^{1''}$), 7.25 (br, 2H, *m*-CH-OTs), 7.81 (br, 2H, *o*-CH-OTs), 8.06 (d, 1H, $(CH)^5$, $^3J_{H5\text{-}H6}$ = 4.5Hz), 8.18 (d, 1H, $(CH)^{5'}$, $^3J_{H5'\text{-}H6'}$ = 4.5Hz), 8.71 (s, 2H, $(CH)^{3,3'}$), 8.78 (d, 1H, $(CH)^6$, $^3J_{H6\text{-}H5}$ = 4.5Hz), 9.22 (d, 1H, $(CH)^{6'}$, $^3J_{H6'\text{-}H5'}$ = 4.5Hz). ^{19}F NMR (376.3 MHz, CD_2Cl_2): δ -81.5 (CF_3), -115.0 (CF_2), -122.4 (CF_2), -122.6 (CF_2), -123.3 (CF_2), -124.0 (CF_2), -126.8 (CF_2).

[Pd(CH₃)(NCCH₃)(L3)][PF₆] (IIIa)

Pale yellow solid (Yield 57 %).

IR (KBr) 1733 cm^{-1} v(COO$^-$). MALDI-TOF calc. for ($C_{37}H_{24}F_{40}N_3O_4PPd$) *m/z*: 1419.9080 [$M^+$-CH₃-PF₆$^-$+Ag$^+$], 1473.0066 [$M^+$+2H$^+$]; found *m/z*: 1419.1599 [M^+-CH₃-PF₆$^-$+Ag$^+$], 1472.9887 [M^++2H$^+$].

^1H NMR (500 MHz, CD_2Cl_2): δ 1.25 (s, 3H, Pd-CH₃), 2.18 (m, 4H, $(CH_2)^{2''}$), 2.32 (m, 4H, $(CH_2)^{3''}$), 2.55 (s, 3H, Pd-NCCH₃), 4.53 (t,4H, $(CH_2)^{1''}$, *J* = 6.25Hz), 8.45 (pst, 2H, $(CH)^{3,3'}$), 8.77 (pst, 2H, $(CH)^{4,4'}$), 9.08 (s, 1H, $(CH)^{6'}$), 9.15 (s, 1H, $(CH)^6$). ^{19}F NMR (376.3 MHz, CD_2Cl_2): δ -73.1 (PF₆, $J_{P\text{-}F}$ = 712 Hz), -81.1 (CF_3), -114.5 (CF_2), -121.9 (CF_2), -122.1 (CF_2), -122.9 (CF_2), -123.5 (CF_2), 126.3 (CF_2). ^{15}N NMR (40 MHz, CD_2Cl_2): δ -205.6 (NCCH₃), -156.6 (N*cis*), -119.0 (N*trans*).

[Pd(CH₃)(NCCH₃)(L3)][OTs] (IIIb)

Green brownish powder (Yield 52 %).

IR (KBr) 1730 cm^{-1} v(COO$^-$). MALDI-TOF calc. for ($C_{44}H_{31}F_{34}N_3O_7PdS$) *m/z*: 1419.9080 [$M^+$-CH₃-OTs$^-$+Ag$^+$], 1474.0462 [$M^+$-NCCH₃+NH₄$^+$]; found *m/z*: 1419.1079 [M^+-CH₃-OTs$^-$+Ag$^+$], 1474.2297 [M^+-NCCH₃+NH₄$^+$].

^1H NMR (500 MHz, CD_2Cl_2): δ 1.15 (s, 3H, Pd-CH₃), 1.27 (s, 3H, CH₃-OTs), 2.16 (m, 4H, $(CH_2)^{3''}$), 2.31 (m, 4H, $(CH_2)^{2''}$), 2.39 (s, 3H, CH₃CN-Pd), 4.51 (psq, 4H, $(CH_2)^{1''}$), 7.24 (d, 2H, *m*-CH-OTs, $^3J_{Hm\text{-}Ho}$ = 9Hz), 7.81 (d, 2H, *o*-CH-OTs, $^3J_{Ho\text{-}Hm}$ = 9Hz), 8.26 (d, 1H, $(CH)^3$, $^3J_{H3\text{-}H4}$ = 8.5Hz), 8.30 (d, 1H, $(CH)^{3'}$, $^3J_{H3'\text{-}H4'}$ = 8.5Hz), 8.67 (m, 2H, $(CH)^{4,4'}$), 9.18 (d, 1H, $(CH)^6$, $^4J_{H6\text{-}H4}$ = 2Hz), 9.71 (d, 1H, $(CH)^{6'}$, $^4J_{H6'\text{-}H4'}$ = 2Hz). ^{19}F NMR (376.3 MHz, CD_2Cl_2): δ -81.5 (CF_3), -115.0 (CF_2), -122.4 (CF_2), -122.5 (CF_2), -123.3 (CF_2), -123.7 (CF_2), -126.8 (CF_2). ^{15}N NMR (40 MHz, CD_2Cl_2): δ -135.0 (N*trans*).

Cationic Pd(II) complexes for CO/vinyl arenes in TFE and CO₂

[Pd(CH$_3$)(NCCH$_3$)(NN)][BArF] (Ic-IIIc)

Two drops of dry acetonitrile were added to a suspension of **Ib-IIIb** (3.4·10^{-2} mmol) and 1.1 equivalents of NaBArF (33 mg, 3.7·10^{-2} mmol) in dry CH$_2$Cl$_2$ (2 mL). . The mixture was stirred for 0.5 h at 0°C and then for 1h at room temperature. The resulting suspension was filtered off, to remove the precipitated NaOTs, which was washed with dry methylenechloride. The filtrate was evaporated in vacuum to yield an oil, which was triturated with pentane yielding a foam.

[Pd(CH$_3$)(NCCH$_3$)(L1)][BArF] (Ic)

Pale brown foam (Yield 97 %).

MALDI-TOF calc. for (C$_{58}$H$_{35}$BF$_{41}$N$_3$Pd) *m/z*: 1600.1373 [M$^+$-CF$_3$], 1643.1613 [M$^+$-CF$_3$+Na$^+$+NH$_4^+$]; found *m/z*: 1599.1922 [M$^+$-CF$_3$], 1643.1685 [M$^+$-CF$_3$+Na$^+$+NH$_4^+$].

^{1}H NMR (400 MHz, CD$_2$Cl$_2$): δ1.09 (s, 3H, Pd-CH$_3$), 1.71 (m, 2H, (CH$_2$)$^{2''}$), 1.78 (m, 2H, (CH$_2$)$^{3''}$), 2.16 (m, 2H, (CH$_2$)$^{4''}$), 2.48 (s, 3H, Pd-NCCH$_3$), 2.55 (d, 3H, (CH$_3$)$^{1'''}$), 2.81 (m, 2H, (CH$_2$)$^{1''}$), 7.54 (s, 4H, BArF), 7.71 (s, 8H, BArF), 7.90-8.10 (m, 4H, (CH)$^{4,4'}$, (CH)$^{3,3'}$), 8.23 (d, 1H, (CH)^6), 8.33 (s, 1H, (CH)$^{6'}$). ^{19}F NMR (376.3 MHz, CD$_2$Cl$_2$): δ -63.3 (CF$_3$, BARF), -81.5 (CF$_3$), -115.1 (CF$_2$), -122.4 (CF$_2$), -122.6 (CF$_2$), -123.4 (CF$_2$), -124.2 (CF$_2$), -126.8 (CF$_2$). ^{15}N NMR (40 MHz, CD$_2$Cl$_2$): δ -165.9 (N*cis*).

[Pd(CH$_3$)(NCCH$_3$)(L2)][BARF] (IIc)

Yellow brownish foam (Yield 65 %).

IR (KBr) 1744 cm^{-1} ν(COO$^-$). MALDI-TOF calc. for (C$_{69}$H$_{36}$BF$_{58}$N$_3$O$_4$Pd) *m/z*: 1393.9049 [M$^+$-NCCH$_3$-BArF+Ag$^+$], 1419.9080 [M$^+$-CH$_3$-BArF+Ag$^+$]; found *m/z*: 1393.0875 [M$^+$-NCCH$_3$-BArF+Ag$^+$], 1419.1705 [M$^+$-CH$_3$-BArF+Ag$^+$].

^{1}H NMR (500 MHz, CD$_2$Cl$_2$): δ 1.23 (s, 3H, Pd-CH$_3$), 2.20 (m, 4H, (CH$_2$)$^{2''}$), 2.30 (m, 4H, (CH$_2$)$^{3''}$), 2.52 (s, 3H, Pd-NCCH$_3$), 4.56 (t, 4H, (CH$_2$)$^{1''}$, $^3J_{\text{H-H}}$ = 6Hz), 7.55 (s, 4H, BArF), 7.71 (s, 8H, BArF), 8.18 (dd, 1H, (CH)^5, $^3J_{\text{H5-H6}}$ = 5.5Hz, $^4J_{\text{H5-H3}}$ = 1Hz), 8.21 (d, 1H, (CH)$^{5'}$, $^3J_{\text{H5'-H6'}}$ = 3.5Hz), 8.66 (d, 1H, (CH)^6, $^3J_{\text{H6-H5}}$ = 5.5Hz), 8.76 (d, 1H, (CH)$^{6'}$, $^3J_{\text{H6'-H5'}}$ = 5.5Hz), 8.82 (s, 2H, (CH)$_{3',3}$). ^{19}F NMR (376.3 MHz, CD$_2$Cl$_2$) : δ -63.3 (CF$_3$, BARF), -81.6 (CF$_3$), -114.9 (CF$_2$), -122.4 (CF$_2$), -122.6 (CF$_2$), -123.4 (CF$_2$), -124.1 (CF$_2$), -126.8 (CF$_2$). ^{15}N NMR (40 MHz, CD$_2$Cl$_2$): δ -204.3 (NCCH$_3$), -149.3 (N*cis*), -111.5 (N*trans*).

[Pd(CH₃)(NCCH₃)(L3)][BARF] (IIIc)

Pale brown foam (Yield 47 %).

IR (KBr) 1741 cm^{-1} ν(COO$^-$). MALDI-TOF calc. for ($C_{69}H_{36}BF_{58}N_3O_4Pd$) *m/z*: 1419.9080 [M$^+$-CH₃-BArF+Ag$^+$], 1477.9755 [M$^+$-BArF+CF₃COO$^-$+K$^+$]; found *m/z*: 1419.0966 [M$^+$-CH₃-BArF+Ag$^+$], 1477.1439 [M$^+$-BArF+CF₃COO$^-$+K$^+$].

^{1}H NMR (400 MHz, CDCl₃): δ 1.27 (s, 3H, Pd-CH₃), 2.18 (m, 4H, (CH₂)$^{2''}$), 2.30 (m, 4H, (CH₂)$^{3''}$), 2.53 (s, 3H, Pd-NCCH₃), 4.52 (psq, 4H, (CH₂)$^{1''}$), 7.55 (s, 4H, BArF), 7.71 (s, 8H, BArF), 8.30 (pst, 2H, (CH)$^{3,3'}$), 8.71 (dd, 1H, (CH)$^{4'}$, $^3J_{H4'-H3'}$ = 8.5Hz, $^4J_{H4'-H6'}$ = 1Hz), 8.75 (dd, 1H, (CH)^4, $^3J_{H4-H3}$ = 8.5Hz, $^4J_{H4-H6}$ = 1Hz), 9.07 (s, 1H, (CH)$^{6'}$), 9.18 (s, 1H, (CH)^6). ^{19}F NMR (376.3 MHz, CD₂Cl₂): δ -63.3 (CF₃, BARF), -81.6 (CF₃), -114.9 (CF₂), -122.4 (CF₂), -122.6 (CF₂), -123.4 (CF₂), -124.1 (CF₂), -126.8 (CF₂). ^{15}N NMR (40 MHz, CD₂Cl₂): δ -204.8 (NCCH₃), -155.9 (N*cis*), -118.2 (N*trans*).

[Rh(L1)(cod)][X] (Ib'-c')

L1 (50 mg, 0.077 mmol) was added to a solution of the complex [Rh(cod)₂][X] (0.077 mmol) in 3 mL of anhydrous dichloromethane. The solution changed from burgundy to orange or brown. Then it was stirred for 5 minutes. Diethyl ether was added to the solution to afford the corresponding solid, which was filtered off, washed with cold diethyl ether and dried under vacuum.

[Rh(cod)(L1)](OTs) (Ib')

Light brown solid (Yield 31 %).

MALDI-TOF calc. for ($C_{38}H_{36}F_{17}N_2O_3RhS$) *m/z*: 1011.0990 [M$^+$-CH₃], 855.1109 [M$^+$-OTs]; found *m/z*: 1011.1529 [M$^+$-CH₃], 855.1777 [M$^+$-OTs].

^{1}H NMR (400 MHz, CDCl₃): δ 1.70 (m, 2H, (CH₂)$^{4''}$), 2.14 (m, 4H, (CH₂)$^{3'',2''}$) 2.16 (d, 4H, (CH₂)^{COD}, $^3J_{H-H}$ = 8.8Hz), 2.30 (s, 3H, (CH₃)$^{1'''}$), 2.39 (s, 3H, OTs-CH₃), 2.62 (m, 4H, (CH₂)^{COD}), 2.70 (t, 2H, (CH₂)$^{1''}$, $^3J_{H-H}$ = 7.6Hz), 4.53 (br, 4H, (CH)^{COD}), 7.07 (d, 2H, *m*-CH-OTs, $^3J_{Hm-Ho}$ = 7.2Hz), 7.43 (s, 2H, (CH)$^{6,6'}$), 7.72 (br, 2H, *o*-CH-OTs), 8.07 (d, 1H, (CH)$^{4'}$, $^3J_{H4'-H3'}$ = 8Hz), 8.15 (d, 1H, (CH)^4, $^3J_{H4-H3}$ = 8.4Hz), 8.92 (d, 1H, (CH)$^{3'}$, $^3J_{H3'-H4'}$ = 8Hz), 9.00 (d, 1H, (CH)^3, $^3J_{H3-H4}$ = 8.4Hz); ^{19}F NMR (376.3 MHz, CDCl₃): δ -81.2 (CF₃), 114.5 (CF₂), -122.0 (CF₂), -122.2 (CF₂), -123.0 (CF₂), -123.8 (CF₂), -126.4 (CF₂).

Cationic Pd(II) complexes for CO/vinyl arenes in TFE and CO₂

[Rh(cod)(L1)](BArF) (Ic')

Orange foam (Yield 73 %).

MALDI-TOF calc. for ($C_{63}H_{41}BF_{41}N_2Rh$) *m/z*: 887.0748 [M^+-CH_3-BArF+2Na^+], 854.1031 [M^+-BArF]; found *m/z*: 887.2039 [M^+-CH_3-BArF+2Na^+], 853.9245 [M^+-BArF].

^{1}H NMR (400 MHz, $CDCl_3$): δ 1.68 (br, 2H, $(CH_2)^{4''}$), 2.10 (m, 4H, $(CH_2)^{3'',2''}$) 2.12 (d, 4H, $(CH_2)^{COD}$, $^3J_{H-H}$ = 8.4Hz), 2.34 (s, 3H, $(CH_3)^{1'''}$), 2.55 (br, 4H, $(CH_2)^{COD}$), 2.67 (t, 2H, $(CH_2)^{1''}$, J = 7.6Hz), 4.51 (m, 4H, $(CH)^{COD}$), 7.50 (s, 4H, BArF), 7.50-7.71 (m, 6H, $(CH)^{6,6',4,4',3,3'}$), 7.71 (s, 8H, BArF); ^{19}F NMR (376.3 MHz, $CDCl_3$): δ -62.8 (CF_3, BArF), -81.2 (CF_3), -114.8 (CF_2), -122.2 (CF_2), -122.4 (CF_2), -124.0 (CF_2), -123.2 (CF_2), -126.6 (CF_2). .

4.5 Supporting information

A pdf file containing all the NMR spectra of complex from **I-III** to **I-IIIa-c**, the ^{1}H-^{1}H NOESY spectra, the ^{19}F-^{1}H HOESY spectra, the MALDI-TOF analysis and IR spectra as well as a pdf of the PGSE calculation and the MALDI-TOF spectra of each catalysis are available in the supporting information as an electronic file.

4.6 References

[1] *(a)* Drent, E., Budzelaar, P.H.M. *Chem. Rev.* **1996**, *96*, 663-681. *(b)* Bianchini, C. and Meli, A. *Coord. Chem. Rev.* **2002**, *225*, 35–66.

[2] *(a)* Durand, J.; Milani, B. *Coord. Chem. Rew.* **2006**, *250*, 542-560. *(b)* Togni, A.; Venanzi, L. M. *Angew. Int. Ed. Engl.* **1994**, *33*, 497-526. *(c)* Sen, A., *Catalytic Synthesis of alkene-carbon monoxide copolymers and cooligomers*, Kluwer Academic Publishers, **2003**, Dordecht, The Netherlands. *(d)* Brookhart, M.; Rix, F. C.; De Simone, J. M.; Barborak, C. J. *J. Am. Chem. Soc.* **1992**, *114*, 5894-5895. *(e)* Brookhart, M.; Wagner, M. I.; Balavoine, G. G. A.; Haddou, H. A. *J. Am. Chem. Soc.* **1994**, *116*, 3641-3642. (f) Brookhart, M.; Wagner, M. L. *J. Am. Chem. Soc.* **1996**, *118*, 7219-7220. *(g)* Bastero, A.; Ruiz, A.; Reina J.A.; Claver, C.; Guerrero, A. M., Jalon, F. A.; Manzano, B. R. *J. Organomet. Chem.* **2001**, *619*, 287-292. *(h)* Bastero, A.; Castillon, S.; Claver, C.; Ruiz, A. *Eur. J. Inorg. Chem.*, **2001**, *12*,

3009-3011. *(i)* Carfagna, C.; Gatti, G.; Martini, D.; Pettinari, C. *Organometallics*, **2001**, *20*, 2175-2082. *(j)* Nozaki, K.; Komaki, H.; Kawashima, Y.; Hiyama, T.; Matsubara, T. *J. Am. Chem. Soc.,* **2001**, *123*, 534-544.

[3] Scarel, A.; Durand, J.; Franchi, D.; Zangrando, E.; Mestroni, G.; Milani, B.; Gladiali, S.; Carfagna, C.; Binotti, B.; Bronco, S.; Gragnoli, T. *J. Organomet. Chem*. **2005**, *690*, 2106-2120.

[4] Durand, J.; Zangrando, E.; Stener, M.; Fronzoni, G.; Carfagna, C.; Binotti, B.; Kamer, P.C.J.; Müller, C.; Carporali, M.; van Leeuwen, P.W.N.M., Vogt, D. and Milani, B. *Chem. Eur. J.* **2006**, *12*, 7639 – 7651.

[5] Giménez-Pedrós, M.; Tortosa-Estorach, C.; Bastero, A.; Masdeu-Bultó, A.M.; Solinas M. and Leitner. W. *Green Chem.*, **2006**, *8*, 875–877.

[6] Milani, B.; Marson, A.; Zangrando, E.; Mestroni, G.; Ernsting, J.M. and Elsevier, C.J. *Inorg. Chim. Acta,* **2002**, *327*, 188-201.

[7] Slootweg J.C. and Chen, P. *Organometallics,* **2006**, *25*, 5863-5869.

[8] Byers, P.K. and Canty, A.J. *Organometallics* **1990**, *9*, 210-220.

[9] Gottlieb, H.E.; Kotlyar, V. and Nudelman, A. *J. Org. Chem.* **1997**, *62*, 7512-7515.

[10] Mason, J. *Chem Rev,* **1981**, *81*, 205-228.

[11] *(a)* Pazderski, L.; Szłyk, E.; Sitkowski, J.; Kamieński, B.; Kozerski, L.; Toušek J. and Marek. R. *Magn. Reson. Chem.* **2006**, *44*, 163–170. *(b)* Pazderski, L.; Toušek, J.; Sitkowski, J.; Kozerski L. and Szłyk. E. *Magn. Reson. Chem.* **2007**, *45*, 1045–1058.

[12] Rülke, L.E.; Ernstig, J.M.; Spek, A.L.; Elsevier, C.S.; van Leeuwen, P.W.N.M. and Vrieze, K. *Inorg. Chem.* **1993**, *32,* 5769-5778.

[13] Gregušová, A.; Perera, S.A. and Bartlett, R.J. *J. Chem. Theory Comput.* **2010,** *6,* 1228–1239.

[14] Bastero, A.; Claver, C.; Ruiz, A.; Castillón, S.; Daura, E.; Bo, C.; Zangrado, E. *Chem. Eur. J.*, **2004**, *10*, 3747-3760.

[15] Pregosin, P.S.; Kumar P.G.A. and Fernández, I. *Chem. Rev.*, **2005**, 2977-2998.

[16] Pregosin, P.S. *Prog. NMR Spectr.*, **2006**, *49*, 261-288.

[17] Schott, D.; Pregosin, P.S.; Albinati A. and Rizzato, S. *Inorg. Chim. Acta*, **2007**, 3203-3212.

[18] Schott D. and Pregosin, P.S. *Organometallics*, **2006**, *25*, 1749-1754.

Cationic Pd(II) complexes for CO/vinyl arenes in TFE and CO₂

[19] Sirbu, D.; Consiglio, G.; Milani, B.; Kumar, P.G.A.; Pregosin P.S. and Gishig. S. *J. Organomet. Chem.*, **2005**, *690*, 2254-2262.

[20] Schott, D.; Pregosin, P.S.; Veiron L.F. and Calhorda, M.J. *Organometallics*, **2005**, *24*, 5710-5717.

[21] Schott D. and Pregosin, P.S. *Inorg. Chem.* **2005**, *44*, 5941-5948.

[22] Kumar, P.G.A.; Pregosin, P.S.; Vallet, M.; Bernardinelli, G.; Jazzar, R.F.; Viton F. and Kundig, E.P. *Organometallics*, **2004**, *23*, 5410-5418.

[23] Martínez-Viviente E. and Pregosin, P.S *Inorg. Chem.*, **2003**, *42*, 2209-2214.

[24] Kumar, P.G.A.; Pregosin, P.S.; Goicoechea J.M. and Whittlesey. M.K. *Organometallics*, **2003**, *22*, 2956-2960.

[25] Pregosin, P.S.; Martínez-Viviente, E. and Kumar. P.G.A. *Dalton Trans.*, **2003**, 4007-4014.

[26] Martínez-Viviente, E.; Ruegger, H.; Pregosin P.S. and López-Serrano, J. *Organometallics* **2002**, *21,* 5841-5846.

[27] Macchioni, A.; Bellachioma, G.; Cardaci, G.; Travaglia, M.; Zuccaccia, C.; Milani, B.; Corso, G.; Zangrando, E.; Mestroni, G.; Carfagna C. and Formica, M. *Organometallics*, **1999**, *18*, 3061-3069.

[28] Strauss, S.H. *Chem. Rev.*, **1993**, *93*, 927-942.

[29] NOESY and HOESY NMR spectroscopy can detect only interionic dipolar interactions that are closer tan 4.5 – 5.0 Å and are useful only when intimate ion-pairs are substantially present (ref. 23).

[30] *(a)* Drago, D.; Pregosin P.S. and Pfaltz. A. *Chem. Comm.* **2002**, *3*, 286-287. *(b)* Macchioni, A.; Zuccaccia, C.; Clot, E.; Gruet K. and Crabtree, R.H. *Organometallics*, **2001**, *20*, 2367-2373. *(c)* Kumar, P.G.A.; Pregosin, P.S.; Schmid T. and Consiglio. G. *Magn. Reson. Chem.*, **2004**, *42*, 795-800.

[31] Scarel, A.; Durand, J.; Franchi, D.; Zangrando, E.; Mestroni, G.; Carfagna, C.; Mosca, L.; Seraglia, R.; Consiglio, G.; Milani, B. *Chem. Eur. J.* **2005**, *11*, 6014-6023.

[32] Milani, B.; Anzilutti, A.; Vicentini, L.; Sessanta o Santi, A.; Zangrando, E.; Geremia, S. and Mestroni, G. *Organometallics* **1997**, *16*, 5064 –5075.

[33] Scarel, A.; Axet, M.R.; Amoroso, F.; Ragaini, F.; Elsevier, C.J.; Holuigue, A.; Carfagna, C.; Mosca L. and Milani, B. *Organometallics* **2008**, *27*, 1486–1494

[34] Pisano, C.; Nefkens, S.C.A. and Consiglio, G. *Organometallics*, **1992**, *11*, 1975-1978.

[35] Tortosa-Estorach, C. *PhD. Thesis*, Universitat Rovira i Virgili, **2007**, Tarragona, Spain.

[36] Santi, R.; Romano, A.M.; Garrone, R.; Abbondanza, L.; Scalabrini, M. and Bacchilega, G. *Macromol. Chem. Phys.* **1999**, *200,* 25–30.

[37] Binotti, B.; Carfagna, C.; Zuccaccia, C. and Macchioni A. *Chem. Commun.* **2005**, 92–94.

[38] Milani, B.; Corso, G.; Mestroni, G.; Carfagna, C.; Formica, M.; Seraglia, R. *Oranometallics*, **2000**, *19*, 3435-3441.

[39] *(a)* Chen, J.T. and Sen, A. *J. Am. Chem. Soc.* **1984**, *106*, 1506-1507. *(b)* Sperrle, M. and Consiglio, G. *J. Organomet. Chem.* **1996**, *506*, 177-180.

[40] Jerschow, A. and Mueller, N. *J. Magn. Reson.* **1997**, *125*, 372-375.

Chapter - 5

Reactivity and Characterization of New Phosphinine Complexes. Application as Catalyst in CO/α-Olefins Copolymerization

The coordination chemistry of the bidentate P,N hybrid ligand 2-(2′-pyridyl)-4,6-diphenylphosphinine (**L4**) towards Pd(II), Pt(II) and Rh(I) was investigated. The molecular structure of the complexes [Rh(cod)(**L4**)]BF$_4$, [PdCl$_2$(**L4**)] and [PtCl$_2$(**L4**)] could be determined by X-ray diffraction, representing the first structurally characterized phosphinine-Pd(II) and Pt(II) complexes. Both Pd(II) and Pt(II) complexes react with (chiral) alcohols and (chiral) amines at the P=C double bond at elevated temperature, leading to the corresponding product [MCl$_2$[**L4**H·XR] (XR = OR or NR$_1$R$_2$). The molecular structure of [PdCl$_2$[**L4**H·OCH$_3$] was determined crystallographically, revealing that the reaction with methanol proceeds selectively via a syn-addition to one of the P=C double bonds. Reaction of [PdCl$_2$(**L4**H·OEt)] with chelating diphosphine (DPPE) at room temperature in CH$_2$Cl$_2$ leads quantitatively to [PdCl$_2$(DPPE)] and **L4** by elimination of ethanol and re-aromatization of the phosphorus heterocycle. Preliminary results in CO/α-olefins copolymerisation were obtained with in situ Pd(II) catalysts.
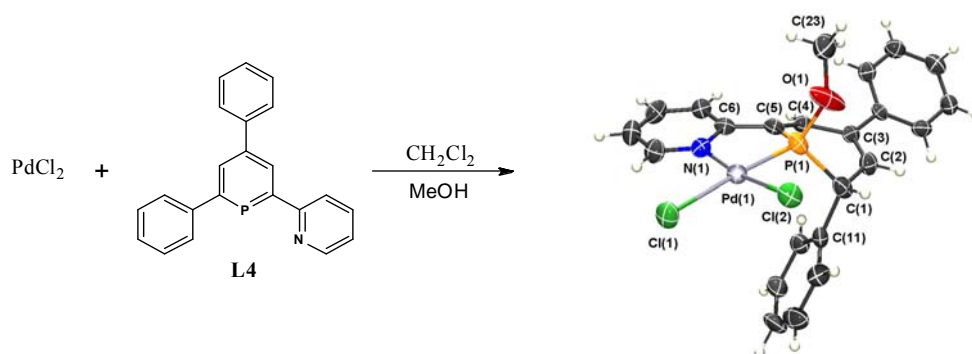
This work has been done in collaboration with Dr. C. Müller (Technische Universiteit Eindhoven, The Netherland)

Reactivity and Characterization of Phosphinine Complexes

5.1   Introduction

Phosphinines are planar, aromatic phosphorus heterocycles, which are more similar to their pyridine analogues than trivalent phosphines. In comparison to pyridines, they are much better π-acceptor, butless good σ-donor ligands.Moreover, they are relatively inert to electrophilic attack.[1]

These aromatic compounds have been known in the literature since 1966 due to the pioneering work of Märkl, who succeed in preparing 2,4,6-triphenylphosphine *via* pyrilium salts (Figure 5.1).[2] In the following years several routes for the synthesis of phosphinines have been described, nevertheless the original synthetic procedure *via* pyrylium salts is highly flexible and modular (Scheme 5.1).[3,4] This synthetic route starts from substituted benzaldehydes and acetophenones, which can also contain different substituents. The key intermediate is the formation of the pyrylium salt, which is converted in the corresponding phosphinines by reaction with an appropriate highly nucleophilic phosphorus source, PH_3-analogues ($P(CH_2OH)_3$ or $P(SiMe_3)_3$). The yields are generally low, between 10-50%. However, they can be obtained highly pure using column chromatography or crystallization.
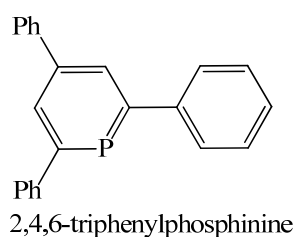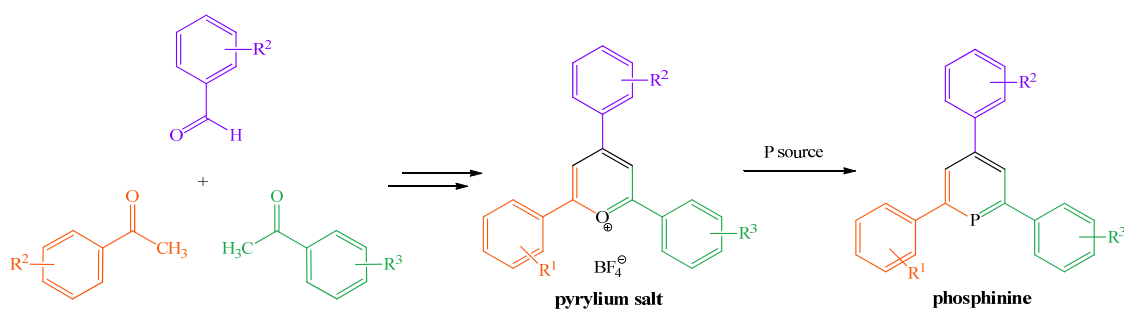

2,4,6-triphenylphosphinine

Figure 5.1. Examples of phosphinine ligands.

Phosphinines are easily characterized by NMR spectroscopy. The ^{31}P NMR spectrum shows a typical downfield shift of about δ = + 200 ppm and all the aromatic protons present chemical shift values downfield from benzene in the ^1H NMR spectrum.[1a]

Scheme 5.1. Modularity of the synthesis of phosphinines.

This kind of ligands possesses two different coordination sites, the phosphorus lone pair and the aromatic system. The coordination through these coordination sites leads to different coordination modes, the most common ones are represented in Figure 5.2. Generally, the most observed coordination mode is through the lone pair of the phosphorus atom (η^1 coordination), which is observed with late transition metals in low oxidation states (for example Rh(I))), due to the strong π-acceptor properties of the phosphinine ligand. However, also the η^6 coordination mode can be observed, which is typically found in complexes with early transition metals in order to compensate the electron deficiency of the metal centre. Some examples are Ti(0), V(0) or LM(CO)$_3$ complexes, where L is the phosphinine and M could be Cr, Mo or W. Moreover, this coordination mode can be imposed by steric effects, for example when *tert*-butyl or Me$_3$Si groups are present in the *ortho* position, preventing the σ-coordination. The mixed η^1- η^6 binding mode is unusual for phosphinines, but it has been found for metals in the centre of the transition series (for example manganese).[1a]

σ- mode; η^1 $\quad$ π- mode; η^6 $\quad$ σ/π- mode; η^1,η^6 $\quad$ σ- mode; μ^2
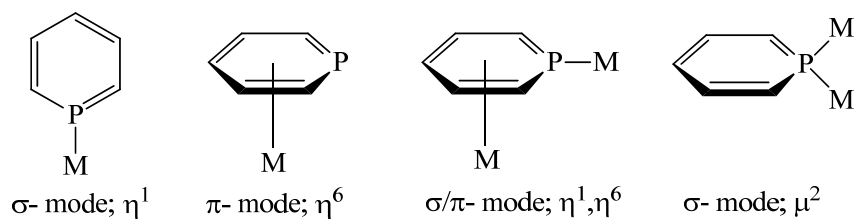
Figure 5.2. Common coordination modes of phosphinines.

2,2'-Bipyridine (bpy) and its derivatives are well studied nitrogen ligands and their rich coordination chemistry has often been exploited for the development of molecular devices, homogeneous catalytic systems or modern materials with interesting photophysical properties.[5] The replacement of a pyridine unit by a π-accepting phosphinine[1,2,6,7] entity leads to 2-(2'-pyridyl)phosphinine, a semi equivalent of bpy containing a low-coordinated "soft" phosphorus and a "hard" nitrogen heteroatom. Such chelates are bidentate hybrid ligands, which have first been described by Mathey *et al*. in 1982 with the synthesis of 2-(2'-pyridyl)-4,5-dimethylphosphinine (NIPHOS, Figure 5.3).[8,9] However, the original synthetic route *via* the pyrilium salt allows easily the incorporation off other additional donor- and heteroatoms in the phosphine moiety.
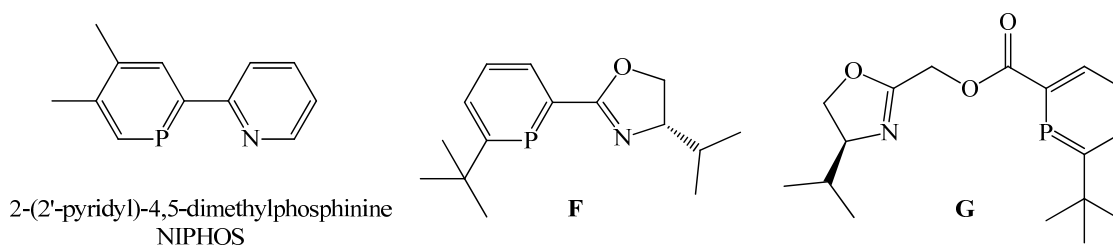
Reactivity and Characterization of Phosphinine Complexes

Figure 5.3. P,N-phosphinine ligands reported previously.

Only a few studies were devoted so far to NIPHOS coordination chemistry as this particular ligand requires a multistep synthesis and is, at the same time, difficult to handle due to its high sensitivity towards nucleophilic attack at the phosphorus atom and facile protonation at the nitrogen centre.[10] The few examples reported in literature are complexes of the type [M(NIPHOS)(CO)$_4$] (M = Cr, Mo, W),[11] the highly water-sensitive Pd(II) and Pt(II) complexes [MCl(L)(NIPHOS)][MCl$_3$(L)] (L = tertiary phosphine),[12] as well as Rh(I) and Ir(I) dimers of the type [Ir$_2$(cod)$_2$(NIPHOS)$_2$][X]$_2$ and [Rh$_2$(nbd)$_2$(NIPHOS)$_2$][X]$_2$ (X = SbF$_6$, cod = 1,5-cyclooctadiene, nbd = norbornadiene),[13] in which the phosphinine ligand adopts a μ^2-bonding mode. Interestingly, reactivity studies have also shown that NIPHOS binds stronger to Ir(I) and Rh(I) than bpy.

Only two more P,N-phosphinine ligands are found in literature (**F** and **G**, Figure 5.3) and applied in homogeneous catalysis. **F** and **G** were used in the Rh-catalysed hydroformylation of styrene by Breit[14] and in the recent literature **F** was used in Ir-catalysed enantioselective hydrogenation of alcohols and imines by Neumann and Pfaltz.[15]
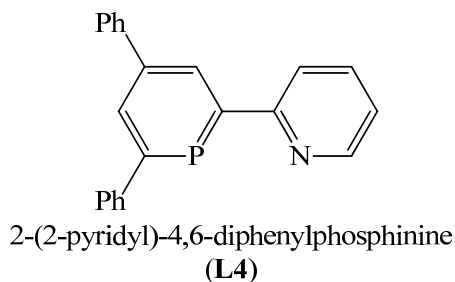

2-(2-pyridyl)-4,6-diphenylphosphinine
(**L4**)

Figure 5.4. Phosphinine ligand (**L4**) of the study.

Since P,N ligands are potential ligands for homogeneous catalysis and the 2,2'-bipyridine derivative 2-(2'-pyridyl)-4,6-diphenyl-phosphinine **L4** (Figure 5.4) is readily available from the corresponding pyridyl-functionalized pyrylium salt and P(SiMe$_3$)$_3$,[16]

144

we report here the coordination chemistry of **L4** towards Pd(II), Pt(II) and Rh(I) and the particular reactivity of Pd(II) and Pt(II) complexes with (chiral) alcohols and (chiral) amines. Some attempts of using the Pd(II) complexes prepared as catalysts in the CO/α-olefins copolymerisation were also done.

5.2   Results and Discussions

5.2.1 Ligand Synthesis

The phosphinine-based ligand **L4** was prepared using the original phosphinine synthesis via pyrylium salts (Scheme 5.2).[16] Here, the scale up to 6 gr and optimization of the synthesis was achieved.

The first step was a Michael addition of benzylidene-2-acetophenone with 2-acetylpyridine to form the 3,5-diphenyl-1-(2-pyridyl)pentane-1,5-dione (diketone), following the synthesis route by Cave *et al.*[17] modified by Müller *et al.*,[16] under solvent free conditions. The diketone was recrystallized from water/ethanol and was isolated by filtration (Scheme 5.2, 82 % yield).
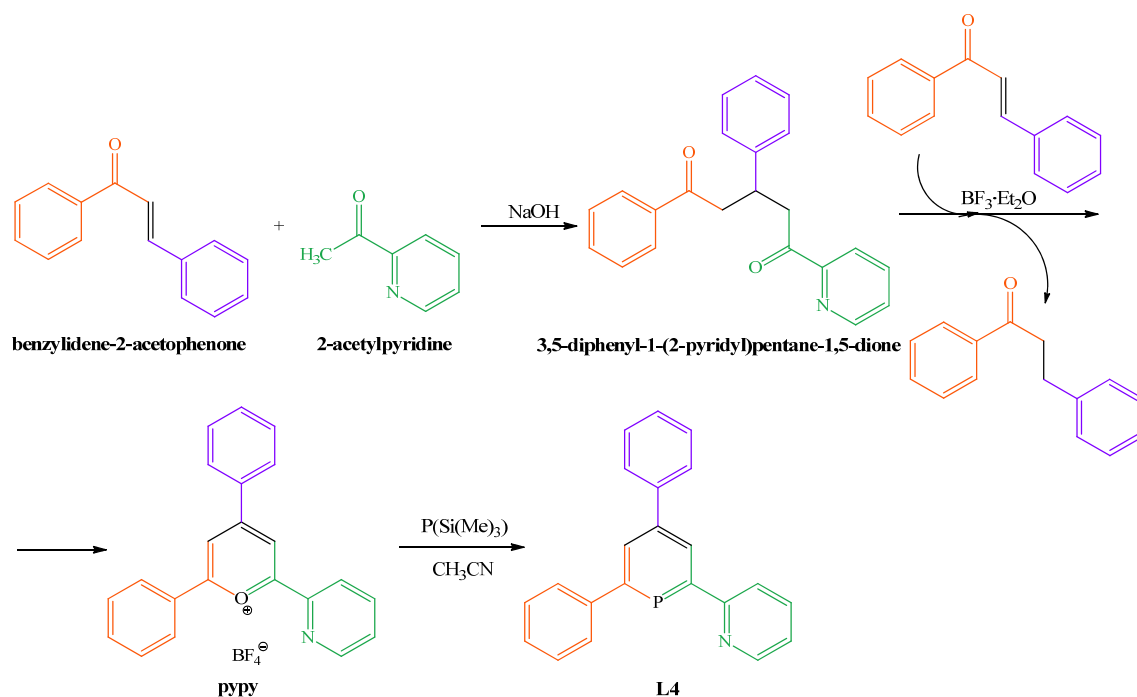
Scheme 5.2. Synthesis of 2-(2-pyridyl)-4,6-diphenylphosphinine (**L4**).

In the second step, the pyridyl-functionalized pyrylium salt **pypy** was prepared according to a modified experimental procedure described by Katritzky *et al.*,[18]

starting from the diketone by subsequent oxidation with one equivalent benzylidene-2-acetophenone in the presence of boron trifluoride diethyl etherate. The **pypy** was obtained as yellow, fluorescent and highly pure crystals (30 % yield).[16]

Finally, **pypy** was converted into the corresponding phosphinine **L4** by reaction with an excess of tris(trimethylsilyl)phosphine, the phosphorus source, in acetonitrile at reflux temperature (Scheme 5.2). Orange crystals were obtained in good yield (54 % yield) by slow recrystallization from hot acetonitrile.[16]

^{1}H and ^{31}P{H} NMR spectra were recorded in benzene (Figure 5.5) to confirm the formation of **L4**. In the phosphorus NMR spectra only one signal at δ 187.4 ppm was observed, which confirmed the incorporation of the phosphorus atom into the ring structure. The proton NMR was a complex spectrum and the aromatic signals appeared between δ 9.4 and δ 6.5 ppm (Figure 5.5). The signal which appeared more deshielded (δ 9.1 ppm) corresponded to proton in α position to the nitrogen atom.[16]
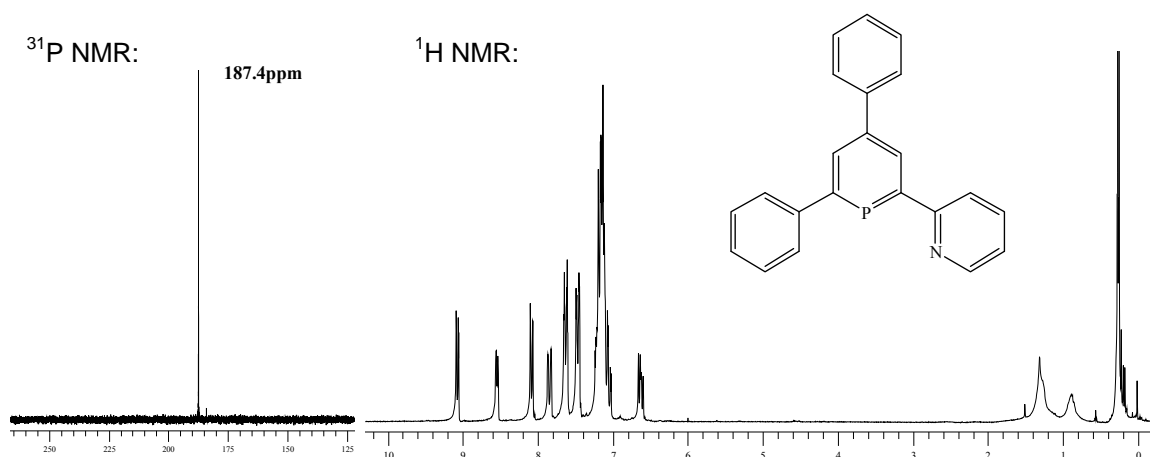

Figure 5.5. ^{31}P{H} and ^{1}H NMR spectra of **L4**.

5.2.2 Coordination Chemistry

5.2.2.1 *Palladium and Platinum Complexes*

Neutral palladium (II) and platinum (II) complexes [M(Cl)$_2$(**L4**)] (**PdL4a**, M = Pd and **PtL4a**, M = Pt) were synthesized starting from [MCl$_2$(cod)] (cod= 1,5-cyclooctadiene, M = Pd or Pt), which reacted with one equivalent of **L4** in dichloromethane solution (Scheme 5.3). **PdL4a** and **PtL4a** were formed in several minutes and isolate as bright orange solid or bright yellow solid, respectively in high yields.
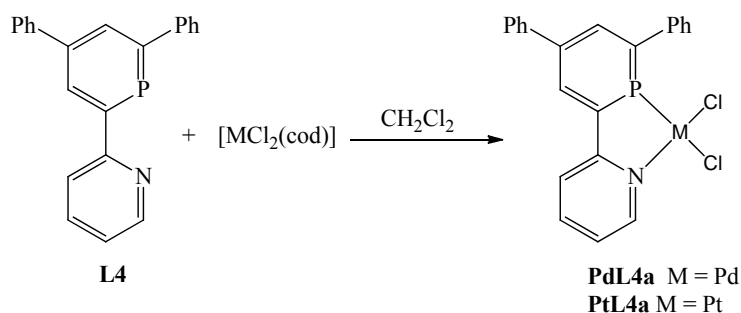
Scheme 5.3. Synthesis of $[M(Cl)_2(L4)]$ (**PdL4a** M = Pd and **PtL4a** M = Pt).

Complex **PdL4a** and **PtL4a** were characterized by ^{1}H and ^{31}P NMR spectroscopy, elemental analysis and X-ray diffraction.

The ^{31}P{^{1}H} NMR spectrum of **PdL4a** showed a singlet at δ 159 ppm in deuterated dichloromethane and a chemical shift difference with the free ligand of $\Delta\delta$= -30 ppm, which is in the expected region for phosphine-metal complexes with a η^1 coordination mode of the phosphorus atom.[13] The ^{31}P{^{1}H} NMR spectrum of **PtL4a** showed a singlet with platinum satellites at δ 141.5 ppm (J_{Pt-P} = 4797 Hz, $\Delta\delta$= -47.5 ppm in CD_2Cl_2). This value is lower than the expected for η^1-coordinationed 2,4,6-triaryl-phosphinines(δ = 160-240 ppm).[13] The ^{1}H NMR spectra from both **PdL4a** and **PtL4a** showed the expected signals of the coordinated ligand in the aromatic region (6.80-10.30 ppm).

Orange crystals of **PdL4a** and yellow crystals of **PtL4a** suitable for X-ray diffraction were obtained by slow diffusion of diethyl ether into a diluted mixture of **L4** and $[PdCl_2(cod)]$ in CH_2Cl_2 or slow recrystallization from CH_2Cl_2, respectively. Complexes **PdL4a** and **PtL4a** complexes crystallized in the monoclinic space group *P2$_1$/c* and the asymmetric unit consisted of two metal complex molecules and one molecule of CH_2Cl_2. Molecular structure is depicted in Figure 5.6a and Figure 5.7a. The crystal structures revealed the mononuclear nature of the compounds with slightly distorted square-planar coordination geometry around the metal centre. The geometries of the two independent molecules are very similar and differ only in the torsions of the phenyl-substituents of the phosphinine-moiety (Figure 5.6b and Figure 5.7b). The phenyl ring in α-position (6-position) is rotated out of the plane of the P-heterocycle (torsion angles P(x)-C1(x)-C11(x)-C12(x) (x = 1 or 2) = -53.1(7) and -44.3(6)° for **PdL4a** and -52.0(6) and -43.8(6)° for **PtL4a**). The non-planarity of the overall molecule prohibits a stacking in the crystal with short intermolecular metal-metal contacts due to

147

Reactivity and Characterization of Phosphinine Complexes

d^8-d^8 interactions,[19] which are e.g. present in the essentially planar [PdCl$_2$(bpy)][20] and [PtCl$_2$(bpy)] complexes.[21]
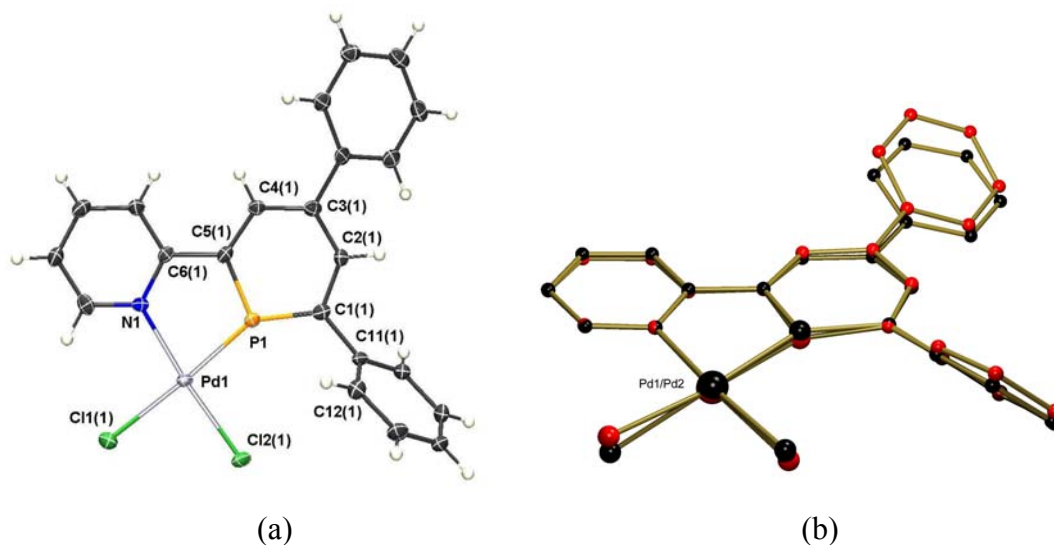

(a)   (b)

Figure 5.6. Complex [Pd(Cl)$_2$(**L4**)] (**PdL4a**) *(a)* ORTEP drawing with 50% probability. Only one independent molecule is shown and the solvent molecule is omitted for clarity. *(b)* Overlay plot (quaternion fit) of the two independent molecules. Phenyl rings were ignored in the calculations of the fit. Hydrogen atoms are omitted in the drawings.

(a)   (b)

Figure 5.7. Complex [Pt(Cl)$_2$(**L4**)] (**PtL4a**) *(a)* ORTEP drawing with 50% probability. Only one independent molecule is shown and the solvent molecule is omitted for clarity *(b)* Overlay plot (quaternion fit) of the two independent molecules. Phenyl rings were ignored in the calculations of the fit. Hydrogen atoms are omitted in the drawings.
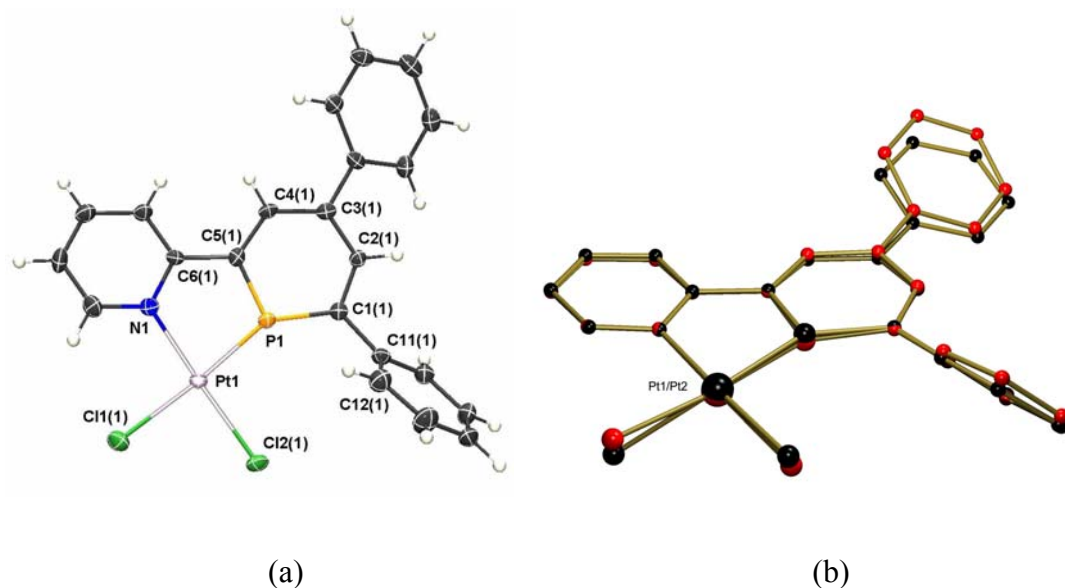
There is a significant difference between the pyridine moiety and the aromatic phosphinine ring, which is best described as a distorted hexagon due to the larger phosphorus atom in comparison to the nitrogen atom. The pyridine and the aromatic phosphinine ring are essentially coplanar with respect to one another in **PdL4a** and **PtL4a**. The intercyclic C5-C6 bonds of 1.470(7)-1.476(7) Å are only slightly shorter than in free 2,2'-bipyridine (1.490(3) Å), while the N-C6 bonds of 1.372(6)-1.386(6) Å are slightly longer than the corresponding bond in 2,2'-bipyridine (1.346(2) Å).[22] The P-C bond lengths of 1.711(5)-1.723(5) Å are somewhat shorter than in free 2,4,6-triarylphosphinines (1.74-1.76 Å),[23] while the carbon-carbon bond distances in the aromatic phosphinine subunit are in the usual range (1.386(7)-1.413(7) Å) observed for both free and complexed phosphinines.

The metal centre is essentially located in the plane formed by the phosphinine-pyridine backbone, with metal-P bond lengths of 2.1866(13) and 2.1973(12) Å for **PdL4a** and 2.1696(12) and 2.1757(12) Å for **PtL4a**. The metal-N distances of 2.096(4) and 2.097(4) Å in **PdL4a** and 2.084(4) and 2.079(4) in **PtL4a** are slightly larger than in the related bipyridine complexes [PdCl$_2$(bpy)] (2.017(2) Å)[20] and [PtCl$_2$(bpy)] (2.015(4) Å).[21] The bite-angles P-metal-N are 81.14(11)-81.75(11)°. Most strikingly, the metal centre is not located in the ideal axis of the phosphorus lone-pair and clearly shifted towards the nitrogen atom (C5-P-metal = 106.77(17)-107.57(17)°, C1-P-metal = 144.35(17)-145.18(17)°). Obviously, this effect is necessary for an efficient complexation of the metal atom by the chelating P,N ligand and enabled by the more diffuse and less directional lone pair of the low-coordinated phosphorus atom compared to the sp^2-hybridized nitrogen atom in pyridines. Consequently, it is not observed for the metal-N interactions (metal-N-C = 120.5(3)-121.4(3)°). A *trans* influence of the P-atom can further be noticed by the longer metal-Cl1 bonds (2.3373(12)-2.3457(12) Å) compared to the metal-Cl2 bonds *trans* to the N-atom (2.2791(12)-2.2947(12) Å), which are close to the reported metal-Cl distances in [PdCl$_2$(bpy)] (2.2942(9) Å)[20] and [PtCl$_2$(bpy)] (2.308(1) Å).[21]

Moreover, we assume that the additional phenyl-substituents in 4- and 6-position of the heterocyclic framework might also contribute to a kinetic stabilization of the metal complex, as no particular sensitivity could be observed for **PdL4a** and **PtL4a**, in contrast to some reported NIPHOS-metal complexes (*vide supra*). The higher the

Reactivity and Characterization of Phosphinine Complexes

electrophilic character of the metal centre, the more prone the complex is for nucleophilic attack.

Table 5.1. Selected bond lengths [Å], angles and torsion angles [º] in the isomorphous crystal structure of **PdL4a** and **PtL4a**.

	compound **PdL4a** (M=Pd)		compound **PtL4a** (M=Pt)	
	mol. 1 (x=1)	mol. 2 (x=2)	mol. 1 (x=1)	mol. 2 (x=2)
M(x)-P(x)	2.1866(13)	2.1973(12)	2.1696(12)	2.1757(12)
M(x)-N(x)	2.096(4)	2.097(4)	2.084(4)	2.079(4)
M(x)-Cl1(x)	2.3406(13)	2.3457(12)	2.3373(12)	2.3444(12)
M(x)-Cl2(x)	2.2886(12)	2.2791(12)	2.2947(12)	2.2872(12)
P(x)-M(x)-N(x)	81.69(11)	81.14(11)	81.75(11)	81.33(11)
Cl1(x)-M(x)-Cl2(x)	90.33(4)	89.19(4)	88.60(4)	87.76(4)
C1(x)-P(x)-M(x)	144.91(17)	145.18(17)	144.35(17)	144.57(18)
C6(x)-N(x)-M(x)	120.7(3)	121.3(3)	120.8(3)	121.3(3)
C10(x)-N(x)-M(x)	121.2(3)	120.0(3)	121.4(3)	120.5(3)
P(x)-C1(x)-C11(x)-C12(x)	-53.1(7)	-44.3(6)	-52.0(6)	-43.8(6)
M(x)-N(x)-C6(x)-C5(x)	-6.8(6)	-1.5(6)	-6.2(5)	-3.0(5)
M(x)-P(x)-C5(x)-C6(x)	-0.2(4)	8.5(4)	0.8(4)	7.3(4)

The dicationic bischelated palladium complexes $[Pd(\textbf{L4})_2][X]_2$ with $X = BF_4^-$ and $BArF^-$ as counterion ($BArF = B[3,5-(CF_3)_2C_6H_3]_4$; Scheme 5.4) were synthesised following a similar two-step procedure described in Chapter 3, but starting from $[PdCl_2(cod)]$, instead of Na_4PdCl_4, and ligand **L4** to get the neutral complex $[PdCl_2(\textbf{L4})]$ (**PdL4a**), which was handled with the corresponding salt and another equivalent of **L4** to obtain the desired dicationic derivatives **PdL4b-c**.[24]
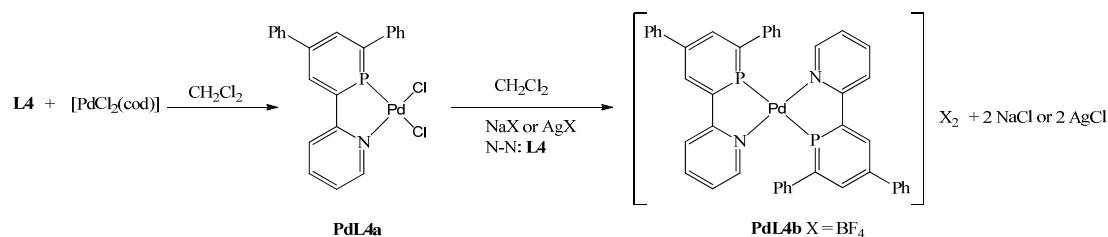
Scheme 5.4. Synthesis of $[Pd(L4)_2]X_2$ (**PdL4b** $X = BF_4$ and **PdL4c** $X = BArF$).

The mass spectra of complex **PdL4b** showed a peak at *m/z* 930, corresponding to the formation of the bischelated complex In the $^{31}P\{^1H\}$ NMR spectrum two signals at δ 36.4 and 35.6 ppm were observed, which were attributed to a mixture of the *cis*- and *trans*- **PdL4b** isomers. Using the salt NaBArF, the $^{31}P\{^1H\}$ NMR spectrum showed also two signals at δ 24.1 and 22.9 ppm, but the MALDI-TOF indicated the formation of a dinuclear species $[Pd(L4)_2]_2(BArF)_4$ **PdL4c** (Figure 5.8), probably similar to the one reported for $[Ir(cod)(\mathbf{NIPHOS})]_2[SbF_6]_2$.[13]
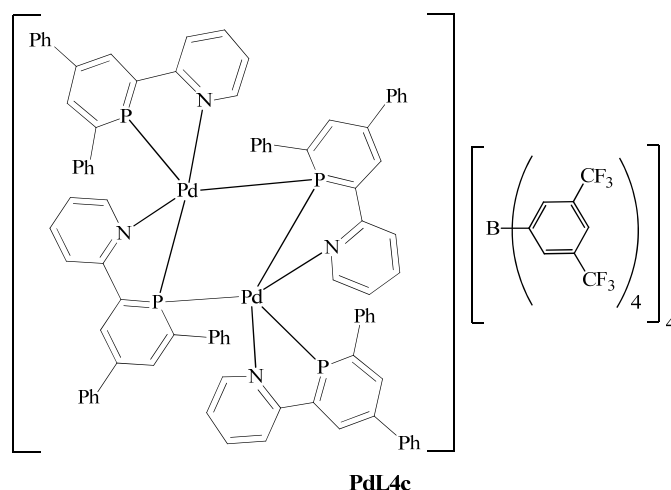

Figure 5.8. Proposed structure for complex **PdL4c**.

The preparation of the analogous monocationic systems $[Pd(CH_3)(CH_3CN)(L-L)][X]$ used in palladium bipyridine CO/styrene copolymerization was attempted, following the procedure described for bipyridines in Chapter 4 (L-L = **L4** and X the counterion).[25] In the first step of the synthesis, $[Pd(CH_3)Cl(cod)]$ was reacted with one equivalent of **L4** to form a solid, which was isolated as a dark-purple powder. However, the $^{31}P\{^1H\}$ NMR spectrum presented an unexpected signal at δ 34.9 ppm, which fell out of the expected chemical shift values for η^1-phosphinines (δ = 160-240 ppm).[13] Moreover, a new doublet signal ($^2J_{P-H}$ = 16Hz) was observed in the ^1H NMR spectrum (see SI), which was detected in the region of a methyl group at δ 2.0 ppm, and

Reactivity and Characterization of Phosphinine Complexes

downfield shifted with respect to the normal singlet attributed to Pd-CH$_3$ (between δ 1.0-0.6 ppm)[26] suggesting the addition of the methyl group to the phosphorus atom. The mass spectra (MALDI-TOF analysis) showed peaks corresponding to a dimeric species [Pd(**L4**·Me)Cl]$_2$ (**PdL4d**). The formation of this species would avoid further reactivity with another equivalent of **L4** or acetonitrile. For this reason the synthesis of monocationic complexes was not continued and no further reactivity was studied with this particular complex.

a) <u>Reactivity with (chiral) alcohols and (chiral) amines</u>

During the course of their investigations on transition metal complexes of NIPHOS, Venanzi and co-workers observed that cationic Pd(II) and Pt(II) complexes [M(Cl)(L)(NIPHOS)] were very reactive and could readily add protic reagents, such as water or alcohols at the external P=C double bond to give dihydrophosphinine complexes of the type [M(Cl)(L)(NIPHOS-H·OR)] (Scheme 5.5).[12] This reactivity was attributed to a disruption of the aromaticity upon complex formation.
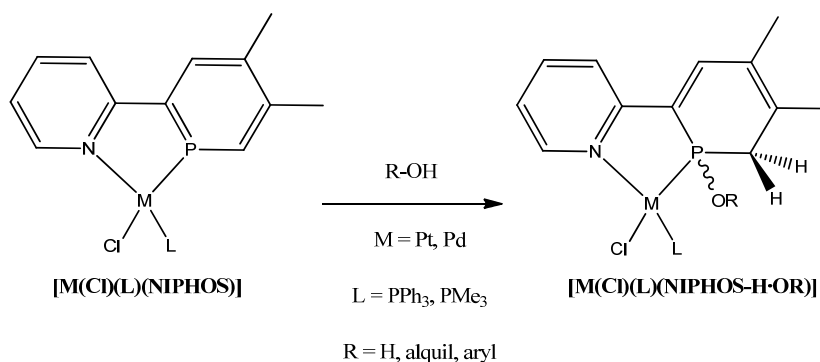

Scheme 5.5. Reactivity of NIPHOS complexes with water and alcohols.

The reaction of **PdL4a** and **PtL4a** with (chiral) alcohols and (chiral) amines was achieved by heating a solution of ligand **L4** and a stoichiometric amount of MCl$_2$ (M = Pd or Pt) in a mixture of CH$_2$Cl$_2$ or THF and the (chiral) alcohols or (chiral) amines (1:1), respectively, at 65ºC overnight. The corresponding phenyl-(hydro or amino)phosphinine-metal complexes of the type **PdL4e** or **PtL4d** – **PdL4f**, respectively (Scheme 5.6) were obtained and characterized only in solution except for **PdL4e$_2$** ([PdCl$_2$(**L4**H·OMe)]) for which single crystals suitable for X-ray diffraction were obtained.

Due to the presence of a phenyl group in C$_\alpha$-position of **L4** in contrast to NIPHOS, the addition of the protic substrate could proceed selectively on the same side

152

of the heterocycle, *via* a concerted mechanism giving the *syn*-product. Alternatively nucleophilic attack of OR^- or $NR_1R_2^-$ to the phosphinine (P atom) followed by the protonation of C_6 or *viceversa* yielding the *anti*-product is possible. In addition, two new stereogenic centres are formed (carbon and phosphorous atom) leading to the formation of four possible stereoisomers (Scheme 5.6).
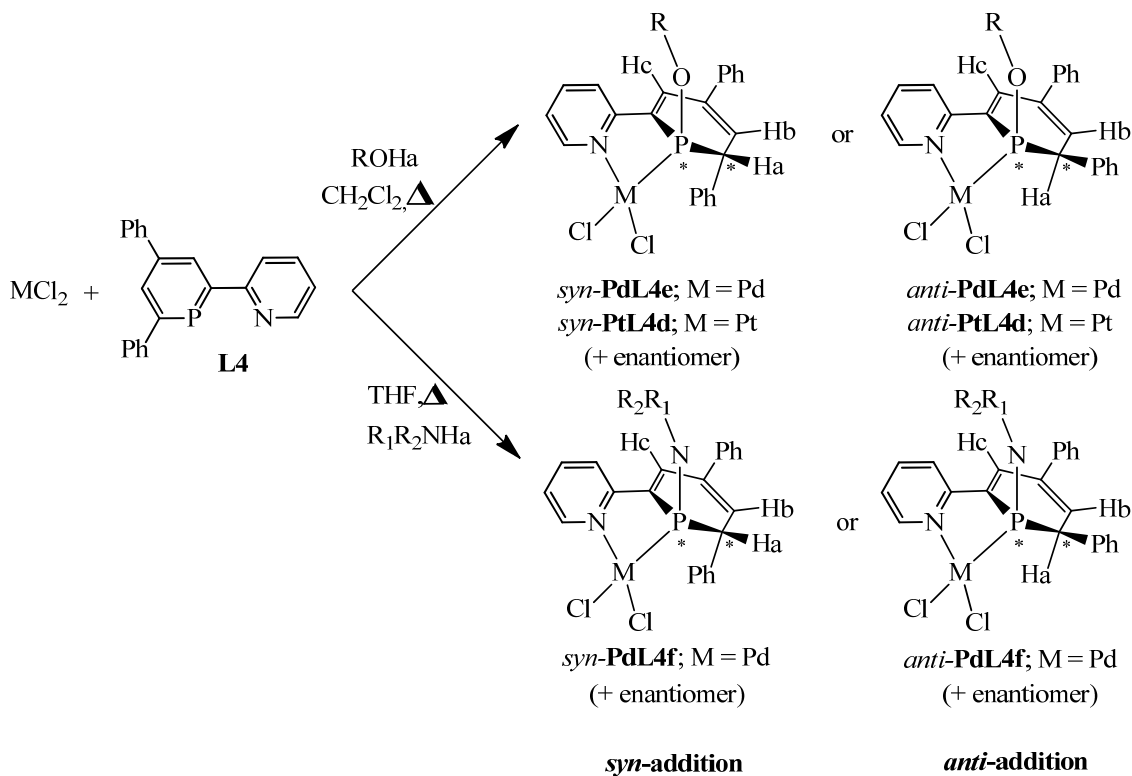
Scheme 5.6. Formation of phenyl-(hydro or amino)phosphinine-palladium complexes.

The reaction of **L4** and $PdCl_2$ or $PtCl_2$, respectively, in a mixture of CH_2Cl_2 and ethanol (1:1) at 65°C for overnight provided a dark red solution, from which the product precipitated after concentration and was isolated as purple-pink or brown powder in 95 % (Pd) or 90 % (Pt) yield, respectively.

The $^{31}P\{^1H\}$ NMR spectra of $[MCl_2(\textbf{L4}H \cdot OEt)]$ (**PdL4e$_1$**, M = Pd; **PdL4d$_1$**, M = Pt) showed only a single resonance at δ 107.9 ppm in **PdL4e$_1$** and a singlet signal with Pt-satellites at δ 71.7 ppm (J_{Pt-P} = 2166 Hz) in **PtL4d$_1$**, pointing to a highly regioselective reaction.

The ^1H NMR spectrum in dichloromethane was recorded for complexes **PdL4e$_1$** and **PtL4d$_1$** and showed only one set of new signals in the region of ethanoate group (δ 1.3 and δ 4.4 ppm) and at δ 4.8 ppm that confirmed the addition of ethoxide on the phosphorus atom. For example in ^1H NMR spectrum for complex **PdL4e$_1$** (Figure 5.9),

Reactivity and Characterization of Phosphinine Complexes

the triplet at δ 1.3 ppm could be due to the methylene group of the ethanolate and the two multiplets between δ 4.2 – 4.6 ppm correspond to the two methylenic protons which are different and show mutual coupling as well as coupling with the methylene group and the phosphorus atom. The most significant evidence, however, is the characteristic resonances for the protons H^a and H^b at δ 4.8 ppm (dd, $^3J_{H-H} = 8.9$, $^2J_{H-P} = 22.2$) and at δ 6.8 ppm (dd, $^3J_{H-H} = 8.9$, $^3J_{H-P} = 17.8$). From these observations it can be concluded that the ethanol addition is regioselective and only one pair of enantiomers is formed, either *syn*-**PdL4e$_1$** (through the same face of the planar skeleton (the top, *re*, or the bottom, *si* face)) or *anti*-**PdL4e$_1$**, since more complex signals would be expected for a mixture of diastereoisomers. The peripheral proton H^c appear as a doublet at δ = 7.7 ppm (d, $^3J_{H-P} = 26.7$ Hz) and the doublet at δ = 9.7 ppm (d, $^3J_{H-H} = 7.1$ Hz) can be assigned to the proton H^d at the C_α atom of the pyridine ring.
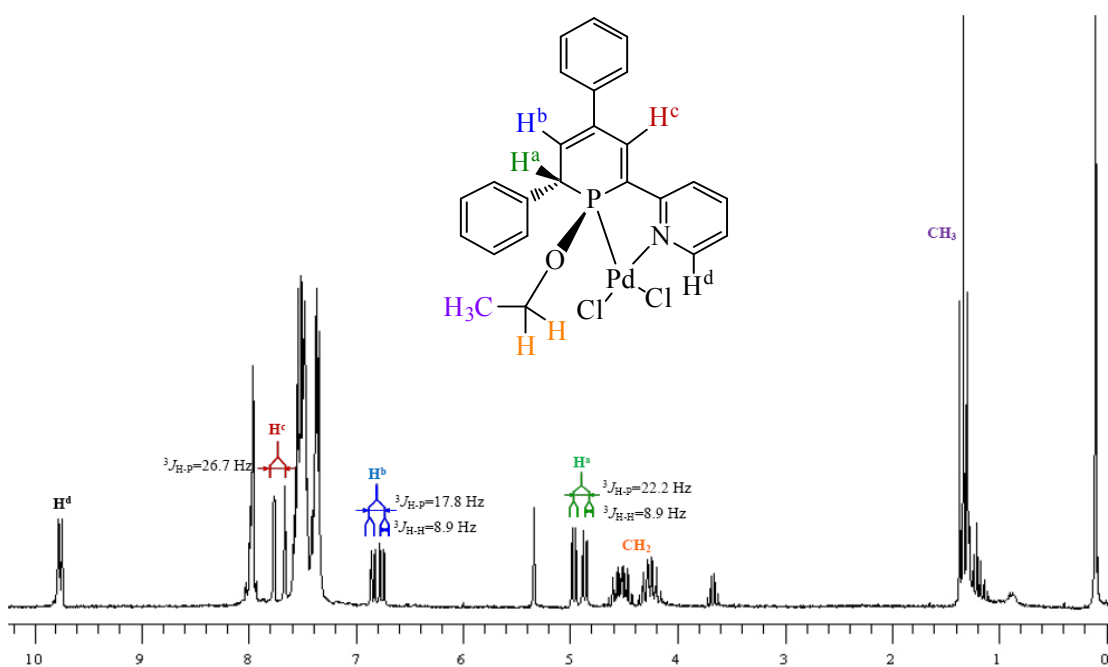

Figure 5.9. ^{1}H NMR spectrum and structure of the complex [PdCl$_2$(**L4H·OEt**)] (**PdL4e$_1$**) (200 MHz, CD$_2$Cl$_2$).

In the ^{1}H NMR spectrum of the Pt-complex [PtCl$_2$(**L4H·OEt**)] (**PdL4d$_1$**) similar signals were observed (see SI). The characteristic resonances for H^a, H^b, H^c and H^d were observed at δ 4.7 (dd, 1H, $^2J_{H-P} = 20.4$ Hz, $^3J_{H-H} = 7.4$ Hz), 6,8 (dd, 1H, $^3J_{H-P} = 17.2$ Hz, $^3J_{H-H} = 7.4$Hz), 7.7 (d, 1H, $J_{H-P} = 21.2$ Hz) and 10.08 (d, 1H, $J_{H-H} = 6.2$ Hz), while the methyl group of the ethoxy-substituent appear as a triplet at δ 1.3 (t, 3H, $^2J_{H-H} = 3.8$ Hz) and the methylene group of the ethanolate as two multiplets between δ 4.2 – 4.5 ppm.

The reaction carried out with methanol led to complex [PdCl$_2$(**L4**H·OMe)] (**PdL4e$_2$**). Crystals of **PdL4e$_2$** suitable for X-ray diffraction were obtained by slow diffusion of pentane into a solution of the complex in CH$_2$Cl$_2$. The compound crystallizes in the orthorhombic space group *Pbca* and the molecular structure is depicted in Figure 5.10a. The crystal structure of **PdL4e$_2$** unambiguously shows that the CH$_3$OH molecule has been added in a *syn*-fashion to the P1=C1 double bond, rather than in an *anti*-fashion. The phosphorus atom shows a distorted tetrahedral structure with a P1-C1 bond length of 1.818(7) Å and a P1-C5 distance of 1.797(5) Å, reflecting the *sp*^{3} hybridization of C1 and the *sp*^{2} hybridization of C5. Moreover, the C-C bond distances in the phosphorus heterocycle are in agreement with a diene structure, showing the expected values of C1-C2 = 1.494(9) Å, C2-C3 = 1.331(8) Å, C3-C4 = 1.478(8) Å and C4-C5 = 1.343(8) Å. The P1-O1 distance of 1.562(5) Å is in the typical range for phosphinite metal complexes.[27] The Pd centre shows a slightly distorted square planar coordination geometry with a Cl1-Pd1-Cl2 angle of 92.86(6)° and a bite angle N1-Pd1-P1 of 84.43(14)°. A *trans* influence of the P-atom can further be noticed in the longer Pd1-Cl1 bond (2.3922(17) Å) compared to the corresponding Pd1-Cl2 bond *trans* to the N-atom (2.2977(15) Å).

(a)   *(b)*
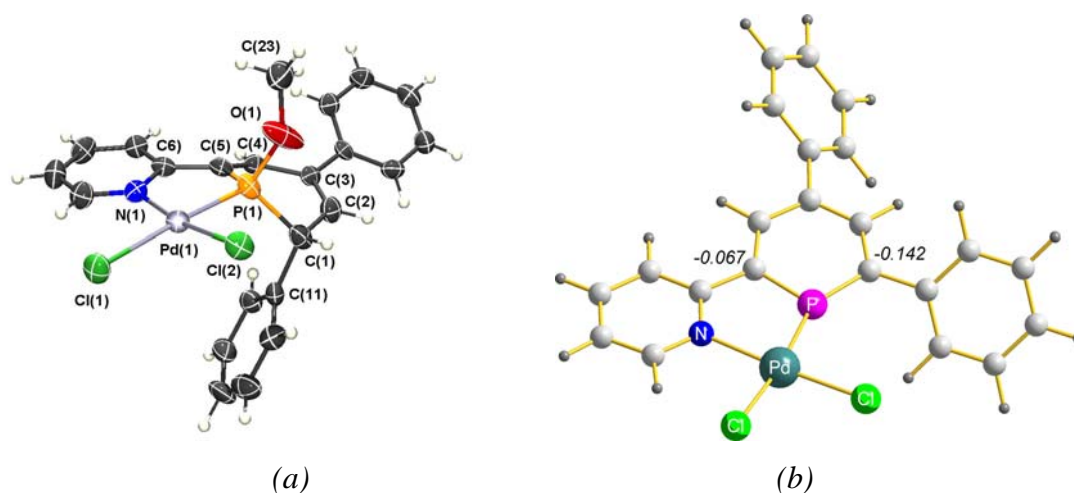
Figure 5.10. *a)* ORTEP drawing of complex [Pd(Cl)$_2$(**L4**H·OMe)] (*syn*-**PdL4e$_2$**). Displacement ellipsoids are shown at the 50% probability level. Selected bond lengths [Å] and angles [°]: Pd1-P1 = 2.151(17), Pd1-N1 = 2.080(5), Pd1-Cl1 = 2.392(18), Pd1-Cl2 = 2.298(16), P1-C1 = 1.818(7) Å, P1-C5 = 1.797(5) Å, C1-C2 = 1.494(9) Å, C2-C3 = 1.331(8) Å, C3-C4 = 1.478(8) Å and C4-C5 = 1.343(8) Å; Cl1-Pd1-Cl2 = 92.86(6)°, N1-Pd1-P1 of 84.43(14)°. *b)* Mulliken charge calculation. Numbers correspond to Mulliken charges on carbon atoms neighboring phosphorus.

Reactivity and Characterization of Phosphinine Complexes

Interestingly, due to the phenyl-substituent in 6-position of the P-heterocycle the addition shows a high regioselectivity excluding the formation of diasteromeric product mixtures generated by a random transfer of a proton to the C_α atom and proceeds exclusively at the P=C double bond, which points away from the pyridyl group (Scheme 5.7). In contrast to the formation of [PdCl$_2$(NIPHOSH·OR)], a structural investigation of **PdL4e** or **PtL4d** by means of X-ray diffraction allowed the differentiation between *anti-* and *syn*-addition.
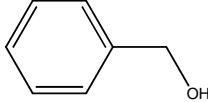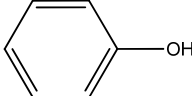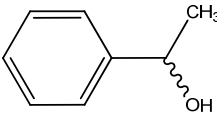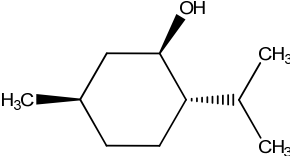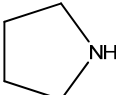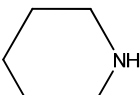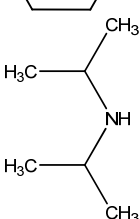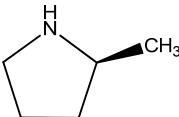
In order to understand the cause of the regioselective addition of methanol exclusively to the P1=C1 double bond, they were performed theoretical calculations for complex [PdCl$_2$(**L4**)] (**PdL4a**). The preferred addition to the P1=C1 double bond might be attributed to the somewhat higher nucleophilicity of the respective carbon atom as is evidenced by the computed Mulliken charges (-0.14 for C1 versus -0.07 for C5, Figure 5.10b). Although the difference is marginal and dependent on the computational method used, it can be explained by the electron-withdrawing character of the pyridine ring. Moreover, it could be proposed that in the *anti*-mechanism, which involves the approach of two molecules of methanol from the opposite site of the Pd-complex, the second methanol is sterically hindered by the phenyl-substituent in the 6-position of the phosphorus-heterocycle leading selectively the formation of *syn*-complex.
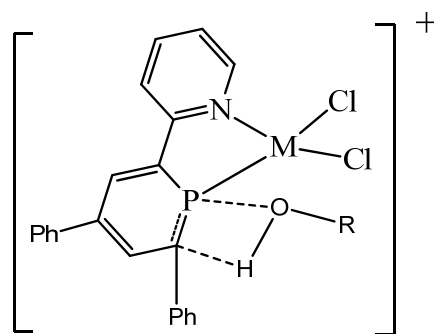
Scheme 5.7. Concerted mechanism proposed for the formation of phenyl-hydrophosphinine-palladium complexes. M = Pd or Pt.

This reaction is quite general, as similar products could be obtained by the addition of different alcohols or amines to the palladium complexes. In Table 5.2 the ^{31}P{^{1}H} NMR chemical shifts for the reaction of PdCl$_2$ and different alcohols and amines are reported (complexes **PdL4e** and **PdL4f)**.

Table 5.2. $^{31}P\{^1H\}$ NMR chemical shifts of the reaction of $PdCl_2$ and ligand **L4** with alcohols and amines (**PdL4e** and **PdL4f**).[a]

Entry	Alcohols and Amines	$^{31}P\{H\}$ NMR (ppm)
1	CH_3CH_2OH	107.9
2	CH_3OH	111.1
3		107.4
4		114.4
5		108.1 / 107.1
6		103.6 / 100.5
7		8.8
8		44.6
9		31.5
10		25.9 / 26.1

[a] recorded in CH_2Cl_2 at 200 MHz.

The most significant result were obtained using enantiomerically pure alcohols or amines, which led to the introduction of three stereogenic centres and the formation of only one diastereoisomeric pair (entry 5, 6 and 10, Table 5.2). This fact was supported by the $^{31}P\{H\}$ NMR spectrum, which showed only one signal for each of the two possible diasteroisomers.

Reactivity and Characterization of Phosphinine Complexes

i.   *Reversibility of alcohol addition*

In order to test the possibility whether the free 1,2-dihydrophosphinine **L4**H·OEt could be generated from the palladium complex *syn*-**PdL4e₁** [PdCl₂(**L4**H·OEt)] and platinum complex *syn*-**PtL4d₁** [PtCl₂(**L4**H·OEt)] by ligand exchange, they were reacted with 1,2-bis(diphenylphosphino)ethane (DPPE).

When the reaction was carried out with complex *syn*-**PdL4e₁** and two equivalents DPPE in CH_2Cl_2 at room temperature, an instantaneous and quantitative conversion of *syn*-**PdL4e₁** into a 1:1 mixture of [Pd(DPPE)₂]Cl₂ and the free pyridyl-phosphinine **L4** was found, rather than the formation of **L4**H·OEt (Scheme 5.8). Both compounds were characterized by their $^{31}P\{^1H\}$ NMR chemical shift. The spectrum showed two singlet signals corresponding to ligand **L4** (δ 188.5 ppm) and complex [Pd(DPPE)₂]Cl₂ (δ 52.8 ppm).[28]
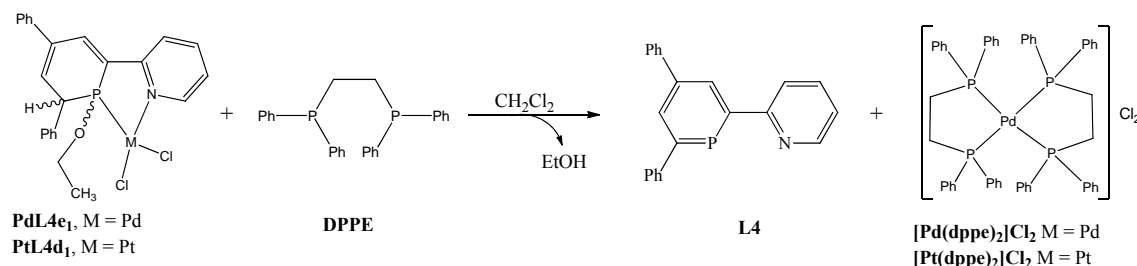
Scheme 5.8. Free ligand **L4** isolation by reaction of **PdL4e₁** or **PtL4d₁** with DPPE.

In attempt to understand the behaviour of this reaction the successive addition of 0.5 equivalents of DPPE up to 2.0 equivalents to complexes *syn*-**PdL4e₁** and *syn*-**PtL4d₁** was performed and monitored by NMR spectroscopy.

In the first addition to complex *syn*-**PdL4e₁** a signal of an unidentified species at δ 65.3 ppm and the singlet signal corresponding to *syn*-**PdL4e₁** (δ 107.9 ppm) were observed. Neither of both free ligands or **L4**H·OEt were detected. In the next addition three new singlet signals appeared, which were attributed to [Pd(DPPE)Cl₂] (δ 62.7 ppm),[28] [Pd(DPPE)₂]Cl₂ (δ 52.8 ppm)[28] and free ligand **L4** (δ 188.5 ppm).Complete disappearance of the signals attributed to complex *syn*-**PdL4e₁** and the signal at δ 65.3 ppm was observed. The palladium (II) complexes were in a relative intensity of 2:1, respectively. The addition of additional 0.5 equivalents only caused changes in the relative ratio of the species shown in the previous experiment, from 2:1 to 1:2. Finally, when 2.0 equivalents were added, only two signals were observed and attributed to the free ligand **L4** and [Pd(DPPE)₂]Cl₂ (see SI).

When the same experiment was repeated with complex *syn*-**PtL4d$_1$** similar results were observed (Scheme 5.8). After addition of 0.5 equivalents of DPPE the singlet signal with platinum satellites corresponding to *syn*-**PtL4d$_1$** (δ 73.9 ppm $^1J_{\text{P-Pt}}$ = 2166 Hz) was observed as well as the singlet signal with platinum satellites at δ 47.8 ppm ($^1J_{\text{P-Pt}}$ = 2369 Hz)[29,30] attributed to [Pt(DPPE)$_2$]Cl$_2$. Moreover, a new signal with platinum satellites at δ 42.4 ppm ($^1J_{\text{P-Pt}}$ = 3623 Hz) appeared. The relative intensity of the latter two species was found to be 1:2. In the following addition the relative intensity of the signals at δ 47.8 ppm and at δ 42.4 ppm changed to 2:1, while the signal of the starting material disappeared. In the following addition only changes of the relative intensity to 4:1 were observed. Finally, in the last addition only two signals were shown, at δ 187.3 ppm attributed to the free ligand and the singlet signal with its satellites corresponding to [Pt(DPPE)$_2$]Cl$_2$ (δ 47.8 ppm, $^1J_{\text{P-Pt}}$ = 2369 Hz).

The main differences in the Pd(II) and Pt(II) NMR experiments is the fact that Pt stabilized better complex **PtL4d$_1$** due to its lower lability, since it needs 2.0 equivalents of diphosphines to observed free ligand.

L4H·OEt was not detected in the NMR experiments with DPPE. Apparently, **L4** is rapidly formed by elimination of ethanol from the 1,2-dihydrophosphinine **L4**H·OEt. This observation suggests that the free species **L4**H·OEt is not stable and the equilibrium favours the formation of **L4** due to the re-aromatization of the phosphorus heterocycle.

5.2.2.2 *Rhodium Complexes*

Reaction of **L4** with one equivalent of [Rh(cod)$_2$]BF$_4$ in CH$_2$Cl$_2$ led instantaneously and quantitatively to the corresponding Rh(I) complex [Rh(cod)(**L4**)]BF$_4$ (**RhL4a**) (Scheme 5.9).
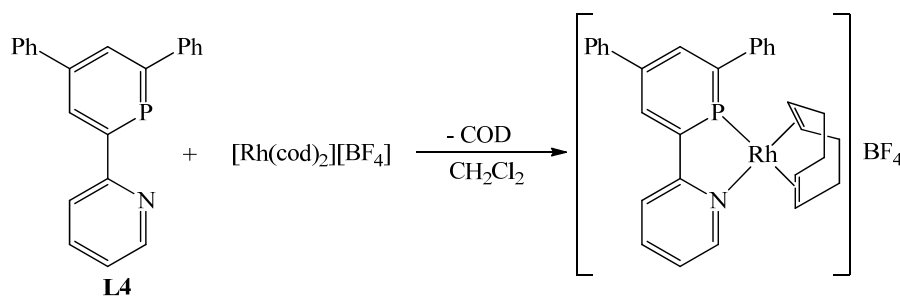
Scheme 5.9. Synthesis of [Rh(cod)(**L4**)]BF$_4$ (**RhL4a**).

Reactivity and Characterization of Phosphinine Complexes

The ^{31}P NMR spectrum of the reaction mixture showed a doublet at δ 175.5 ppm (CD_2Cl_2, $^1J_{P-Rh}$ = 188.6 Hz), which was very similar to the reported values for [Rh(cod)L_2]BF_4 containing two monodentate 2,3,5,6-tetraphenyl-phosphinine ligands (δ175.15 ppm, d, $^1J_{P-Rh}$ = 166.5 Hz).[31]

Orange crystals of **RhL4a** suitable for X-ray diffraction were obtained from a mixture of [Rh(cod)$_2$]BF_4 and **L4** in THF/CH_2Cl_2 upon standing at room temperature for one week. The rhodium complex crystallizes in the space group $P\overline{1}$ (no. 2) and the molecular structure is depicted in Figure 5.11. It confirms the observed spectroscopic data and reveals the mononuclear nature of **RhL4a** with slightly distorted square-planar coordination geometry around the metal centre. The crystallographic representation of **RhL4a** in Figure 5.11a shows the difference between the pyridine moiety and the aromatic phosphinine ring, which is best described as a distorted hexagon, as was observed with previously described Pd(II) and Pt(II) complexes. As a consequence, the phenyl-substituent in α-position of the P-heterocycle is shifted away from the coordination site and can additionally rotate out of the plane of the P-heterocycle (torsion angle P(1)-C(1)-C(11)-C(12) = -53.8(4)°).[31,32] Moreover, as we assume for Pd(II) and Pt(II), the additional phenyl-substituents in 4- and 6-position of the heterocyclic framework might also contribute to a kinetic stabilization of the metal complex, as no particular sensitivity could be observed for **RhL4a**.

The two heterocyclic rings in **RhL4a** are essentially coplanar with respect to one another (interplanar angle between the least-square planes = 5.73(13)°). The intercyclic C-C bond is 1.472(4) Å and thus only slightly shorter than in free 2,2'-bipyridine (1.490(3) Å), while the N-C(6) bond is with 1.372(3) Å slightly longer than the corresponding bond in 2,2'-bipyridine (1.346(2) Å).[22] The P-C(1) and P-C(5) bond lengths are with 1.729(3) Å and 1.721(3) Å somewhat shorter than in free 2,4,6-triarylphosphinines (1.74-1.76 Å), while the internal C(1)-P-C(5) angle is with 105.25(14)° larger compared to free 2,4,6-triarylphosphinines (101.24-101.76°).[23] The carbon-carbon bond lengths in the aromatic phosphinine subunit are in the usual range (1.392(4)-1.404(4) Å) observed for both free and complexed phosphinine ligands.

The Rh-centre is essentially located in the plane formed by the phosphinine-pyridine backbone (torsion angle N(1)-Rh(1)-P(1)-C(5) = -4.01(12)°). The Rh-P bond length in **RhL4a** is with 2.2250(8) Å shorter than in [Rh(cod)L_2]BF_4 (L = 2,3,5,6-

tetraphenyl-phosphinine) (2.281 and 2.301 Å), which might be a consequence of steric repulsion between the α,α'-diphenyl-substituents of the two monodentate phosphinine ligands in the latter complex.
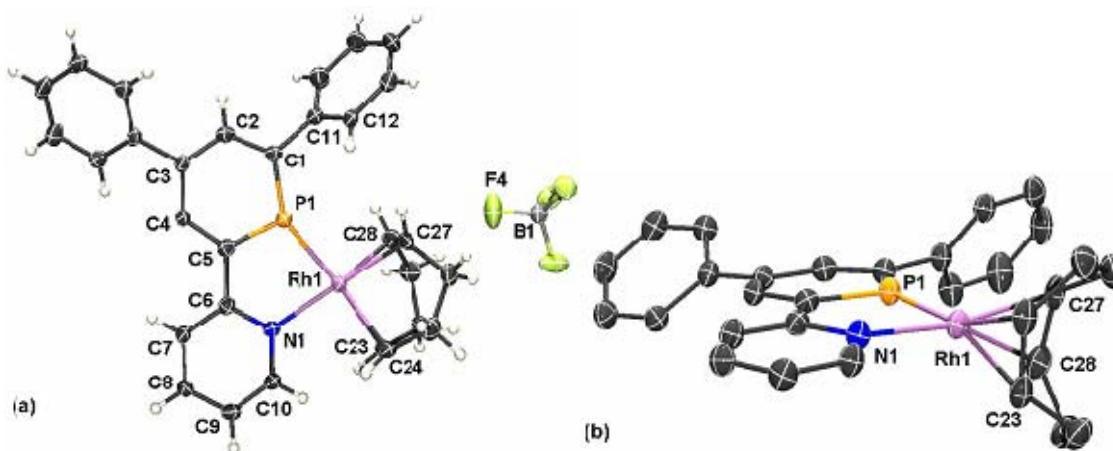
Figure 5.11. *(a)* Molecular structure of **RhL4a** in the crystal. Displacement ellipsoids are shown at the 50% probability level. The solvent molecule CH_2Cl_2 is omitted for clarity. *(b)* Side-view of the cationic part of **RhL4a**, hydrogen atoms are not represented. Selected bond lengths [Å] and angles [°]: Rh1-P1: 2.225, Rh1-N1: 2.159, Rh1-C23: 2.236, Rh1-C24: 2.213, Rh1-C27: 2.167, Rh1-C28: 2.150, P1-C1: 1.729, P1-C5: 1.721, N1-C6: 1.371, N1-C10: 1.348, P1-Rh1-N1: 79.77, C23-Rh1-C27: 87.45, C23-Rh1-C28: 80.96, C24-Rh1-C27: 80.50, C24-Rh1-C28: 96.29.

Moreover, the metal centre in **RhL4a** is not located in the ideal axis of the phosphorus lone-pair and clearly shifted towards the nitrogen atom (C(5)-P(1)-Rh(1) = 107.89(10)°, C(1)-P(1)-Rh(1) = 146.23(10)°). Obviously, this effect is necessary for a proper complexation of the Rh atom by the chelating P,N ligand and enabled by the more diffuse and less directional lone pair of the low-coordinated phosphorus atom compared to the sp^2-hybridized nitrogen atom in pyridines. Consequently, it is not observed for the N(1)-Rh interaction (N(1)-Rh(1) = 2.159(2) Å), Rh(1)-N(1)-C(6) = 121.35(18)°, Rh(1)-N(1)-C(10) = 121.23(19)°. A *trans* influence of the P-atom can further be noticed in the longer Rh-cod bonds Rh(1)-C(23) (2.136(3) Å) and Rh(1)-C(24) (2.213(3) Å) compared to the corresponding bonds *trans* to the N-atom (Rh(1)-C(27) = 2.167(3) Å, Rh(1)-C(28) = 2.150(3) Å).[33] The coordination to the metal centre proceeded in the same way observing the same characteristic trends as was reported for **PdL4a** and **PtL4a** (metal displacement for coordination and *trans* influence).

Reactivity and Characterization of Phosphinine Complexes

5.2.3 Catalysis

The catalytic activity of Pd(II)/**L4** systems in the copolymerisation of CO/α-olefins (ethylene and styrene, Scheme 5.10) was studied. The cationic palladium (II) catalyst were prepared *in situ* mixing the neutral complexes **PdL4d** or **PdL4e$_2$** and one or two equivalents of silver hexafluoroantimonate (AgSbF$_6$), respectively.
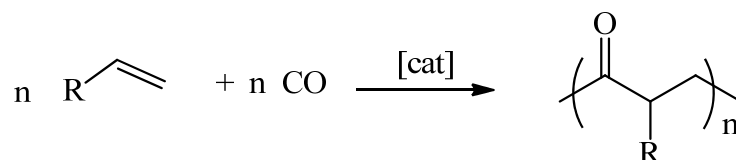
Scheme 5.10. Alternating copolymerisation of CO/α-olefins (R = H or Ph).

The CO/ethylene copolymerisation was performed in CH$_2$Cl$_2$ or MeOH with precatalyst **PdL4d** or **PdL4e$_2$**, respectively, at 60ºC, 25 bars CO, 25 bars ethylene, 0.062 mmol precatalyst and during 18h.[34] Complex **PdL4d** gave small amounts of oligomeric polyketones and high amount of Pd-black. For that reason 1,4-benzoquinone (BQ) in [BQ]/[Pd] = 10 was added.[35] Nevertheless, no improvement was observed and the MALDI-TOF showed signals corresponding to oligomers with a repetitive unit of 56 g/mol with a maximum of *ca* 100 repetitive units of polyketones. In the case of precatalyst **PdL4e$_2$** no polyketones were observed. The solution showed a green fluorescence color, indicating the transformation of the precatalyst in the catalytic conditions.

The CO/styrene copolymerisation was run at 10 bars of CO, 3 mL styrene, 5mL solvent (CH$_2$Cl$_2$ or MeOH), $4.2 \cdot 10^{-3}$ mmols of catalyst, [BQ]/[Pd] = 10, at 30ºC and during 18h.[36] Catalyst **PdL4e$_2$** provided no polyketone and the same deactivation process, while with precatalyst **PdL4d** only polystyrene was formed, even if 50 bars CO were used. No deactivation of the catalyst to palladium black was observed with precatalyst **PdL4d**.

In summary, the catalytic studies with catalysts **PdL4d** presented moderate catalytic activity for the CO/ethylene copolymerisation reaction with the formation of oligomers, while it was not active in CO/styrene copolymerisation. Precatalyst **PdL4e$_2$** showed no activity for both substrates.

162

5.3   Conclusion

During the course of the investigation the scale up (up to 6.2 g) and optimization of the synthesis of 2-(2-pyridyl)-4,6-diphenylphosphinine (**L4**) was achieved.

New palladium and platinum complexes with ligand **L4** were isolated and fully characterized by NMR spectroscopy, mass spectrometry and X-ray diffraction analysis of [PdCl$_2$**L4**] (**PdL4a**) and [PtCl$_2$**L4**] (**PtL4a**). Complexes [Pd(**L4**)$_2$][BF$_4$]$_2$ (**PdL4b**) and [Pd(**L4**)$_2$]$_2$[BArF]$_4$ (**PdL4c**) were also obtained. The reactivity of [Pd(cod)MeCl] with **L4** lead to [PdCl(**L4**·CH$_3$)]$_2$ (**PdL4d**), which is proposed to show a methyl transfer to the phosphorus atom.

MCl$_2$ (M= Pd or Pt) reacted with **L4** and alcohols (HOR) or amines (HNR$_2$R$_1$) under formation of the complexes of the general formula [MCl$_2$(**L4**H·OR)] or [MCl$_2$(**L4**H·NR$_2$R$_1$)]. These coordination compounds were formed most likely through a concerted mechanism, the reaction proceeds selectively via a syn-addition to one of the P=C double bonds. Furthermore, when chiral alcohols or amines were used, three stereogenic centres at once could be introduced and only one pair of diastereoisomers were formed. Complexes [PdCl$_2$(**L4**H·OEt)] (**PdL4e$_1$**) and [PtCl$_2$(**L4**H·OEt)] (**PdL4d$_1$**) showed reactivity with diphosphines to form free ligand **L4**. [Rh(cod)(**L4**)]BF$_4$ (**RhL4a**) was isolated and characterized by NMR spectroscopy, mass spectrometry and X-ray diffraction.

The catalytic studies in the CO/α-olefins copolymerisation with precatalyst **PdL4d** and **PdL4e$_2$** showed that precatalyst **PdL4d** presented only moderate catalytic activity in CO/ethylene copolymerisation and precatalyst **PdL4e$_2$** was inactive for both substrates.

5.4   Experimental Section

General Comments. All manipulations were carried out under argon atmosphere, using modified Schlenk techniques unless otherwise stated. All glassware was dried prior to use by heating under vacuum. All common solvents and chemicals were commercially available and purchased from Aldrich Chemical Co. and Merck. P(SiMe$_3$)$_3$ was prepared according to the literature.[37] The solvents were taken from custom-made solvent purification columns filled with Al$_2$O$_3$. **The elemental analyses** were obtained from H. Kolbe, Mikroanalytisches Laboratorium, Mülheim a.d. Ruhr (Germany). **NMR spectroscopy** ^{1}H, ^{13}C{^{1}H}, ^{31}P{^{1}H} and ^{19}F{^{1}H} NMR spectra were

Reactivity and Characterization of Phosphinine Complexes

recorded on a Varian Mercury 200 or 400 spectrometer and all chemical shifts are reported relative to the residual proton resonance in the deuterated solvents or referred to an 85% aqueous solution of H_3PO_4, respectively. **MALDI-TOF measurements of complexes:** Voyager-DE-STR (Applied Biosystems, Franingham, MA) instrument equipped with a 337 nm nitrogen laser. All spectra were acquired in the positive ion reflector mode and were accelerated at 20 keV. α-cyano-4-hydroxycinnamic acid (CHCA) was used as matrix. The matrix was dissolved in THF at a concentration of 20 mg·mL^{-1}. The complex was dissolved in THF (50 mg·L^{-1}). The matrix and the samples were premixed in the ratio 1:1 (Matrix : sample) and then the mixture was deposited (1 μL) on the target. For each spectrum 100 laser shots were accumulated.

Standard copolymerisation experiment in organic solvent. Copolymerization reactions were carried out in a 75 mL stainless steel autoclave equipped with a glass insert and a magnetic stirring bar at different bars of CO. After introduction of the catalyst precursor **PdL4d** or **PdL4e$_2$**, 1 or 2 equivalents AgSbF$_6$ (6.2·10^{-2} mmol catalyst in CO/ethylene or 4.2·10^{-3} mmol catalyst in CO/styrene) and BQ into the purged autoclaved, the solvent and substrate were added under argon atmosphere. The autoclave was pressurized with carbon monoxide and 25 bars ethylene, if necessary, and heated to the desired temperature. After the desired time, the reactor was vented out and the reaction mixture was filtered through celitte. The solution was analyze and dried under vacuum.

5.4.1 Ligands and Complexes Synthesis

3,5-diphenyl-1-(2-pyridyl)pentane-1,5-dione [16]
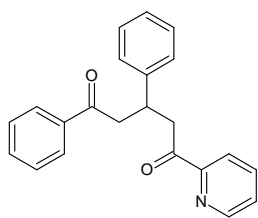
In a mortar 2-acetylpyridine (7.08 g, 58.5 mmol, 1 equiv.) was added to a mixture of chalcone (12.18 g, 58.5 mmol, 1 equiv.) and NaOH (2.34 g, 58.5 mmol, 1 equiv.). All reactants were mingled by the use of a pestle for about ten minutes until a sticky yellow gum was obtained. The gum was transferred to a flask and heated in a water-ethanol mixture (1:2) until the gum was completely dissolved. The solution was stirred and was filtered off and washed with ethanol (30 mL) to obtain the pure product as a white powder (15.27 g, 79 %). Melting point: 104ºC. ^{1}H NMR (400 MHz, CDCl$_3$): δ (ppm)= 8.64 (d, 1H, pyridyl-H$_3$), 7.94 (d, 1H, pyridyl-H$_6$), 7.90 (d, 2H, acetylphenyl-H$_o$), 7.79 (dt, 1H, pyridyl-H$_5$), 7.53 (t, 1H,

acetylbenzyl-H_p), 7.43 (m, 3H, acetylbenzyl-H_m, pyridyl-H_4), 7.33 (d, 2H, phenyl-H_o), 7,26 (t, 2H, phenyl-H_m), 7.15 (t, 1H, phenyl-H_p), 4.11 (q, 1H, methine), 3.70 (dd, 2H, methylene), 3.41 (dd, 2H, methylene).

2-(2-pyridyl)-4,6-diphenylpyrylium tetrafluoroborate (pypy) [16]
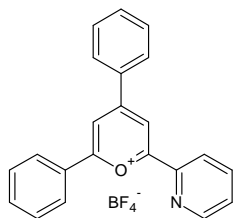
$BF_3 \cdot Et_2O$ (22.3 g, 157.3 mmol, 8 equiv.) was added dropwise to a mixture of 1,3-diphenyl-5-(2-pyridyl)-1,5-pentanedione (6.5 g, 19.7 mmol, 1 equiv.) and chalcone (4.1 g, 19.8 mmol, 1 equiv.) at room temperature. The reaction mixture was then heated to 70ºC for 3 hours. After allowing the reaction mixture to cool down to room temperature a yellow solid precipitated on addition of diethyl ether. The yellow solid was collected on a glass filter, washed with diethyl ether and recrystallized from methanol to obtain the pyrylium salt as yellow needles (1,86 g, 30 %). Mp.: 243°C (decomp.). Anal. Calc. For $C_{22}H_{16}BF_4NO$ (397.18 g/mol): C, 66.53; H, 4.06; N, 3.53. Found: C, 67.51; H, 4.13; N, 3.42. ^1H NMR (200 MHz, DMSO-d_6): δ (ppm)= 7.90 – 7.76 (m, 7H, pyridyl-H_4, pyryliumphenyl-$H_{m,p}$, phenyl-$H_{m,p}$), 8.26 (dt, 1H, J_{H-H} = 7.8 Hz, pyridyl-H_5), 8.79 – 8.49 (m, 5H, pyridyl-H_6, pyryliumphenyl-H_o, phenyl-H_o), 9.20 (s, 1H, pyrylium-H_5), 9.00 (d, 1H, J_{H-H} = 4.4 Hz, pyridyl-H_2), 9.28 (s, 1H, pyrylium-H_3). ^{13}C NMR (DMSO-d_6): δ (ppm)= 115.7, 116.9, 125.0, 129.1, 129.3, 129.5, 130.4, 130.5, 132.7, 136.0, 139.1, 146.7, 151.5, 160.1, 168.2, 171.1. ^{19}F NMR (DMSO-d_6): δ (ppm)= -148.3.

2-(2-pyridyl)-4,6-diphenylphosphinine (L4) [16]
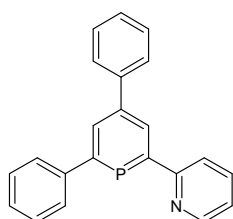
Under argon atmosphere at room temperature, tris-(trimethylsilyl)phosphine (18.57 g, 74.1 mmol, 2.1 equiv.) was added dropwise to a solution of 2-(2-pyridyl)-4,6-diphenylpyrylium tetrafluoroborate (14.02 g, 35.3 mmol, 1 equiv.) and acetonitrile (84 mL) in a 250 mL Schlenk flask. Upon adding a dark reaction mixture was obtained which was refluxed at 85ºC for 6 hours. Subsequently, all volatiles were removed *in vacuum* to obtain a dark solid. The crude product was purified by means of column chromatography over neutral alumina with ethyl acetate-petroleum ether (1:5) to yield the product as a yellow-orange solid (6.2 g, 54 %). A small amount (25 mg) was recrystallized very slowly from hot acetonitrile to obtain

Reactivity and Characterization of Phosphinine Complexes

yellow-orange needles. Mp.: 146.5°C. Anal. Calc. for $C_{22}H_{16}NP$ (M_w = 325.35 g/mol): C, 81.22; H, 4.96; N, 4.31. Found: C, 80.84; H, 5.24; N, 3.97. ^{1}H NMR (200 MHz, C_6D_6) : δ (ppm) = 6.77 (dd, 1H, J = 1.4 Hz), 7. 19 – 7.35 (m, 7H), 7.61 (d, 2H, J = 3.6 Hz), 7.77 (d, 2H, J = 3.8 Hz), 8.00 (d, 1H, J = 4.0 Hz), 8.24 (d, 1H, J = 3.0 Hz), 8.70 (d, 1H, J = 2.4 Hz), 9.23 (d, 1H, J = 2.8 Hz). ^{13}C NMR (C_6D_6): δ (ppm) = 120.8, 121.2, 122.4, 128.8, 132.0 (d, J_{C-P} = 13.0 Hz, $C^{3/5}$), 132.9 (d, J_{C-P} = 11.9 Hz, $C^{3/5}$), 136.2, 142.3 (d, J_{C-P} = 3.5 Hz, C^4), 143.5, 144.0, 144.2 (d, J_{C-P} = 22.2 Hz), 149.8, 159.1 (d, J_{C-P} = 26.1 Hz), 169.5 (d, J_{C-P} = 50.6 Hz, $C^{2/6}$), 171.5 (d, J_{C-P} = 50.6 Hz, $C^{2/6}$). ^{31}P NMR (C_6D_6): δ (ppm) = 187.3.

[Pd(Cl)₂(L4)] (PdL4a)

A solution of **L4** (20 mg, 0.0615 mmol) in CH_2Cl_2 (0.5 mL) was added dropwise to a solution of [PdCl₂(cod)] (17.5 mg, 0.061 mmol) in CH_2Cl_2 (0.5 mL). A red solution was formed instantaneously. The product was formed within several minutes and precipitated as an orange solid from the reaction mixture. The solid was filtered off, washed several times with diethyl ether and dried under vacuum. **PdL4a** was obtained as an orange solid (23 mg, 0.045 mmol, 73 %).

Analysis calcd. for $C_{22}H_{16}Cl_2NPPd$ x 0.5 CH_2Cl_2 (M_w = 545.15 g/mol): C: 49.57%; H: 3.14%; N: 2.57%. Found: C: 49.84; H: 3.21; N: 2.64.

^{1}H NMR (C_6D_6), 400 MHz): δ (ppm) = 6.87-6.93, (m, 4H), 7.16 (resonances covered by solvent peak), 7.31 (br, 1H, phosphinine-H_β), 7.58-7.60 (m, 4H), 8.11 (d, 1H, J_{H-H} = 6.4 Hz), 9.44 (d, $^3J_{H-H}$ = 6.0 Hz, 1H, pyridine-H_α). ^{31}P NMR (CD_2Cl_2, 162 MHz): δ (ppm) = 159.3. (Due to the low solubility of **PdL4a** an acceptable ^{13}C NMR spectrum could not be obtained)

[Pt(Cl)₂(L4)] (PtL4a)

Under argon atmosphere at room temperature, 2-(2-pyridyl)-4,6-diphenylphosphinine (**L4**) (20 mg, 0.061 mmol, 1 equiv.) in CH_2Cl_2 was added dropwise to a solution of [PtCl₂(cod)] (23 mg, 0.061 mmol, 1 equiv) in 0.5 mL of CH_2Cl_2. A red solution was formed instantaneously. The product was formed within several days as a bright orange, crystalline material, which was filtered off, washed several times with diethyl ether and dried under vacuum. **PtL4a** was obtained as a bright orange solid (24 mg, 0.04 mmol, 65 %).

Analysis calcd. for $C_{22}H_{16}Cl_2NPPt$ x 0.5 CH_2Cl_2 (M_w = 633.81 g/mol): C: 42.64%; H: 2.70%; N: 2.21%. Found: C: 42.81; H: 2.91; N: 2.42.

^{1}H NMR (CD_2Cl_2, 400 MHz): δ (ppm) = 7.19-7.30 (m, 5H), 7.48-7.60 (m, 6H), 7.73 (2xd, $^3J_{H-P}$ = 21.2, 20.8 Hz, $^3J_{H-H}$ = 7.4 Hz, 2H, phosphinine-H_β), 8.12 (m, 2H), 10.26 (d, $^3J_{H-H}$ = 5.2 Hz, 1H, pyridine-H_α). ^{31}P NMR (CD_2Cl_2, 162 MHz): δ (ppm) = 141.5 (s with Pt-satellites, $^1J_{Pt-P}$ = 4797 Hz). Due to the low solubility of **PtL4a** an acceptable ^{13}C NMR spectrum could not be obtained.

$[Pd(L4)_2]_n[X]_{n\cdot2}$ (PdL4b or PdL4c)

To a suspension of $[PdCl_2(\textbf{L4})]$ (**PdL4a**) (0.068 mmol) in 2 mL of dichloromethane, a solution of the ligand (**L4**) (0.068 mmol) and the corresponding sodium salt (0.143 mmol) in 2 mL of dichloromethane were added slowly. The mixture was heated overnight at 50°C. The product was filtered off over celitte to remove the sodium chloride and the solvent was evaporated under reduced pressure. An oil was obtained which was reevaporated with diethyl ether, obtaining the product as a solid.

$[Pd(L4)_2][BF_4]_2$ (PdL4b): Brown solid (50 mg, 91 %).

HR MASS MALDI-TOF calc. for ($C_{44}H_{32}B_2F_8N_2P_2Pd$) (*m/z*): 930.12 [$M^+$], 807.19 [$M^+$ +3NH_4^+]; found *m/z*: 930.21 [M^+], 807.30 [M^+ +3NH_4^+]. ^{19}F NMR (376.5 MHz, CD_2Cl_2): δ (ppm) = -149.7; ^{31}P NMR (162 MHz, CD_2Cl_2): δ (ppm) = 36.4, 35.3.

$[Pd(L4)_2]_2[BArF]_4$ (PdL4c): Brown solid (128 mg, 85 %).

HR MASS MALDI-TOF calc. for ($C_{216}H_{112}B_4F_{96}N_4P_4Pd_2$) (*m/z*): 1590.13 [$M^+$-4BArF − 2$H^+$ + 2K^+]; found *m/z*: 1590.02 [M^+-4BArF − 2H^+ + 2K^+]. ^{19}F NMR (376.5 MHz, CD_2Cl_2): δ (ppm) = -62.3; ^{31}P NMR (162 MHz, CD_2Cl_2): δ (ppm) = 24.1, 22.9.

Reaction of $[Pd(cod)(CH_3)Cl]$ with L4: $[Pd(L4\cdot CH_3)Cl]_2$ (PdL4d)

The synthesis was carried out according to a modification of literature procedure of bipyridine analogue.[5] 2-(2-pyridyl)-4,6-diphenylphosphinine **L4** (20 mg, 0.062 mmol, 1 equiv.) was added to a solution of $[Pd(cod)(CH_3)Cl]$ (16 mg, 0.062 mmol, 1 equiv) in 2 mL of dichloromethane at room temperature and under argon atmosphere at room temperature. After 5 h stirring at room temperature, diethyl ether was added and the product precipitated as purple solid, which were filtered off, washed with diethyl ether and the dried under vacuum. (65 mg, 84 %).

Reactivity and Characterization of Phosphinine Complexes

HR MASS MALDI-TOF calc. for ($C_{46}H_{36}Cl_2N_2P_2Pd_2$) (*m/z*): 1032.97 [$M^+$+3$Na^+$], 965.00 [$M^+$+$H^+$], 806.10 [$M^+$-Pd-$CH_3$-Cl]; found *m/z*: 1032.92 [M^++3Na^+], 965.01 [M^++H^+], 806.16 [M^+-Pd-CH_3-Cl].

^{1}H NMR (400 MHz, CD_2Cl_2): δ (ppm) = 2.00 (d, 3H, P-CH_3, $J_{P\text{-}H}$ = 16Hz), 6.66 (dd, 1H, $J_{P\text{-}H}$= 16Hz, $J_{H\text{-}H}$= 8Hz), 7.00-8.40 (m, 15H), 9.70 (d, 1H, $J_{H\text{-}H}$ = 4Hz); ^{31}P NMR (162 MHz, CD_2Cl_2): δ (ppm) = 34.9.

Reactivity of PdL4a and PtL4a with ROH and R^1RNH

[PdCl$_2$(L4H·OR)] (PdL4e)
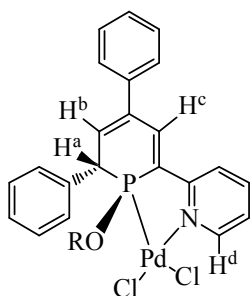
Under an argon atmosphere at room temperature, a mixture of 2-(2-pyridyl)-4,6-diphenylphosphinine **L4** (0.093 g, 0.285 mmol, 1 equiv.) and PdCl$_2$ (0.051 g, 0.285 mmol, 1 equiv.) in CH_2Cl_2/ROH (2 mL/2 mL) was refluxed at 65°C overnight to give a dark red solution, which was concentrated in vacuum to aprox. 1 mL until a red precipitated appeared. Addition of ROH (3 mL) induced formation of more precipitate. Afterwards the solvent was removed by the use of a syringe and the solid was dried in vacuum.

Ethanol (PdL4e₁): Purple-pink solid (160 mg, 95 %).

^{1}H NMR (200 MHz, CD_2Cl_2): δ (ppm) = 1.3 (t, 3H, *J* = 9.09Hz), 4.25 (m, 1H), 4.51 (m, 1H), 4.8 (dd, 1H, H$_a$, $^2J_{H\text{-}P}$ = 22.2 Hz, $^3J_{H\text{-}H}$ = 8.9 Hz), 6.8 (dd, 1H, H$_b$, $^3J_{H\text{-}P}$ = 17.8 Hz, $^3J_{H\text{-}H}$ = 8.9Hz), 7.35 – 7.5 (m, 11H), 7.73 (d, 1H, H$_c$, $^3J_{H\text{-}P}$ = 26.7 Hz), 7.98 (m, 2H), 9.65 (d, 1H, H$_d$, $^3J_{H\text{-}H}$ = 7.1 Hz). ^{13}C NMR (200 MHz, CD_2Cl_2): δ (ppm) =16.2, 16.4 (-CH_3), 68.0 (-CH_2-), 120.1, 120.3, 124.7, 125.3, 126.4, 126.5, 127.5, 128.4, 128.7, 128.7, 128.9, 129.0, 129.2, 130.0, 130.1, 130.3, 131.7, 131.9, 133.7, 136.7, 137.7, 137.9, 138.2, 138.7, 139.0, 139.3, 140.0, 153.3, 153.8, 156.9. ^{31}P NMR (162 MHz, CD_2Cl_2): δ (ppm) = 107.9.

Methanol (PdL4e₂): Bright yellow solid obtained by recrystallization from CH_2Cl_2 and pentane (109 mg, 0.204 mol, 71 %).
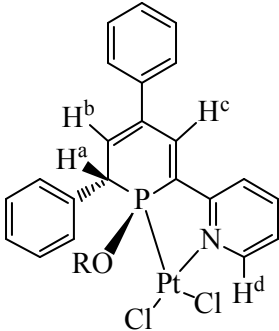
Analysis calcd. for $C_{23}H_{20}Cl_2NOPPd$ (M$_w$ = 534.72 g/mol): C: 51.66%; H: 3.77%; N: 2.62%. Found: C: 51.48; H: 3.74; N: 2.58. ^{1}H NMR (400 MHz, CD_2Cl_2): δ (ppm) = 3.97 (d, 3H, -OCH_3, $^3J_{H\text{-}P}$ = 14.4 Hz), 4.93 (dd, 1H, H$_a$, $^3J_{H\text{-}H}$ = 7.2 Hz; $^2J_{H\text{-}P}$ = 20.2 Hz), 6.79 (dd, 1H, H$_b$, $^3J_{H\text{-}H}$ = 7.2 Hz; $^3J_{H\text{-}P}$ = 17.1 Hz), 7.32-7.40 (m, 4H, Aryl-H),

7.44-7.53 (m, 5H, Aryl-H), 7.54-7.59 (m, 2H, Aryl-H), 7.74 (d, 1H, H_c, $^3J_{H\text{-}P}$ = 20.6 Hz), 7.97 (m, 2H, Aryl-H), 9.74 (d, 1H, pyridine-H_α, $^3J_{H\text{-}H}$ = 6.0 Hz). ^{13}C NMR (100 MHz, CD_2Cl_2): δ (ppm) = 42.7 (d, phosphinine-C_1, $^1J_{P\text{-}C}$ = 48.6 Hz), 57.7 (-OCH_3), 120.4 (d, $J_{P\text{-}C}$ = 11.1 Hz), 125.4, 126.4, 128.5, 128.7, 128.9, 129.0, 130.1, 131.6 (d, $J_{P\text{-}C}$ = 11.8 Hz), 132.6 (d, $J_{P\text{-}C}$ = 36.8 Hz), 138.1, 138.9, 138.6, 139.4, 140.0, 153.6, 157.1 (d, $J_{P\text{-}C}$ = 21.3 Hz). ^{31}P NMR (162 MHz, CD_2Cl_2): δ (ppm) = 111.1.

[PtCl$_2$(L4H·OEt)](PtL4d)

The same procedure as complex **PdL4e** was followed; however the reaction time was increase until 24 h.

Ethanol (PtL4d$_1$): brown solid (176 mg, 90 %).

^1H NMR (200 MHz, CD_2Cl_2): δ (ppm) = 1.3 (t, 3H, $J_{H\text{-}H}$ = 3.8 Hz), 4.2 (m, 1H), 4.47 (m, 1H), 4.73 (dd, 1H, H_a, $^3J_{H\text{-}P}$ = 20.4 Hz, $^2J_{H\text{-}H}$ = 7.4 Hz), 6.8 (dd, 1H, H_b, $^3J_{H\text{-}P}$ = 17.2 Hz, $^3J_{H\text{-}H}$ = 7.4Hz), 7.35 – 7.5 (m, 11H), 7.7 (d, 1H, H_c, $^3J_{H\text{-}P}$ = 21.2 Hz), 7.97 (m, 2H), 10.08 (d, 1H, H_d, $^3J_{H\text{-}H}$ = 6.2 Hz); ^{13}C NMR (200 MHz, CD_2Cl_2): δ (ppm)= 16.1, 16.2 (-CH_3), 66.7 (-CH_2-), 120.5, 125.6, 126.4, 128.3, 128.8, 129.0, 130.1, 130.2, 131.1, 131.8, 134.3, 137.6, 138.4, 138.8, 139.2, 152.2, 157.6; ^{31}P NMR (162 MHz, CD_2Cl_2): δ (ppm) = 71.7 ($J_{P\text{-}Pt}$ = 2166 Hz).

Methanol (PtL4d$_2$): brown solid (130 mg, 0.209 mmol, 76 %). The product contains approximately 10% of an unidentified side-product with a resonance in the ^{31}P NMR spectrum at δ (ppm) = 64.3 ($J_{Pt\text{-}P}$ = 4338 Hz).

^1H NMR (CD_2Cl_2, 400 MHz): δ (ppm) = 3.87 (d, $^3J_{H\text{-}P}$ = 14.0 Hz, 3H, -OCH_3), 4.74 (dd, 1H, H_a, $^3J_{H\text{-}H}$ = 6.8 Hz; $^2J_{H\text{-}P}$ = 19.6 Hz), 6.83 (dd, 1H, H_b, $^3J_{H\text{-}H}$ = 6.8 Hz; $^3J_{H\text{-}P}$ = 17.6 Hz), 7.32-7.35 (m, 2H, aryl-H), 7.42-7.46 (m, 5H, aryl-H), 7.48-7.58 (m, 4H, aryl-H), 7.74 (d, 1H, H_c, $^3J_{H\text{-}P}$ = 20.8 Hz), 7.93 (t, 1H, aryl-H, ^3J = 7.6 Hz), 8.0 (t, 1H, aryl-H, $^3J_{H\text{-}H}$ = 7.6 Hz), 10.06 (d, 1H, pyridine-H_α, $^3J_{H\text{-}H}$ = 6.0 Hz). ^{31}P NMR (CD_2Cl_2, 162 MHz): δ (ppm) = 77.7 (s with Pt-satellites, $J_{Pt\text{-}P}$ = 4349.4 Hz).

Reactivity and Characterization of Phosphinine Complexes

[PdCl$_2$(L4H·NR^{1}R)](PdL4f)

Under an argon atmosphere at room temperature, a mixture of 2-(2-pyridyl)-4,6-diphenylphosphinine **L4** (0,093 g, 0,285 mmol, 1 equiv.) and PdCl$_2$ (0,051 g, 0,285 mmol, 1 equiv.) in THF/R$_1$R$_2$NH (2 mL/2 mL) was refluxed at 65°C overnight to give a dark brown solution, which was concentrated in vacuum to aprox. 1 mL until a brown precipitated appeared. Addition of Et$_2$O (3 mL) induces formation of more precipitate. Afterwards the solvent was removed by the use of a syringe. The solid was dried in vacuum.

[Rh(cod)(L4)]BF$_4$ (RhL4a)

[Rh(cod)$_2$]BF$_4$ (37 mg, 0.092 mmol) and 2-(2'-pyridyl)4,6-diphenylphosphinine (**L4**) (30 mg, 0.092 mmol) was dissolved in CH$_2$Cl$_2$ (2.0 mL). The dark red solution was stirred for 1h. Subsequently, Et$_2$O (6.0 mL) was added until a solid precipitated. The solution was decanted and the solid was dried under vacuum. Complex **RhL4a** was obtained as an orange-brown powder (38 mg, 0.06 mmol, 66 %). Orange crystals of **RhL4a** suitable for X-ray diffraction and elemental analysis were obtained by slow crystallization from a mixture of [Rh(cod)$_2$]BF$_4$ (25 mg, 0.0615 mmol) and **L4** (20 mg, 0.0615 mmol) in THF/CH$_2$Cl$_2$ (2.0 mL) after filtration over Celitte.

Anal. Calcd. for C$_{30}$H$_{28}$BF$_4$NPRh (M$_w$ = 623.24 g/mol): C: 57.82; H: 4.53; N: 2.25. Found: C: 57.43; H: 4.48. N: 2.18. HR MASS MALDI-TOF calc. for (C$_{32}$H$_{34}$BF$_4$NPRh) (*m/z*): 570.15 [M$^+$-BF$_4^-$+2NH$_4^+$], 535.09 [M$^+$-BF$_4^-$]; found *m/z*: 570.21 [M$^+$-BF$_4^-$+2NH$_4^+$], 535.22 [M$^+$-BF$_4^-$].

^{1}H NMR (400 MHz, CD$_2$Cl$_2$): δ 2.26 (m, 4H, (CH)$_{COD}$), 2.55 (m, 4H, (CH$_2$)$_{COD}$), 5.31 (m, 4H, (CH$_2$)$_{COD}$), 7.50-7.70 (m, 10H), 7.74 (d, 2H, J_{H-H}= 8Hz), 8.17 (m, 2H), 8.26 (d, 1H, J_{H-H}= 8Hz), 8.57 (dd, 1H, J_{P-H}= 16Hz, J_{H-H}= 4Hz); ^{19}F NMR (376.5 MHz, CD$_2$Cl$_2$): δ -149.7; ^{31}P NMR (162 MHz, CD$_2$Cl$_2$): δ 175.4 (d, $^1J_{Rh-P}$= 188Hz). ^{13}C NMR (50.3 MHz, CD$_2$Cl$_2$): δ (ppm) = 29.7 ((CH$_2$)^{COD}), 107.5, 107.6 ((CH)^{COD}), 120.8 (d, $^1J_{C-P}$ = 13.5 Hz), 126.9, 127.6, 127.7, 127.9, 128.7, 129.3, 129.4, 129.6, 131.8 (d, $^1J_{C-P}$ = 13.0 Hz), 139.0 (m), 140.4, 141.5, 143.4, 151.7, 158.2 (m).

5.4.2 X-ray crystal structure determination

X-ray intensities were measured on a Nonius KappaCCD diffractometer (rotating anode, graphite monochromator, λ = 0.71073 Å) [compounds **PdL4a**, **PtL4a**, **RhL4a**] or a Bruker Kappa ApexII diffractometer (sealed tube, triumph monochromator, λ = 0.71073 Å) [compound **PdL4e$_2$**] at a temperature of 150(2) K. Data were integrated with the EVAL14[38] [compounds **PdL4a**, **PtL4a**, **PdL4e$_2$**] or with the HKL2000[39] [compound **RhL4a**] software. Scaling and absorption correction was performed using SADABS.[40] The structures were solved with Direct Methods using the program SHELXS-97[41] [compound **PdL4a**, **PtL4a**, **PdL4e$_2$**] and SIR-97[42] [compound **RhL4a**]. Least-squares refinement was performed with SHELXL-97[41] on F^2 of all reflections. Non-hydrogen atoms were refined with anisotropic displacement parameters. Hydrogen atoms were located in difference-Fourier maps [compound **PtL4a**] or introduced in calculated positions [compounds **PdL4a**, **PdL4e$_2$**]. All hydrogen atoms were refined with a riding model. Structure calculations and checking for higher symmetry were performed with the PLATON software.[43] Structural graphics were generated by ORTEP-3 v2.02 and POV-Ray v3.6. [Compounds **PdL4a**, **PtL4a**, **PdL4e$_2$**]. All hydrogen atoms were located in difference-Fourier maps. Hydrogen atoms at the double bonds of the *cod* ligands were refined freely with isotropic displacement parameters; all other hydrogen atoms were refined as rigid groups with the PLATON software.[43] [Compound **RhL4a**].

Compound PdL4a: [$C_{22}H_{16}Cl_2NPPd$]·0.5CH$_2$Cl$_2$, Fw = 545.09, dark orange needle, 0.54 x 0.16 x 0.09 mm^3, monoclinic, P2$_1$/c (no. 14), a = 18.2129(6), b = 7.3165(2), c = 33.1753(11) Å, β = 111.376(2)°, V = 4116.7(2) Å^3, Z = 8, D$_x$ = 1.759 g/cm^3, μ = 1.38 mm^{-1}. 24487 Reflections were measured up to a resolution of (sin $\theta/\lambda)_{max}$ = 0.55 Å^{-1} of which 5712 were unique reflections (R$_{int}$ = 0.036), and 4839 were observed [I>2σ(I)]. Absorption correction range = 0.57-0.75. 514 Parameters were refined with no restraints. R1/wR2 [I > 2σ(I)]: 0.0354 / 0.0811. R1/wR2 [all refl.]: 0.0474 / 0.0881. S = 1.190. Residual electron density between -0.73 and 1.32 e/Å^3.

Compound PtL4a: [$C_{22}H_{16}Cl_2NPPt$]·0.5CH$_2$Cl$_2$, Fw = 633.78, orange needle, 0.60 x 0.15 x 0.06 mm^3, monoclinic, P2$_1$/c (no. 14), a = 18.2499(4), b = 7.3203(2), c = 33.1920(7) Å, β = 111.382(2)°, V = 4129.07(17) Å^3, Z = 8, D$_x$ = 2.039 g/cm^3, μ = 7.27

Reactivity and Characterization of Phosphinine Complexes

mm^{-1}. 51545 Reflections were measured up to a resolution of $(\sin \theta/\lambda)_{max}$ = 0.61 Å^{-1} of which 7676 were unique reflections (R_{int} = 0.041), and 6641 were observed [I>2σ(I)]. Absorption correction range = 0.18-0.69. 514 Parameters were refined with no restraints. R1/wR2 [I > 2σ(I)]: 0.0266 / 0.0589. R1/wR2 [all refl.]: 0.0364 / 0.0630. S = 1.162. Residual electron density between -1.30 and 1.32 e/Å^3.

Compound PdL4e$_2$: $C_{23}H_{20}Cl_2NOPPd$, Fw = 534.67, yellow block, 0.24 x 0.21 x 0.18 mm^3, orthorhombic, Pbca (no. 61), a = 8.8039(3), b = 16.9366(8), c = 28.1738(10) Å, V = 4200.9(3) Å^3, Z = 8, D_x = 1.691 g/cm^3, μ = 1.23 mm^{-1}. 30502 Reflections were measured up to a resolution of $(\sin \theta/\lambda)_{max}$ = 0.56 Å^{-1} of which 3014 were unique reflections (R_{int} = 0.045), and 2531 were observed [I>2σ(I)]. Absorption correction range = 0.59-0.75. 263 Parameters were refined with no restraints. R1/wR2 [I > 2σ(I)]: 0.0419 / 0.0909. R1/wR2 [all refl.]: 0.0539 / 0.0996. S = 1.263. Residual electron density between -0.89 and 0.68 e/Å^3.

Compound RhL4a: $[C_{30}H_{28}NPRh]BF_4 \cdot 0.4(CH_2Cl_2)$, Fw = 657.19, orange plate, 0.21x0.12x0.02 mm^3, triclinic, P 1 (no. 2), a = 9.7987(2), b = 10.3575(2), c = 14.5382(3) Å, α = 84.8750(6), β = 85.4051(6), γ = 71.0572(8)°, V = 1387.95(5) Å^3, Z = 2, Dcalc = 1.573 g/cm^3, μ = 0.80 mm^1. 21889 Reflections were measured up to a resolution of (sin θ/λ) max = 0.65 Å^{-1} of which 6367 were unique (Rint = 0.044) and 5109 observed [I > 2σ(I)]. The CH_2Cl_2 molecule was located close to an inversion centre and refined with partial occupancy. Absorption correction range: 0.88-0.98. 377 Parameters were refined with one restraint. R1/wR2 [I > 2σ(I)]: 0.0396/0.0872, R1/wR2 [all refl.]: 0.0586/0.0949. S = 1.047. Δρmin/max = -0.47/1.03 eÅ^3.

5.5   Supporting information

CCDC 787659 (compound **PdL4a**), 787660 (**PtL4a**), 787661 (**PdL4e$_2$**) and 762388 (**RhL4a**) contain the supplementary crystallographic data for these complexes. These data can be obtained free of charge from The Cambridge Crystallographic Data Centre via www.ccdc.cam.ac.uk/data_request/cif and moreover, the NMR spectra and MALDI-TOF analysis from the complexes studied are included in the supporting information as an electronic file.

5.6 References

[1] *(a)* Müller, C. and Vogt, D. *Dalton Trans.* **2007**, 5505-5523. *(b)* Müller, C. and Vogt, D. *C. R. Chimie* **2010**, *13*, 1127-1143.

[2] Märkl, G., *Angew. Chem.* **1966**, *78*, 907-908.

[3] *(a)* Müller, C., Guarrotxena-Lopéz, L., Kooijman, H., Spek, A.L. and Vogt, D. *Tetrahedron Lett.*, **2006**, *47*, 2017-2020; *(b)* Müller, C., Pidko, E.A., Staring, A.J.P.M., Lutz, M., Spek, A.L., van Santen, R.A. and Vogt, D. *Chem. Eur. J.*, **2008**, *14*, 4899-4905; *(c)* Müller, C., Freixa, Z., Lutz, M., Spek, A.L., Vogt, D. and van Leeuwen, P.W.N.M. *Organometallics*, **2008**, *27*, 834-838; *(d)* Müller, C., Pidko, E.A., Lutz, M., Spek, A.L. and Vogt, D. *Chem. Eur. J.*, **2008**, *14*, 8803-8807.

[4] *(a)* Breit, B., Winde, R., Mackewitz, T., Paciello, R. and Harms, K. *Chem. Eur. J.*, **2001**, *7*, 3106-3121. *(b)* Wallis, C., McGuinness, D., Newman, P.D., Tooze, R.P. and Edwards, P. G. *Dalton Trans.*, **2009**, 2178-2184.

[5] Kaes, C., Katz, A. and Hosseini, M.W. *Chem. Rev.*, **2000**, *100*, 3553-3590.

[6] Ashe, III, A.J. *J. Am. Chem. Soc.*, **1971**, *93*, 3293-3295.

[7] *(a)* Le Floch, P. *Coord. Chem. Rev.*, **2006**, *250*, 627-681; *(b)* Mézailles, N., Mathey, F. and Le Floch, P. *Prog. Inorg. Chem.*, **2001**, 455-450; *(c)* Le Floch, P. and Mathey, F. *Coord. Chem. Rev.*, **1998**, *179-180*, 771-791.

[8] Alcaraz, J.-M., Brèque, A. and Mathey, F. *Tetrahedron Lett.*, **1982**, *23*, 1565-1568.

[9] Le Floch, P., Carmichael, D., Ricard, L. and Mathey, F. *J. Am. Chem. Soc.*, **1993**, *115*, 10665-10670.

[10] Lesnard, H., Cantat, T., Le Floch, P., Demanchy, I. and Jean, Y. *Chem. Eur. J.*, **2007**, *13*, 2953-2965.

[11] Brèque, A., Santini, C.C., Mathey, F., Fischer, J. and Mitschler, A. *Inorg. Chem.*, **1984**, *23*, 3463-3467.

[12] Schmid, B., Venanzi, L.M., Albinati, A. and Mathey, F. *Inorg. Chem.*, **1991**, *30*, 4693-4699.

[13] Schmid, B., Venanzi, L.M., Gerfin, T., Gramlich, V. and Mathey, F. *Inorg. Chem.* **1992**, *31*, 5117-5122.

[14] Breit, B. *Chem. Commun.* **1996**, 2071-2072.

[15] Neumann, E. *PhD. Thesis*, Universität Basel, **2006**, Switzerland.

[16] Müller, C.; Wasserberg, D.; Weemers, J. J. M.; Pidko, E. A.; Hoffmann, S.; Lutz, M.; Spek, A. L.; Meskers, S. C. J.; Janssen, R. A. J.; van Santen, R. A.; Vogt, D. *Chem. Eur. J.* **2007**, *13*, 4548-4559.

[17] Cave, G. W. V.; Raston, C. L. *J. Chem. Soc. Perkin Trans. 1* **2001**, 3258-3264.

[18] Katritzky, A. R.; Elisseou, E. M.; Patel, R. C.; Plau, B. *J. Chem. Soc. Perkin Trans. 1* **1982**, 125-130.

[19] Aullón, G.; Alemany, P. and Alvarez, S. *Inorg. Chem.* **1996**, *35*, 5061-5067.

[20] Maekawa, M.; Munakata, M.; Kitagawa, S. and Nakamura, M. *Analytical Sciences* **1991**, *7*, 521-522.

[21] Connick, W.B.; Henling, L.M.; Marsh, R.E. and Gray, H.B. *Inorg. Chem.* **1996**, *35*, 6261-6265.

[22] *(a)* Chrisholm, M.H.; Huffman, J.C.; Rothwell, I.P.; Bradley, P.G.; Kress, N. and Woodruff, W.H. *J. Am. Chem. Soc.* **1981**, *103*, 4945-4947; *(b)* Szalda, D.J.; Creutz, C.; Mahajan, D. and Sutin, N. *Inorg. Chem.* **1983**, *22*, 2372-2379.

[23] Müller, C.; Lutz, M.; Spek, A.L. and Vogt, D. *J. Chem. Crystallogr.* **2006**, *36*, 869-874.

[24] *(a)* Chatt, J.; Vallarino, L. M.; Venanzi, L. M. *J. Chem. Soc.* **1957,** 3413-3416. *(b)* A. Zucca, M.A. Cinellu, M.V. Pinna, S. Stoccoro, G. Minghetti, M. Manassero, M. Sansoni, *Organometallics* **2000**, 19, 4295-4304. *(c)* Stoccoro, S.; Alesso, B.; Cinellu, M. A.; Minghetti, G.; Zucca, A.; Bastero, A.; Claver, C.; Manassero, M. *J. Organomet. Chem.* **2002**, 664, 74-84.

[25] Milani, B.; Marson, A.; Zangrando, E.; Mestroni, G.; Ernsting, J.M. and Elsevier, C.J. *Inorg. Chim. Acta* **2002**, *327*, 188-201.

[26] P.K Byers, A.J. Canty, *Organometallics* **1990**, *9*, 210-220.

[27] In 2,6-Me$_3$Si-substituted phosphinines and the corresponding metal complexes the internal C-P-C angle can be even higher. See for example: N. Mézailles, L. Ricard, F. Mathey, P. Le Floch, *Eur. J. Inorg. Chem.* **1999**, 2233-2241.

[28] Lindsay, C. H.; Benner, L. S. and Balch, A. L. *Inorg. Chem.* **1980**, *19*, 3503-3508.

[29] Hope, E.G.; Levason, W. and Powell, N.A. *Inorg. Chim. Acta* **1986**, *115*, 187-192.

[30] Al-Najjar, I.M. *Inorg. Chim. Acta* **1987**, *128,* 93-104.

[31] Doux, M., Ricard, L., Mathey, F., Le Floch, P. and Mézailles, N. *Eur. J. Inorg. Chem.*, **2003**, 687-698.

[32] Mézailles, N., Ricard, L., Mathey, F. and Le Floch, P. *Organometallics*, **2001**, *20*, 3304-3307.

[33] Yang, H., Lugan, N. and Mathieu, R. *Organometallics* **1997**, *16*, 2089-2095.

[34] Caporali, M.; Müller, C.; Staal, B. B. P.; Tooke, D. M.; Spek, A. L.; van Leeuwen, P. W. N. M. *Chem. Commun.* **2005**, 3478-3480.

[35] Drent, E. and Budzelaar, P. H. M. *Chem. Rev.* **1996,** 96, 663-681.

[36] Milani, B.; Durand, J.; Zangranado, E.; Stener, M.; Fronzoni, G.; Carfagna, C.; Binotti, B.; Kamer, P. C. J.; Müller, C.; Caporali, M.; van Leeuwen, P. W. N. M.; and Vogt, D. *Chem. Eur. J.* **2006**, *12*, 7639 – 7651.

[37] Niecke, E. and Westermann, H. *Synthesis* **1988**, *4*, 330.

[38] Duisenberg, A.J.M.; Kroon-Batenburg, L.M.J. and Schreurs, A.M.M. *J. Appl. Cryst.* **2003**, *36*, 220-229.

[39] Otwinowski, Z., Minor, W., *Methods in Enzymology, Volume 276* (C.W. Carter, Jr. & R.M. Sweet, Eds) Academic Press (1997) 307-326.

[40] Sheldrick, G.M. **1999**. SADABS: Area-Detector Absorption Correction, v2.10, Universität Göttingen, Germany.

[41] Sheldrick, G.M. *Acta Cryst.* **2008**, *A64*, 112-122.

[42] Altomare, A.; Burla, M.C.; Camalli, M.; Cascarano, G.L.; Giacovazzo, C.; Guagliardi, A.; Moliterni, A.G.G.; Polidori, G. and Spagna, R. *J. Appl. Cryst.* **1999**, *32*, 115-119.

[43] Spek, A.L. *Acta Cryst.* **2009**, *D65*, 148-155.

PART - 2

CO2 as C1 building block

Chapter - 6

Zinc Catalytic Systems with Amino-Alcohol Ligands in Polycarbonate Synthesis by Copolymerization of Cyclohexene Oxide and Carbon Dioxide.

A series of chiral amino-alcohol ligands were tested in zinc catalysed copolymerization of cyclohexene oxide and carbon dioxide giving almost 100% carbonate linkage in the polycarbonate product. The effect in the productivity and polycarbonate selectivity of the different substituents in the carbon α to the –OH (R_4) and –NR group (R_3) as well as the amino-substituents of the ligand (R_1 and R_2) were studied. The polycarbonates were obtained with low activities (up to 2.90 g PCHC/ g Zn) and the molecular weight ranged 15000 – 50000 (M_w).
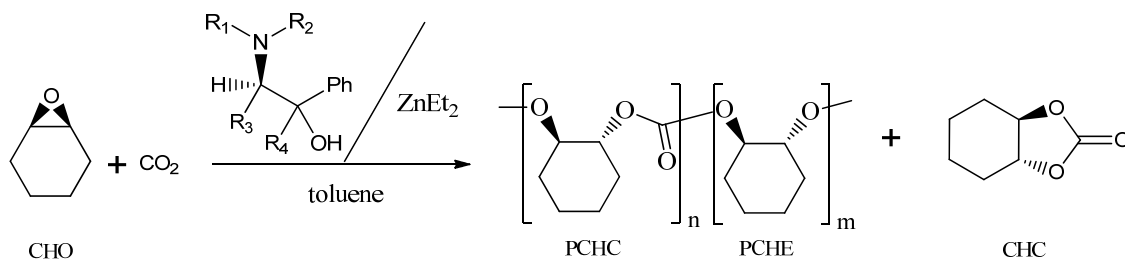
This work has been done in collaboration with Prof. Dr. M. A. Pericàs and Dra. A. Bastero (ICIQ, Institut Català d'Investigació Química, Tarragona)

Zinc catalytic systems with amino-alcohol ligands in polycarbonates synthesis

6.1 Introduction

As discussed in Chapter 1, in the recent years it has been growing the interest for *polycarbonates*, since they have good biodegradability, are highly transparent to visible light, have better light transmission characteristics than many kinds of glass, are hard and could be employed to develop other specialty polymers.[1,2,3] Nevertheless, the industrial production of polycarbonates involves the polycondensation of phosgene and diols, being phosgene notorious for its high toxicity and corrosiveness. Therefore, an alternative procedure avoiding phosgene would lead to a completely green process.

An attractive alternative for *polycarbonates* synthesis is using carbon dioxide as C_1 building block by copolymerization with epoxides due to it is an inexpensive, non-toxic and non-flammable gas.[4] Although owing to the thermodynamical stability of carbon dioxide requires the use of a catalyst.

Furthermore, this reaction offers the possibility of asymmetric alternating copolymerization of *meso*-epoxide with CO_2 (Scheme 6.1) when a chiral catalyst is used.[5] The chiral catalyst could control the absolute stereochemistry of the asymmetric ring-opening leading to optically active aliphatic polycarbonate with (*R,R*)- or (*S,S*)-1,2-diol units. The model *meso* epoxide used is normally cyclohexene oxide (CHO). In copolymerization of CO_2 and CHO cyclic species (cyclic carbonate) are common by-products since they are thermodynamically more stable than polycarbonates.[6,7] Even more, in this reaction can be observed a consecutive epoxide enchainment leading to the formation of ether linkage, another important by-product.[6]
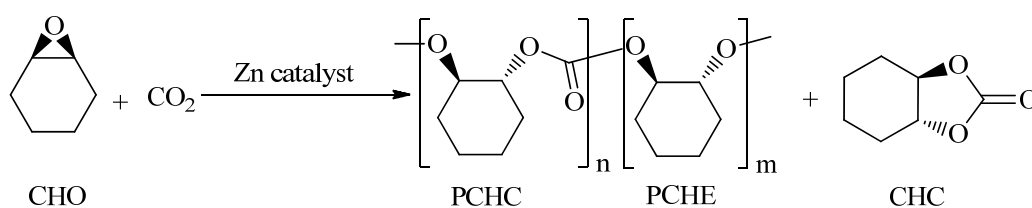
Scheme 6.1. Alternating copolymerization of *meso*-cyclohexene oxide (CHO) with carbon dioxide.

In the literature the best enantioselective catalytic systems for asymmetric CHO/CO_2 copolymerisation was obtained with a chiral amino-alcohol ((*S*)-**C**) with ZnEt$_2$ and the addition of 0.2-1.0 equivalents of EtOH. This precatalyst system reported by Nozaki *et al.*[8,9] gave 80% e.e. corresponding (*R,R*)-*trans*-cyclohexane-1,2-diol and was isolated and characterised by X-ray diffraction as a dimer ((*S,S*)-**C$_1$**). This system

provided good results in terms of yield leading to polycarbonates with 100% of carbonate linkage (PCHC) and no cyclic cyclohexene carbonate (CHC) was present.

(S)-**C**   *(S,S)*-**C₁**
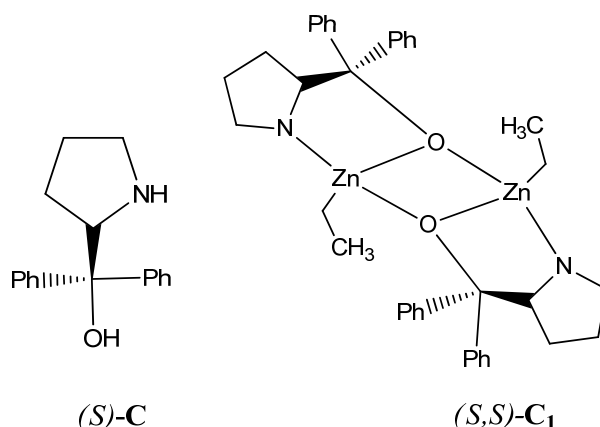
Figure 6.1. Chiral ligand and chiral zinc catalysts for the asymmetric alternating copolymerisation of CHO and CO_2 reaction.

In base of these results, taking system **C₁** as a model, a family of amino-alcohol ligands (**L5-L12,** Figure 6.2) were selected to be tested in the zinc catalyzed copolymerization of cyclohexene oxide with CO_2 using the reaction conditions reported by Nozaki *et al.* [8,9]
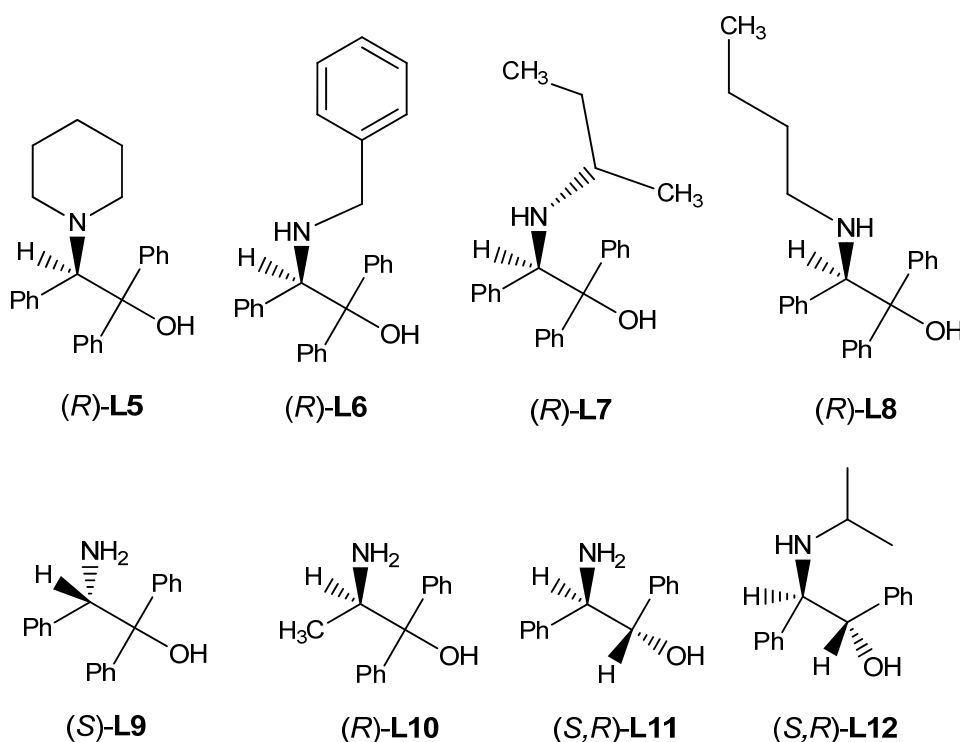
Figure 6.2. Amino-alcohols used as ligands in copolymerization of CHO with CO_2.

Zinc catalytic systems with amino-alcohol ligands in polycarbonates synthesis

6.2 Results and discussion

The ligands **L5-L8** were synthesized at the Institut Català d'Investigacions Químiques (ICIQ, group of Prof. M. A. Pericàs) according to described procedures[10,11] and ligands **L9-L12** were commercially available (Figure 6.2). The catalyst precursors were prepared *in situ* by addition of stoichiometric amounts of the ligand to a solution of $ZnEt_2$ in toluene.

The results obtained with the catalytic systems $ZnEt_2$/ **L5-L12** are shown in Table 6.1. The reactions were carried out at 60ºC and 30 atm of CO_2 during 24h to ensure that the polymer was formed. The final products were extracted from the reaction solution, once the catalyst was hydrolysed, and the reaction products were further purified by reprecipitation from methylene chloride with methanol. The copolymers were analyzed by NMR and IR spectroscopy after purification.

The presence of the cyclic carbonate was confirmed by FTIR and ^{1}H NMR spectroscopy. FTIR was only used to determine the presence of *trans*-cyclohexane carbonate (CHC) isomer, which shows in methylene chloride a $v(CO_2)$ stretching vibration at 1820 and 1803 cm^{-1}, while the asymmetric $v(CO_2)$ stretching vibration of the polycarbonate linkage was observed at 1750 cm^{-1}.[12] A representative IR spectra of a mixture CHC-PCHC and isolated PCHC is shown in Figure 6.3.
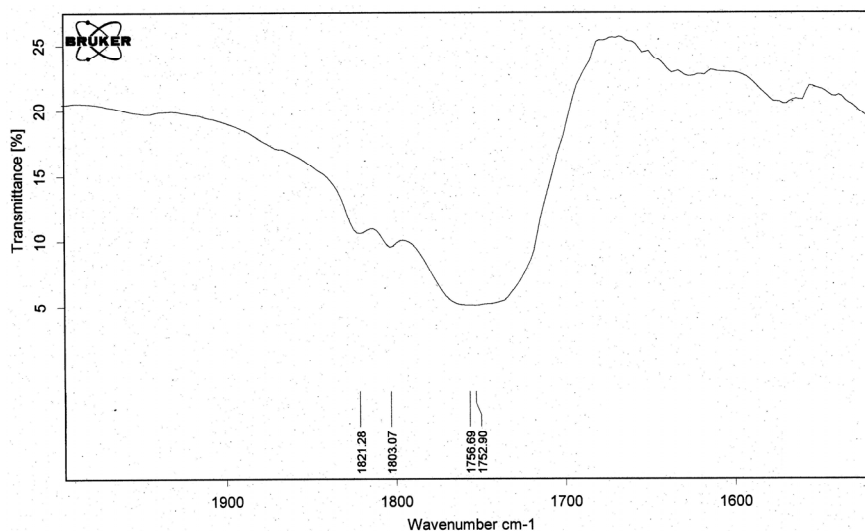

Figure 6.3a. Infrared spectrum of reaction product at 60ºC using precatalyst **L11**/$ZnEt_2$ (entry 7, Table 6.1).
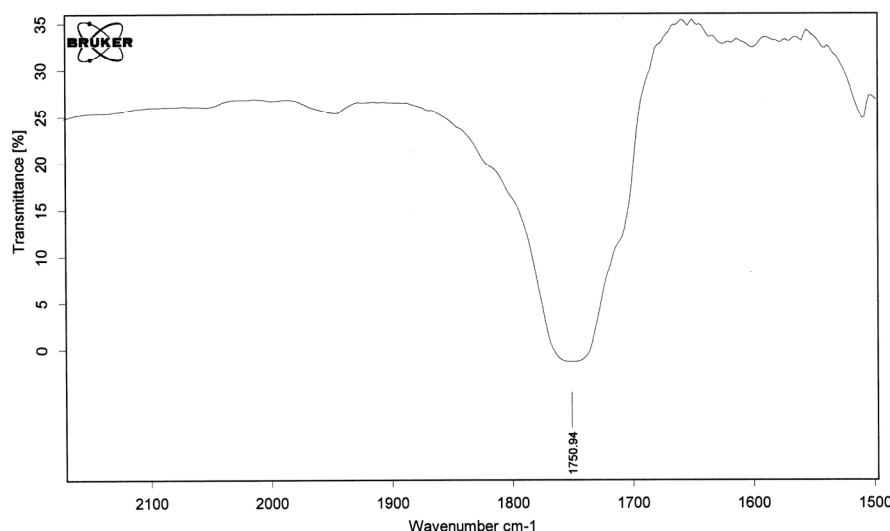
Figure 6.3b. Infrared spectrum of reaction product at 60ºC using precatalyst **L10**/ZnEt$_2$ (entry 6, Table 6.1).

The percentage of polycarbonate selectivity was calculated from the relative intensities of the ^{1}H NMR signals of the methylene protons next to the carbonate linkage, δ 4.60 ppm for polycyclohexanecarbonate (PCHC) and δ 3.9 ppm for *trans*-CHC.[12] In the carbonyl region of the ^{13}C NMR (Figure 6.4) spectra appears two signal at δ 154.2 ppm and δ 153.6 ppm which confirm the formation of carbonate linkage and no CHC, which signal appears at δ 154.7 ppm (entry 1, Table 6.1).[12] The two peaks are assigned according to literature data to syndiotactic (two diols units with the opposite absolute configuration connected through a carbonate bond, relative configuration *RR-SS*) and isotactic (with relative configuration *RR-RR*) copolymer chain tacticity on the basis of corresponding ^{13}C NMR data from the model compound 2,2'-oxydicyclohexanol.[13,14]

The degree of carbonate that was incorporated in the co-polycarbonate polyether polymer, *f*CO$_2$, can be evaluated as was described by Hsu and Tan[15] by the ratio (%) of the integration of the methine proton geminal to oxygen, which give a broad signal in the ^{1}H NMR at δ 4.6 ppm, for the polycarbonate fraction; and a δ 3.5 ppm, for the polyether fraction. In most of the experiments the degree of carbonate incorporation was relatively high, leading more than 90% in almost all cases.

Zinc catalytic systems with amino-alcohol ligands in polycarbonates synthesis

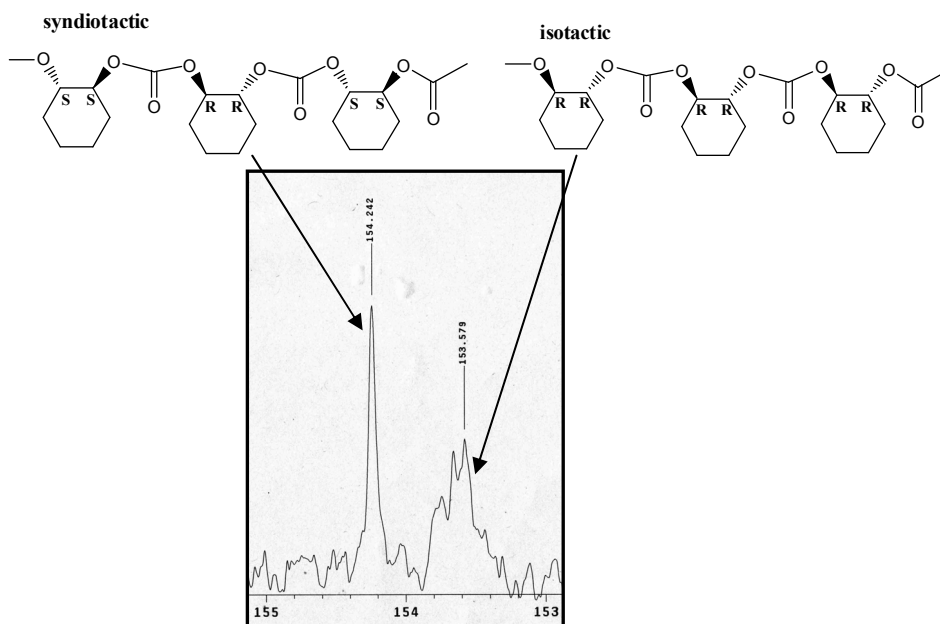**Figure 6.4.** Example of ^{13}C NMR spectrum from PCHC formed with **4**/ZnEt$_2$ (entry 1, Table 6.1).

In general the productivities obtained were low (up to *ca.* 3-4 g product/g Zn). The catalytic system ZnEt$_2$/**L5** presented the best combined results of productivity 2.90 g PCHC/g Zn and high selectivity in polymer formation (100%) with high degree of carbonate incorporation (94%) (entry 1, Table 6.1). Comparing this catalytic system with the ones with ligands **L6-L9**, it is observed that a bulky substituent seems important to obtain as a main product the polycarbonate with noteworthy productivity (entry 1 - 3 *vs.* entry 4 and 5, Table 6.1).[16] The steric hindrance may avoid the degradation of the polymer (decreasing of the M$_w$) (entry 1 and 3 *vs.* entry 5, Table 6.1).[17,18]

Once we analysed the effect of the nitrogen substituent, we moved on to study the effect in *C1* and *C2* substituents (α-substituent on the C-OH and C-NR$_2$, respectively). Position α to the amino group affected the carbonate incorporation, as was observed comparing the catalytic systems ZnEt$_2$/**L9** (entry 5, Table 6.1) and ZnEt$_2$/**L10** (entry 6, Table 6.1). Both catalytic systems presented similar productivities, but when a small α-substituent on the amino group was used (ZnEt$_2$/**L10**; entry 6, Table 6.1) small increase in the carbonate incorporation was observed. On the other hand, the *C1* position affected the selectivity in polycarbonates *vs.* CHO. The comparison between the catalytic system ZnEt$_2$/**L9** and ZnEt$_2$/**L11** (entry 5 and 7, Table 6.1) showed an increase in the productivity of 4.5 times, but a decreased of selectivity was observed.

184

Table 6.1. Results obtained in the copolymerization of CO_2/CHO with $ZnEt_2$/**L5-L12**.[a]

Entry	L	T(ºC)	g prod/ g Zn	IR[b]	Selectivity (%)[c]	fCO_2 (%)[d]	Mw (Mw/Mn)[e]	% e.e.[f]
1	**L5**	60	2.90	1743	100	94	28670 (1.2)	3 (*R,R*)
2	**L6**	60	4.89	1738, 1802	77	88	-	-
3	**L7**	60	2.47	1738	100	92	34387 (3.8)	nd[h]
4	**L8**	60	0.37	1739	100	94	nd	nd
5	**L9**	60	0.87	1750	100	93	16741 (1.9)	7 (*S,S*)
6	**L10**	60	0.74	1751	100	100	30925 (2.4)	nd
7	**L11**	60	3.88	1753, 1803	95	83	-	-
8	**L11**	40	1.88	1749	100	96	48993 (2.5)	nd
9	**L12**	60	2.37	1752, 1803	97	90	-	-
10[g]	**L12**	60	0.92	1740	100	76	43981 (2.1)	nd

[a] Conditions: $[ZnEt_2]$ = 0.16 M; [L]:[Zn] = 1; [CHO]:[Zn] = 20; P_{CO2} = 30 atm; time = 24 hours. [b] $\upsilon(CO_2)$ stretching vibrations in CH_2Cl_2. [c] Selectivity of PCHC in front of CHC, calculate based on integrals in ^{1}H NMR. [d] Degree of carbonate incorporated in the co-polycarbonate polyether polymer. [e] Determined by GPC, calibrated with polystyrene standard in THF. [f] Determined by GC, as 2,2-dimethylhexahydro-1,3-benzodioxole (trans-cyclohexane-1,2-diol derivatization). [g] P = 50 atm. [h] nd = not determined.

Decreasing the temperature from 60ºC to 40ºC produced an increase in the selectivity, using $ZnEt_2$/**L11**, showing as the only product PCHC, but the productivity was affected decreasing 2.0 times (entry 7 *vs.* entry 8, Table 6.1). The increase of selectivity to polycarbonate at low temperature might be attributed to a suppression of the backbiting mechanism leading to the cyclic carbonate. This is in agreement with literature, where backbiting mechanism was reported to be favoured with temperature.[6,7,19]

The catalytic system $ZnEt_2$/**L12** was selected to confirm the effect of the amine's substituent (entry 9, Table 6.1) in a direct comparison with the catalytic system $ZnEt_2$/**L11** (entry 7 and 8, Table 6.1). Increasing the bulk of the amine's substituent increased the selectivity for PCHC and the carbonate incorporation, although the productivity decreased. This observation may be related with the formation of the active species, which could not be favoured by the introduction of too bulky substituents in the amino group.

Zinc catalytic systems with amino-alcohol ligands in polycarbonates synthesis

Increasing the pressure until 50 bars (ZnEt$_2$/**L12** entry 9 *vs.* entry 11, Table 6.1), the selectivity increased until 100% of PCHC, but the productivity decreased 2.5 times, which may be due to a competition between CHO and CO$_2$ for coordination site and disfavouring the rate determining step.

The analysis of the molecular weight (M$_w$) revealed that substituents in the amino group were necessary for increasing the copolymer's M$_w$ (entry 5 *vs.* 1 and 4, Table 6.1). Even more, the bulkiness of the substituent in the carbon α to –OH group could block the propagation steps decreasing the M$_w$ (entry 5 and 6 *vs.* entry 8, Table 6.1).

The polycarbonate obtained with catalytic systems were hydrolyzed to the 1,2-cyclohexanediol[8] and the enantiomeric excess (% e.e.) of this product was determined by derivatization to the ketal species[20] using GC analysis with a chiral column (Scheme 6.2). The % e.e. obtained with this catalytic systems were very low and lower than the one reported for the ZnEt$_2$/**C** system at the same conditions.[9] The low enantiomeric excess could be attributed to a weak interaction of the ligand with the metal centre, which may lead to ligand dissociation allowing the insertion of the cyclohexene oxide in two different ways. In attempt to increase the enantiomeric excess, the catalytic system ZnEt$_2$/**L5** was tested decreasing the temperature to 40ºC, but no significant increasing was observed. However, it can be notice that the copolymers formed had the same chiral configuration than the catalytic systems used (*R,R*-copolymer unit for (*R*)-**L5**/ZnEt$_2$ catalytic system and *S,S*-copolymer unit for (*S*)-**L9**/ZnEt$_2$ catalytic system; entry 1 and 5, Table 6.1, respectively).
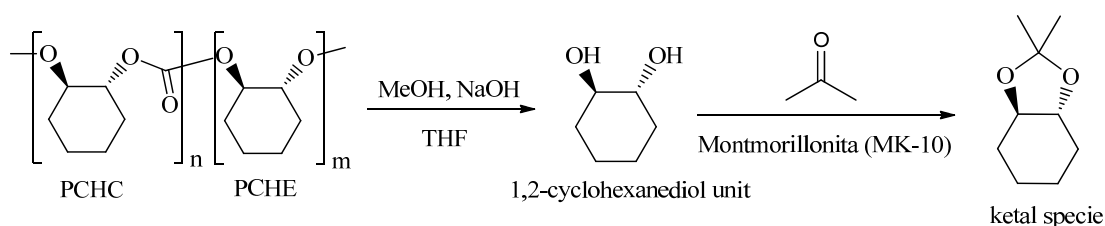
Scheme 6.2. Hydrolyzation of the polymer and subsequently derivatization.

In conclusion, bulky substituents in the amino group seemed necessary to achieve polycarbonates in moderate yield and selectivity, but at the same time too bulky substituents were not beneficial. The substituents in the carbon α to –OH group strongly affected the productivity and in a small scale the selectivity, being more effective less

bulky substituents. On the other hand, the bulkiness of the substituent in the carbon α to –NR$_2$ group had less effect in the productivity and in the selectivity than in the carbonate incorporation.

6.3 Conclusions

The catalytic systems ZnEt$_2$/amino-alcohol (**L5-L12**) presented low activity (up to 2.90 g PCHC/ g Zn) in the copolymerization of cyclohexene oxide and carbon dioxide and the polycarbonate formed showed moderate molecular weight between 15000 – 50000 (M$_w$).

The best results in terms of selectivity was obtained with the catalytic system ZnEt$_2$/**L5** (2.90 g PCHC / g Zn and 100% selectivity) and the highest molecular weight of the polycyclohexene carbonate was up to 50000 (M$_w$) with ZnEt$_2$/**L11**.

In these experiments it was observed that the substituent in the carbon α to –OH group (*C1*) and the amine substituent group affects the productivity and the selectivity. The bulkiness of the substituent in the *C1* atom could block the propagation steps, whereas the steric effects generated in *C2* had less effect in the productivity and in the selectivity than in carbonate incorporation. On the other hand, the amine's substituent has a stronger effect in the selectivity; it needs to generate steric repulsion to avoid the backbiting mechanism.

6.4 Experimental Section

General Comments. Commercial available ligands **L9-L12** (Sigma-Aldrich and Alfa Aesar) were used as received. Cyclohexene oxide (Alfa Aesar) was dried over CaH$_2$, distilled, and stored under inert atmosphere. Toluene was dried over sodium and freshly distilled. Carbon dioxide (SCF Grade, 99.999 %, Air Products) was used introducing an oxygen/moisture trap (Agilent) in the line. **IR spectra** (range 4000-400 cm^{-1}) were recorded on a Midac Grams/386 spectrometer in KBr pellets. **NMR spectra** were recorded at 400 MHz Varian, with tetramethylsilane (^{1}H NMR and ^{13}C NMR). **Molecular weight measurements of polycarbonates:** The molecular weight (Mw) of copolymers and the molecular weight distributions (Mw/Mn) were determined by gel permeation chromatography versus polystyrene standards. Measurements were made in THF on a Millipore-Waters 510 HPLC Pump device using three-serial column system (MZ-Gel 100Å, MZ-Gel 1000 Å, MZ-Gel 10000 Å linear columns) with UV-Detector

Zinc catalytic systems with amino-alcohol ligands in polycarbonates synthesis

(ERC-7215) and IR- Detector (ERC-7515a). The software used to get the data was NTeqGPC 5.1. Samples were prepared as follow: 10 mg of the copolymer was solubilised with 2 mL of tetrahydrofuran (HPLC grade) and toluene (HPLC grade) as internal standard.

Standard copolymerization experiment in organic solvent. In a typical experiment, a flame dried Schlenk tube (80 mL) was charged with the amino-alcohol ligand (0.5 mmol) and toluene (17 mL) under argon. With stirring, a hexane solution of diethyl zinc (1 M, 0.5 mL, 0.5 mmol) was added at room temperature. After ethane gas evolution ceased, the solution was stirred at room temperature for 0.5 h. This solution was transferred into a 50 mL autoclave followed by the introduction of cyclohexene oxide (CHO, 1.0 mL, 10 mmol) and carbon dioxide (30 atm). After stirring at 60ºC for 24 h, the mixture was cooled down to room temperature by means of an ice bath. After the unreacted gases were released, the mixture was diluted with toluene (100 mL) and washed with aqueous solution of HCl (1 M, 30 mL x 2) and then with brine, saturated solution of NaCl (30 ml x 2). The organic layer was dried over $MgSO_4$, filtered and transferred into a flask where the solution was dried in vacuum until a solid appear. The solid was diluted with 5 mL dichloromethane and poured into 20 mL methanol and the copolymer precipitate. The solid was filtered and the methanol fraction was dried in vacuum until a solid appear. The solids were analyzed with ^{1}H,^{13}C NMR and IR. **Enantiomeric exces determination.** A round-bottomed flask was charged with copolymer (0.14 g, corresponds to 1.0 mmol of the repeating unit), THF (50 mL), MeOH (10 mL) and aqueous sodium hydroxide solution (2M, 10 mL). The resulting colourless homogeneous mixture was stirred under reflux for 15 h. After cooling, the mixture was neutralized with aqueous chloride acid solution (1M) and concentrated to *ca.* 30 mL by evaporation. The solution was extracted with AcOEt (80 mL x 4). The combined organic layer was dried over $MgSO_4$ and concentrated by evaporation. Purification of the crude residue by silica-gel column chromatography (AcOEt as an eluant) gave (*1R, 2R*)-cyclohexane-1,2-diol (98 % yield).[8] The enantiomeric excess was determined by GLC analysis with a chiral column (β-Chiraldex, 100ºC) after derivatisation of the (*1R, 2R*)-cyclohexane-1,2-diol into 2,2-dimethylhexahydro-1,3-benzodioxole by the reaction of the diol with acetone in presence of Montmorillonite K-10 (MK-10) stirred during 12 h.[20]

Safety warning. Experiments involving pressurized gases can be hazardous and must be conducted with suitable equipment and follwing appropriate safety conditions only.

***trans*-Cyclohexenecarbonate** ^{1}H NMR (400 MHz, CDCl$_3$, 298 K): δ 1.35-2.25 (m, 8H, CH$_2$), 3.96 (m, 2H, CH-carbonate). ^{13}C NMR (100.5 MHz, CDCl$_3$, 298 K): δ 18.6, 26.1, 75.3, 154.7 (C=O). IR v(C=O), CH$_2$Cl$_2$: 1881 cm^{-1} (w), 1820 cm^{-1} (m), 1803 cm-1 (s).[12]

Polycyclohexenecarbonate ^{1}H NMR (400 MHz, CDCl$_3$, 298 K): δ 1.33-2.10 (m, 8H, CH$_2$), 4.60 (m, 2H, CH-carbonate). ^{13}C NMR (100.5 MHz, CDCl$_3$, 298 K): δ 23.1, 29.7, 67.8, 154.2 (C=O, syndiotactic), 153.3-153.6 (C=O, isotactic and atactic). IR v(C=O), CH$_2$Cl$_2$: 1750 cm^{-1}.[12]

(*1R, 2R*)-cyclohexane-1,2-diol ^{1}H NMR (400 MHz, CDCl$_3$, 298 K): δ 1.22 (m, 4H, CH$_2$), 1.66 (m, 2H, CH$_2$), 1.93 (m, 2H, CH$_2$), 2.91 (br, 2H, OH), 3.32 (m, 4H, CH). ^{13}C NMR (100.5 MHz, CDCl$_3$, 298K) δ 24.5, 29.9, 33.0, 76.1.

6.5 *Supporting Information Available*

An example of ^{1}H NMR, ^{13}C NMR, IR, GPC and GC spectra of the copolymers and the mixture PCHC-CHC are available in the supporting information as an electronic file.

6.6 *References*

[1] Anastas, P.T. (Ed.) and Crabtree R.H. (Ed.) *Handbook of Green Chemistry-Green Catalysis Vol. 1: Homogeneous Catalysis*, WILEY-VCH, **2009**, Weinheim (Deutschland).

[2] *(a)* Allen, G. (Ed.) *Comprehensive Polymer Science,* Pergamon Press, Oxford (UK) **1989**; *(b)* Fried, J.R. *Polymer Science and Technology*, Prentice Hall, **1995**, Englewood Cliffs (USA).

[3] Anastas, P.T. and Williamson, T.C. *Green Chemistry: Designing Chemistry for Environment*, American Chemical Society, **1994**, Washington DC (USA).

[4] *(a)* Darensbourg, D. J. and Holtcamp, M.W. *Coord. Chem. Rev.*, **1996**, *153*, 155-174. *(b)* Coates, G. W.; Moore, D. R. *Angew. Chem. Int. Ed.* **2004**, *43*, 6618-6639. *(c)* Sugimoto, H. and Inoue, S. *J. Polym. Sci. Part A: Polym. Chem.* **2004**, *42*, 5561-5573. *(d)* Darensbourg, D.J.; Mackiewicz, R.M.; Phelps, A.L. and Billodeaux, D.R. *Acc. Chem. Res.*, **2004**, *37*, 836-844. *(e)* Zevenhoven, R.; Eloneva, S. and Teir, S. *Catal. Today* **2006**, *115*, 73-79. *(f)* Darensbourg, D.J. *Chem. Rev.* **2007,** 107, 2388-2410.

[5] *(a)* Nakano, K.; Kosaka, N.; Hiyama T. and Nozaki K. *Dalton Trans.* **2003**, 4039-4050. *(b)* Nozaki, K. *J. Polym. Sci., Part A: Polym. Chem.* **2004**, *42*, 215-221.

[6] Coates, G.W.; Moore, D.R. *Angew. Chem. Int. Ed.* **2004**, *43*, 6618-6639.

[7] Rokicki, G. *Prog. Polym. Sci.* **2000**, *25*, 259 – 342.

Zinc catalytic systems with amino-alcohol ligands in polycarbonates synthesis

[8] Nozaki, K; Nakano, K; Hiyama, T. *J. Am. Chem. Soc.* **1999**, *121*, 11008-11009.

[9] Nozaki, K; Nakano, K; Hiyama, T. *J. Am. Chem. Soc.* **2003**, *125*, 5501-5510.

[10] *(a)* Vidal-Ferran, A.; Moyano, A.; Pericàs, M.A.; Riera, A. *J. Org. Chem*. **1997**, *62*, 4970-4982. *(b)* Solà, Ll.; Reddy, K.S.; Vidal-Ferran, A.; Moyano, A.; Pericàs, M.A.; Riera, A.; Larena-Alvarez, A. and Pinilla, J-F. *J. Org. Chem*. **1997**, *62*, 4970-4982.

[11] García-Delgado,N.; Reddy, K.S.; Solà, L.; Riera, A.; Pericàs, M.A. and Verdaguer, X. *J. Org. Chem.,* **2005**, *70*, 7426-7428.

[12] Darensbourg, D.J.; Lewis, S.J.; Rodgers, J.L. and Yarbrough, J.C. *Inorg. Chem*. **2003**, *42*, 581-589.

[13] Hasebe, Y. and Tsuruta, T. *Makromol. Chem.* **1987**, *188*, 1403-1414.

[14] Nakano, K., Nozaki, K. and Hiyama, T. *Macromolecules*, **2001**, *34*, 6325-6332.

[15] Hsu, T.J.; Tan, C.S.M. *Polymer*, **2001**, *42*, 5143-5150.

[16] Moore, D.R.; Cheng, M.; Lobkovsky, E.B. and Coates, G.W. *J. Am. Chem. Soc.* **2003**, *125*, 11911-11924.

[17] Darensbourg, D.J. and Holtcamp, M.W. *Coord. Chem. Rev.*, **1996**, *153*, 155-174.

[18] Darensbourg, D.J. and Holtcamp, M.W. *Coord. Chem. Rev.*, **1996**, *153*, 155-174.

[19] Allen, S. D.; Moore, D. R.; Lobkovsky, E. B.; and Coates, G. W. *J. Am. Chem. Soc.* **2000**, *124*, 14284-14285.

[20] *(a)* Segarra, A.M.; Guerrero, R.; Claver, C.and Fernandez, E. *Chem. Commun.* **2001**, 1808-1809. *(b)* Segarra, A.M.; Guerrero, R.; Claver, C.and Fernandez, E. *Chem. Eur. J.* **2003**, *9*, 191-200. *(c)* Yañez, X.; Claver, C.; Castillón, S. and Fernandez, E. *Tetrahedron Lett.* **2003**, *44*, 1631–1634.

Chapter - 7

Zinc Schiff Base Complexes in Polycarbonate Synthesis by Copolymerization of Cyclohexene Oxide and Carbon Dioxide.

New zinc (II) Schiff base complexes were synthesized and characterized by NMR, IR, MALDI-TOF spectrometry and X-ray diffraction structure for a zinc (II) acetate derivative, which showed a polymeric structure. Preliminary catalytic studies of the copolymerisation of cyclohexene oxide and carbon dioxide had been done using the new complexes affording low activity (3.22 g PCHC/g Zn), 100% polycarbonate selectivity and moderate molecular weight (Mw up to 46000).
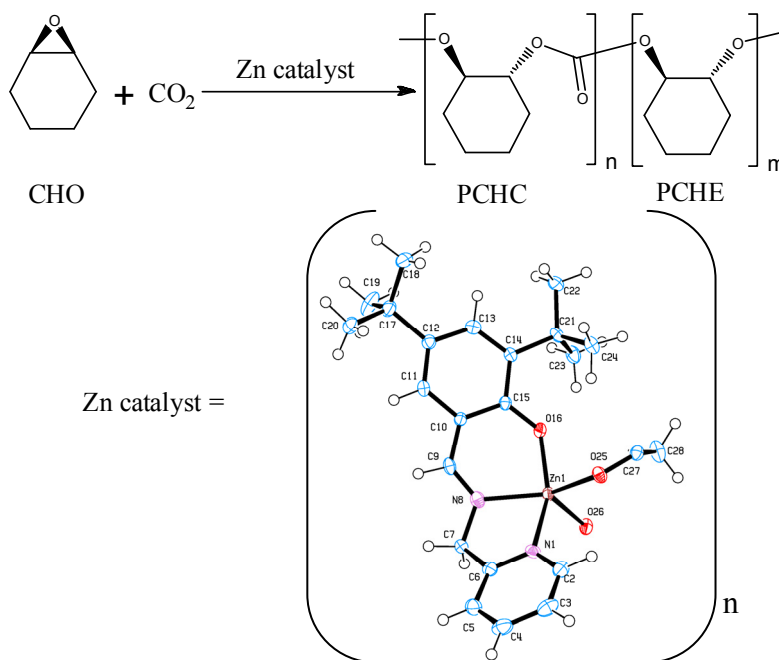
This work has been done in collaboration with Dr. Ali Aghmiz (Universitat Rovira i Virgili, Tarragona)

Zinc Schiff base complexes in polycarbonates synthesis.

7.1 Introduction

As discussed in Chapter 1 and Chapter 6, metal-catalyzed copolymerisation reactions of CO_2 and epoxides that give polycarbonates and/or cyclic carbonates have been extensively investigated as a potentially effective CO_2 fixation. In the copolymerization of CO_2 and epoxides are used mainly three model substrates, ethylene oxide, propylene oxide and cyclohexene oxide; among them the most widely studied is cyclohexene oxide (Scheme 7.1), which gives highest activities.[1,2] In 1969, this copolymerization was first reported by Inoue and Tsuruta who used a Zn catalyst.[3] Since then, there have been a number of reports on polycarbonate formation from CO_2 and epoxides with Zn-based catalysts in organic solvents,[4] where the polymerization times were relatively long, significant amounts of cyclic carbonate were produced, and some times alternating copolymer (100% carbonate) could be generated.[5]
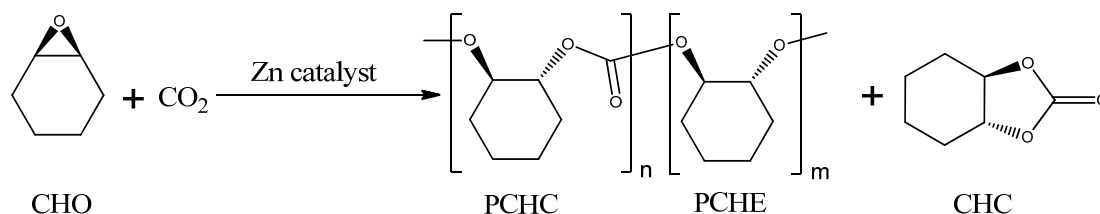
Scheme 7.1. Alternating copolymerization of *meso*-cyclohexene oxide (CHO) with carbon dioxide.

In the literature there are described zinc (II) complexes containing bis-salicylaldimine ligand (D_{1-5} and $E-G_{1-5}$, Figure 7.1) found to display catalytic activity for the alternating copolymerisation of CO_2 and CHO. There was a difference in catalytic activity depending on steric and electronic effects provided by the substituents on the Schiff base ligand.[6,7] The activities of these bis(salicylaldiminato)zinc complexes were investigated at 80°C and 55 bar and the efficacy of these catalysts precursors decreased in the order $G_1 > G_5 > G_2 > G_4 > G_3$, with turnover frequencies (TOFs) 15 > 7.3 > 5.0 > 1.2 > trace (g PCHC/g Zn·h), respectively and all have >99% carbonate linkage polymers. The good catalytic result of G_1 is attributed to the electron donating and no hindered phenolic ring, thereby facilitating the CO_2 insertion.

1 $R^1 = 3\text{-Me}; R^2 = 2,6\text{-}^i\text{Pr}$
2 $R^1 = 3,5\text{-}^t\text{Bu}; R^2 = 2,6\text{-}^i\text{Pr}$
3 $R^1 = 3,5\text{-Cl}; R^2 = 2,6\text{-}^i\text{Pr}$
4 $R^1 = 5\text{-OMe}; R^2 = 2,6\text{-}^i\text{Pr}$
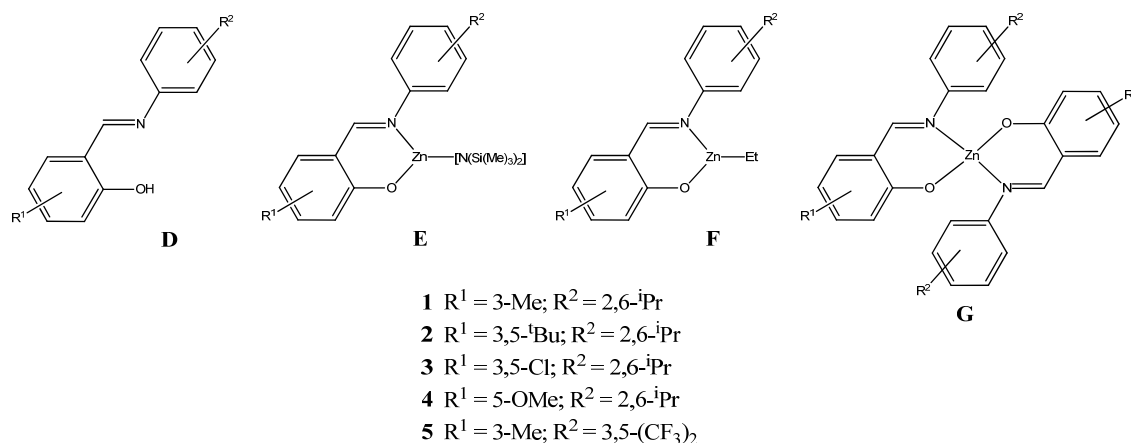**5** $R^1 = 3\text{-Me}; R^2 = 3,5\text{-(CF}_3)_2$

Figure 7.1. Bis-salicylaldimine ligands and zinc complexes.

On the other hand, the introduction of a pendant N, O or P arm attached to the imine nitrogen leads to a new class of ligands (**H**, Figure 7.2),[8,9] which has been successfully applied in aluminium (III) catalysed ethylene polymerization[10] and in calcium (II) and zinc (II) catalysed ring-opening polymerization of cyclic monomers.[11,12] Due to the fact that they are successfully applied in different substrate polymerisations, we thought that they could also lead to good catalysts in zinc (II) copolymerisation of epoxides and carbon dioxide. Moreover, tridentate ligands may offer different possibilities to stabilize the intermediate species. Therefore we decided to check their catalytic activity.

N,X,O-Schiff based ligands

L13 R = 2,6-ditertbutyl L = 3
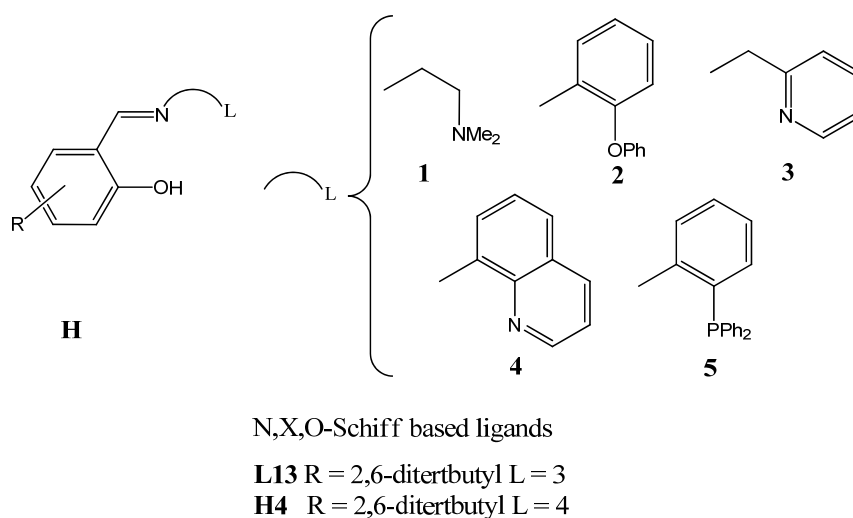**H4** R = 2,6-ditertbutyl L = 4

Figure 7.2. N,X,O-Schiff base ligands (X = O, N or P).

Based on the literature results we chose ligand **L13** (Figure 7.2) to synthesise a new variety of zinc complexes derived from this ligand and subsequent application in copolymerization of CO_2 and *meso*-cyclohexene oxide.

Zinc Schiff base complexes in polycarbonates synthesis.

7.2 Results and discussion

7.2.1 Zinc Schiff Base Complexes Synthesis

Ligand **L13** was synthesized following the procedure described by Finney and Mitchell starting with 3,5-di-*tert*-butyl salicylaldehyde and 2-methylaminopyridine (Scheme 7.2).[8] Treatment of **L13** with $Zn(OAc)_2$ under reflux during 4 hours formed **L13a** as a toasted cream powder (Scheme 7.2).
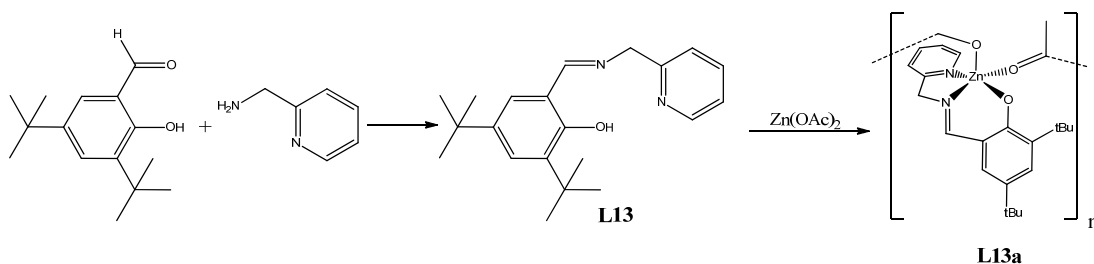
Scheme 7.2. Synthesis of zinc (II) complexes **L13a**.

In the MALDI-TOF mass spectra of **L13a** appeared a molecular ion peak at *m/z* = 898 corresponding to a dinuclear fragment $[Zn(\mathbf{L13})(OAc)]_2$ (M_2). The spectra also contained peaks due to molecular cations formed by los of $- CH_3$, $- CH(CH_3)_3$ and $-$ OAc form this dinuclear frangment. However, the most important observation is the confirmation of at least a dimeric zinc (II) acetate complex was formed.

The infrared spectral data of the zinc(II) complex **L13a** was recorded and compared with the literature data of Schiff-base ligand **L13**.[9] Ligand **L13** showed a medium intensity band at 1632 cm^{-1} and two weak intense band at 1591 cm^{-1} and 1571 cm^{-1} assigned to the azomethine ν(C=N) stretching vibration and ν(C=C) vibration.[9] On complexation the band at 1632 cm^{-1} had shifted to the lower region 1606 cm^{-1} in **L13a** indicating coordination of the azomethine nitrogen atom,[13] Furthermore, the ring skeletal vibration (C=C) of Schiff base ligand were also shifted to lower region 1530 and 1439 cm^{-1} upon coordination. [13,14] Also high intensity band of **L13** at 1252 cm^{-1} due to the phenolic ν(C-O) vibration appeared in the vicinity 1350 cm^{-1}. These observations emphasize that the –OH group of the ligand had reacted with zinc(II) *via* deprotonation.[13] The ν(Zn-N) and ν(Zn-O) stretching vibrations were observed at about 499 and 409 cm^{-1}, respectively. Moreover, information from the coordination type of the acetate could be obtained from IR spectra.[15] In complex **L13a** two strong bands were observed at 1557 and 1414 cm^{-1} assigned to ν_a(COO) and ν_s(COO), respectively.

The Δν value of 143 cm^{-1} is in agreement with a bridging coordination of the acetate ion, where one oxygen atom is coordinated to one metal centre and the second oxygen to a second zinc atom.

The ^{1}H NMR spectrum of compound **L13a** exhibited broad signals. The disappearance of the signal at δ 13.65 ppm from the OH group indicated the coordination to the zinc (II) precursor by phenol deprotonation. The upfield shifted signal of the methyl group from the acetate also indicates the coordination of this ligand. The signal characteristic of the imine CH=N group was observed as a broad signal at δ 8.40 ppm (upfield shifted Δδ = -0.16) and the signal corresponding to the backbone NCH$_2$ group appeared as a singlet signal at δ 4.88 ppm (Δδ = -0.06 ppm). The most surprising was that the signals corresponding to both *tert*-butyl groups collapse in one broad signal at δ 1.32 ppm. The ^{13}C NMR spectrum was assigned by ^{1}H-^{13}C HSQC and ^{1}H-^{13}C HMBC NMR experiments. The most down field signal appeared at δ 179.7 ppm attributed to CO group from the acetate, the following signals was δ 170.2 ppm corresponding to the imine CH carbon and at high field were the methyl carbon atoms from the acetate group at δ 23.3 ppm. The resonance signal attributable to NCH$_2$ group occurred at δ 58.5 ppm. The signals corresponding to the pyridyl carbons and salicylaldehyde aromatic carbon atoms were present in the expected range between δ 170.2 – 117.4 ppm.[9]

Single crystals of **L13a**, suitable for X-ray diffraction analysis, were obtained by recrystallization from chloroform/diethyl ether after one week at room temperature. X-ray diffraction analysis revealed that **L13a** has a polymeric structure (Figure 7.3). The geometry at zinc (Figure 7.3b) is best described as a distorted trigonal bipyramidal, with N(8), O(26) and O(25) occupying the equatorial sites, while N(1) and O(16) occupying the axial positions. Importantly, the relatively weak interaction of the N(8) pendant group with the zinc centre is apparent from the long Zn-N(1) bond [length of 2.230(3) Å] than that to the equatorial imino centre N(1) [2.072(3) Å]. Moreover, both Zn-N distances are similar than in bischelated zinc (II) complex with **H4** ligand (Figure 7.2), molecular formula [Zn(**H4**)$_2$] [2.238(3) Å and 2.104(3) Å, respectively].[16] Within the six-membered chelated ring the binding to zinc is unsymmetrical, with the bond to the oxygen atom being typical of an alkoxide [1.990(2) Å], whilst that to the imino nitrogen atom is, as expected, appreciably longer at 2.072(3) Å. All these distances are similar than in [Zn(**H4**)$_2$] complex.[16] The chelated C=N bond retains its double bond character

Zinc Schiff base complexes in polycarbonates synthesis.

[C(9)-N(8) 1.271(4) Å], there being no evidence of significant delocalization into any of the adjacent linkage. The C=N bond had similar length than in bis(salicylaldimine) ligands [average 1.281(5) Å].[7] The six-membered metallacycle has a half-boat conformation. The five-membered chelated ring has an envelope conformation, the NCH$_2$CN portion of the ligand adopting a *gauche* geometry. Similar structure was adopted by ligand **L13** in reported dimethylaluminium complex.[10]

(a)   **(b)**
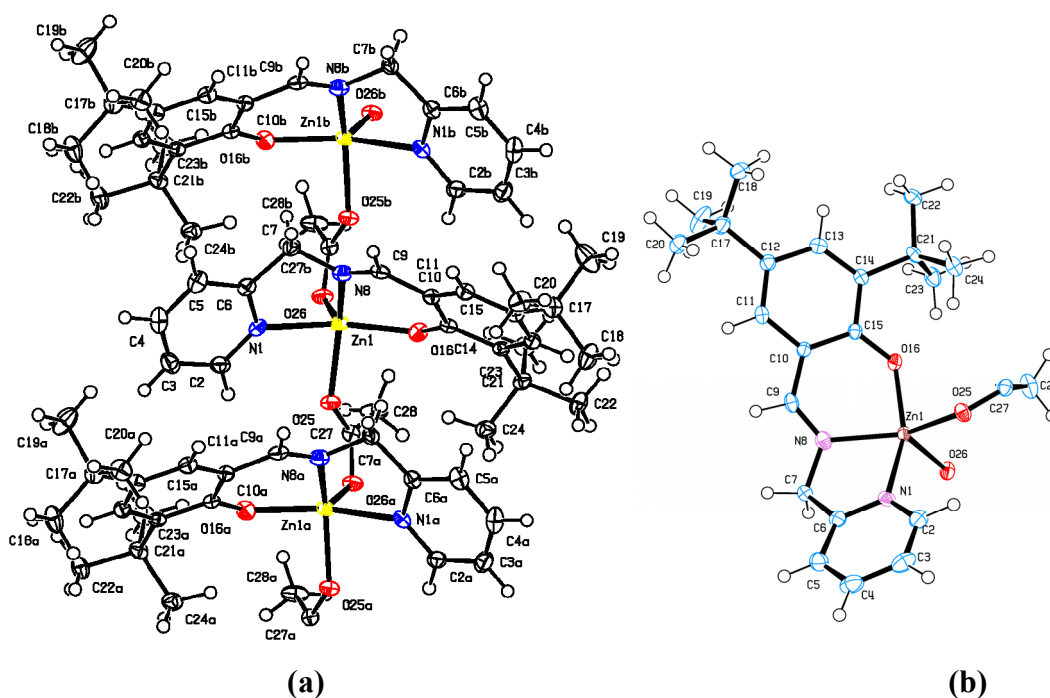
Figure 7.3. ORTEP drawing of complex **L13a**. **(a)** Polymeric structure. **(b)** Repetitive unit. Selected bond lengths [Å] and angles [°]: Zn1-O26: 1.988(2). Zn1-O16: 1.990(2). Zn1-O25: 2.032(2). Zn1-N8: 2.072(3). Zn1-N1: 2.230(3). N(8)-C(9): 1.271(4). O26-Zn1-O25: 98.46(10). O16-Zn1-O25: 91.17(10). O26-Zn1-N8: 121.83(10). O25-Zn1-N8: 137.60(9). O26-Zn1-N1: 101.06(10). O16-Zn1-N1: 149.27(10). O25-Zn1-N1: 85.57(10). N8-Zn1-N1: 74.97(11).

Treatment of **L13** with 5 equivalents of diethylzinc in dry hexane at room temperature caused the evolution of ethane affording a yellow solid **L13b** (Scheme 7.3). This compound was unstable in solution and was characterized by mass spectrometry and NMR spectroscopy under inert atmosphere.

In the MALDI-TOF mass spectra of **L13b** appeared the molecular ion peak at $m/z = 875$ ([M$^+$+K$^+$]) corresponding to a dimeric zinc (II) structure [Zn(Et)(**L13**)]$_2$.
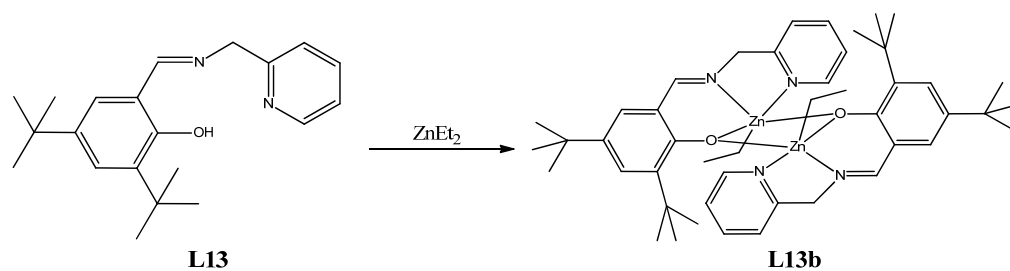
Scheme 7.3. Synthesis of zinc (II) complex **L13b**.

The ^{1}H NMR spectrum of compound **L13b** (C_6D_6, 298K and 400MHz, Figure 7.4), showed the signal attributed to the ethyl group bonded to the zinc (II) at high field as a triplet for $-CH_2-$ (δ 0.87 ppm, [3]J_{H-H} = 6.6 Hz) and a broad signal for $-CH_3$ group (δ 1.26 ppm), which are in the expected range.[17] The signal corresponding to the imine CH=N group was observed as a singlet at δ 7.81 ppm and the one attributed to the backbone $-NCH_2-$ group exhibited a singlet signal at δ 4.22 ppm. The signals corresponding to pyridil protons and salicyladehyde derived aromatic signals were present between 6.5 – 8.26.[9]

Figure 7.4. ^{1}H NMR spectrum of **L13b** in C_6D_6 (400MHz).

Zinc Schiff base complexes in polycarbonates synthesis.
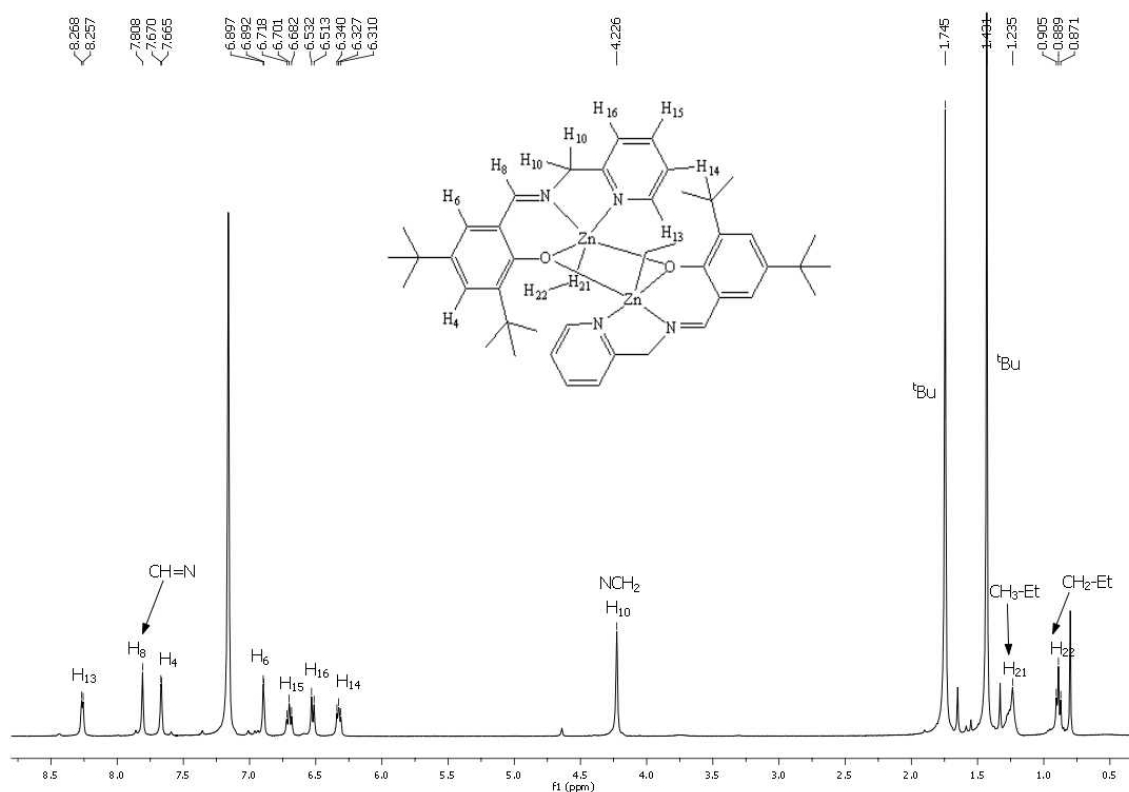
The signals of the ^{13}C NMR spectrum were assigned by ^{1}H-^{13}C HSQC and ^{1}H-^{13}C HMBC NMR experiments. The most down field signal appeared at δ 171.5 ppm corresponding for the imine CH carbon and at high field they were the signals of the methyl and methylene carbon atoms from the ethyl group at δ 14.4 and δ 23.1 ppm, respectively. The resonance signal attributable to -NCH$_2$- group occurred at δ 62.3 ppm. The pyridyl carbons and salicylaldehyde aromatic carbon atoms were present in the expected range between δ 171.2 – 118.1 ppm.[9]

To sum up, new zinc Schiff base complexes **L13a** [Zn(**L13**)(OAc)]$_n$ and **L13b** [Zn(Et)(**L13**)]$_2$ were obtained in moderate yields and were characterized by NMR, IR and MALDI-TOF spectrometry.

7.2.2 Catalysis results

The zinc (II) complexes **L13a** and **L13b** were tested as catalysts for alternating CO$_2$/cyclohexene oxide (CHO) copolymerisation in toluene at 60 ºC and 30 atm of CO$_2$. The reactions were carried out during 24h to ensure that the polymer was formed. The final products were extracted from the reaction solution, once the catalyst was hydrolysed, and the reaction products were further purified by reprecipitation from methylene chloride in methanol to obtain a methanol-insoluble (high molecular weight) products. The copolymers were analyzed by NMR and IR spectroscopy after the purification. A reference experiment using ZnEt$_2$ as catalyst showed no formation of copolymer demonstrating the important role of the ligand.

Only traces of co-polycarbonate polyether product were obtained using polymeric complex **L13a** as catalyst.

The use of precatalyst **L13b** provided 3.22 g PCHC/ g Zn with a molecular weigh of 46000 (M$_w$). The presence and percentage of cyclic cyclohexenecarbonate (CHC) was analyzed by ^{1}H NMR spectroscopy.[18] Catalytic system **L13b** presented 100% selectivity *versus* polycarbonate formation (δ 4.60 ppm) and no *trans*-CHC (δ 3.9 ppm) was observed.

The percentage of carbonate incorporated in the co-polycarbonate polyether polymer, *f*CO$_2$, was evaluated by the ^{1}H NMR spectrum.[19] In the ^{1}H NMR spectrum (see SI) of the copolymer obtained with precatalyst **L13b**, it was found PCHC as the only product (δ 4.60 ppm), however it presented 30% of polyether linkage (δ 3.60 ppm),

as well some signals related with the free **L13** or as end group of the copolymer could also be observed.

From the results obtained in the copolymerisation of CHO with CO_2 we observed moderate activity for catalytic systems **L13b** with 100% selectivity for polycarbonate formation. The different catalytic activity between **L13a** and **L13b** may be due to the polymeric nature of **L13b**, which avoided the formation of dimeric active species.[4,20]

7.3 Conclusions

New zinc (II) Schiff base complexes were synthesized and characterized. Single crystals of **L13a** were obtained suitable for X-ray diffraction characterization showing a polymeric structure.

Preliminary catalytic results were obtained with precatalyst **L13a** and **L13b**. Precatalyst systems **L13b** was moderate active in CO_2/CHO copolymerisation affording 3.22 g PCHC/g Zn, while with complex **L13a** only traces of PCHC were obtained. Complex **L13b** showed 100% selectivity for PCHC with 70% carbonate linkage and moderate molecular weight co-polycarbonate polyether (M_w up to 46000).

These preliminary results show that these systems have potential as catalyst for this reaction. In the future, the solubility of these systems in compressed carbon dioxide could be studied and later on tested under solvent free conditions, using CO_2 both as reagent and solvent, as was already reported by several groups leading to significant improvement in the activity of polycarbonates synthesis.[21-24] Moreover, due to the easily synthesis of Schiff base ligands, which allow the variation in steric and electronic properties,[8,25] new zinc (II) complexes with electrondonating and no steric demanding groups may be prepared and tested in CHO/CO_2 copolymerisation.

7.4 Experimental Section

General Comments. Ligands **L13** were prepared following described procedures.[8] $Zn(OAc)_2$ (Merk) was dried under 30ºC and under vacuum overnight before be used and $ZnEt_2$ (1M in hexane, Sigma-Aldrich) was used in the glove-box without further purification. Cyclohexene oxide (Alfa Aesar) was dried over CaH_2, distilled, and stored under inert atmosphere. Toluene and pentane were dried over sodium and freshly distilled. Carbon dioxide (SCF Grade, 99.999 %, Air Products) was

Zinc Schiff base complexes in polycarbonates synthesis.

purified with an oxygen/moisture trap (Agilent). **IR spectra** (range 4000-400 cm^{-1}) were recorded on a Midac Grams/386 spectrometer in CH_2Cl_2 or KBr pellets, when indicated. **IR spectra in ATR mode** (range 4000-600 cm^{-1}) were recorded on a JASCO FTIR 680 plus as solid, spectra analysis software used was spectra manager for Win 95/NT v1.53.04 Build 1 JASCO Corporation. **NMR spectra** were recorded at 400 MHz Varian, with tetramethylsilane (^{1}H NMR and ^{13}C NMR) as the internal standards. **MALDI-TOF measurements of complexes:** Voyager-DE-STR (Applied Biosystems, Franingham, MA) instrument equipped with a 337 nm nitrogen laser. All spectra were acquired in the positive ion reflector mode. α-cyano-4-hydroxycinnamic acid (CHCA) was used as matrix. The matrix was dissolved in THF at a concentration of 10 mg·mL^{-1} + 1mg/mL KTFA or AgTFA. The complex was dissolved in THF or $CHCl_3$ (50 mg·L^{-1}), depends on the solubility. The matrix and the samples were premixed in the ratio 1:1 (Matrix : sample) and then the mixture was deposited (1 μL) on the target. For each spectrum 100 laser shots were accumulated. **Molecular weight measurements of polycarbonates:** The molecular weights (Mw) of copolymers and the molecular weight distributions (Mw/Mn) were determined by gel permeation chromatography versus polystyrene standards. Measurements were made in THF on a Millipore-Waters 510 HPLC Pump device using three-serial column system (MZ-Gel 100Å, MZ-Gel 1000 Å, MZ-Gel 10000 Å linear columns) with UV-Detector (ERC-7215) and IR- Detector (ERC-7515a). The software used to get the data was NTeqGPC 5.1. Samples were prepared as follow: 5 mg of the copolymer was solubilised with 1,5 mL of tetrahydrofurane (HPLC grade) and 7,5 μL of toluene (HPLC-grade) as internal standard.

Standard copolymerization experiment in organic solvent. In a typical experiment, the catalyst precursor **L13a**, **L13b** (0.5 mmol) was introduced into a 50 mL autoclave. Cyclohexene oxide (CHO, 1.0 mL, 10 mmol) was introduced and followed by carbon dioxide (30 atm). After stirring at 60ºC for 24 h, the mixture was cooled down to room temperature by means of an ice bath. After the unreacted gases were released, the mixture was diluted with toluene (100 mL) and washed with aqueous solution of HCl (1 M, 30 mL x 2) and then with brine, saturated solution of NaCl (30 mL x 2). The organic layer was dried over $MgSO_4$, filtered and transferred into a flask where the solution was dried in vacuum until a solid appear. The solid was redisolved in MeOH and filtered. The precipitation was analyzed with ^{1}H NMR and IR spectroscopy.

Safety warning. Experiments involving pressurized gases can be hazardous and must be conducted with suitable equipment and following appropriate safety conditions only.

Polycyclohexenecarbonate ^{1}H NMR (400 MHz, CDCl$_3$, 298 K): δ 1.33-2.10 (m, 8H, CH$_2$), 4.60 (m, 2H, CH-carbonate). ^{13}C NMR (CDCl$_3$): δ 23.1, 29.7, 67.8, 154.0 (C=O, syndiotactic), 153.3-153.5 (C=O, isotactic and atactic). IR v(C=O), CH$_2$Cl$_2$: 1750 cm^{-1}.[18]
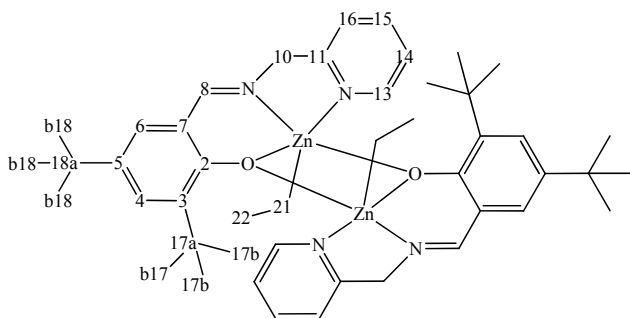
7.4.1 Complexes synthesis

[Zn(OAc)(L13)]$_n$ (L13a).
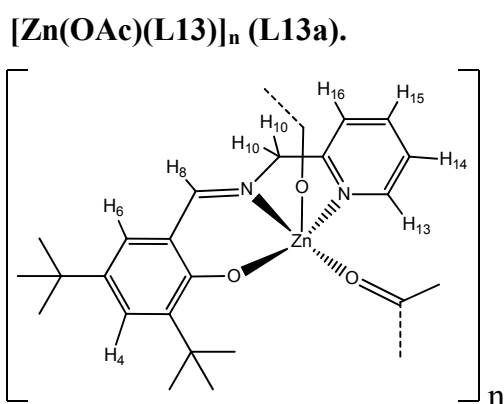
To a solution of **L13** (109 mg, 0.335 mmol) in dry methanol (10 mL) was added a solution of Zn(OAc)$_2$ (61 mg, 0.335 mmol) in methanol (10 mL). The mixture was refluxed for 4 h and then cooled to room temperature. The solid precipitated from the reaction mixture and was filtered and washed with methanol, diethyl ether and dried in vacuum. Toasted cream solid, 82 mg, (Yield 55 %).

MALDI-TOF calc for (C$_{23}$H$_{30}$N$_2$O$_3$Zn)$_n$ *m/z*: n=2 897.3135 [M$_2$$^+$+H$^+$], n=2 877.2856 [M$_2$$^+$-CH$_3$]; found *m/z*: n=2 897.5544 [M$_2$$^+$+H$^+$], n=2 877.5402 [M$_2$$^+$-CH$_3$]. IR (KBr) 1642 cm^{-1} v(C=N), 1347 cm^{-1} v(C-O), 499 cm^{-1} v(Zn-N), 409 cm^{-1} v(Zn-O).

^{1}H NMR (400 MHz, CD$_2$Cl$_2$): δ 1.29 (br, 18H, *tert*-butyl), 1.87 (br, 3H, CH$_3$-OAc), 4.90 (br, 2H, (CH$_2$N)[10]), 6.92 (br, 1H, (CH)[6]), 7.23 (br, 1H, (CH)[14]) 7.33-7.35 (br, 2H, (CH)[4,16]), 7.81 (br, 1H, (CH)[15]), 8.41 (br, 1H, (CH=N)[8]), 8.80 (br, 1H, (CH)[13]). ^{13}C NMR (75.43 MHz, CD$_2$Cl$_2$): δ 23.3 (CH$_3$-OAc), 29.2 (C[17b]), 31.2 (C[18b]), 33.6 (C[17a]), 35.2 (C[18a]), 58.5 (C[10]), 117.4 (C[2]), 121.9 (C[6,4]), 123.3 (C[14,16]), 128.6 (C[5]), 138.6 (C[15]), 140.9 (C[3]), 149.0 (C[13]), 156.1 (C[11]), 170.2 (C[7,8]), 179.7 (CO-OAc).

Zinc Schiff base complexes in polycarbonates synthesis.

[ZnEt(L13)]$_2$ (L13b).

A solution of ZnEt$_2$ (1.0 mL, 1.0 mmol, 1M in hexane) was added to a stirred solution of **L13** (66 mg, 0.2 mmol) in dry hexane (3 mL). The solution was stirred at room temperature 2 hours. The desired product precipitates from the reaction mixture and was collected by filtration, washed with cold diethyl ether and dried in vacuum. Yellow solid, 127 mg, (Yield 75 %).

MALDI-TOF calc for (C$_{46}$H$_{64}$N$_4$O$_2$Zn$_2$) *m/z*: 875.3209 [M$^+$+K$^+$], 777.3059 [M$^+$-2Et]; found *m/z*: 875.3743 [M$^+$+K$^+$], 777.4563 [M$^+$-2Et].

^{1}H NMR (400MHz, CDCl$_3$): δ 0.89 (t, 6H, CH$_3$-Et, ^3J = 6.6 Hz), 1.23 (br, 4H, CH$_2$-Et), 1.43 (s, 18H, (*tert*-butyl)^{18}), 1.74 (s, 18H, (*tert*-butyl)^{17}), 4.23 (s, 4H, (CH$_2$N)^{10}), 6.33 (pst, 2H, (CH)^{15}), 6.52 (d, 2H, (CH)^{16}, ^3J = 7.2 Hz), 6.70 (pst, 2H, (CH)^{14}), 6.89 (d, 2H, (CH)^6, ^4J = 2.4 Hz), 7.67 (d, 2H, (CH)^4, ^4J = 2.4 Hz), 7.81 (s, 2H, (CH=N)^8), 8.26 (d, 2H, (CH)^{13}, ^3J = 4.4 Hz); ^{13}C NMR (75.43 MHz, CDCl$_3$): δ 14.4 (C^{22}), 23.1 (C^{21}), 30.1 (C^{17b}), 31.9 (C^{18b}), 34.0 (C^{18a}), 36.0 (C^{17a}), 62.3 (C^{10}), 118.1 (C^2), 121.7 (C^{16}), 122.1 (C^{14}), 128.9 (C^4), 129.4 (C^6), 133.1 (C^5), 136.7 (C^{15}), 141.9 (C^3), 148.5 (C^{13}), 156.9 (C^{11}), 171.2 (C^7), 171.4 (C^8).

7.4.2 X-ray crystallography

Diffraction data for the structures reported were carried out on a Smart CCD 1000 Bruker diffractometer system with Mo Kα radiation (λ = 0.71073 Å). Cell refinement, indexing and scaling of the data sets were carried out using programs Bruker Smart and Bruker Saint. All the structures were solved by *SIR97* [26] and refined by *SHELXL97* [27] and the molecular graphics with ORTEP-3 *for Windows*.[28] All the calculations were performed using the *WinGX* publication routines.[29]

Compound L13a: [$C_{23}H_{30}N_2O_3Zn$], F_w = 447.88, colourless prism, 0.6 x 0.11 x 0.22 mm^3, monoclinic P2$_1$/c, a = 8.895 (2) Å, b = 29.114 (7) Å, c = 9.417 (2) Å, β = 115.012 (4)º, V = 2210.0 (9) Å^3, Z = 4, D_x = 1.346 Mg·m^{-3}, μ = 1.14 mm^{-1}. 21900 Reflections were measured up to a resolution of (sin θ/λ)$_{max}$ = 0.63 Å^{-1} of which 4515 were unique reflections (R_{int} = 0.090), and 3044 were observed [I>2σ(I)]. 269 Parameters were refined with no restraints. R1/wR2 [I > 2σ(I)]: 0.041/ 0.094. S = 1.01. Residual electron density between -0.50 and 0.41 e/Å^3.

7.5 *Supporting Information Available*

NMR spectra, FTIR and MALDI-TOF mass spectra of zinc (II) complex, the NMR, IR and GPC spectra of the catalytic products and the pdf file containing CIF files giving crystallographic data for **L13a**, are available in the supporting information as an electronic file.

7.6 *References*

[1] Anastas, P.T. and Williamson, T.C. *Green Chemistry: Designing Chemistry for Environment*, **1994**, American Chemical Society, Washington DC (USA).

[2] Jessop, P. G.; Noyori, I. and Noyori, R. *Chem. Rev.* **1995**, *95*, 259-272.

[3] Inoue, S.; Koinuma, H. and Tsuruta, T. *J. Polym. Sci., Polym. Lett. B.* **1969**, *7*, 287-292.

[4] Coates, G. W.; Moore, D. R. *Angew. Chem. Int. Ed.* **2004**, *43*, 6618-6639.

[5] Beckman, E.J. *J. of Supercritical Fluids*, **2004**, *28*, 121-191.

[6] Younkin, T.R.; Connor, E.F.; Henderson, J.I.; Friedrich, S.K.; Grubbs, R.H. and Bansleben D.A. *Science* **2000**, *287*, 460-462.

[7] Darensbourg, D.; Rainey, P. and Yarbrough, J. *Inorg. Chem.* **2001**, *40*, 986-993.

[8] Mitchell, J.M. and Finney, N. S. *J. Am. Chem. Soc.* **2001,** *123,* 862-869.

[9] Cameron, P.A.; Gibson, V.C.; Redshaw, C.; Segal, J.A.; White, A.J.P. and Williams, D.J. *J. Chem. Soc., Dalton Trans.* **2002**, 415-422.

[10] Cameron, P.A.; Gibson, V.C.; Redshaw, C.; Segal, J.A.; Bruce, M.D.; White, A.J.P. and Williams, D.J. *Chem. Commun.* **1999**, 1883-1884.

[11] Darensbourg, D.J.; Choi, W. and Richers C.P. *Macromolecules*, **2007**, *40*, 3521-3523.

[12] Darensbourg, D.J.; Choi, W.; Karroonnirun, O. and Bhuvanesh, N. *Macromolecules* **2008**, *41*, 3493-3502.

Zinc Schiff base complexes in polycarbonates synthesis.

[13] Annigeri, S.M.; Sathisha, M.P. and Revankar, V.K. *Trans. Metal Chem.*, **2007**, *32*, 81-87.

[14] Asadi, M.; Mohammadikish, M.; Mohammadi, K.; Mousavi, P.; Javidnia, K. and Miri, R. *Inorg. Chim. Acta* **2009**, *362*, 4906-4912.

[15] Szécsényi, K.M.; Leovac, V.M.; Jácimović, Ž.K.; Češljević, V.I., Kov-acs, A.M.; Pokol, G. and Gál, S. *J. Termal Analysis and Calorimetry*, **2001**, *63*, 723-732.

[16] Orio, M.; Philouze, C.; Jarjayes, O.; Neese, F. and Thomas, F. *Inorg. Chem.* **2010**, *49*, 646-658.

[17] Nozaki, K; Nakano, K; Hiyama, T. *J. Am. Chem. Soc.* **1999**, *121*, 11008-11009.

[18] Darensbourg, D.J.; Lewis, S.J.; Rodgers, J.L. and Yarbrough, J.C. *Inorg. Chem.* **2003**, *42*, 581-589.

[19] Hsu, T.J.; Tan, C.S.M. *Polymer*, **2001**, *42*, 5143-5150.

[20] Moore, D. R.; Cheng, M.; Lobkovsky, E. B.; Coates, G. W. *J. Am. Chem. Soc.* **2003**, *125*, 11911-11924.

[21] DeSimone, J.M. and Tumes, W. *Green Chemistry using liquid and supercritical carbon dioxide,* **2003**, Oxford University Press, Inc.; New York.

[22] Darensbourg, D. J.; Holtcamp, M. W.; Struck, G. E.; Zimmer, M. S.; Niezgoda, S. A.; Rainey, P.; Robertson, J. B.; Draper, J. D.; Reibenspies, J. H. *J. Am. Chem. Soc.* **1999**, *121,* 107-116.

[23] Darensbourg, D. J.; Holtcamp, M. W. *Macromolecules,* **1995**, *28,* 7577-7579.

[24] Super, M., Berluche, E., Costello, C. and Beckman, E. *Macromolecules* **1997**, *30*, 368-372.

[25] Asadi, M.; Hemmateenejad, B. and Mohammadikish, M. *J. Coord. Chem.* **2010**, *63*, 124-135.

[26] Altomare, A.; Burla, M.C.; Camalli, M.; Cascarano, G.L.; Giacovazzo, C.; Guagliardi, A.; Moliterni, A.G.G.; Polidori, G. and Spagna, R. *J. Appl. Cryst.* **1999**, *32*, 115-119.

[27] Sheldrick, G. M. **1997**. SHELXS97 and SHELXL97. University of Göttingen, Germany.

[28] Ortep-3 for Windows - A Version of ORTEP-III with a Graphical User Interface (GUI). L. J. Farrugia, *J. Appl. Crystallogr.* **1997**, *30*, 565-566.

[29] WinGX Suite for Single Crystal Small Molecule Crystallography. L. J. Farrugia, *J. Appl. Cryst.* **1999**, *32*, 837-838.

Chapter - 8

Conclusions

Conclusions (English)

8.1 Conclusions

In this chapter are summarized the conclusions extracted from each part.

Part 1. *CO_2 as solvent in CO/ST and TBS copolymerisation reaction.*

➢ We have synthesised a new family of perfluorinated bipyridine ligands (**L1-L3**) soluble in compressed carbon dioxide.

➢ The dicationic palladium (II) complexes [Pd(**L2-L3**)$_2$][BArF]$_2$ (modified with ester groups) showed a dynamic behaviour attributed by DFT calculations to the different disposition of the carbonyl group.

➢ The FTIR spectroscopy studies of the [Rh(CO)$_2$(**L1-L3**)][PF$_6$] complexes allowed to conclude that there were only slightly differences between both families (with and without ester groups) and similar electronic properties were exhibited between fluorinated and non perfluorinated ligands.

➢ The cationic palladium (II) complexes [Pd(CH$_3$)(NCCH$_3$)(**L1-L3**)][X] (X = PF$_6^-$, OTs$^-$ or BArF$^-$) showed in ^{1}H NMR anion dependence, which was attributed by PGSE and NOESY or HOESY to interionic interaction for complexes with PF$_6^-$ and OTs$^-$. In solution, PF$_6^-$ and OTs$^-$ appeared to be localized close to the bipyridine ring *trans* to palladium methyl and acetonitrile, while BArF did not show any significant interionic contact.

➢ The dicationic Pd (II) complexes [Pd(**L1-L3**)$_2$][BArF]$_2$ were active in CO/styrene (ST) and CO/4-*tert*-butylstyrene (TBS) copolymerisation. The catalytic results obtained had comparable productivities in CO/ST (2.3 kg CP/g Pd) and CO/TBS (6.1 kg CP/g Pd obtained with [Pd(**L3**)$_2$][BArF]$_2$) copolymerisation in liquid expanded carbon dioxide than the best literature results in 2,2,2-trifluoroethanol (TFE), but with better molecular weight (M$_w$ = 693000 in ST and 222000 in TBS) and high stereoregularity (% uu > 90 % in ST and 73-97 % in TBS).

➢ The catalytic activity of the cationic complexes [Pd(CH$_3$)(NCCH$_3$)(**L1-L3**)][X] (X = PF$_6^-$, OTs$^-$ or BArF$^-$) in the CO/ST and TBS copolymerisation in TFE and compressed CO_2 exhibited good productivities. In TFE, the best catalytic results in CO/ST copolymerisation required the use of BQ (4.65 kg CP/g Pd, M$_w$ up to 580000

using [Pd(CH$_3$)(NCCH$_3$)(**L2**)][PF$_6$]), while in compressed CO$_2$ were not required (1.09 kg CP/g Pd using [Pd(CH$_3$)(NCCH$_3$)(**L3**)][BArF]) providing a long living system (M$_w$ up to 914000).

➢ The catalytic conditions optimisation in compressed CO$_2$ using [Pd(CH$_3$)(NCCH$_3$)(**L1-L3**)][X] revealed CO$_2$ phase as the most important parameter showing the best results in liquid expanded CO$_2$ (65 atm total pressure and 38ºC) in combination with the increase of TBS ([TBS]/[Pd] = 3100) and CO (10 atm).

➢ The counterion dependence in CO/ST and CO/TBS showed different behaviour depending on the medium. In TFE the productivity was the following: PF$_6^-$ > OTs$^-$ ≈ BArF$^-$, while in compressed CO$_2$ the best results were obtained with BArF$^-$.

➢ The initiation and termination steps study by MALDI-TOF spectrometry showed that there was only one initiation step in both substrates; through substrate insertion in Pd-H bond, and the termination steps depended on the substrate, the medium and the catalyst used.

➢ The most important conclusion drawn is the potential of compressed CO$_2$ as green medium for copolymerisation reaction.

➢ The scale up (to 6.2 g) and optimisation of the synthesis of **L4** was achieved.

➢ The coordination chemistry towards Pd(II), Pt(II) and Rh(I) led to the syntheses of complexes [PdCl$_2$**L4**], [PtCl$_2$**L4**] and [Rh(cod)(**L4**)]BF$_4$, which were characterised by X-ray diffraction.

➢ MCl$_2$ (M= Pd or Pt) reacted with **L4** and alcohols (HOR) or amines (HNR$_2$R$_1$) at the P=C double bond at elevated temperature regio- and stereo-selective (*syn*-addition), leading to [MCl$_2$(**L4**H·OR)] or [MCl$_2$(**L4**H·NR$_2$R$_1$)]. When chiral alcohols or amines were used, three stereogenic centres at once could be introduced and only one pair of diastereoisomers was formed. Complexes [PdCl$_2$(**L4**H·OEt)] and [PtCl$_2$(**L4**H·OEt)] showed reactivity with DPPE to form quantitatively [Pd(DPPE)$_2$]Cl$_2$ and free ligand **L4**.

➢ The catalytic studies in the CO/α-olefins copolymerisation with *in situ* Pd(II) precatalyst showed only moderate catalytic activity in CO/ethylene copolymerisation and inactive in CO/ST copolymerisation.

Conclusions (English)

Part 2. *CO_2 as C1 building block in polycarbonate synthesis.*

➢ Catalytic systems for the copolymerisation of CO_2/epoxides to form polycarbonates, formed by $ZnEt_2$ and amino alcohols provided low activities(up to 2.90 g PCHC/ g Zn), high selectivity (80-100 % polycarbonate *vs.* cyclic carbonate), high carbonate incorporation (80-100 %) and the molecular weight up to 50000 (M_w).

➢ We observed important effects of the substituents of the amino-alcohol ligands in the carbon α to –OH (*C1*), to NR_2 (*C2*) and the amine's substituent in the productivity and selectivity. The bulkiness of the substituent in the *C1* atom could block the propagation steps, whereas the steric effects generated in *C2* had less effect in the productivity and in the selectivity than in carbonate incorporation. On the other hand, the amine's substituent has a stronger effect in the selectivity; it needs to generate steric repulsion to avoid the backbiting mechanism. The low enantiomeric excess (up to 7 %) could be attributed to a weak interaction of the ligand with the metal centre, which may lead to ligand dissociation allowing the insertion of the cyclohexene oxide in two different ways.

➢ New zinc (II) Schiff base complexes were obtained in moderate yield leading to polymeric structure in [Zn(**L13**)(OAc)]$_n$ and dimeric structure in [Zn(Et)(**L13**)]$_2$.

➢ Precatalyst systems [Zn(Et)(**L13**)]$_2$ was moderate active in copolymerisation of CO_2/CHO affording 3.22 g PCHC/g Zn, 100% selectivity for PCHC with 70% carbonate linkage and moderate molecular weight (M_w up to 46000), while the zinc (II) acetate derivative only traces of PCHC was observed. The difference may be due to the polymeric nature of [Zn(**L13**)(OAc)]$_n$, which could avoid the formation of dimmeric active species.

➢ These preliminary results show that zinc (II) Schiff base systems have potential as catalyst for this reaction.

8.2 Conclusions

En aquest capítol es troben resumides les conclusions extretes de cada part.

Part 1. *Ús del diòxid de carboni com a dissolvent en la copolimerització de CO amb estirè i tert-butilestirè.*

➢ Es va sintetitzar una nova família de lligands bipiridina perfluorats (**L1-L3**) solubles en diòxid de carboni comprimit.

➢ Els complexes dicationic de pal·ladi (II) [Pd(**L2-L3**)$_2$][BArF]$_2$ (modificats amb grups ester) van mostrar un comportament dinàmic atribuït a la posició relativa adoptada pels grups carbonil mitjançant càlculs DFT.

➢ L'estudi realitzat als complexos [Rh(CO)$_2$(**L1-L3**)][PF$_6$] amb espectroscòpia FTIR va permetre concloure que només existien petites diferencies entre les dues famílies de lligands (amb i sense el grup ester) i que les propietats electròniques entre els lligands fluorats i els no fluorats eren molt similars.

➢ La caracterització dels complexos catiònics de pal·ladi (II) [Pd(CH$_3$)(NCCH$_3$)(**L1-L3**)][X] (X = PF$_6^-$, OTs$^-$ o BArF$^-$) per RMN de ^{1}H va mostrar dependència aniònica, la qual va esser atribuïda per PGSE i NOESY o HOESY a una interacció interiònica en els complexos amb PF$_6^-$ i OTs$^-$. En solució, PF$_6^-$ i OTs$^-$ van localitzar-se en les immediacions de l'anell de bipiridina *trans* al pal·ladi metil i pròxim al lligand acetonitril, mentre que l'anió BArF$^-$ no va mostrar cap contacte interiònic significatiu.

➢ Els complexos dicatiònics de Pd (II) [Pd(**L1-L3**)$_2$][BArF]$_2$ són actius en la copolimerització de CO/estirè (ST) i CO/4-*tert*-butilestyrè (TBS). Le*s pro*ductivitats obtingudes en la copolimerització de CO/ST (2.3 kg CO/g Pd obtingut amb [Pd(**L3**)$_2$][BArF]$_2$) i de CO/TBS (6.1 kg CP/g Pd obtingut amb [Pd(**L3**)$_2$][BArF]$_2$) en diòxid de carboni comprimit van ser comparables als millors resultats reportats en la bibliografia amb 2,2,2-trifluoretanol (TFE), però amb millors pesos moleculars (M$_w$ = 693000 en ST i 222000 en TBS) i elevada estereoregularitat (% uu > 90 % en ST i 73-97 % en TBS).

➢ L'activitat catalítica dels complexos catiònics de [Pd(CH$_3$)(NCCH$_3$)(**L1-L3**)][X] (X = PF$_6^-$, OTs$^-$ o BArF$^-$) en la copolimerització de CO/ST i CO/TBS en TFE i CO$_2$ comprimit van mostrar bones productivitats. En TFE, els millors resultats catalítics en la copolimerització de CO/ST va requerir l'ús de BQ (4.65 kg CP/g Pd, M$_w$ fins a 580000 fent servir el complex [Pd(CH$_3$)(NCCH$_3$)(**L2**)][PF$_6$]), en tant que en CO$_2$ comprimit no va ser necessàri l'ús de la BQ (1.09 kg CP/g Pd amb [Pd(CH$_3$)(NCCH$_3$)(**L3**)][BArF]) donant lloc a un sistema altament viu (M$_w$ fins a 914000).

➢ L'optimització de les condicions de reacció amb [Pd(CH$_3$)(NCCH$_3$)(**L1-L3**)][X] en CO$_2$ comprimit revela com el paràmetre més important en la productivitat la fase del CO$_2$, produint els millors resultats en CO$_2$ líquid (P$_T$ = 65 atm i 38ºC) en combinació amb l'augment de la concentració de TBS ([TBS]/[Pd] = 3100) i pressió de CO (10 atm).

➢ L'estudi de l'efecte del contraió en la productivitat en la reacció de copolimerització de CO/ST i CO/TBS mostra diferent comportament segons el medi de reacció. Per una banda en TFE la productivitat varia en funció de l'anió segons: PF$_6^-$ > OTs$^-$ ≈ BArF$^-$, per altra banda en CO$_2$ comprimit els millors resultats s'obtenen amb el BArF$^-$.

➢ L'estudi del mecanisme d'iniciació i terminació mitjançant l'espectrometria MALDI-TOF va revelar que la reacció s'inicia mitjançant la inserció del substrat en l'enllaç Pd-H, i el mecanisme de terminació depèn del substrat, el medi i el catalitzador usat.

➢ Les conclusions més importants que es poden extreure d'aquest estudi és el potencial del CO$_2$ comprimit com a medi sostenible per a la reacció de copolimerització.

➢ Es va dur a terme l'optimització i la síntesi a gran escala (fins a 6.2 g) del lligand fosfinina **L4**.

➢ La química de coordinació amb Pd(II), Pt(II) i Rh(I) va donar lloc a la síntesi dels complexos [PdCl$_2$**L4**], [PtCl$_2$**L4**] and [Rh(cod)(**L4**)]BF$_4$, dels quals es van caracteritzar mitjançant difracció de raig-X.

➢ La reacció de MCl$_2$ (M= Pd o Pt) amb **L4** i alcohols (HOR) o amines (HNR$_2$R$_1$) mitjançant el doble enllaç P=C a elevada temperatura de manera regio- i estereo-selectiva (adició-*syn*) va donar lloc als complexos [MCl$_2$(**L4**H·OR)] o

[MCl$_2$(**L4**H·NR$_2$R$_1$)]. Quan els alcohols o les amines usades van ser quirals es van formar tres centres esterogènics i només un parell iònic va ser observat. Aquests complexos [PdCl$_2$(**L4**H·OEt)] i [PtCl$_2$(**L4**H·OEt)] van reaccionar amb DPPE per formar de manera quantitativa [Pd(DPPE)$_2$]Cl$_2$ i lligand lliure **L4**.

➢ L'estudi catalític de la copolimerització de CO/α-olefines amb precatalitzadors de Pd(II) *in situ* van mostrar una activitat moderada en la copolimerització de CO i etilè i inactivitat quan es va dur a terme la copolimerització CO/estirè.

Part 2. *L'ús del diòxid de carboni com a matèria prima en la síntesi de policarbonats.*

➢ En la copolimerització asimètrica de CO$_2$ i òxid de ciclohexè (CHO) per l'obtenció de policarbonats catalitzada amb ZnEt$_2$ i lligands aminoalcohols quirals es van obtenir baixes activitats (fins a 2.90 g PCHC/g Zn), elevada selectivitat (80-100 % policarbonat *vs.* carbonat cíclic), elevada incorporació del carbonat (80-100 %) i un pes molecular de fins a 50000 (M$_w$).

➢ Nosaltres vam observar importants efectes en la productivitat i la selectivitat per part dels substituents dels lligands aminoalcohol en el carboni α al grup –OH (*C1*), al grup NR$_2$ (*C2*) i els substituents del grup amina. La voluminositat dels substituents en el carboni *C1* s'observa que poden esser els responsables de bloquejar la propagació, mentre que els efectes estèrics generats en el *C2* tenen menys efecte en la productivitat i la selectivitat que en la incorporació del carbonat. Per altra banda, el volum dels substituents en el grup amina tenen un efecte elevat en la selectivitat, aquests són necessaris per tal de generar repulsions estèriques i evitar el mecanisme de *backbiting*. El baix excés enantiomèric (fins a un 7 %) pot esser atribuït a la interacció feble del lligand amb el centre metàl·lic, el qual pot donar lloc a la dissociació del lligand permetent la inserció del CHO en dues posicions diferents.

➢ Nous complexos de zinc (II) amb el lligand N,N,O-donador **L13** es van obtenir rendiments moderats donant lloc a estructures polimèriques en [Zn(**L13**)(OAc)]$_n$ i estructures dimèriques [Zn(Et)(**L13**)]$_2$.

➢ El sistema [Zn(Et)(**L13**)]$_2$ va presentar una activitat catalítica moderada en la copolimerització de CHO/CO$_2$ donant lloc a 3.22 g PCHC/g Zn, 100 % de selectivitat

pel PCHC amb un 70 % d'enllaços carbonat i un pes molecular moderat (M_w fins a 46000), mentre que el complex derivat de zinc (II) acetat només va donar lloc a traces de copolímer PCHC-PCHE. Les diferencies en la productivitat poden venir degudes a la naturalesa polimèrica del complex [Zn(**L13**)(OAc)]$_n$, el qual pot evitar la formació de l'espècie activa dimèrica.

➢ Aquests resultants preliminars mostren que els sistemes de zinc (II) amb el lligand N,N,O-donador té potencial com a catalitzador en la síntesi de policarbonats mitjançant la copolimerització CO_2/CHO.

Chapter - 9

Summary & Resum

9.1 Summary

In the last decades chemistry has experienced an important change, which is focused on minimizing the hazard and maximizing the efficiency of any chemical process. This leads to explore the possibilities of reuse, recover and recycle the emissions (basically carbon dioxide) prior to their release into the environment. One possible application of carbon dioxide is as an environmental benign reaction medium in its compressed form (liquid or supercritical, scCO$_2$), also providing opportunities for facilitating the recovery and recycling of the catalyst. Many investigations are also focusing on the reuse of CO$_2$ as a remarkable C$_1$ feedstock because of its low cost, its natural abundance and relatively low toxicity.

In **Chapter one**, the literature dealing with the use of carbon dioxide, as an alternative solvent and as C$_1$ building block to perform copolymerisation reactions, is reviewed. Specially, carbon dioxide as an alternative solvent to perform copolymerisation reactions of CO and vinyl arenes to obtain polyketones and the use of CO$_2$ as C$_1$ building block in CO$_2$/epoxides copolymerisation reactions producing polycarbonates. The main conclusions that can be drawn from this chapter are *a)* the copolymerisation of CO and vinyl arenes are extensively studied with a wide number of ligands, and 2,2'-bipyridine and 1,10-phenantroline derivative ligands give the best results *b)* however, only few attempts to do the reaction environmentally friendly were explored. *c)* The polycarbonates synthesis is a field of growing interest using a greener alternative to the actual industrial process, consequently, the CO$_2$/epoxides copolymerisation reactions with a huge variety of metal alkoxide or metal carboxylate species have been studied *d)* even more this reaction could lead to the formation of optically active aliphatic polycarbonate, which are hardly explored to date.

The objectives of this Thesis are presented and detailed in **Chapter 2**.

Chapter three is dedicated to the synthesis and characterisation of new perfluorinated bipyridine ligands (**L1-L3**) soluble in compressed carbon dioxide. The coordination chemistry towards Pd(II) and Rh(I) was described, obtaining complexes with general formula [Pd(**L1-L3**)$_2$][BArF]$_2$ (BArF = B[3,5-(CF$_3$)$_2$C$_6$H$_3$]$_4$), [Rh(CO)$_2$(**L1-L3**)]PF$_6$. NMR, IR spectroscopy techniques and DFT calculations are

used to gain insight the new complexes synthesised. Bischelated palladium catalysts containing these perfluorinated bipyridine ligands were tested in the CO/styrene (ST) and CO/*tert*butylstyrene (TBS) copolymerisation in compressed carbon dioxide and 2,2,2-trifluoroethanol (TFE). For both substrates high activities were obtained, showing the best results in productivity in liquid expanded CO_2, 6.1 kg CP/g Pd and 222000 of M_w in CO/TBS copolymerisation.

Based on the results obtained with bischelated palladium catalyst, **Chapter four** extended the use of the **L1-L3** ligands to the synthesis of monochelated palladium complexes with general formula $[Pd(CH_3)(NCCH_3)(\textbf{L1-L3})][X]$, where X is PF_6^-, OTs^- and $BArF^-$. The chemical structure of the complexes was examined and evidences of interionic interactions were found by PGSE and NOESY or HOESY. The PF_6^- and OTs^- are localized close to the bipyridine ring *trans* to palladium methyl and the acetonitrile, while $BArF^-$ did not show any significant interionic contact. The monochelated palladium (II) complexes were applied in the CO/ST and CO/TBS copolymerisation in compressed carbon dioxide and TFE showing good results in both media. MALDI-TOF analysis of the initiation and end group from the copolymers was studied, being observed the most accepted mechanism for CO/TBS, initiation by the substrate and termination by β-H elimination.

The coordination chemistry of the bidentate P,N-donor phosphinine ligand **L4** towards Pd(II), Pt(II) and Rh(I) was investigated in **Chapter five**. The molecular structure of the complexes $[Rh(cod)(\textbf{L4})]BF_4$, $[PdCl_2(\textbf{L4})]$ and $[PtCl_2(\textbf{L4})]$ were determined by X-ray diffraction. Both phosphinine-Pd(II) and Pt(II) complexes reacted with (chiral) alcohols and (chiral) amines at the P=C double bond at elevated temperature regio- and stereo-selective (*syn*-addition), leading to $[MCl_2[\textbf{L4}H\cdot XR]$ (M = Pd or Pt, XR = OR or NR_1R_2). Reaction of the new complexes with chelating diphosphine (DPPE) at room temperature in CH_2Cl_2 lead quantitatively to $[Pd(DPPE)_2]Cl_2$ and **L4** by elimination of ethanol and re-aromatization of the phosphorus heterocycle. Preliminary results in CO/olefins copolymerisation were obtained with *in situ* Pd(II) catalysts, but they showed moderate activity for ethylene and no activity for styrene in copolymerisation reaction.

Summary & Resum

Chapter six involves the environmental friendly polycarbonates synthesis using carbon dioxide as C_1 building block by copolymerisation with cyclohexene oxide (CHO). As a first approach different chiral amino-alcohol ligands were used with Zn (II) catalyst for the reaction. The effect in the productivity and polycarbonate selectivity of the different substituents in the carbon α to the –OH (*C1*) and –NR group (*C2*) as well as the amino-substituents of the ligand have been analysed. The bulkiness of the substituent in the *C1* affects the productivity and the selectivity, while in *C2* had no important effect. On the other hand, the amine's substituent has a stronger effect in the selectivity. The polycarbonates were obtained with low activities, high selectivity, high carbonate incorporation and the molecular weight up to 50000 (M_w).

Chapter seven deals with the synthesis and characterization of new zinc (II) N,N,O-Schiff base complexes by NMR, IR, MALDI-TOF spectroscopy techniques and X-ray structure for zinc (II) acetate derivative showing a polymeric structure. The preliminary results in the copolymerisation of CO_2 and CHO using these complexes as catalyst produced low activity (3.22 g PCHC/g Zn), 100% polycarbonate selectivity and moderate molecular weight (M_w up to 46000).

9.2 Resum

En les últimes dècades la química ha experimentat importants canvis centrats en la minimització de l'ús de productes tòxics i la maximització del rendiment en qualsevol procés químic. Això ha donat lloc a explorar les possibilitats de la recuperació, reutilització i el reciclatge de les emissions (bàsicament de diòxid de carboni) abans d'enviar-les a l'atmosfera. Una de les possibles aplicacions del diòxid de carboni és com a dissolvent no nociu per al medi ambient en la seva forma comprimida (ja sigui com a líquid o com a diòxid de carboni supercrític), donant lloc a la vegada a una millor recuperació i reciclatge dels catalitzadors usats en reaccions catalítiques. Per altra banda, moltes investigacions es centren també en reutilitzar el diòxid de carboni com a matèria prima per a la síntesi de nous productes degut al seu baix cost, la seva abundància natural i la seva relativa baixa toxicitat.

En el **Capítol u** es fa una revisió de la bibliografia publicada fins al moment en el camp dels usos del diòxid de carboni com a dissolvent alternatiu i com a matèria prima en reaccions de copolimerització. Concretament, es presenta l'ús del diòxid de carboni com a dissolvent en reaccions de copolimerització entre el monòxid de carboni i arens vinílics per obtenir policetones. Per altra banda s'analitza l'ús del CO_2 com a matèria prima en la copolimerització amb epòxids donant lloc a policarbonats. Les principals conclusions que es poden extreure d'aquest capítol són *a)* la copolimerització de CO amb arens vinílics està extensament estudiada amb un gran nombre de lligands, i concretament els lligands derivats de la 2,2'-bipiridina i la 1,10-phenantrolina són els que donen millors resultats, *b)* només s'han explorat pocs exemples de convertir la reacció en menys contaminant pel medi ambient. *c)* La síntesi de policarbonats és un camp de creixent interès fent servir processos menys contaminants que el procés industrial actual, com a conseqüència, han aparegut una gran varietat de metalls en forma d'espècies metall alcòxid o metall carboxilat per dur a terme la reacció de copolimerització amb CO_2 i epòxids *d)* a més aquesta reacció dóna l'opció d'obtenir policarbonats alifàtics òpticament actius, els quals han estat rarament investigats.

Els objectius d'aquesta Tesi estan presentats i detallats en el **Capítol dos**.

El **Capítol tres** està dedicat a la síntesis i caracterització de nous lligands bipiridines perfluorats (**L1-L3**) solubles en diòxid de carboni comprimit. S'ha estudiat la química de coordinació amb aquests lligands en complexos de Pd(II) i Rh(I), obtenint-se complexos amb fórmula general [Pd(**L1-L3**)$_2$][BArF]$_2$ (BArF = B[3,5-(CF$_3$)$_2$C$_6$H$_3$]$_4$), [Rh(CO)$_2$(**L1-L3**)]PF$_6$. Per tal d'aprofundir en aquests nous complexos s'han fet servir tècniques espectroscòpiques com l'RMN, l'IR i càlculs DFT. Els complexos dicatiònics de pal·ladi sintetitzats amb les bipiridines d'estudi han estat provats com a catalitzadors en les reaccions de copolimerització de CO amb estirè (ST) i *tert*butilestirè (TBS) en diòxid de carboni comprimit i 2,2,2'-trifluoroetanol (TFE) com a medis per la reacció. Amb ambdós substrats s'han obtingut altes activitats, donant lloc als millors resultats publicats en CO$_2$ comprimit com a solvent, 6.1 kg CP/g Pd i 222000 de pes molecular en la copolimerització de CO/TBS.

En base als resultats obtinguts amb els catalitzadors bisquelats de pal·ladi, en el **Capítol quatre** s'ha estès l'ús dels lligands **L1-L3** en la síntesi de complexos catiònics de pal·ladi amb fórmula general [Pd(CH$_3$)(NCCH$_3$)(**L1-L3**)][X], on X és PF$_6^-$, OTs$^-$ o BArF$^-$. L'estructura química d'aquests complexos ha estat examinada i s'han obtingut evidències d'interaccions interiòniques mitjançant PGSE i NOESY o HOESY. Els anions PF$_6^-$ i el OTs$^-$ es troben localitzats en les proximitats de l'anell de bipiridina *trans* a l'enllaç pal·ladi metil i a prop del lligand acetonitril, mentre que l'anió BArF$^-$ no va mostrar cap tipus de contacte iònic. Aquests complexos catiònics de pal·ladi (II) es van aplicar com a catalitzadors en la copolimerització de CO/ST i CO/TBS en diòxid de carboni comprimit i TFE, donant lloc a bons resultats en ambdós medis. Per altra banda, es va estudiar el mecanisme de la reacció fent servir l'estudi dels grups finals i inicials dels copolímers mitjançant el MALDI-TOF, on es va veure el mecanisme més acceptat en CO/TBS, en el qual la iniciació té lloc a partir de la inserció del substrat i la terminació mitjançant la β-eliminació.

La química de coordinació del lligand bidentat P,N-fosfinina (**L4**) amb Pd(II), Pt(II) i Rh(I) es va investigar en el **Capítol cinc**. L'estructura molecular dels complexos [Rh(cod)(**L4**)]BF$_4$, [PdCl$_2$(**L4**)] i [PtCl$_2$(**L4**)] es va determinar mitjançant difracció de raig-X. Els complexos fosfinina de Pd(II) i de Pt(II) reaccionen a elevada temperatura amb alcohols i amines (quirals) a través de l'enllaç P=C de forma regio- i estero-selectiva (addició *syn*), donant lloc a complexos de fórmula molecular [MCl$_2$[**L4**H·XR]

(M = Pd o Pt, XR = OR o NR_1R_2). L'estudi de la reactivitat d'aquests nous complexos amb difosfines quelat (DPPE) a temperatura ambient i en CH_2Cl_2 dóna lloc a compostos de fórmula $[Pd(DPPE)_2]Cl_2$ i al lligand lliure **L4**, el qual es forma mitjançant l'eliminació d'etanol i la re-aromatització de l'anell de fòsfor. Els resultats preliminars en la copolimerització de CO i olefines amb catalitzadors de Pd(II) sintetitzats *in situ* mostren que aquests catalitzadors són moderadament actius en la copolimerització CO/etilè i no són actius en la copolimerització CO/estirè en aquesta reacció.

El **Capítol sis** es dedica a la síntesi poc contaminant dels policarbonats fent servir el diòxid de carboni com a matèria prima mitjançant la copolimerització amb l'òxid de ciclohexè (CHO). Com una primera aproximació s'han fet servir aminoalcohols quirals en complexos de zinc (II) com a catalitzadors per aquesta reacció. S'ha estudiat l'efecte en la productivitat i la selectivitat en vers el policarbonat tenint en compte l'efecte produït pels diferents substituents en el carboni α del grup –OH (*C1*) i del grup –NR (*C2*), al igual que l'efecte dels substituents de l'amina. Es va observar que els impediments estèrics dels substituents en el *C1* afectaven la productivitat i la selectivitat, mentre que en el *C2* aquests efectes no eren tan importants. Per altra banda, els substituents de l'amina influeixen considerablement a la selectivitat pel policarbonat envers al carbonat cíclic. Els policarbonats han estat obtinguts amb baixa activitat, alta selectivitat, alta incorporació del carbonat i pesos moleculars fins a 50000 (M_w).

El **Capítol set** tracta sobre la síntesi i caracterització de nous catalitzadors de zinc (II) amb lligands N,N,O-tridentats mitjançant espectroscòpia de RMN, IR, MALDI-TOF i la determinació estructural per raig-X del complex derivat de l'acetat de zinc(II), el qual mostra una estructura polimèrica. Els resultats preliminars de la copolimerització del CO_2 amb el CHO fent servir els complexos de zinc (II) sintetitzats donen lloc a activitats baixes (3.22 g PCHC/g Zn), 100% de selectivitat pel policarbonat i pesos moleculars moderats (M_w fins a 46000).

Chapter - 10

Appendix

Appendix

10.1 List of publications

Authors: Ariadna Campos-Carrasco, Evgeny A. Pidko, Anna M. Masdeu-Bultó, Martin Lutz, Anthony L. Spek, Dieter Vogt and Christian Müller.

Title: 2-(2'-pyridyl)-4,6-diphenylphosphinine versus 2-(2'-pyridyl)-4,6-diphenylpyridine: Synthesis, characterization and coordination chemistry towards Rh(I)

Journal: New Journal of Chemistry

Number or authors: 7

Volume: 34 **Number:** 8 **Pages, Initial:** 1547 **final:** 1550 **Year:** 2010 **Place of publication:** (ENGLAND) **ISSN:**1144-0546 **Legal Deposit:** DOI: 10.1039 / C0NJ00030B

Key: Letter **article code:** 516342 **Order:** 001

Authors: Ariadna Campos-Carrasco, Leen E.E. Broeckx, Jarno J.M. Weemers, Evgeny A. Pidko, Martin Lutz, Anna M. Masdeu-Bultó, Dieter Vogt and Christian Müller.

Title: Pd(II) and Pt(II) complexes of 2-(2'-pyridyl)-4,6-diphenylphosphinine: Synthesis, Structure and Reactivity

Journal: Chemistry A European Journal - *printed online*

Number or authors: 7

Volume: --- **Number:** --- **Pages, Initial:** --- **final:** --- **Year:** 2011 **Place of publication:** Weinheim, Germany **ISSN:** 0947-6539 **Legal Deposit:** DOI: 10.1002/chem.201002586

Key: Article **article code:** --- **Order:** 002

Authors: Ariadna Campos-Carrasco, Clara Tortosa-Estorach, M.M. Reguero, Barbara Milani, Giancarlo Franció, Walter Leitner and Anna M. Masdeu-Bultó.

Title: New Efficient Dicationic Palladium (II) Complexes for the CO/vinyl arenes copolymerisation in condensed and supercritical carbon dioxide.

Journal: in preparation

Number or authors: 7

Volume: --- **Number:** --- **Pages, Initial:** --- **final:** --- **Year:** 2011 **Place of publication:** --- **ISSN:** --- **Legal Deposit:** ---

Key: Article **article code:** --- **Order:** 003

Authors: Ariadna Campos-Carrasco, Angela D'Amora, Walter Leitner, Barbara Milani and Anna M. Masdeu-Bultó.

Title: New Efficient Monocationic Palladium (II) Complexes with Perfluorinated Bipyridines used for CO/aromatic α-Olefins Copolymerization in Conventional and Green Media.

Journal: in preparation

Number or authors: 5

Volume: --- **Number:** --- **Pages, Initial:** --- **final:** --- **Year:** --- **Place of publication:** --- **ISSN:** --- **Legal Deposit:** ---

Key: Article **article code:** --- **Order:** 004

Authors: Ariadna Campos-Carrasco, Arantxa Orejón, Amaia Bastero, Miquel A. Pericàs and Anna M. Masdeu-Bultó.

Title: Zinc catalytic systems with amino-alcohol ligands in polycarbonates synthesis by copolymerisation of cyclohexene oxide and carbon dioxide.

Journal: in preparation

Number or authors: 5

Volume: --- **Number:** --- **Pages, Initial:** --- **final:** --- **Year:** --- **Place of publication:** --- **ISSN:** --- **Legal Deposit:** ---

Key: Article **article code:** --- **Order:** 005

10.2 Meeting contributions

Authors: <u>A. Campos-Carrasco</u>, A. Orejón, A. M. Masdeu-Bultó, A. Bastero, M. A. Pericàs

Title: Polycarbonates by copolymerization of cyclohexene oxide and carbon dioxide

Kind of participation: Poster

Conference: RENACOM, Symposium International sur la Chimie Organometallique et la Catalyse

Number or authors: 5

Place of celebration: Tetouan (MORROCCO) **Year:** 2009

Authors: <u>A. Campos-Carrasco</u>, C. Tortosa-Estorach, A. D'Amora, B. Milani, A. M. Masdeu-Bultó

Title: New Perfluorinated 2,2'-Bipyridine ligands applied to the Pd-catalyzed CO/styrene copolymerization in green and conventional media

Kind of participation: Poster

Conference: RENACOM, Symposium International sur la Chimie Organometallique et la Catalyse

Number or authors: 5

Place of celebration: Tetouan (MORROCCO) **Year:** 2009

Authors: <u>A. Campos-Carrasco</u>, C. Tortosa-Estorach, A. D'Amora, B. Milani, A. M. Masdeu-Bultó

Title: New Perfluorinated 2,2'-Bipyridine ligands applied to the Pd-catalyzed CO/styrene copolymerization in green and conventional media oxides

Kind of participation: Poster

Conference: ICCDU-X, 10th International Conference on Carbon Dioxide Utilization

Number or authors: 5

Place of celebration: Tianjin (CHINA) **Year:** 2009

Appendix

Authors: A. Campos-Carrasco, C. Tortosa-Estorach,M. Giménez-Pedrós W. Leitner, G. Franciò, A. D'Amora, B. Milani, <u>Anna M. Masdeu-Bultó</u>
Title: Pd-catalysed CO/arene copolymerization in supercritical carbon dioxide
Kind of participation: Participation in oral comunication
Conference: RENACOM, Symposium International sur la Chimie Organometallique et la Catalyse
Number or authors: 8
Place of celebration: Tetouan (MORROCCO) **Year:** 2009

Authors: <u>A. Campos-Carrasco,</u> C. Tortosa-Estorach, A. M. Masdeu-Bultó, W. Leitner.
Title: New Perfluorinated 2,2'-Bipyridine ligand used for CO/Tert-butylstyrene copolymerization in supercritical carbon dioxide
Kind of participation: Poster
Conference: 16 International Symposium on Homogeneous Catalysis
Number or authors: 4
Place of celebration: Florencia (ITALY) **Year:** 2008

Authors: <u>A. Campos-Carrasco</u>, C. Tortosa-Estorach, A. M. Masdeu-Bultó, W. Leitner
Title: New Perfluorinated 2,2'-Bipyridine ligand used for CO/Tert-butylstyrene copolymerization in supercritical carbon dioxide
Kind of participation: Poster
Conference: XXVI Reunión del Grupo especializado en Química Organometálica
Number or authors: 4
Place of celebration: Santiago de Compostela (SPAIN) **Year:** 2008

Activity: COST D40 - Inovation II
Dates: 18/05/2008 - 21/05/2008
Broad field: Internacional
Classification: Attendance at Cientific meetings (without presentation or publication)

10.3 Research stays abroad

Center: Technische Universiteit Eindhoven
Place: Eindhoven   **Country:** NETHERLANDS   **Year:** 2009   **Duration:** 02M
Issue: "Synthesis of Phosphabenzene-based Ligands and Coordination Chemistry".
Key: PhD – 19 May – 8 July

Center: Università di Trieste
Place: Trieste   **Country:** ITALY   **Year:** 2008   **Duration:** 03M
Issue: 'New perfluorinated 2,2'-bipyridine ligand used for CO/Styrene copolymerization in conventional media'
Key: PhD - 01 September - 30 November

Center: Technische Universiteit Eindhoven
Place: Eindhoven   **Country:** NETHERLANDS   **Year:** 2007   **Duration:** 04M
Issue: "Synthesis of Phosphabenzene-based Ligands, Coordination Chemistry and Applications in Homogeneous Catalysis".
Key: PhD – 16 March – 16 July

10.4 Other important activities

Activity: CERTIFICATE OF HONORABLE MENTION for Poster Award. Tittle: NEW PERFLUORINATED 2,2'-BIPYRIDINE LIGANDS APPLIED TO THE Pd-CATALYZED CO/STYRENE COPOLYMERIZATION IN GREEN AND CONVENTIONAL MEDIA
Dates: 17/05/2009 - 21/05/2009
Broad field: International
Conference: ICCDU-X, 10th International Conference on Carbon Dioxide Utilization
Place of celebration: Tianjin (CHINA) **Year:** 2009
Classification: Price - CERTIFICATE OF HONORABLE MENTION for Poster Award.